

UNIVERSITY OF GLASGOW
FACULTY OF ENGINEERING
DEPARTMENT OF NAVAL ARCHITECTURE AND OCEAN ENGINEERING
ACADEMIC YEAR: 1995 - 1996

Research study title leading to an MSc degree:

**ADHESIVELY BONDED STEEL SANDWICH STRUCTURES
FOR MARINE APPLICATIONS**

MSc THESIS

Postgraduate student: **Eleni Apollon's KONSTANTINOU**

Supervisor: **Mr. Ian E. WINKLE**

© Eleni KONSTANTINOU
GLASGOW * March 1996 *

ProQuest Number: 13833381

All rights reserved

INFORMATION TO ALL USERS

The quality of this reproduction is dependent upon the quality of the copy submitted.

In the unlikely event that the author did not send a complete manuscript and there are missing pages, these will be noted. Also, if material had to be removed, a note will indicate the deletion.



ProQuest 13833381

Published by ProQuest LLC (2019). Copyright of the Dissertation is held by the Author.

All rights reserved.

This work is protected against unauthorized copying under Title 17, United States Code
Microform Edition © ProQuest LLC.

ProQuest LLC.
789 East Eisenhower Parkway
P.O. Box 1346
Ann Arbor, MI 48106 – 1346

Theris
10568
Copy 1

GLASGOW
UNIVERSITY
LIBRARY

*I would like to dedicate the present MSc study to
Ignatios and Alexandros*

Three kinds of souls, three prayers:

- 1. I am a bow in your hands, Lord. Draw me, lest I rot.**
- 2. Do not overdraw me, Lord. I shall break.**
- 3. Overdraw me, Lord, and who cares if I break!**

... And while I waited, the stones seemed to shift. I heard great breaths.

"Behold Him!" I murmured. "He has come!"

I turned with a shudder. But it was not Jehovah. It was not Jehovah, it was you, grandfather, from the beloved soil of Crete. You stood before me, a stern nobleman, with your small snow-white goatee, dry compressed lips, your ecstatic glance so filled with flames and wings. And roots of thyme were tangled in your hair.

You looked at me, and as you looked at me I felt that this world was a cloud charged with thunderbolts and wind, man's soul a cloud charged with thunderbolts and wind, that God puffs above them, and that salvation does not exist.

Lifting my eyes, I glanced at you. I was about to ask, Grandfather, is it true that salvation does not exist? But my tongue had stuck to my throat. I was about to go near you, but my knees gave way beneath me.

At that point you held out your hand as if I were drowning and you wished to save me.

I clutched it avidly. It was spattered with multicoloured paints. You seemed to be painting still. The hand was burning. I gained strength and momentum by touching it, and was able to speak.

"Give me a command, beloved grandfather."

Smiling, you placed your hand upon my head. It was not a hand, it was multicoloured fire. The flame suffused my mind to the very roots.

Reach what you can, my child."

Your voice was grave and dark, as though issuing from the deep larynx of the earth.

It reached the roots of my mind, but my heart remained unshaken.

"Grandfather," I called more loudly now, "give me a more difficult, more Cretan command."

Hardly had I finished speaking when, all at once, a hissing flame cleaved the air. The indomitable ancestor with the thyme roots tangled in his locks vanished from my sight; a cry was left on Sinai's peak, an upright cry full of command, and the air trembled:

"Reach what you cannot!" ...

ABSTRACT

Sandwich panels, consisting of two facing plates separated by a core of stiffeners, are known to possess high strength and high stiffness to weight ratios. This form of construction is appropriate for structures where the self weight is one of the governing design criteria. This is particularly applicable in cases where the self weight could be reduced while the strength is maintained.

The present study deals specifically with the understanding of the performance of adhesively bonded steel corrugated core sandwich structures used for marine applications under realistic loading, namely bending and axial compression. That was done through review on the relevant subjects, theoretical work as well as experimentation.

Review on the subjects of adhesion, adhesives, sandwich construction, theory of sandwich construction and the concept of structural connections within the field of sandwich construction are concisely covered from Chapter 1 to Chapter 4, giving in a rather informative way the main outline of each aforementioned subject. As far as the experimental part is concerned, ten models were manufactured especially for the purposes of the present study. More specifically, their components - namely the flat plates and the webs - were joined together by means of a structural adhesive. Therefore, this study demonstrates - and this is clearly shown from Chapter 5 to Chapter 6 - that any failure occurring at this kind of structures is due to buckling either of the flat plate or the web, instead of being due to failure of the adhesive bonding.

Two types of bending tests were performed: four point and three point bending tests. Buckling of the webs and any other deformation occurred only adjacent to the points of load application causing some local but not global adhesive and further model damage. Besides, none of the models collapsed. Prediction of the stresses conforms to simple beam theory, although there seem to be some discrepancies between theoretical and experimental values. These could be attributed to imperfections occurring during the manufacture of the models, the material properties from which they are constructed, the installation of the strain gauges, the measuring of the strain gauge values and the important fact that both kinds of bending tests followed either the creep

or compression tests.

The four point bending tests revealed that the adhesive can influence the performance of the models. In a few words, in terms of real life performance, the strength of the adhesively bonded corrugated core sandwich structures can be seriously affected by the creep of the adhesive. This performance seems to be common for any corrugated core structure irrespective of the combination of face and core geometry. This would seem to preclude use of such structures where significant continuous loading is concerned (for example, heavy weights on deck structure).

In contrast to what happens in bending, in compression of this type of structures theory agrees almost perfectly with experiments and this happens mainly because a lot of serious studies have been done in the past by a number of scientists as far as this matter is concerned which results in small deviations to exist. Buckling of the faces and any other deformation occurred only adjacent to the points of load application causing some local but not global adhesive debonding.

In conclusion, the model structures designed for the purposes of the present project proved to be stable and strong. The concept of adhesively bonded steel corrugated core sandwich structures specifically designed for marine applications is still new and is worth developing much further by encouraging further research. The findings of the present work have been set all together in Chapter 7 and a number of interesting conclusions accompanied by proposals for future research work appear in Chapter 8.

PREFACE

This thesis describes fifteen months work concerned with understanding the performance of adhesively bonded steel sandwich structures used for marine applications. It represents a development of research at Glasgow undertaken within SERC/MoD contract GR/E96832, entitled "Adhesively Bonded Sandwich Structures in Marine Technology", which investigated the feasibility of bonding corrugated steel cores into steel sandwich beams typical of potential bulkhead and deck structures for ships.

Its main objectives included:

- The establishment, design, production and analysis of one of the design concepts illustrated in the figure at the end of the text.
- A further understanding of its behaviour under realistic loading.
- The extraction of useful information which industry could use on design, fabrication as well as associated performance.

The project consisted of both an experimental and a theoretical part. The experimental part included the manufacture of ten models of corrugated core sandwich construction. Five of the them were tested in four point bending, three were used in axial compression tests and the rest were tested in three point bending. The models were manufactured within the premises of the University workshops so that control of the parameters involved in the system would be possible. The joining of the parts which constitute each of them was done by means of a structural adhesive for which a substantial amount of test data already existed through the work of the research team of Glasgow Marine Technology Center. Tensile tests were also performed to determine the modulus of elasticity of the material of each model - cold rolled steel.

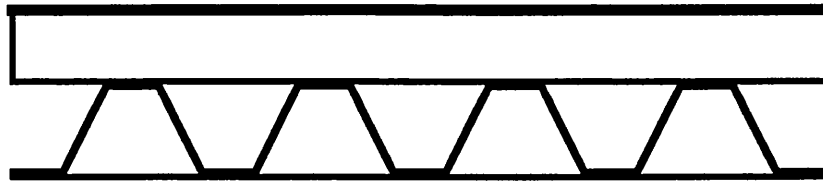
The theoretical part included a review of the present standing of theoretical work on the subject of the present research. Also, theoretical

predictions of bending and compression strength have been compared with the experimental results.

A number of useful conclusions have been drawn which should be a guide for any further work.



single corrugated core



double corrugated core - orthogonal corrugations

Figure: The design concepts of the present project

ACKNOWLEDGEMENTS

The present work would not have been completed without the generous help I received from my supervisor Mr. Ian E. Winkle. To him I would like to give my heartfelt thanks.

Also, I am grateful to Professor Faulkner for allowing this project to take place and offering me advice and comments as far as certain references were concerned.

Furthermore, I am indebted to Professor Cowling, Dr. Das, Dr. Hashim and E. Smith for certain information they offered me.

I am deeply grateful to the technical staff of Naval Architecture and Mechanical Engineering departments for their help during the manufacture and testing of the models.

Finally, I have to mention that the present project gave me the opportunity to make a little 'exploration' into the world of other engineering domains such as Mechanical, Civil and Aeronautical Engineering, mainly through papers and textbooks.

AUTHOR'S DECLARATION

Except where reference is made to the work of others, this thesis is believed to be original.

Note: Where there are tables, figures or illustrations, each appears as near as possible to the first reference to it in the text.

CONTENTS

Page

CHAPTER 1:

ADHESIVES	1
1.1 Definitions	1
1.2 Introduction	2
1.3 Historical development	4
1.4 Advantages - limitations of adhesive bonding	9
1.5 Mechanisms of adhesion	13
1.6 Choice of an adhesive	15
1.7 Surface pretreatment	15
1.8 Adhesive properties	16
1.9 Marine and offshore applications of adhesives	17

CHAPTER 2:

SANDWICH CONSTRUCTION	21
2.1 Definitions	21
2.2 Introduction	22
2.3 Core materials	29
2.4 Advantages - limitations of sandwich construction	29
2.5 Fire resistance	30
2.5.1 General	30
2.5.2 Marine fire resistance	31
2.5.3 Methods of protection	32
2.6 Designing a sandwich	35
2.7 Design steps	36
2.8 Modes of failure	38

CHAPTER 3:

THEORY OF CORRUGATED CORE SANDWICH CONSTRUCTION	41
3.1 Definitions	41
3.2 Introduction	42
3.3 Theory	43
3.3.1 Physical constants	43

3.3.2 Theoretical results	47
3.3.2.1 Bending stiffness D	47
3.3.2.2 Poisson's ratios μ associated with bending	48
3.3.2.3 Torsional stiffness D_{xy}	49
3.3.2.4 Transverse shear stiffness D_{Qy} in planes perpendicular to corrugation axis	49
3.3.2.5 Transverse shear stiffness D_{Qx} in planes parallel to corrugation axis	52
3.3.3 Principal results of the Libove and Batdorf [31] small deflection theory for flat sandwich plates	53
3.3.4 Stability of flat, simply supported corrugated core sandwich plates under compression [27]	57

CHAPTER 4:

THE DESIGN OF STRUCTURAL CONNECTIONS	62
4.1 Definitions	62
4.2 General	63
4.3 The ideal structural connection	63
4.4 Structural connections in composite structures	65
4.4.1 Bulkhead/shell connections	66
4.4.2 Stiffener intersections	67
4.4.3 Deck/edge connections	67
4.4.4 Single-skin shell/sandwich components connections	69

CHAPTER 5:

THE PROJECT: SELECTION AND MANUFACTURE OF THE MODELS	72
5.1 Introduction	72
5.2 The selection of the models	78
5.3 The manufacture of the models	79
5.4 The tensile tests	93

CHAPTER 6:

THE PROJECT: THE MODELS TESTS AND FINAL RESULTS	96
6.1 Introduction	96
6.2 Strain gauges installation	97

6.3 The four point bending tests	100
6.4 The axial compression tests	107
6.5 Additional three point bending tests	114
6.6 The results	117

CHAPTER 7:

DISCUSSION	166
7.1 General	166
7.2 Bending tests	167
7.3 Creep tests	170
7.4 Tensile tests	172
7.5 Compression tests	172
7.6 Conclusion	174

CHAPTER 8:

CONCLUSIONS-PROPOSED FUTURE WORK	175
8.1 Conclusions	175
8.2 Proposed future work	178

REFERENCES	180
------------	-----

APPENDIX A:

STEELWORK IN FIRE	A1
-------------------	----

APPENDIX B:

STRUCTURAL OPTIMIZATION OF CORRUGATED CORE AND WEB CORE SANDWICH PANELS SUBJECTED TO UNIAxIAL COMPRESSION (selected parts from [58])	B1
--------------------------------------------------------------------------------------------------------------------------------------	----

APPENDIX C:

STRAIN GAUGE INSTALLATION INSTRUCTIONS	C1
----------------------------------------	----

APPENDIX D:

CALCULATIONS FOR THE DETERMINATION OF THE BENDING AND COMPRESSION STRESSES	D1
----------------------------------------------------------------------------	----

APPENDIX E:

THE ORION PROCEDURE

E1

APPENDIX F:

**FORMULAE FOR CALCULATING THE PRINCIPAL STRESSES AND PRINCIPAL
AXES USING A 45-ANGLE ROSETTE**

F1

FIGURES**Page****CHAPTER 1:****ADHESIVES** 1

- 1.1 Technical and economic advantages gained from the use of adhesives [34] 3

CHAPTER 2:**SANDWICH CONSTRUCTION** 21

- 2.1 Structural sandwich 23
2.2 Corrugated core sandwich construction 23
2.3 Sandwich panel with honeycomb core [24] 26
2.4 Sandwich panel with corrugated core [4] and its elements 27
2.5 Variations of the corrugated core sandwich construction [4] 28

CHAPTER 3:**THEORY OF CORRUGATED CORE SANDWICH CONSTRUCTION** 41

- 3.1 Forces and moments acting on differential element $dx dy$ [28] 44
3.2 Sample of charts which give S directly for the common type of sandwich with corrugated core [28] 51
3.3 (Fig. E3 [28]) 52
3.4 (Fig. E1 [28]) 53
3.5 Sample of charts for the value of compressive-buckling-load parameter k vs the plate aspect ratio β [27] 61

CHAPTER 4:**THE DESIGN OF STRUCTURAL CONNECTIONS** 62

- 4.1 Bulkhead/shell connection 66
4.2 Stiffener intersections 68
4.3 Deck/edge connections 68
4.4 Joints between sandwich and single-skin components 69
4.5 Bolted joints in composite/sandwich structure 70
4.6 Edge treatments and suggestions for corner designs, edge close-outs and splices 71

CHAPTER 5:

THE PROJECT: SELECTION AND MANUFACTURE OF THE MODELS	72
5.1 The design concepts of the project	73
5.2 Elements of a corrugated core sandwich beam	73
5.3 Comparison of stiffness and section area between sandwich construction and conventionally stiffener plates	77
5.4 Diagrammatic illustration of the models	81
5.5 Sketch of the cross section of the bonding frame	82
5.6 Sketch of the plan view of the top and bottom plates	83
5.7 Sketch of the profile of a clamp	84
5.8 Sketch of the section of the frame base	85
5.9 The dimensions of each tensile test specimen	93
5.10 Diagrammatic illustration of E variation	94

CHAPTER 6:

THE PROJECT: THE MODELS TESTS AND FINAL RESULTS	96
6.1 The points where strain gauges were installed	98
6.2 Compression test rig [18]	107
6.3 The position and numbering of strain gauges on models 0-4b, 1-4b, 2-4b and 3-4b	118
6.4 The position and numbering of strain gauges on model 4-4b	119
6.5 The position and numbering of strain gauges on models 2-c and 1-c	120
6.6 The position and numbering of strain gauges on model 4-c	121
6.7 The position and numbering of strain gauges on models 0-3b and 3-3b	122
6.8 Records of the load vs deflection relationship of all four point bending tests	128
6.9 Diagrams showing the maximum bending load and deflection levels for each model of the four point bending tests	129
6.10 Test 8: four point bending test of model 0-4b. Diagrams of bending stresses vs deflection	130
6.11 Test 8: Comparison between the gradients of the experimentally obtained curves and the SBT ones	131
6.12 Test 16: four point bending test of model 3-4b. Diagrams of bending	

stresses vs deflection	132
6.13 Test 16: Comparison between the gradients of the experimentally obtained curves and the SBT ones	133
6.14 Test 12: four point bending test of model 2-4b. Diagrams of bending stresses vs deflection	134
6.15 Test 12: Comparison between the gradients of the experimentally obtained curves and the SBT ones	135
6.16 Test 14: four point bending test of model 4-4b. Diagrams of bending stresses vs deflection	136
6.17 Test 14: Comparison between the gradients of the experimentally obtained curves and the SBT ones	137
6.18 Test 10: four point bending test of model 1-4b. Diagrams of bending stresses vs deflection	138
6.19 Test 10: Comparison between the gradients of the experimentally obtained curves and the SBT ones	139
6.20 Creep tests of all models. Diagrams of bottom plate deflection vs time	144
6.21 Curve fit of the linear part of creep curves of all models	144
6.22 Test 7: creep test of model 0-4b. Diagrams of longitudinal strains and stresses vs time	145
6.23 Curve fit of the linear part of strain creep curves of model 0-4b	146
6.24 Test 15: creep test of model 3-4b. Diagrams of longitudinal strains and stresses vs time	147
6.25 Curve fit of the linear part of strain creep curves of model 3-4b	148
6.26 Test 11: creep test of model 2-4b. Diagrams of longitudinal strains and stresses vs time	149
6.27 Curve fit of the linear part of strain creep curves of model 2-4b	150
6.28 Test 13: creep test of model 4-4b. Diagrams of longitudinal strains and stresses vs time	151
6.29 Curve fit of the linear part of strain creep curves of model 4-4b	152
6.30 Test 9: creep test of model 1-4b. Diagrams of longitudinal strains and stresses vs time	153
6.31 Curve fit of the linear part of strain creep curves of model 1-4b	154
6.32 Diagrams showing the relationship between Load/Section modulus factor and strain or deflection gradient	155

6.33 Test 17: axial compression test of model 2-c	158
6.34 Test 18: axial compression test of model 1-c	159
6.35 Test 19: axial compression test of model 4-c	160
6.36 Axial compression tests of models 2-c, 1-c and 4-c. Diagrams of compression load and stress levels for all models	161
6.37 Test 20: three point bending test of model 0-3b. Diagrams of bending stresses vs deflection	164
6.38 Test 21: three point bending test of model 3-3b. Diagrams of bending stresses vs deflection	165

TABLES**Page****CHAPTER 1:****ADHESIVES**

1

1.1 General characteristics of current toughened adhesives [34]

7

1.2 Benefits of structural bonding with toughened adhesives [34]

8

1.3 General comparison of joining process characteristics [34]

10

CHAPTER 2:**SANDWICH CONSTRUCTION**

21

2.1 Fire-related properties of metallic and FRP materials [18]

33

CHAPTER 5:**THE PROJECT: SELECTION AND MANUFACTURE OF THE MODELS**

72

5.1 The properties of a range of conventionally stiffened flat plate

74

5.2 The properties of a corrugated core sandwich beam

75

5.3 The ten bending and compression test models

80

5.4 The results of the tensile tests

94

5.5 The final values of E for all models

95

PHOTOS

Page

CHAPTER 5:

THE PROJECT: SELECTION AND MANUFACTURE OF THE MODELS	72
5.1 Cross section of model 0-4b and frame	86
5.2 View of model 0-4b and frame	86
5.3 Model 0-4b in the oven	87
5.4 Model 0-4b	90
5.5 Model 1-4b	91
5.6 Model 2-4b	91
5.7 Model 3-4b	92
5.8 Model 4-4b	92

CHAPTER 6:

THE PROJECT: THE MODELS TESTS AND FINAL RESULTS	96
6.1 Model 0-4b after the strain gauges installation and wiring	99
6.2 Model 0-4b at INSTRON machine before the four point bending test	99
6.3 Model 0-4b: the edge failure during the bending test	103
6.4 Model 0-4b: the buckling of the webs is apparent	103
6.5 Model 0-4b: the local deformation of the top plate	104
6.6 Model 0-4b after the four point bending test	104
6.7 Model 2-4b after the four point bending test	105
6.8 Model 3-4b: detail of the buckling of the webs	105
6.9 Model 3-4b: internal detail of the local deformation of the top plate	106
6.10 Model 3-4b: detail of the local deformation of the top plate	106
6.11 Model 2-c before the axial compression test	109
6.12 Model 2-c: the beginning of adhesive debonding and local buckling of the upper edge	109
6.13 Model 2-c: the adhesive debonding and local deformation become more severe	110
6.14 Model 2-c after the axial compression test	110
6.15 Model 1-c: the first signs of buckling	111
6.16 Model 1-c: local buckling continues	111

6.17 Model 1-c: a characteristic view of the continuing deformation	112
6.18 Model 1-c: adhesive debonding	112
6.19 Model 1-c after the axial compression test	113
6.20 Model 4-c: adhesive debonding and local deformation	113
6.21 Model 4-c after the axial compression test	114
6.22 Model 0-3b before the three point bending test	115
6.23 Model 0-3b after the three point bending test	116
6.24 Model 3-3b after the three point bending test	116

LIST OF ABBREVIATIONS

x	axial or longitudinal coordinate (mm)
y	lateral coordinate of plate (mm)
z	coordinate normal to faces of sandwich (mm)
w	deflection of middle surface of plate, measured in z direction (mm)
q	intensity of lateral loading (N/mm ²)
Q _x	intensity of internal shear acting in z direction in a cross section originally parallel to yz plane (N/mm)
Q _y	intensity of internal shear acting in z direction in a cross section originally parallel to xz plane (N/mm)
M _x	intensity of internal bending moment acting upon a cross section originally parallel to yz plane (Nmm/mm)
M _y	intensity of internal bending moment acting upon a cross section originally parallel to xz plane (Nmm/mm)
M _{xy}	intensity of internal twisting moment acting in a cross section originally parallel to yz plane or xz plane (Nmm/mm)
N _x	intensity of middle plane tensile force parallel to xz plane (N/mm)
N _y	intensity of middle plane tensile force parallel to yz plane (N/mm)

N_{xy}	intensity of middle plane shearing force parallel to yz plane and xz plane (N/mm)
D_x, D_y	flexural stiffnesses of plate with anticlastic bending unrestrained (Nmm)
D_{xy}	torsional stiffness of plate (Nmm)
D	flexural stiffness of ordinary plate (Nmm)
D_{Q_x}, D_{Q_y}	shear stiffnesses of plate (N/mm)
μ_x, μ_y	Poisson ratios for plate
μ	Poisson ratio for ordinary plate
γ_x, γ_y	shear-strain angles due to shears Q_x and Q_y , respectively
a	length of rectangular plate (mm)
b	width of rectangular plate (mm)
V	total potential energy of system (Nmm)
$[D], [M],$	differential operators
$[N], [P]$	
m	number of half waves in the x direction
n	number of half waves in the y direction
$\beta=a/b$	aspect ratio
P_{cr}	critical buckling end load per mm of the sandwich panel of infinite length (parallel to the x direction), i.e., critical value of $-N_x$
r_x, r_y	transverse-shear-flexibility parameters, $\frac{\pi^2 E_f I_f}{b^2 D_{Q_x}}$ and $\frac{\pi^2 E_f I_f}{b^2 D_{Q_y}}$ respectively
k	compressive-buckling-load parameter, $\frac{b^2 N}{\pi^2 E_f I_f}$

E_f	Young's modulus of elasticity of face material
E_c	Young's modulus of elasticity of core material
I_f	moment of inertia per unit width of faces, considered as membranes, taken about sandwich- plate middle surface ($0.5t_f h^2$)
I_c	moment of inertia per unit width of corrugation cross section in planes perpendicular to x or y axis, taken about sandwich-plate middle surface
η	flexural-stiffness ratio, $\frac{E_c I_c}{E_f I_f}$
SBT	simple beam theory
OBP	one-sided bulb plate
e	microstrain
e_x	longitudinal microstrain of the rosette
e_d	diagonal microstrain of the rosette
e_y	transverse microstrain of the rosette
e_1	principal microstrain along the 1 axis of the plate (see Appendix F)
e_2	principal microstrain along the 2 axis of the plate (see Appendix F)
s	stress (N/mm ²)
s_x	stress along the x axis of the plate (N/mm ²)
s_y	stress along the y axis of the plate (N/mm ²)

CHAPTER 1: ADHESIVES

The science of adhesion is truly multi-disciplinary, demanding a consideration of concepts from such diverse topics as surface chemistry, polymer chemistry, rheology, stress analysis and fracture mechanics.

It is, nevertheless, important for the technologist to possess a qualitatively correct overall picture of the various factors influencing adhesion and controlling joint performance in order to make rational judgements concerning the selection and use of adhesives.

1.1 DEFINITIONS

Adhesive: Generally speaking one takes it to refer to a material used to join two solids together by forming between them a thin layer which sticks to both. At some stage in its application the adhesive must be liquid or at least plastic. When the bond is formed it is solid, though it may or may not be flexible.

Adhesion: The attraction between substances whereby when they are brought into contact work must be done in order to separate them. The engineer uses experimentally determined values, which describe joint behaviour under specific conditions, in order to classify the bond or adhesion between two phases.

Adherends or Substrates: The materials being joined.

Composite (plastic): Plastic containing a filler which may be fibrous or particulate.

Creep: The dimensional change with time of a material under sustained load; usually relatively low loads and long periods are involved.

Prepreg: Woven cloth or tows of fibres preimpregnated with partially cured

resin.

Rheology: Study of the flow behaviour of materials.

Structural Adhesive: Adhesive which produces bonds capable of bearing an appreciable and sustained load for the period of service, without creep or other loss of performance. Most structural adhesives have been toughened by the addition of an additional flexible or rubbery molecular phase.

1.2 INTRODUCTION

The possible use of adhesives in a new design should always be considered because of the economic and technical benefits that they can confer. This statement is justified when one considers the benefits summarised in Fig. 1.1.

Adhesives are not a panacea, but they do have a great deal to offer as is shown by the vital role they play in modern production engineering. Yet, despite this, they are not generally regarded with enthusiasm by engineers and designers. The reason for this is not hard to find [9]. There are so many adhesives with such diverse properties that, in the absence of a unifying science which can explain not only why adhesives stick but why they behave as they do, a very strong incentive is required to guarantee perseverance.

In addition, although the polymeric structures of adhesives are well understood, this knowledge is usually of little help to the engineer who is used to dealing in precise terms and may be readily put off by a subject which he tends to regard as being arcane and woolly. Nevertheless, from the point of view of the designer, one of the most inviting avenues in his search for lighter and more economical structures and mechanisms leads inevitably towards the use of adhesives.

(continued on page 4)

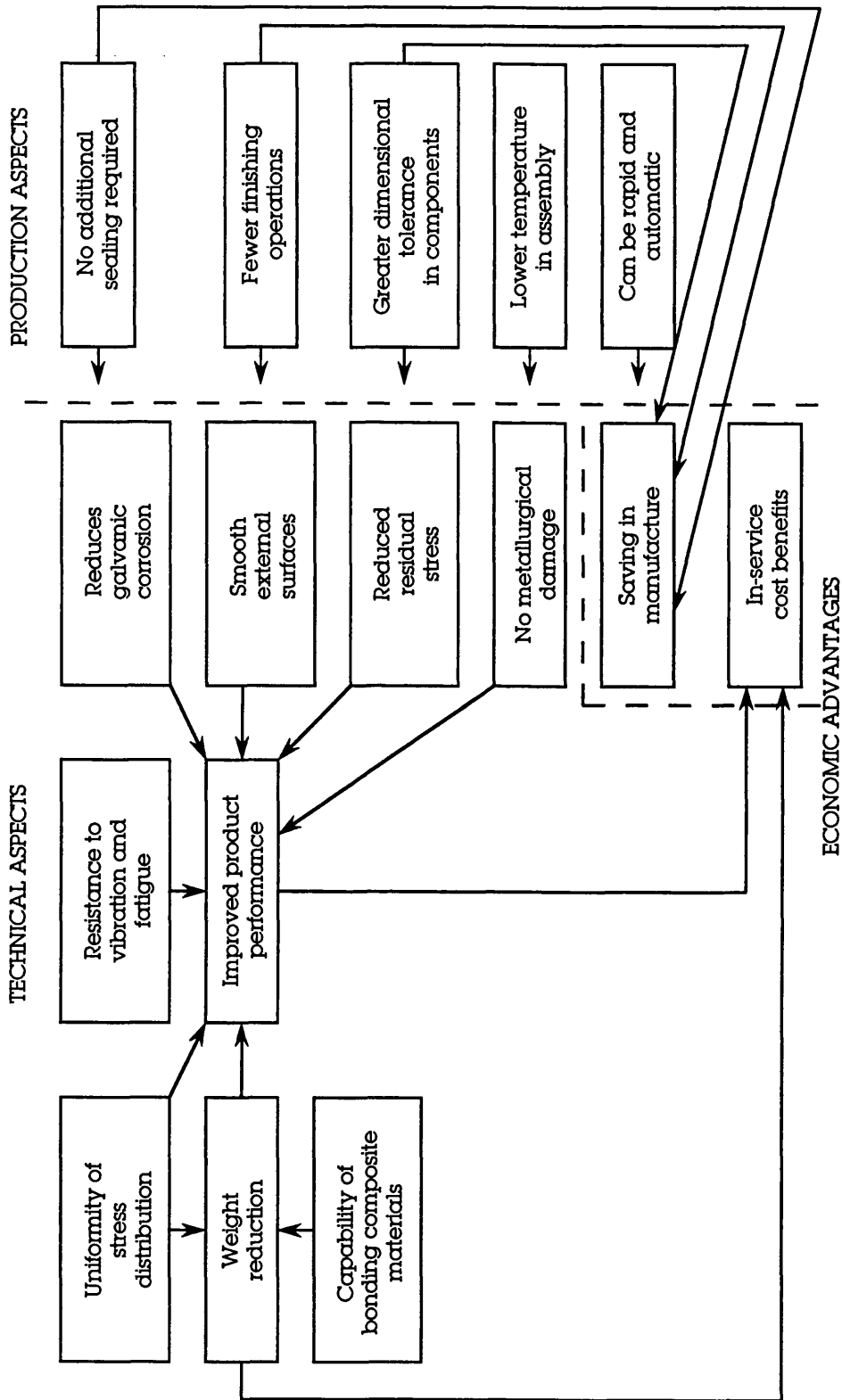


Fig. 1.1 Technical and economic advantages gained from the use of adhesives [34]

1.3 HISTORICAL DEVELOPMENT

Sticking things together is a common enough task, and materials exhibiting adhesive properties have been employed in a sophisticated manner since earliest times. Natural adhesives such as starch, animal glues and plant resins have been used for centuries, and are still used widely today for packaging and for joining wood. Rubber-based adhesives were introduced in the shoe and tyre industries towards the end of the 19th century, but the birth of modern structural adhesives is generally dated from the early 20th century with the introduction of phenol-formaldehyde resins. Mainly as a result of the Second World War, many natural products were not available in the early 1940s and this spurred the further development of synthetic resins. The construction of wooden wartime aircraft was, nevertheless, facilitated by the availability of phenol-resorcinol- and urea-formaldehyde adhesives, and since then reactive formaldehyde-based adhesives have continued to be used in the manufacture of timber-based building elements such as plywood, chipboard and laminated timber beams.

Over the past four or five decades the natural adhesives have been improved, and there has been an intense development of synthetic adhesives to meet more technically demanding applications. These synthetic polymers and ancillary products, which include thermoplastic and thermosetting types, have been developed to possess a balance of properties that enables them to adhere readily to other materials, to have an adequate cohesive strength and appropriate mechanical characteristics when cured, to possess good durability and to meet various application and manufacturing requirements.

Thermoplastic adhesives may be softened by heating and rehardened by cooling, and included in this group are polyvinyl acetates [10, 11, 12, 33]. Since the 1950s they have been used extensively as general-purpose adhesives for bonding slightly porous materials, from floor screeds to timber; they are, however, sensitive to wet alkaline service conditions, effectively restricting them to indoor use. Similar adhesives suitable for external situations are based on other polymer dispersions such as styrene butadiene rubbers, acrylic polymers and copolymers of vinyl

acetate with other monomers. Cyanocrylates, or so called 'superglues', also belong to this class of thermoplastic adhesives and are very useful for bonding small parts involving plastics, rubber, metal, glass and even human tissue.

Thermosetting materials are so called because, when cured, the molecular chains are locked permanently together in a large three-dimensional molecular structure; they may, therefore, be regarded as structural resins. Unlike thermoplastics they do not melt or flow when heated, but become more rubbery and lose strength with increasing temperature. Phenolic resins, and their modifications, belong to this group of adhesives and are numbered among the early structural adhesives used extensively within the aerospace industry for bonding metal parts [11, 12]. Epoxides and polyesters also belong to this group of thermosetting adhesives and they find widespread use in civil and marine engineering applications [6, 22, 35, 38]. Unsaturated polyesters are often used as binders in glass-reinforced plastics, or as mortars in conjunction with stone and cementitious materials. However, high shrinkage on curing, poor resistance to creep and low tolerance of damp conditions significantly restricts their application. Epoxides, on the other hand, are generally tolerant of many surface and environmental conditions, possess relatively high strength, and shrink very little on curing. A range of epoxy materials are available which cure at ambient or elevated temperatures, whose mechanical and physical characteristics vary widely [12, 33]. Indeed the general term epoxy may include materials which vary from flexible semi-elastic coatings and sealants to epoxy resin based concretes. Epoxy adhesives are available as single- or two-component materials in liquid, paste or film forms, which may additionally be 'toughened'. General information about toughened adhesives is given in Tables 1.1 and 1.2.

The increasing use of adhesives in a diversity of demanding situations has given confidence in the successful application of synthetic polymers and has provided the spur for further fundamental research and the development of improved products. In the future it is possible that acrylates and polyurethanes, and their toughened variants, may challenge the epoxides - particularly as they are perceived to be safer to use and less environmentally harmful. Structural silicone adhesives may

also be introduced for certain applications where gap-filling and flexibility are required, but where high strength is relatively unimportant; they also possess the added advantage of quite high thermal and environmental stability.

TABLE 1.1
General characteristics of current toughened adhesives [34]

ACRYLIC

Two-part (mixed). Usually mixed in ratio 1:1, 1:2, 1:5 and 1:10; general purpose gap-filling adhesives; overall performance not usually as good as non-mixed versions

Two-part (not mixed). One component, a catalyst, is applied sparingly onto either or both surfaces to be bonded; adhesive is then applied; use limited to relatively thin bond lines

Viscosity: viscous liquids to thixotropic pastes
Strength: shear - up to 35 MPa

T-peel - usually 100-120 N/25 mm width
impact - stops standard ASTM pendulum

Cure time (25°C): from 15 s to 15 min according to formulation

EPOXY

Single-part. Heat cured high performance adhesives with general utility in both mechanical and structural applications; particularly suited to the harsher environments

Viscosity: thixotropic gels to stiff pastes; some are intended to flow like solder when hot

Strength: generally somewhat higher (approximately 50% higher)

Cure time: from 1 min according to material, mass, method and temperature; usually about 30 min at 180°C for sheet steel assemblies

Two-part. General purpose high performance adhesives with good environmental resistance; variety of mix ratios

Viscosity: low viscosity resins to thick pastes

Strength: lower than hot cure

Cure time (25°C): not less than 2 h unless warmed

TABLE 1.1a

Main mechanical properties of current toughened adhesives [12]

	Tensile Strength N/cm ² * 10 ³	Elasticity Modulus N/cm ² * 10 ⁵	% Elongation	Compressive Strength N/cm ² * 10 ³	Flexural Strength N/cm ² * 10 ³
Melamine formaldehyde	5.9	7.12	0-2.5	12-38	6-13
Phenol formaldehyde	4.6	4.34	0-60	10-35	4-12
Resorcinol formaldehyde	4.5-7	4.8	-	16-22	6-13
Urea formaldehyde	4.9	6.11	-	16-24	6-11
Phenolic/nitrile	5.5-8	0.1	2-10	8-23	-
Phenolic epoxy	3-8	-	0.5	11-16	7-12
Silicone resins	2-3	0.0.5	80-97.5	11-17	4.8
Epoxy+polyamide	3-5	2-3	2-4	4-12	4.9
Epoxy+polyamine	4-6	1-3	2-10	5-12	6.9
Epoxy+polyamine (aromatic)	4.5-6.5	1.5-3	-	6-10	5.7
Epoxy novolac	5.5-8	-	2.5	11-12	7-11
Epoxy (cycloaliphatic)	6-7	-	2.5	19-21	7-10
Epoxy polysulphide	3-3.5	-	10-80	1-10	1.9
Polyimide	7.5-10.5	4.5	5.9	12-17	12-17
Polyurethane	-	-	-	-	-

TABLE 1.1b
General characteristics of the more important engineering adhesives [34]

Adhesive	Toxicity	Capital cost	Material cost	Process complexity	Process temperature	Solvent resistance	Heat resistance	General durability	Use
Anaerobic	1	1	2-3	1	E	3	2-3	3	Assembly for machines, coaxial components
Cyanoacrylate	1	1	3	1	C	2	1	1-2	Almost every type of small plastics, metal and rubber assembly
Epoxide	1-3	1-2	2	2	E	3	2-3	3	Usually used on larger objects where good performance required
Toughened acrylic	1-2	1	2-3	1-2	E	2-3	2-3	2-3	Excellent general performance, particularly structures
Toughened epoxide (heat cured)	1	1	2-3	1-2	H	3	3	3	Superb structural adhesives; also used for dynamically loaded mechanisms
Phenolic	1-2	3	2	3E	2-3	2-3	2-3	2-3	Usually used in large stressed and critical structures
Polyurethane	3	3	2	2-3	C	2-3	2-3	2	Used when rapid assembly needed in large structures

1=low; 2=medium; 3=high; H=hot; C=cold; E=either.

TABLE 1.2

Benefits of structural bonding with toughened adhesives [34]

Initial design

- Enhanced stiffness allows use of lighter alloys and/or thinner gauges
- Allows combination of many different materials
- Avoids high local loads
- Greater design freedom due to absence of dimensional and access restraints induced by conventional welding techniques

Construction

- No metallurgical damage
- No distortion or defacement
- Very accurate assembly possible without undue expense
- Little or no residual stress
- Can simplify assembly techniques
- Capital costs usually lower
- Overall costs can be reduced
- Reduced health hazard

Ultimate use

- Repair can be simpler than welding
 - No metallurgical damage during repair
 - Corrosion reduced or eliminated
 - Old composites may be repaired well
 - Fatigue resistance enhanced
-

1.4 ADVANTAGES - LIMITATIONS OF ADHESIVE BONDING

A driving force for the development and continual growth of the adhesives market is the many advantages that they offer compared with other, more traditional techniques for fastening materials, such as welding, brazing and soldering and mechanical fastening.

This is obviously true when one takes into consideration the information of Table 1.3.

Therefore, the advantages that adhesives can offer include:

- The ability to join dissimilar materials; e.g. the joining of metals, plastics, rubbers, fibre-composites, wood, paper products, etc. Specifically for marine applications, joining between aluminium and steel structural parts.
- The ability to join thin sheet-material efficiently. This is a major use of adhesives for joining both metallic and non-metallic materials. Compared to metallic substrates, adhesives, being based largely upon organic polymers, do not possess anywhere near the level of tensile fracture strengths exhibited by most metals but when used to join relatively thin sheets of metal their strengths are usually more than adequate. Specifically for marine applications, joining plates of considerable difference in thickness is performed satisfactorily.
- An improved stress distribution in the joint which imparts, for example, a very good dynamic-fatigue resistance to the bonded component.

In marine industry, an elimination of residual stresses due to welding joining techniques.

- The fact that they frequently represent the most convenient and cost-effective technique.

(continued on page 12)

TABLE 1.3
General comparison of joining process characteristics [34]

<i>Welding</i>	<i>Brazing and soldering</i>	<i>Mechanical fastening</i>	<i>Adhesive bonding</i>
Permanent joints	Usually permanent (soldering may be non-permanent)	Threaded fasteners permit disassembly	Permanent joints
Local stress points in structure	Fairly good stress distribution	Points of high stress at fasteners	Good uniform load distribution over joint area (except in peel)
Joint features	Joint appearance usually acceptable some dressing necessary for smooth surfaces	Surface discontinuities sometimes unacceptable	No surface marking; joint almost invisible
	Generally limited to similar material groups	Most forms and combinations of materials can be fastened	Ideal for joining most dissimilar materials
	Very high temperature resistance	High temperature resistance	Poor resistance to elevated temperatures
	Special provision often necessary to enhance fatigue resistance	Special provision for fatigue and resistance to loosening	Excellent fatigue properties; electrical resistance reduces corrosion at joints

(continued)

TABLE 1.3 - contd
 General comparison of joining process characteristics [34]

	<i>Welding</i>	<i>Brazing and soldering</i>	<i>Mechanical fastening</i>	<i>Adhesive bonding</i>
Joint preparation	Little or none on thin material; edge preparation for thick plates	Pre-fluxing often required (except for special brazing processes)	Hole preparation and often tapping for threaded fasteners	Cleaning often necessary
Post-processing	Heat treatment sometimes necessary	Corrosive fluxes must be cleaned off	Usually no post-processing; occasionally retightening in service	Not often required
Equipment	Relatively expensive, bulky and often requires heavy power supply	Manual equipment cheap; special furnaces and automatic units expensive	Relatively cheap, portable and can be used for 'on-site' assembly	Only large multi-feature epoxide and polyurethane dispensers are expensive
Consumables	Wire, rods etc. fairly cheap	Some special brazing fillers expensive; soft solders cheap	Quite expensive	Structural adhesives quite expensive
Production rate	Can be very fast	Automatic processes quite fast	Joint preparation and manual tightening slow; mechanical tightening fairly rapid	Seconds to hours, according to type
Quality assurance	NDT methods applicable to most processes	Inspection difficult particularly on soldered electrical joints	Reasonable confidence in torque-control tightening	NDT methods limited

Indeed, the bonding operation can often be automated. This obviously removes the necessity for any human operator to mix together the various components of the adhesive, if required, apply the adhesive to the correct location and repeat the procedure correctly many hundreds of times a day.

- An increase in design flexibility which enables novel design concepts to be implemented and allows a wider choice of materials to be available to the designer. A good example of these advantages is in corrugated core sandwich structures.
- An improvement in the appearance of the fastened structure; for example, if adhesives are used instead of spot-welding then the smooth, blemish-free appearance of the bonded structure is more appealing to the consumer.
- An improvement in corrosion resistance especially for marine structures operating in the sea environment. The above comparison to the spot-welded component serves as a good example where the use of a well-selected adhesive system will inherently result in far less corrosion.

However, as with any technology, there are some disadvantages:

- In order to attain long service-life from adhesive joints in very severe, hostile environments may often require the use of a surface pretreatment process for the substrates being joined. Particularly for marine applications this means extra time and cost.
- Compared to other fastening techniques the upper service-temperatures that adhesives can withstand are limited. Therefore, they are vulnerable in areas such as machinery spaces.

- As remarked above, the strength and toughness of adhesives in tension or shear is relatively low compared to many metals. Hence, whilst adhesives are very effective at joining thin sheets of metal, they are not typically used for joining thick metallic components, unless the bonded area is large or the adhesive is kept in compression.
- Non-destructive test methods for adhesive joints are relatively limited compared to those used with other fastening methods.
- Fairly long curing times are frequently involved and especially in the marine industry, large ovens would have to be provided.

1.5 MECHANISMS OF ADHESION

There are four general theories of adhesion which have been advanced:

Mechanical: This is the oldest, simplest theory which in essence suggests interlocking [10, 33]. It underlies the layman's instinctive procedure of roughening surfaces to improve adhesion. Any proper consideration of quantitative data shows that this cannot be the true general explanation, although there are special cases where it is significant. When adhesively bonding leather, it is important to roughen the surface to raise the fibres of the corium and for the adhesive to surround and embed them. Similarly, in the adhesion between textiles and rubber the extent of embedding of fibres of the staple yarn is the governing factor in achieving really strong bonds. In both cases penetration of adhesive into the structure is no substitute for penetration of the fibres into the adhesive. More recently with metal surfaces, evidence indicates that a very much smaller scale of roughness or porosity is important. Provided that the surface itself is strong and coherent, then a roughness with fibres or pores of micron diameter will increase strength in an adhesive bond.

Adsorption: This essentially depends upon the utilisation of the surface forces. Provided that the molecules of the adhesive and of the adherend can be brought close enough together, then the van der Waals forces will give rise to physical adsorption. This phenomenon of adsorption has been widely explored in pure physical chemistry and is quite well understood in simple cases [10, 33]. It can be shown that the forces of physical adsorption are adequate for much more than the observed strength of adhesive bonds.

It is also certain that, in many cases, there is the possibility of chemical interaction and bonding across the interface. Electron donor-acceptor bonds may be formed to add to the adhesive strength from the dispersion forces. Hydrogen bonding is a particular case but acid-base interactions may also be involved.

Diffusion: This is largely due to a school of Russian chemistry lead by Voyutskii and Vasenin and is largely accepted as valid in adhesion between two surfaces of the same polymer and for the heat sealing of thermoplastic materials [10].

The concept is quite simple, one end of the polymer molecule chain from one surface diffuses into the structure of the second surface so that that molecule forms a bridge or bond across the interface. Using theories of diffusion and polymer structure, this has been developed to provide substantial theoretical background which correlates very well with experimental results.

Electrostatic: This theory was developed by another Russian, Deryagin, particularly for pressure-sensitive tape [10]. The adhesive and the adherend are likened to the two plates of a capacitor, and the work of separation is equated to that required to separate the two charged capacitor plates. Again the theoretical basis developed correlates with experiment.

This theory is not widely accepted as of general importance, but the mechanism probably contributes to certain rather special instances of adhesion.

1.6 CHOICE OF AN ADHESIVE

From the user's point of view, the considerations involved in choosing an adhesive fall into four main groups. There is first the nature of the adherends - the actual materials to be joined - and obviously it will be necessary to find an adhesive which will bond to both.

Secondly there is the kind of bond required, whether structural or non-structural, rigid or flexible; the bond-strength needed; the service conditions - temperature, moisture, dynamic stresses, etc. - to which it will be exposed and the service life expected.

Third there are the processing requirements - preparation of surfaces, methods of applying the adhesive, positioning of joints, use if necessary of heat and pressure, equipment and time schedules involved.

Finally, but by no means least important, there is the question of cost. Here the price per kilogram or per tonne of the adhesive itself, or even the price per square metre, is only one element. Labour costs together with overheads on specialised equipment will usually be at least equally important and the time and factory space required for a given operation may be vital for fitting it into a continuous production line.

1.7 SURFACE PRETREATMENT

Quite contrary to popular belief (a belief founded upon the experience of using traditional adhesives), reliable joints can be formed on a variety of unprepared surfaces - provided that the operational conditions are not extreme.

This follows the introduction of adhesives capable of accommodating surface contamination and has given users a degree of freedom which was previously unknown. Of course, there can be no denying that the better the preparation the better the overall performance. However, providing contamination is not gross, perfectly adequate levels of performance can normally be obtained from the principal adhesives likely to be used in structural and mechanical engineering - the toughened acrylic and heat cured epoxides and the various anaerobic

compositions [9, 12, 33, 35].

However, the subject of surface preparation should be treated with respect and the knowledge that preparation may not be necessary should be considered as an inducement to explore carefully rather than as a licence to proceed without caution. In general, a level of surface preparation can be chosen to give the following properties:

- Optimum adhesion with excellent environmental resistance
- Excellent adhesion with good environmental resistance
- Moderate to good adhesion with moderate environmental resistance

Typically, and for most materials, these levels are obtained from the following processes:

- Some form of chemical pre-treatment
- Surface abrasion and degreasing
- Degreasing only, or no treatment at all

Safety precautions should be observed strictly where chemical solutions and solvents are employed for pretreatment procedures.

Methods of surface pretreatment include:

- Preliminary degreasing and cleaning
- Vapour degreasing
- Alkaline wash treatment
- Mechanical pretreatment
- Chemical and electro-chemical pretreatment

1.8 ADHESIVE PROPERTIES

The engineer will be concerned with the behaviour and performance of the selected adhesive from the time he first purchases it from the manufacturer, through the mixing, application and curing phases

to its properties in the hardened state within a joint over the intended design life. Thus the properties of interest in approximate chronological order are likely to include:

Unmixed - shelf life

Freshly mixed - viscosity
 usable life
 wetting ability
 joint open time

During cure - rate of strength developed

Hardened - strength and stress/strain
 characteristics
 fracture toughness
 temperature resistance
 moisture resistance
 creep
 fatigue

More detailed information on the previously mentioned adhesive properties can be found in [12, 33, 34, 35].

1.9 MARINE AND OFFSHORE APPLICATIONS OF ADHESIVES

It is clearly impossible to identify and to document all of the applications of adhesives in engineering assembly and fabrication. Many uses are, anyway, either of a relatively trivial nature or else do not place great demands on the adhesive material. Different engineering sectors where adhesives are already used include: Aerospace, Building, Civil engineering, Railway, Vehicle and Automotive.

Casein and later formaldehyde resin compositions have been used as adhesives and gap fillers in wooden boat construction for many years. The most significant use of resorcinol-formaldehyde resins was for the

construction of wooden minesweepers for the Royal Navy, each vessel requiring some 3 to 5 tonnes - used mostly for laminating the hull [35]. Polyester resins were then introduced to the marine industry and in 1950 the Scott-Bader Company recorded the construction of the first polyester-glass vessel [35]. Intense development led to virtually all boat-builders producing moulds or finished GRP (glass reinforced plastic) craft, with wooden boat construction assuming a minority or specialist role. Many GRP-hulled boats, both naval and civilian, now rely significantly on resins for laminating, stiffening, the fabrication of sandwich panels and for bonding attachments. Indeed the fitting out of many vessels is conducted with the large-scale use of non-structural sandwich- and insulating panels using various bonded skin and core combinations. Epoxides were introduced into the industry for a range of bonding and gap-filling applications, one of the latter being for accommodating the tolerances and consolidating the bearings in large mooring buoys for oil tankers.

The most significant marine use of resins is actually in the form of paint corrosion protection systems for hulls. These include polyurethane and epoxide systems, the latter giving good alkali and solvent resistance in addition to providing superior adhesion to most substrates. Such systems take the form of zinc-rich epoxy and epoxy coal-tar combination hull paints. Epoxy powder coatings are also commonly used for the protection of steel pipelines, both on land and offshore.

A number of interesting structural applications of adhesives lie with the development of bonded stiffened plate structures for hulls [1, 6, 8, 14], sandwich construction [7, 38], the development of lighter-weight composite superstructures (by bonding fibre-reinforced plastics to steel portals and frames) [18, 19] and with the repair of aluminium superstructures [16]. The latter application arose because fatigue cracking developed in Type 21 Frigates, which was difficult to stop from propagating further by such means as drilling out the crack tips [35]. Instead steel plates, up to 6 mm thick, were bonded over the cracks using a two-part cold-curing epoxide; carbon fibre laminate material was later used in place of the steel. The technique provides a rapid repair method with sufficient strength to contain cracking and minimise water leakage until such time as major replating can be carried out. The possibility of

developing the procedure to provide sufficient durability and integrity as a permanent solution is being investigated by the Admiralty.

Nearly a decade has passed since a considerable amount of research and development effort has been expended at Glasgow Marine Technology Centre (especially in the naval architecture and mechanical engineering sector) within the field of the structural applications mentioned at the beginning of the paragraph. A final year student project [1] formed the first step in investigating a number of possible adhesives and their application to bonding short sections of beam elements, typical of the warship structures, using I beams instead of Tee sections. Due to the successful results of that work, a two-year program of research began in order to survey available adhesives, develop methods of fabrication and determine the material and structural properties of bonded stiffener to plate connections in lightweight ship grillages [8]. Subsequent developments followed [6] which focused on further topics such as, temperature and creep effects, fatigue strength, durability in the marine environment, first thoughts on steel sandwich structures and bonding steel to other materials. It is worth mentioning that this paper highlighted the possibility that adhesives can offer to their use in subwater structures and environments in the next century. Some interesting results of experiments performed within the area of the previously mentioned topics were presented in [14]. Also, a number of reports described the work and experiments done to test the practicality and feasibility of the idea of sandwich construction in the marine industry, the final one being [7]. The research is still continuing and draws much interest to representatives of the engineering community.

Many offshore steel structures are subjected to major damage due to accidents and collisions, or through stress fatigue failure of welded joints. As well as damage repair there are instances where it is necessary to modify or to strengthen existing structures. Conventional modification or repair techniques, often involving underwater welding, are extremely expensive and the development of the technique of underwater bonding of steel substrates represents a major technical advance in recent years. Adhesive-assisted repair methods for submerged steel structures have been developed by the Admiralty in conjunction with the Department of

Energy, together with industry [35]. This has required the formulation of hydrophobic filled cold-curing epoxides, as well as a sacrificial pretreatment technique; an adhesive-compatible hydrophobic film is deposited on the surface to be bonded which is then absorbed, or displaced, by the adhesive and enables adhesion to be gained underwater.

Another major offshore application, albeit still potential, lies with the stiff lightweight adoption of aluminium and/or polymer composite topside structures in order to reduce weight. Structural aluminium sections may be created by bonding together individual extrusions, and a most convincing demonstration of the potential has been developed by British Alcan [16].

CHAPTER 2: SANDWICH CONSTRUCTION

'Then the officers of the children of Israel came and cried unto Pharaoh, saying, "Wherefore dealest thou thus with thy servants? There is no straw given unto thy servants, and they say to us 'Make brick': and, behold, thy servants are beaten; but the fault is in thine own people."

But he said "Ye are idle, ye are idle: therefore ye say 'Let us go and do sacrifice to the Lord'. Go therefore now, and work; for there shall be no straw given to you, yet shall ye deliver the tale of bricks."

Exodus, Chapter I.

Ever since Pharaoh had labour troubles about putting straw into bricks there have been reinforced materials and structures of one kind or another although they have only come into prominence as strong materials and structures quite recently. It seems almost certain that the purpose of putting chopped straw into the Egyptian bricks was just the same as that of the Inca and Maya in putting plant fibres into their pottery, that is to prevent cracking when the wet clay was dried rapidly in the sun [55].

2.1 DEFINITIONS

Sandwich construction: Defined as a three-layer type of construction, consisting of two sheets of high-strength material between which a thicker layer of low average strength and density is sandwiched. The two outer sheets are called *the faces* and the intermediate layer is *the core* of the sandwich. The primary function of the face sheets is to provide the required bending and in-plane shear stiffness and to carry the axial, bending and in-plane shear loading. That of a core is to stabilise the facings and carry most of the shear loads through the thickness.

Structural sandwich: Structural sandwich consisting of three elements, as

shown in Fig. 2.1:

- 1) a pair of thin, strong facings
- 2) a thick, lightweight core to separate the facings and carry loads from one facing to the other and
- 3) an attachment which is capable of transmitting shear and axial loads to and from the core.

Corrugated-core sandwich construction: Consists of a corrugated metal sheet fastened at its crests and troughs to two ordinary metal sheets, as shown in Fig. 2.2.

2.2 INTRODUCTION

Although there were some earlier applications, sandwich construction aroused great interest only after the Second World War, when the speed of aircraft became so high that laminar-flow sections were considered to be an extremely desirable design feature and when it was disclosed that the famous Mosquito airplane was largely constructed in this manner.

More specifically, although the employment of a sandwich design to produce lightweight or special purpose load-carrying members is thought to have originated as early as 1820, routine commercial use of the idea did not occur until about 110 years later [31]. What started this sudden acceptance was the successful commercial production of structural adhesives, starting in both England and the United States in the 1930's. This early production resulted from the development of the rubber-phenolics and the vinyl-phenolics. Such materials as 'cycleweld', 'plycosite' and 'Redux' adhered well to both wood and metals, possessed rather high and predictable strength and began a revolution in bonding technology. Many further developments followed in only a few years. They included improved cleaning methods for metal skins; low weight, high strength/stiffness honeycomb core materials; 'B' staged tape adhesives;

(continued on page 24)

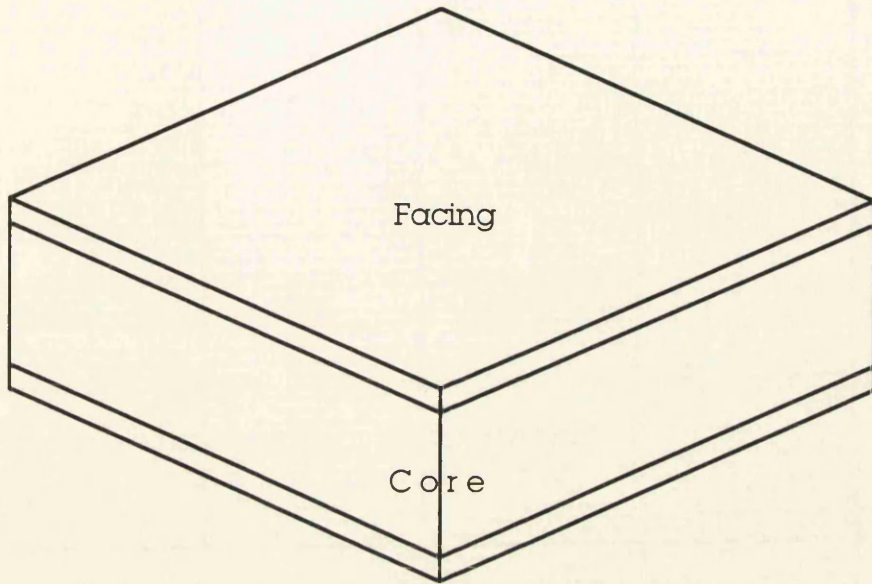


Fig. 2.1 Structural sandwich

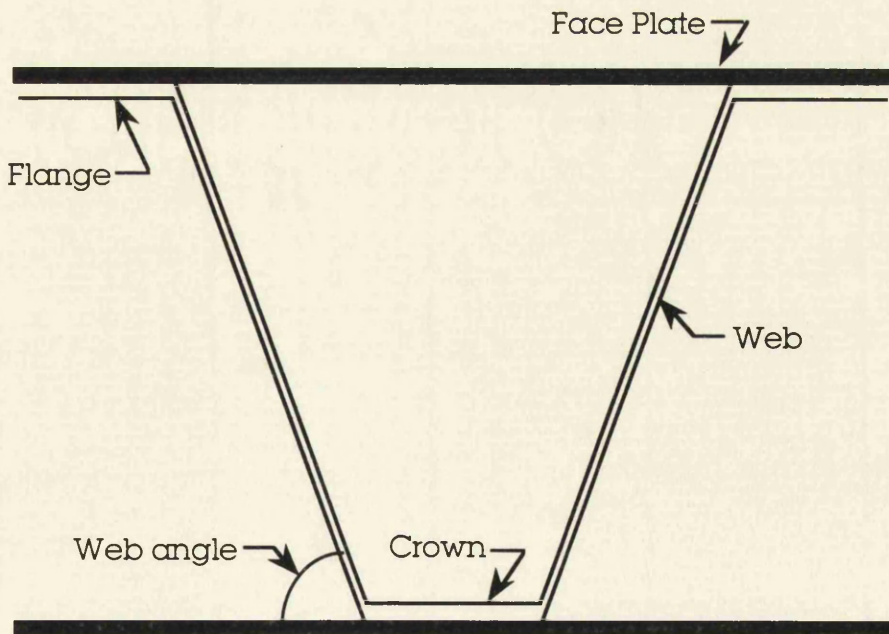


Fig. 2.2 Corrugated core sandwich construction

glass fabrics and collimated tapes preimpregnated with accurately measured amounts of 'B' staged resins; high strength resins; tough, high peel adhesives and lower cure temperature and pressures; as well as the discovery of the resistance of sandwich to sonic fatigue [4, 5, 18, 31].

Structural sandwich construction is one of the first forms of composite structures to have attained broad acceptance and usage. Virtually all commercial airliners and helicopters and nearly all military air and space vehicles make extensive usage of sandwich construction.

In addition to air and space vehicles, the system is commonly used in the manufacture of cargo containers, movable shelters and airfield surfacing, navy ship interiors, small boats and yachts, die models and production parts in the automobile and recreational vehicle industry, snow skis, display cases, residential construction materials, interior partitions, doors, cabinets and a great many other everyday items.

Although various publications dealing with theoretical and experimental investigations of the strength and the stability of sandwich beams, columns and plates had already appeared during the war years and many other useful papers were published between 1945 and 1950, practical applications of sandwich construction lagged behind except for secondary structural elements. Some of the reasons for this lag seem to be that better core materials, better methods of connecting cores to faces, more reliable procedures of inspection and repair of sandwich structures, had still to be developed.

The correct design of the details of sandwich construction is at least as important as the analysis of deflections, stresses and buckling loads. These details include nature of the edge members, splices and joints in the cores and faces, stiffeners and inserts to distribute concentrated loads, type of adhesive, method of fabrication and so forth.

Civil and aircraft industries have applied the idea of sandwich construction for many decades. Nearly eleven years ago [1], the concept that modern structural adhesives might have potential as the primary joining process between similar, dissimilar and nonmetallic materials in major marine structures and could therefore be ideally suited for use in sandwich construction was introduced by a research group at the University of Glasgow [6, 7, 8, 14, 38].

Since then, a substantial body of research experience has been gained [7] in the field of bonded design of steel structures within the framework of the MTD Marine Technology Programme at the University of Glasgow. This research has shown that adhesive bonding is a potential substitute for fillet welding in plated grillage structures to be used in the marine environment, as well as a serious opponent to laser welding, despite the fact that the inherent properties of such adhesives are those associated with most polymers (low strength, low modulus, low toughness and high temperature sensitivity) [8, 14].

Also, Smith et al. [7] has demonstrated that a unidirectional corrugated core provides a simple design basis for sandwich panel structures, affording plenty of scope for design variation. With the increasing need to find practical, stiff but lightweight structures for the major structural panels of multihulled vessels, it has been proposed to research the feasibility of developing practical bonded sandwich designs using this corrugated core concept.

Sandwich panels for aircraft structures almost invariably employ metal faces with metal honeycomb or corrugated cores. The honeycomb is formed from strips of thin aluminium alloy or steel foil deformed and joined together, as shown in Fig. 2.3. The corrugated core is a fluted metal sheet attached alternately to the upper and lower faces, as shown in Fig. 2.4.

Some variations of the corrugated core are shown in Fig. 2.5. The simple parallel-strip arrangement of Fig. 2.5a is sometimes stiffened by the addition of expanded plastics to fill the voids. The tubular core of Fig. 2.5b and the double truss-core of Fig. 2.5c are rather rare. The dimpled core shown in Fig. 2.5d is similar in appearance to the pulpboard commonly used for packing eggs. Unlike the corrugated core it has similar properties in the two principal directions, but it retains the advantages of easy fabrication and good adhesion to the faces.

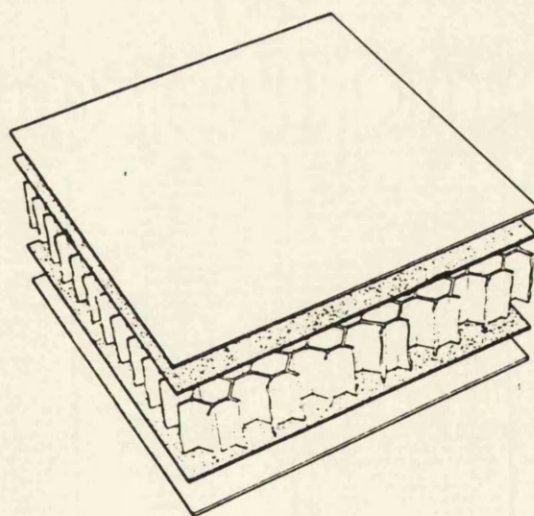
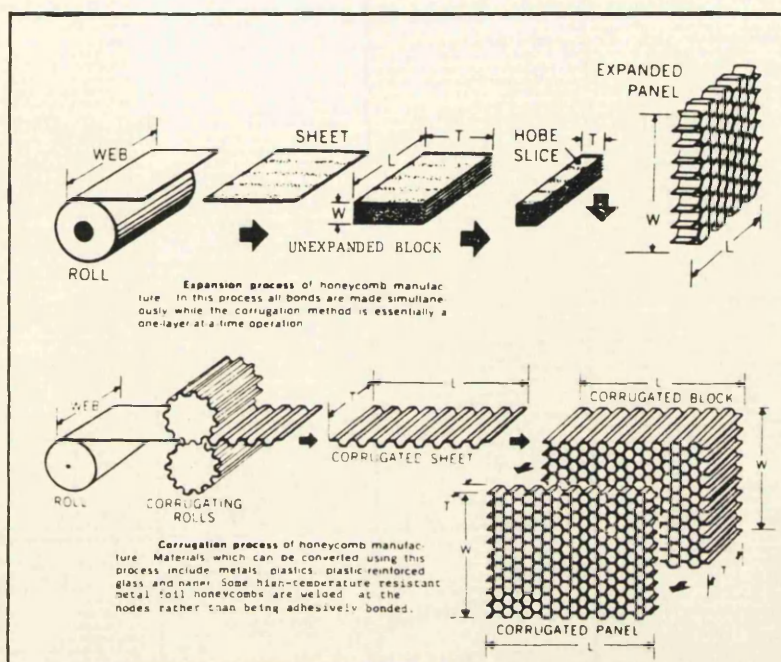


Fig. 2.3 Sandwich panel with honeycomb core [24]

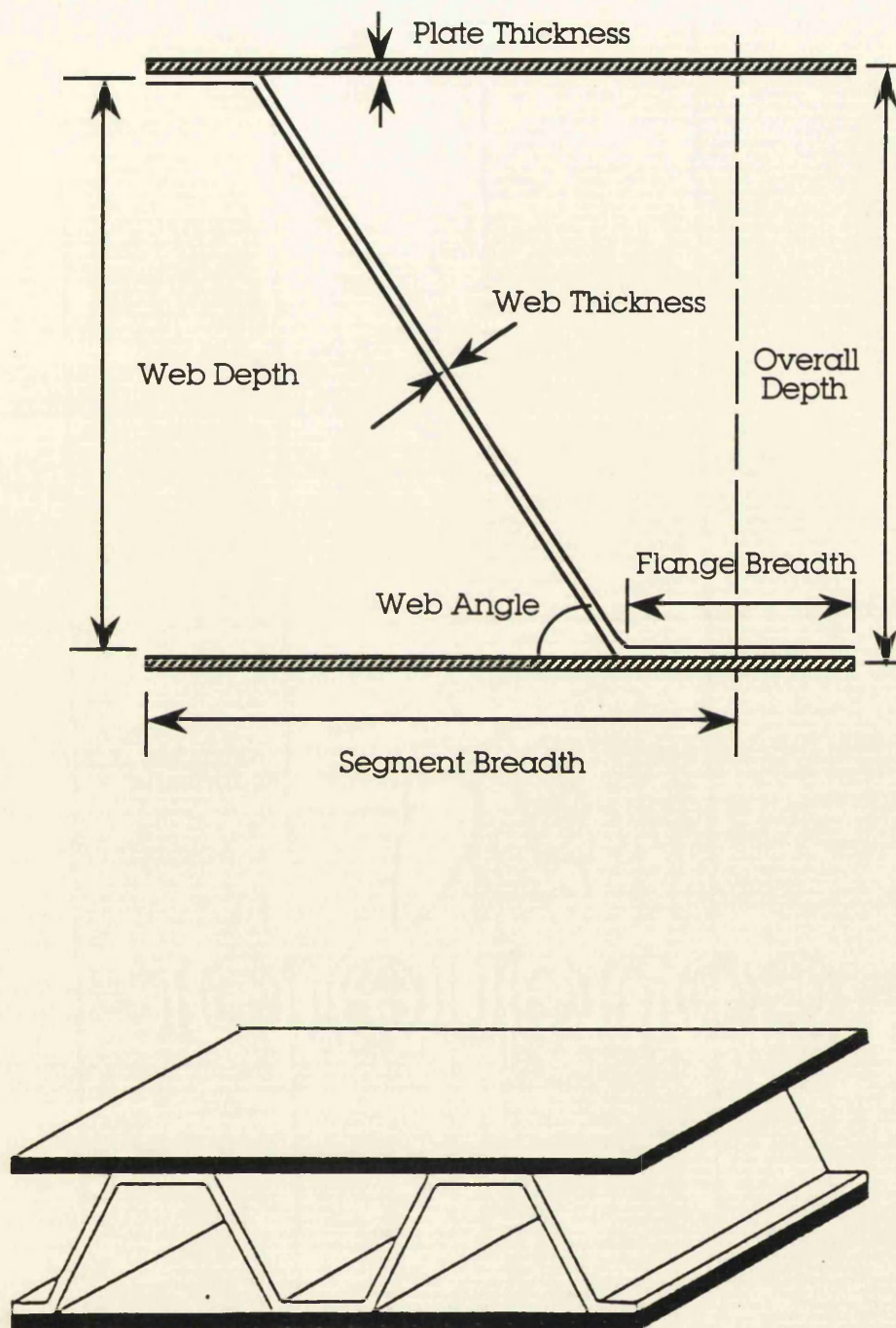


Fig. 2.4 Sandwich panel with corrugated core [4] and its elements

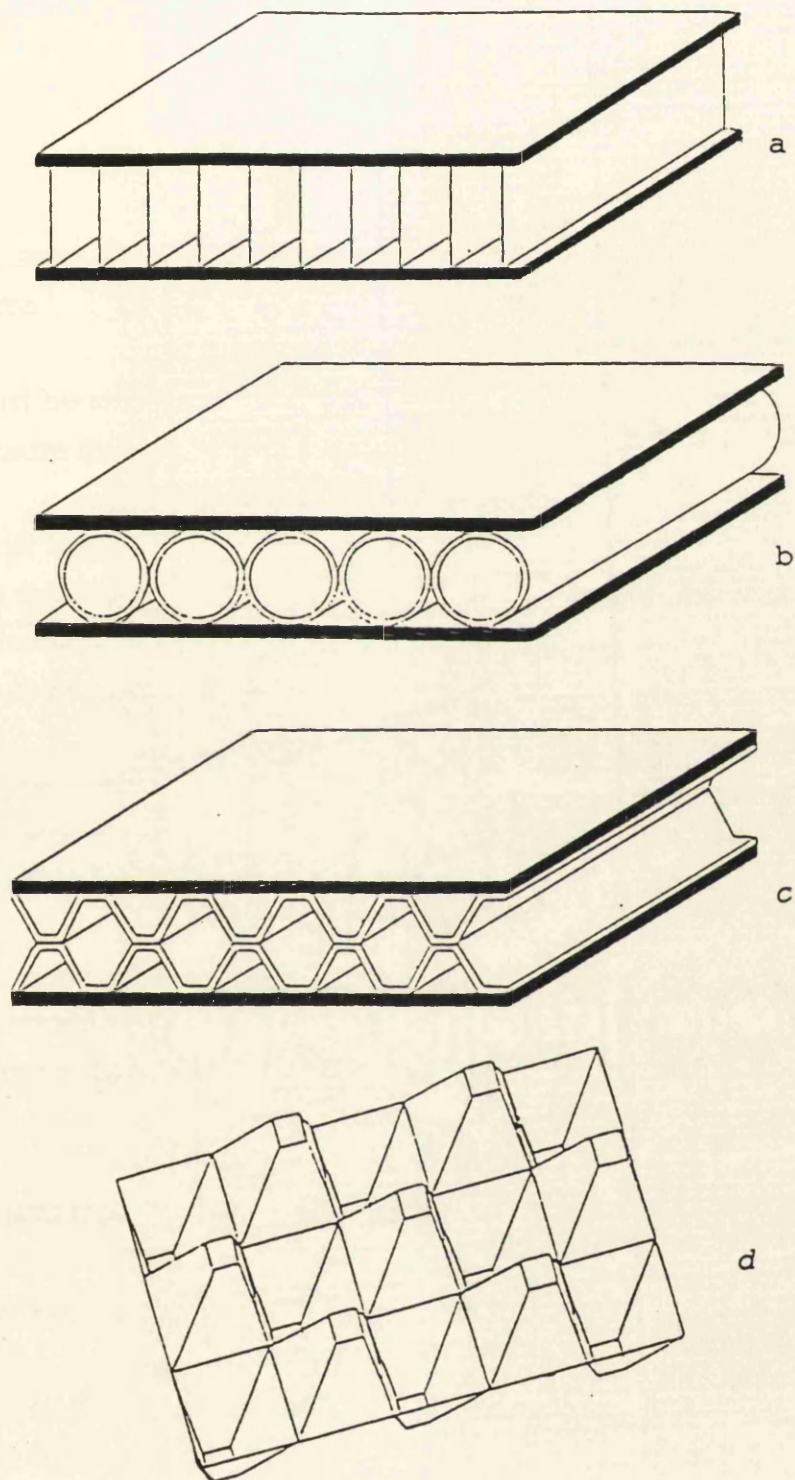


Fig. 2.5 Variations of the corrugated core sandwich construction [4]

2.3 CORE MATERIALS

The primary function of a core in sandwich structures is that of stabilising the facings and carrying most of the shear loads through the thickness.

More specifically, the core should succeed in satisfying the following vital functions:

- It must be stiff enough in the direction perpendicular to the faces to ensure that they remain the correct distance apart.
- It must be stiff enough in shear to ensure that when the panel is bent the faces do not slide over each other. If this last condition is not fulfilled the faces merely behave as two independent beams or panels and the sandwich effect is lost.
- It must also be stiff enough to keep the faces nearly flat; otherwise it is possible for a face to buckle locally (wrinkle) under the influence of compressive stress in its own plane.
- The core must satisfy all these requirements and it is also important that the adhesive should not be sufficiently flexible to permit substantial relative movements of the faces and the core.

2.4 ADVANTAGES - LIMITATIONS OF SANDWICH CONSTRUCTION

The main advantages of sandwich construction are:

- In certain types of structures weight savings up to 30% over conventional structures can be achieved. This is particularly advantageous in the case of SWATH ships.
- The good surface finish and the resistance to local deformations.

- Outstanding rigidity.
- Good fatigue properties, also with regard to acoustical fatigue.
- Good thermal and acoustical insulation.
- Increased interior space and ease of equipment installation.
- Ease of mass production.

Serious objections to sandwich construction include:

- The risk of local separation (and subsequent propagation of debonding) between core and skins caused by initial bonding imperfections and load conditions causing tension across bonded interfaces.
- Difficulty of inspection and repair.
- The risk of absorption and migration of water within the sandwich, where water environment is involved.

2.5 FIRE RESISTANCE

2.5.1 GENERAL

Fire safety must be regarded as a major priority at the earliest stage as it can have a major impact on the design of a structure and particularly its form. Nevertheless, it should not stifle aesthetic or functional freedom: 'fire engineering' techniques are now available which permit a more rational treatment of fire development and fire protection in structures.

The strength of all materials reduces as their temperature increases. Steel and structural adhesives are no exception. It is essential that the structure should not weaken in fire to the extent that collapse occurs prematurely, while the occupants are seeking to make their way to safety.

For this reason it is necessary to provide a minimum degree of 'fire resistance' to the structure.

There are two basic ways to provide fire resistance. First, to design the structure using the ordinary temperature properties of the material and then to insulate the members so that the temperature of the structure remains sufficiently low, or secondly, to take into account the high temperature properties of the material, in which case no insulation may be necessary.

The first method, the 'fire protection' approach, is the most common at present but is a prescriptive method. Recent research [42] has shown that the failure temperature of a member depends upon load, temperature gradient, dimensions and stress distribution. By quantifying these effects a more rational 'fire resistance' approach is being developed which is the basis of the recently published BS 5950 Part 8 of [59].

2.5.2 MARINE FIRE RESISTANCE

Fires in a ship, submarine or offshore platform may be caused by electrical faults, by spillage and ignition of hydraulic or fuel oil, by gas ignition, by welding or flame-cutting operations during construction or repair and in warships by weapon effects. In addition to normal manned fire-extinguishing procedures, automatic countermeasures including water sprinkling and/or halon gas drenching are likely to be provided in all fire-susceptible spaces and are of course an important factor in assessing the consequences of a fire.

Requirements of a structure under fire conditions are:

- prevention of spread of flames from one compartment to another
- limitation of temperature and hence damage in adjoining compartments
- preservation of strength and stiffness for prescribed periods of time until a fire is extinguished
- minimisation of smoke and toxic fumes

Some of the fire-resistance characteristics of alternative structural materials are summarised in Table 2.1.

Steel structure, while in other respects effective under fire conditions, has a high thermal conductivity which undermines its ability to meet the first two requirements mentioned above. Scope exists for structural combination of GFRP panels, offering effective fire containment by virtue of low conductivity, with steel framing which provides good strength and stiffness retention at high temperatures.

Sandwich panels offer particularly good thermal insulation but care must be taken in the choice of core, face and adhesive materials. Face laminates are likely to be thin, exposing the core-face bond and core material to high temperature under fire conditions. Decomposition of foam cores may involve expansive vapour emission, combined with failure of the core-face bond, and mechanical breakdown of the sandwich, further exposing the core material directly to flames. PVC foam, which is widely used in marine sandwich construction, decomposes at temperatures over 200°C with emission of HCl gas which is both toxic and highly corrosive. Other high performance, high-cost fire-resistant core materials include blown polyetherimide (PEI) and polyethersulphone (PES) foams. In contrast, bonded steel sandwich structures can offer satisfactory fire containment by means of low conductivity since steel can inherently provide for good strength and stiffness retention at high temperatures. However, care should be taken in the choice of structural adhesive since its properties tend to deteriorate with increasing temperature [7]. Therefore, if some methods of protection are applied to the steel part of the sandwich panel, the whole structure including the adhesive could resist a fire event more efficiently.

2.5.3 METHODS OF PROTECTION

Basic information on methods of protection is summarised in Appendix A.

(continued on page 34)

TABLE 2.1
Fire-related properties of metallic and FRP materials [18]

Material	Melting temp. (°C)	Thermal conductivity (W/m°C)	Heat distortion temp. (°C) (BS2782)	Self-ignition temp. (°C)	Flash-ignition temp. (°C)	Oxygen index (%) (ASTM D2863)	Smoke density (DM) (ASTM E662)
Aluminium	660	240	-	-	-	-	-
Steel	1430	50	-	-	-	-	-
E-Glass	840	1.0	-	-	-	-	-
Polyester resin	-	0.2	70	-	-	20-30	-
Phenolic resin	-	0.2	120	-	-	35-60	-
GRP (polyester based)	-	0.4	120	480	370	25-35	750
GRP (phenolic based)	-	0.4	200	570	530	45-80	75

i. Spray-applied protection

Sprays are the cheapest method with costs depending on the fire rating required and the size of the job. As implied, spray protection is applied around the exposed perimeter of the member and therefore the relevant section factors are for profile protection [40, 42, 44]. Application is fast and it is easy to protect complex shapes or connections. However, they are applied wet, which can create problems in winter conditions, they can be messy and the appearance is often poor. For this reason they are generally used in hidden areas.

ii. Board protection

Boards tend to be more expensive because of the higher labour content in fixing. The price depends on the rating required and the surface finish chosen but tends to be less sensitive to job size. Board systems form a box around the section and therefore have a reduced heated perimeter in comparison to spray systems. They are dry fixed by gluing, stapling or screwing, so there is less interference with other trades on site and the box appearance is often more suitable for frame elements.

iii. Intumescent coatings

Intumescent coatings achieve insulation in a totally different way: the insulating layer is formed only by the action of heat when the fire breaks out.

The coating is applied as a thin layer, perhaps as little as 1 mm, but it contains a compound in its formulation which releases a gas when heat is applied. This gas inflates the coating into a thick carbonaceous foam, which provides heat insulation to the material underneath. The coatings are available in a range of colours and may be used for aesthetic reasons on visible steelwork.

Two types of intumescent coating are currently available [42]. The first, which is water resistant, has a maximum rating of 2 hours but is expensive. The second type has maximum ratings up to 1 and 1/2 hours but is not so resistant to moisture and so is not recommended for wet applications.

iv. Concrete encasement

In comparison with these lightweight materials, protection by in situ concrete is a 'heavier' protection.

However, concrete is often perceived as a 'traditional' fire-protection material. Of course, this could not form a marine solution due to the weight factor involved.

2.6 DESIGNING A SANDWICH

The usual objective of a sandwich design is to save weight or increase stiffness or to use less of an expensive skin material, or both. Sometimes other objectives, such as reducing tooling or other costs, achieving aerodynamic smoothness, reducing reflected noise or increasing durability under exposure to acoustic energy, are also involved. The designer's problems resolve to relatively few, such as getting the loads in, getting the loads out and attaching small or large load-carrying members, under constraints of deflection, contour, weight and cost.

To achieve such objectives, sandwich structures should be designed to meet the basic structural criteria listed below, where these criteria pertain to the type of loading under consideration:

- The facings should be thick enough to withstand the tensile, compressive and shear stresses induced by the design load.
- The core should have sufficient strength to withstand the shear stresses induced by the design loads.
- The core should be thick enough and have sufficient shear modulus to prevent overall buckling of the sandwich under load.
- Compressive modulus of the core and the compressive strength of the facings should be sufficient to prevent wrinkling of the faces under the design load.
- The core should have sufficient compressive strength to resist crushing by design loads acting normal to the panel facings or by compressive stresses induced through flexure.

A typical design approach may include consideration of the following factors [24]:

- **Understand the fabrication sequence and methods.**
The cost of a sandwich structure is fundamentally fixed at the design stage and considerable cost variations result from other solutions to the design problem.
- **Use the right core.**
Several **densities** (for sandwich structures consisting of more than one materials) or **depths** (as in the case of this project) of core can be used in a single panel, each appropriate to the load carried in the area and adhesively bonded to its neighbour.
- **Do not hesitate to use several joining methods in the same part.**
Fittings to be included in a bonded sandwich may be produced from weldments, forgings or riveted assemblies, or may themselves be bonded assemblies. Available adhesives permit secondary bonding to be performed at temperatures from 16°C up to 177°C without degrading the integrity of the bonded sub-assemblies.

2.7 DESIGN STEPS

The following design steps have been outlined by Marshall [24] and may form a general guide for the construction of any structural sandwich.

- **Define loads.**
- **Define beam type.**
Some care in using the fixed end type of support is needed, as in actual practice total fixity is not realised and the resulting deflection is greater than that calculated.

- **Determine deflection limitations.**

For most applications, the allowable deflection of the structure is usually limited to $L/360$ according to recommendations by Marshall [24]. In some cases, greater deflections may be used.

- **Select skin material.**

Skin considerations include the weight target, possible abuse and local loads, corrosion or decorative constraints and costs. Select standard thicknesses and make the initial calculation as outlined below. The facing thickness directly affects both the skin stress and the deflection.

- **Calculate first approximation.**

After the first sandwich thickness is determined, another selection of facing thickness and Young's modulus may be made to arrive at more desirable or practical values of sandwich thickness. Most sandwich structures in ordinary usage are in the thickness range of 1.5-150 mm.

- **Select skin thickness.**

Keep in mind that materials such as fiberglass cloth and aluminium are available in specific, standard thicknesses. After the skin thickness for deflection is selected, it should be checked for stress. The formula for facing deflection is used and a factor of safety determined.

- **Select core.**

Calculate the core shear stress. Make a preliminary selection of the materials. Note that the core strength is not the same in the longitudinal and transverse directions. Refine the selection, including considerations of material compatibility, cell sizes and types. Determine the corrections needed to account for the effects of thickness on strength. Check the factor of safety using the calculated stress and the corrected allowable stress. Other considerations include crushing and compression strengths,

modulus in shear, weight and costs.

- **Check deflection.**

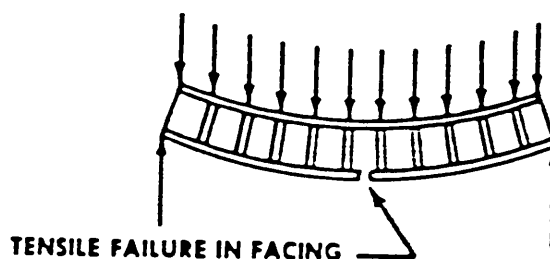
For many applications, the calculation of the expected deflection may omit the shear deflection portion. With a very small deflection limitation, with a very thick sandwich or with a very short span, the shear component should be calculated and the core selection may be influenced by the shear modulus needed.

2.8 MODES OF FAILURE

Typical modes of failure in sandwich structures which must be resisted include:

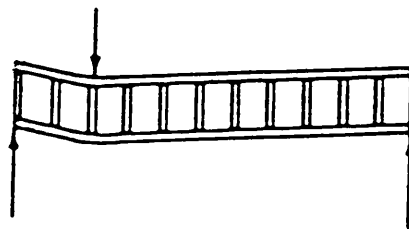
FACING FAILURE

Initial failure may occur in either compression or tension face. It is caused by insufficient panel thickness, facing thickness or facing strength.



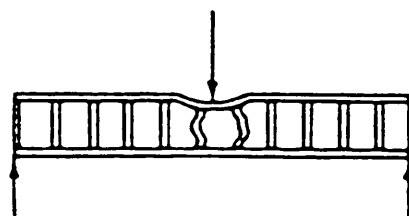
TRANSVERSE SHEAR FAILURE

This is caused by insufficient core shear strength or panel thickness.



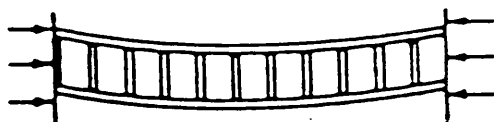
LOCAL CRUSHING OF CORE

This is caused by low core compression strength.



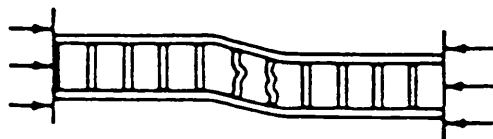
GENERAL BUCKLING

This is caused by insufficient panel thickness or insufficient core shear rigidity.



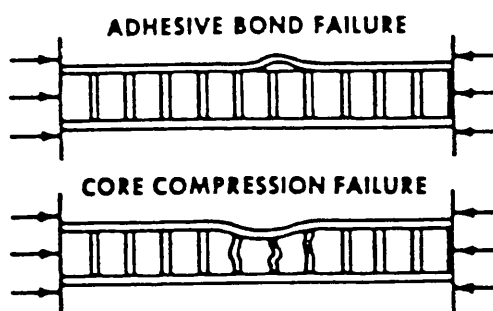
SHEAR CRIMPING

This sometimes occurs following, and as a consequence of, general buckling. It is caused by low core shear modulus or low adhesive shear strength.



FACE WRINKLING

Facing may buckle as a 'plate on elastic foundation'. It may buckle inward or outward depending on relative strengths of core in compression and adhesive in tension.



During some earlier work undertaken by Glasgow Marine Technology Centre team [7], the failure mechanisms (for the three point bending tests) of the corrugated core sandwich panels with corrugations running along the y axis, initiated mainly due to face post yield and web buckling [3 models out of 4], rather than bond failure [1 model out of 4]. The failure mechanisms (for the axial compression tests) developed because of face plate buckling [2 models out of 3] rather than complete bond failure [1 model out of 3]. With the corrugations running along the x axis, it can be expected that the models of the present project would be stronger and failure would occur due to any reason but adhesive failure.

CHAPTER 3:
THEORY OF CORRUGATED CORE
SANDWICH CONSTRUCTION

A corrugated core sandwich plate differs from sandwich plates with isotropic faces in that the core has orthotropic flexural (bending) and transverse shear properties. The transverse shear stiffness in planes parallel to the axis of the corrugations is usually many times the stiffness in planes perpendicular to the axis of the corrugations. The flexural properties are such that the corrugated core can to some extent resist bending moments applied in planes parallel to the axis of the corrugations, whereas its resistance to bending moments applied in planes perpendicular to the axis of the corrugations is much reduced.

3.1 DEFINITIONS

Creep: Continuous increase in deformation under constant or decreasing stress. The term is ordinarily used with reference to the behaviour of metals under tension at elevated temperatures but is particularly important in relation to the performance of adhesives under constantly high loading.

Isotropic: Having the same properties in all directions. In discussions pertaining to strengths of materials, isotropic usually means having the same strength and elastic properties (modulus of elasticity, modulus of rigidity and Poisson's ratio) in all directions.

Orthotropic: The material properties differ only in three (or two) orthogonal directions and are uniform within each direction. In other words, the material has three or two planes of symmetry with respect to its elastic properties.

3.2 INTRODUCTION

Because the face sheets or core (or both) may have orthotropic stretching properties, the sandwich plate will in general be orthotropic in its flexural properties. As a result, ordinary plate theory, which is based on the assumptions that the plate is isotropic and that deflections due to shear may be neglected, cannot be used to determine the stresses, deflections or buckling loads of sandwich plates.

A general small-deflection theory for flat orthotropic plates [31] has therefore been developed in which deflections due to shear are taken into account. The theory is applicable to any type of orthotropic or isotropic sandwich that behaves essentially as a plate, provided certain physical constants are known. These physical constants (two flexural stiffnesses, two shear stiffnesses, a twisting stiffness and two Poisson ratios defined in terms of curvatures) serve to describe the plate deformations associated with simple loading conditions and may be regarded as fundamental properties of the plate. For simpler types of sandwich construction the physical constants can be evaluated theoretically from the geometry and physical properties of the materials used. For more complicated types of construction, these constants can be evaluated by means of simple tests on samples of the assembled sandwich, as described in [31].

As is the case with ordinary plate theory, orthotropic plate theory consists of two parts, each complete in itself. These parts are a set of six differential equations, three of which express the equilibrium of an infinitesimal plate element and three of which relate the curvatures and twist of the element to the forces and moments acting upon it, and an expression for the total potential energy of the system comprising the plate and the forces acting upon it. However, it has been shown [31] how these simultaneous equations can be reduced to a single equation of sixth order involving any one of the variables alone.

The consideration of deflections due to shear makes necessary the specification of one more boundary condition than in ordinary plate theory. Because of some arbitrariness in the choice of the additional boundary condition, two types of simple support and two types of

clamped edges are possible. Furthermore, three boundary conditions can be specified for a free edge, in contrast to ordinary plate theory.

3.3 THEORY

3.3.1 PHYSICAL CONSTANTS

The physical properties of a plate are described by means of seven constants:

- D_x and D_y , the flexural stiffnesses
- D_{xy} , the torsional stiffness
- D_{Qx} and D_{Qy} , the transverse shear stiffnesses
- μ_x and μ_y , the Poisson ratios

Definitions of these constants are obtained by considering the distortions of the differential element of Fig. 3.1 under simple loading conditions.

Let all forces and moments acting on the element be zero, except for the moments M_x acting on two opposite faces. The effect of M_x is to produce a primary curvature $\partial^2 w / \partial x^2$ in the middle surface of the element and also a secondary curvature $\partial^2 w / \partial y^2$ which is a poisson effect. Then D_x is defined as the negative of the ratio of moment to primary curvature or:

$$D_x = -\frac{M_x}{\frac{\partial^2 w}{\partial x^2}} \quad (1)$$

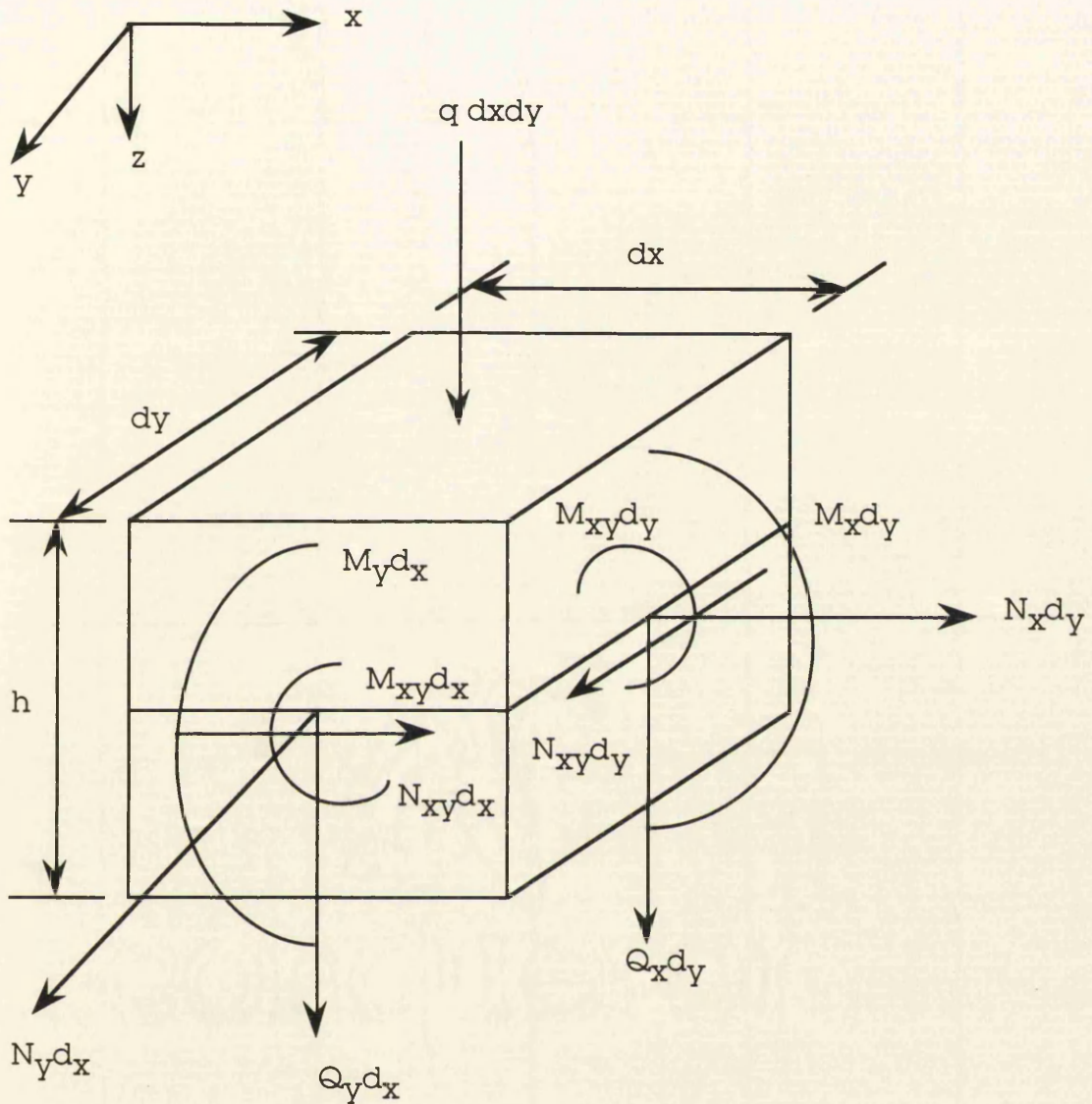


Fig. 3.1 Forces and moments acting on the differential element $dx \, dy$ [28]

when only M_x is acting, and μ_x is defined as the negative of the ratio of Poisson curvature to primary curvature or:

$$\mu_x = -\frac{\frac{\partial^2 w}{\partial y^2}}{\frac{\partial^2 w}{\partial x^2}} \quad (2)$$

when only M_x is acting. No other distortions are assumed but $\partial^2 w / \partial x^2$ and $\partial^2 w / \partial y^2$ when M_x acts.

The minus signs are introduced in order to make D_x and μ_x essentially positive quantities.

Similarly:

$$D_y = -\frac{M_y}{\frac{\partial^2 w}{\partial y^2}} \quad (3) \quad m_y = -\frac{\frac{\partial^2 w}{\partial x^2}}{\frac{\partial^2 w}{\partial y^2}} \quad (4)$$

when only M_y is acting.

If now, all of the forces and moments are equal to zero except M_{xy} acting on all four faces, the only distortion produced is a twist $\partial^2 w / \partial x \partial y$, and D_{xy} is defined as the ratio of torsional moment to twist or:

$$D_{xy} = \frac{M_{xy}}{\frac{\partial^2 w}{\partial x \partial y}} \quad (5)$$

when only M_{xy} is acting.

The transverse shear stiffness D_{Q_x} is defined by letting only the shear Q_x act on opposite faces of the element (except for an infinitesimal moment of magnitude $Q_x dx dy$ required for equilibrium). The distortion is assumed for the moment to be essentially a sliding of one face of the element with respect to the opposite face, both faces remaining plane. As a result of this sliding, the two faces parallel to the xz plane are distorted from their rectangular shape into parallelograms by an amount γ_x , which is the shear angle measured in the xz plane. The shear stiffness D_{Q_x} is defined as the ratio of shear to shear angle or:

$$D_{Q_x} = \frac{Q_x}{\gamma_x} \quad (6)$$

when only Q_x is acting. If the sides of the element are kept parallel to the z axis, the slope of the middle surface is:

$$\frac{\partial w}{\partial x} = \gamma_x = \frac{Q_x}{D_{Q_x}} \quad (7)$$

when only Q_x is acting.

In a similar manner, the shear stiffness D_{Q_y} is defined as the ratio of the shear on the faces parallel to the xz plane to the shear angle measured in the yz plane when only Q_y is acting or:

$$D_{Q_y} = \frac{Q_y}{\gamma_y} \quad (8)$$

when only Q_y is acting. If all sides of the element are kept parallel to the z axis, the slope produced is:

$$\frac{\partial w}{\partial y} = \gamma_y = \frac{Q_y}{D_{Q_y}} \quad (9)$$

when only Q_y is acting.

The constants just discussed serve to define the orthotropic sandwich plate; they can be evaluated theoretically if the properties of the component parts of the sandwich are known and if the plate is of simple construction. In any event, the constants can be determined experimentally by means of bending tests and torsional tests on beams and panels of the same sandwich construction as the plate.

Although seven physical constants have been discussed, they

need not all be independently determined for if any three of the four constants D_x , D_y , μ_x and μ_y are known the fourth can be evaluated from the relationship:

$$\mu_x D_y = \mu_y D_x \quad (10)$$

This relationship, which is based on a generalisation of Maxwell's reciprocal law, is derived by Libove and Batdorf [31].

3.3.2 THEORETICAL RESULTS

Libove and Hubka [28] derive the formulae for the elastic constants for the general corrugated core sandwich plate. Generally, the subscript c denotes the core and the subscript f denotes the face. In this section only symmetrical sandwiches are considered, i.e. both lower and upper faces are of the same thickness.

3.3.2.1 Bending stiffness D

$$D_x = EI_x \quad (11)$$

$$D_y = \frac{EI_y}{1 - \mu_f^2 \left(1 - \frac{EI_y}{EI_x} \right)} \quad (12)$$

where:

$$EI_x = E_c I_c + (1/2) E_f t_f h^2$$

$$EI_y = (1/2) E_f t_f h^2$$

μ_f : Poisson's ratio of face sheet material

E_f : modulus of elasticity of face sheet material [N/mm²]

E_c : modulus of elasticity of core material [N/mm²]

I_c : moment of inertia per unit width of corrugation cross-sectional area about middle plane [mm³]

t_f : thickness of face plate [mm]

h : distance between middle surfaces of face sheets [mm]

For practical sandwiches the moment of inertia I_c contributed by the core is often small compared with the moment of inertia which the faces contribute to cross sections perpendicular to the corrugations. In such cases (E_y/E_x) is very nearly unity and the following approximation to equation (12) may be made:

$$D_y \approx E I_y \quad (13)$$

This approximation implies a neglect of the restraining effect of the corrugation on the Poisson expansion or contraction of the face sheets. The error in the approximate value has been seen [28] to be small over a large part of the range of configurations considered by Libove and Hubka and in extreme cases no more than 6%.

3.3.2.2 Poisson's ratios μ associated with bending

$$\mu_x = \mu_f \quad (14)$$

$$\mu_y = \mu_x \frac{D_y}{D_x} \quad (15)$$

where:

μ_f : Poisson's ratio of face sheet material

3.3.2.3 Torsional stiffness D_{xy}

$$D_{xy} = 2GJ \quad (16)$$

where:

$$GJ = (1/2)G_f t_f h^2$$

G_f : shear modulus of elasticity of face sheet material [N/mm²]

t_f : thickness of face plate [mm]

h : distance between middle surfaces of face sheets [mm]

The stiffness D_{xy} is independent of the properties of the core since symmetry requires that the shear flow in the corrugated core sheet be zero.

3.3.2.4 Transverse shear stiffness D_{Qy} in planes perpendicular to corrugation axis

$$D_{Qy} = Sh \left(\frac{E_c}{1 - \mu_c^2} \right) \left(\frac{t_c}{h_c} \right)^3 \quad (17)$$

where:

h_c : depth of corrugation, measured vertically from center line at crest to center line at trough [mm]

t_c : thickness of core material [mm]

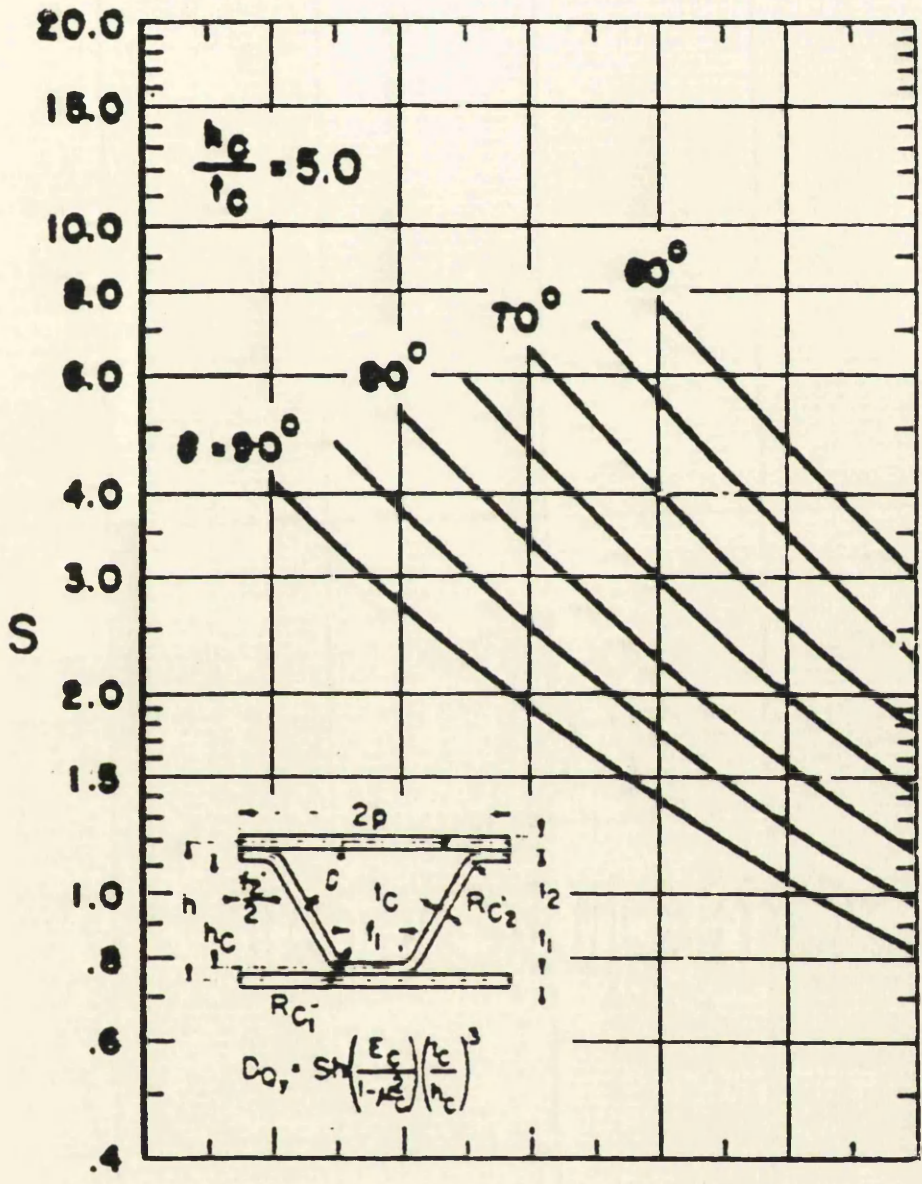
E_c : modulus of elasticity of core material [N/mm²]

μ_c : Poisson's ratio of core material

S: nondimensional coefficient depending on shape of corrugation, relative proportions of sandwich cross section and the material properties of the component parts

h: distance between middle surfaces of face sheets [mm]

Because of the complexity of the formulae for evaluating S [28], a number of charts were computed which give S directly for the common type of sandwich with corrugation cross-sectional shape consisting of straight lines and circular arcs. A sample of these charts is presented in Fig. 3.2.



$t_c/t_f = 0.30$

Fig. 3.2 Sample of charts which give S directly for the common type of sandwich with corrugated core [28]

3.3.2.5 Transverse shear stiffness D_{Q_x} in planes parallel to corrugation axis

$$D_{Q_x} = \frac{G_c I_c h}{P \int_0^l Q ds} \quad (18)$$

where:

I : moment of inertia of width $2p$ of cross section parallel to yz plane, taken about centroidal axis parallel to y axis [mm^4]

$2p$: corrugation pitch [mm]

l : length of one corrugation leg measured along the center line [mm] as in Fig. 3.3

s : coordinate measured along center line of corrugation leg [mm] as in Fig. 3.3

Q : static moment about the centroidal axis (middle plane for symmetrical sandwich) of the cross-hatched area as in Fig. 3.4

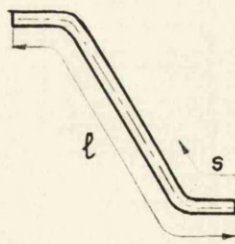


Fig. 3.3 (Fig. E3 [28])

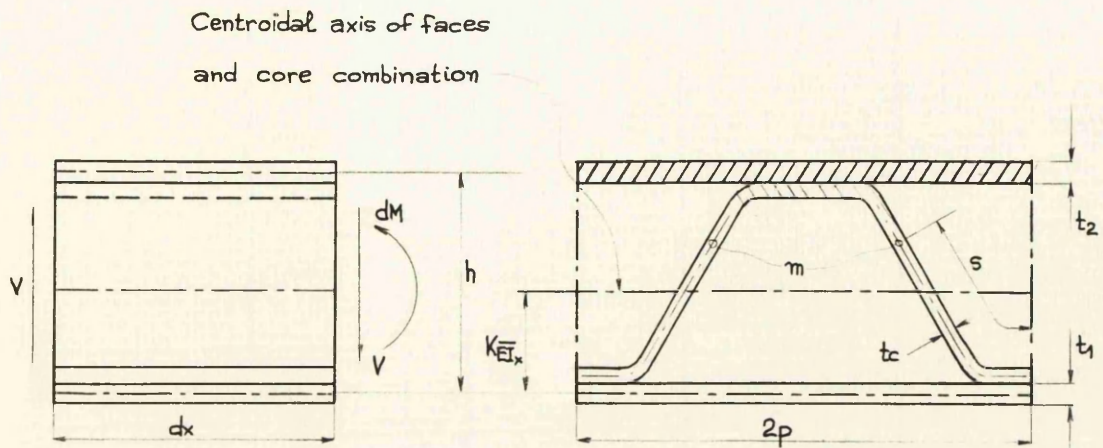


Fig. 3.4 (Fig. E1 [28])

An approximate formula, which is more practicable, is presented by Libove and Hubka [28]:

$$D_{Q_x} \approx \frac{G_c t_c h^2}{pl} = \frac{G_c t_c^2}{A_c} \left(\frac{h}{p} \right)^2 \quad (19)$$

where:

p : half corrugation pitch [mm]

h : distance between middle surfaces of face sheets [mm]

A_c : area per unit width of corrugation cross section parallel to yz plane [mm]

t_c : thickness of core material [mm]

l : length of one corrugation leg measured along the center line [mm] as in Fig. 3.3

G_c : shear modulus of elasticity of core material [N/mm²]

3.3.3 PRINCIPAL RESULTS OF THE LIBOVE AND BATDORF [31] SMALL DEFLECTION THEORY FOR FLAT SANDWICH PLATES

The differential equations relating the deflections w , the lateral

load q and the internal forces and moments N_x , N_y , N_{xy} , Q_x , Q_y , M_x , M_y and M_{xy} are:

$$\frac{\partial^2 w}{\partial x^2} = -\frac{M_x}{D_x} + \mu_y \frac{M_y}{D_y} + \frac{1}{D_{Q_x}} \frac{\partial Q_x}{\partial x} \quad (20)$$

$$\frac{\partial^2 w}{\partial y^2} = -\frac{M_y}{D_y} + \mu_x \frac{M_x}{D_x} + \frac{1}{D_{Q_y}} \frac{\partial Q_y}{\partial y} \quad (21)$$

$$\frac{\partial^2 w}{\partial x \partial y} = \frac{M_{xy}}{D_{xy}} + \frac{1}{2} \frac{1}{D_{Q_x}} \frac{\partial Q_x}{\partial y} + \frac{1}{2} \frac{1}{D_{Q_y}} \frac{\partial Q_y}{\partial x} \quad (22)$$

relating distortions to distorting moments and forces, and

$$\frac{\partial Q_x}{\partial x} + \frac{\partial Q_y}{\partial y} = - \left(q + N_x \frac{\partial^2 w}{\partial x^2} + N_y \frac{\partial^2 w}{\partial y^2} + 2N_{xy} \frac{\partial^2 w}{\partial x \partial y} \right) \quad (23)$$

$$Q_x = -\frac{\partial M_{xy}}{\partial y} + \frac{\partial M_x}{\partial x} \quad (24)$$

$$Q_y = -\frac{\partial M_{xy}}{\partial x} + \frac{\partial M_y}{\partial y} \quad (25)$$

for equilibrium.

Equations 20-22 can be solved for M_x , M_y and M_{xy} to obtain:

$$M_x = -\frac{D_x}{1 - \mu_x \mu_y} \left[\frac{\partial}{\partial x} \left(\frac{\partial w}{\partial x} - \frac{Q_x}{D_{Q_x}} \right) + \mu_y \frac{\partial}{\partial y} \left(\frac{\partial w}{\partial y} - \frac{Q_y}{D_{Q_y}} \right) \right] \quad (26)$$

$$M_y = -\frac{D_y}{1 - \mu_x \mu_y} \left[\frac{\partial}{\partial y} \left(\frac{\partial w}{\partial y} - \frac{Q_y}{D_{Q_y}} \right) + \mu_x \frac{\partial}{\partial x} \left(\frac{\partial w}{\partial x} - \frac{Q_x}{D_{Q_x}} \right) \right] \quad (27)$$

$$M_{xy} = \frac{1}{2} D_{xy} \left[\frac{\partial}{\partial x} \left(\frac{\partial w}{\partial y} - \frac{Q_y}{D_{Q_y}} \right) + \frac{\partial}{\partial y} \left(\frac{\partial w}{\partial x} - \frac{Q_x}{D_{Q_x}} \right) \right] \quad (28)$$

Substitution of these expressions into equations 23-25 and solution of the resulting equations by means of operational determinants give the following differential equations with variables separated, for the case in which N_x , N_y and N_{xy} are constant throughout the plate:

$$[D]w = -[M]q \quad (29)$$

$$[D]Q_x = -[N]q \quad (30)$$

$$[D]Q_y = -[P]q \quad (31)$$

where $[D]$, $[M]$, $[N]$ and $[P]$ are differential operators defined by Libove and Batdorf [31].

Three types of support commonly assumed at the boundaries of a plate are no support (free edge), simple support and clamping. These types of support can be described in terms of deflections, shears and moments for an edge parallel to the y axis as follows:

For a free edge:

$$M_x = 0 \quad M_{xy} = 0 \quad Q_x + N_x \frac{\partial w}{\partial x} + N_{xy} \frac{\partial w}{\partial y} = 0 \quad (32)$$

For a simple supported edge at which the support is applied over the entire thickness:

$$w = 0 \quad M_x = 0 \quad \frac{Q_y}{D_{Q_x}} = 0 \quad (33)$$

For a simply supported edge at which the support is applied only to the middle surface:

$$w = 0 \quad M_x = 0 \quad M_{xy} = 0 \quad (34)$$

For a clamped edge at which the support is applied over the entire thickness:

$$w = 0 \quad \frac{\partial w}{\partial x} - \frac{Q_x}{D_{Q_y}} = 0 \quad \frac{Q_y}{D_{Q_x}} = 0 \quad (35)$$

For a clamped edge at which the support is applied only to the middle surface (a type of support very unlikely to be met in practice):

$$w = 0 \quad \frac{\partial w}{\partial x} - \frac{Q_x}{D_{Q_y}} = 0 \quad M_{xy} = 0 \quad (36)$$

The conditions for an edge parallel to the x axis can be written by replacing x by y and vice versa, except in the subscripts of M_{xy} and N_{xy} . Boundary conditions can also be written for more general types of support.

The potential energy of a plate in which the middle surface forces are assumed to remain unchanged in the course of the plate's deflection and for which the moments and vertical forces at the boundaries do no work is given by equation (37).

The most important types of boundary to which this expression applies are free, simply supported or clamped. For more general types of support, in which the boundary reactions do work in the course of the plate's deflection, the potential energy expression must be extended to include terms representing the potential energy of the reactions.

$$\begin{aligned}
V = \frac{1}{2} \iint \left\{ \right. & \left. \left[\frac{D_x}{1 - \mu_x \mu_y} \left[\frac{\partial}{\partial x} \left(\frac{\partial}{\partial x} - \frac{Q_x}{D_{Q_x}} \right) \right]^2 + \frac{D_x \mu_y + D_y \mu_x}{1 - \mu_x \mu_y} \left[\frac{\partial}{\partial x} \left(\frac{\partial w}{\partial x} - \frac{Q_x}{D_{Q_x}} \right) \right] \right] \right. \\
& \left. \left[\frac{\partial}{\partial y} \left(\frac{\partial w}{\partial y} - \frac{Q_y}{D_{Q_y}} \right) \right] + \frac{D_y}{1 - \mu_x \mu_y} \left[\frac{\partial}{\partial y} \left(\frac{\partial w}{\partial y} - \frac{Q_y}{D_{Q_y}} \right) \right]^2 + \frac{D_{xy}}{2} \right. \\
& \left. \left[\frac{\partial}{\partial x} \left(\frac{\partial w}{\partial y} - \frac{Q_y}{D_{Q_y}} \right) + \frac{\partial}{\partial y} \left(\frac{\partial w}{\partial x} - \frac{Q_x}{D_{Q_x}} \right) \right]^2 + \frac{Q_x^2}{D_{Q_x}} + \frac{Q_y^2}{D_{Q_y}} \right. \\
& \left. \left. \frac{1}{2} \iint \left[-2\alpha w + N_x \left(\frac{\partial w}{\partial x} \right)^2 + N_y \left(\frac{\partial w}{\partial y} \right)^2 + 2N_{xy} \frac{\partial w}{\partial x} \frac{\partial w}{\partial y} \right] dx dy \right. \right\} dx dy +
\end{aligned}
\tag{37}$$

The calculus of variations can be used to show [31] that in order for the potential energy to be a minimum the differential equations of equilibrium and the boundary conditions must be satisfied.

3.3.4 STABILITY OF FLAT, SIMPLY SUPPORTED CORRUGATED CORE SANDWICH PLATES UNDER COMPRESSION [27]

Combining the work of Libove and Batdorf [31] together with the physical constants derived by Libove and Hubka [28], makes possible the determination of the elastic over-all buckling loads of flat corrugated core sandwich plates with symmetric corrugated cores which is done by Seide [27]. By over-all buckling is meant buckling of the sandwich plate as a whole, without regard to local buckling of the faces between corrugations or of the corrugations themselves. Criteria for the problem of stability under longitudinal compression of flat symmetric corrugated core sandwich plates with simply supported loaded edges and simply supported or clamped unloaded edges have been derived by Seide [27]. The assumptions made to derive the stability criteria include:

- Straight lines in the plate that are originally perpendicular to the undeformed plate middle surface remain straight but not

necessarily perpendicular to the plate middle surface after bending occurs.

- The plate has no local deformations. This assumption permits the analysis of only the overall stability of sandwich plates.

Corrugated core sandwich plates can be analysed by this approach provided that limitations are imposed on the relative dimensions of the sandwich faces and of the core. The pitch of the core corrugations should be small compared with the plate width perpendicular to the axis of the corrugations so that the plate can be treated adequately as a continuous orthotropic medium. The thickness of the faces should be small compared with the overall plate thickness in order that bending of each face about its own middle surface may be neglected. The core should be sufficiently stiff so that changes in the panel thickness are negligible. Libove and Hubka [28] indicate that limitations should also be placed on the type of corrugated core sandwich plate that may be analysed by the sandwich-plate theory by Libove and Batdorf [31]. The Poisson's ratios of the materials of the two faces must be equal, the neutral plane of bending of the faces alone must coincide with the plane passing through the centroidal axis of the corrugation cross section, and load resultants must be applied in specified planes between the plate faces. Symmetric corrugated core sandwich plates - that is, plates with faces of equal thickness and of the same material and with a corrugated core having symmetrical corrugations - satisfy these conditions, provided that load resultants are applied in the plane of the plate middle surface.

For many practical structures, the transverse shear stiffness in planes parallel to the axis of the corrugations is very much greater than the transverse shear stiffness in planes perpendicular to the axis of the corrugations and may be assumed to be **infinite**.

Finally, the stability criterion or buckling coefficient for simply supported corrugated core sandwich plates under longitudinal

compression is given by the following expression:

$$k = \frac{\left\{ \left(\frac{m}{\beta} + n^2 \frac{\beta}{m} \right)^2 + (1 - \mu_f^2) \eta \frac{m^2}{\beta^2} + \left[\frac{1}{2(1 + \mu_f)} \left(\frac{m}{\beta} + n^2 \frac{\beta}{m} \right)^2 + \eta \left(n^2 + \frac{1 - \mu_f}{2} \frac{m^2}{\beta^2} \right) \right] \left(n^2 r_x + \frac{m^2}{\beta^2} r_y \right) \right\}}{\left\{ 1 - \mu_f^2 + \left[\frac{1 - \mu_f}{2} n^2 + \frac{m^2}{\beta^2} + (1 - \mu_f^2) \eta \frac{m^2}{\beta^2} \right] r_x + \left(n^2 + \frac{1 - \mu_f}{2} \frac{m^2}{\beta^2} \right) r_y + \left[\frac{1}{2(1 + \mu_f)} \left(\frac{m^2}{\beta^2} + n^2 \right)^2 + \eta \frac{m^2}{\beta^2} \left(n^2 + \frac{1 - \mu_f}{2} \frac{m^2}{\beta^2} \right) \right] r_x r_y \right\}} \quad (38)$$

where:

m : number of half waves in the x direction

$\beta = a/b$: aspect ratio

r_x, r_y : transverse-shear-flexibility parameters,

$\frac{\pi^2 E_f I_f}{b^2 D_{Q_x}}$ and $\frac{\pi^2 E_f I_f}{b^2 D_{Q_y}}$ respectively

k : compressive-buckling-load parameter, $\frac{b^2 N}{\pi^2 E_f I_f}$

η : flexural-stiffness ratio, $\frac{E_c I_c}{E_f I_f}$

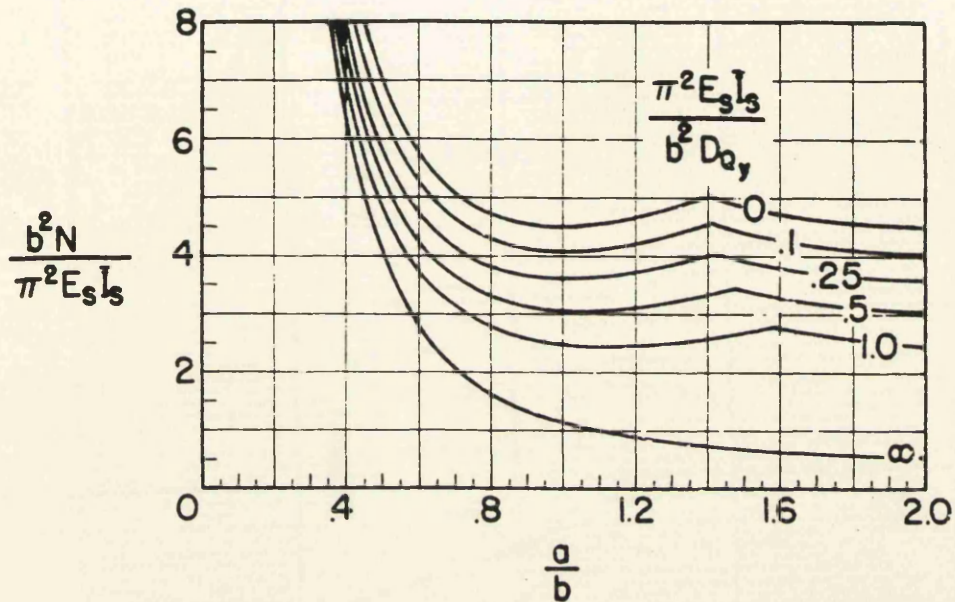
In the analysis of corrugated core sandwich plates in which the corrugations are oriented in the direction of either the x or the y axis, it is often assumed that D_{Q_x} , or D_{Q_y} respectively, is infinite. Then either r_x or r_y is zero and equation (38) reduces to a simpler expression. In our case it becomes:

$$k = \frac{\left\{ \left(\frac{m}{\beta} + n^2 \frac{\beta}{m} \right)^2 + (1 - \mu_f^2) \eta \frac{m^2}{\beta^2} + \left[\frac{1}{2(1 + \mu_f)} \left(\frac{m}{\beta} + n^2 \frac{\beta}{m} \right)^2 + \eta \left(n^2 + \frac{1 - \mu_f}{2} \frac{m^2}{\beta^2} \right) \right] \frac{m^2}{\beta^2} r_y \right\}}{1 - \mu_f^2 + \left(n^2 + \frac{1 - \mu_f}{2} \frac{m^2}{\beta^2} \right) r_y} \quad (39)$$

When equation (38) is used, m and n are assigned different integer values until the lowest value of the compressive-buckling-load parameter k is obtained. Computations indicate that n should always be given the value 1 in these calculations so that the corrugated core sandwich plate buckles with one sinusoidal half-wave in the y direction.

By use of the more general equations derived for corrugated core sandwich plates with finite transverse shear stiffness in both directions, it is concluded by Seide [27] that the charts for the value of k vs β , a sample of which appears in Fig. 3.5, may be considered adequate for plates of practical dimensions for which the transverse shear stiffness in planes parallel to the axis of the corrugations is 10 or more times the transverse shear stiffness in planes perpendicular to the axis of the corrugations, provided that the panel aspect ratio (β) is greater than about 0.6.

Appendix B shows very clearly how all these theoretical results apply in the case of a corrugated core sandwich panel similar to that we are dealing with in this project and contains all governing equations for this kind of panels.



$$\eta=0$$

$a/b=\beta$: aspect ratio

$\frac{\pi^2 E_s I_s}{b^2 D_{Q_y}} = \tau_y$: transverse-shear-flexibility parameter,

$\frac{b^2 N}{\pi^2 E_f I_f} = k$: compressive-buckling-load parameter or the stability

criterion

$\frac{E_c I_c}{E_f I_f} = \eta$: flexural-stiffness ratio

Fig. 3.5 Sample of charts for the value of compressive-buckling-load parameter k vs the plate aspect ratio β [27]

CHAPTER 4:

THE DESIGN OF STRUCTURAL CONNECTIONS

The design of structural connections is a neglected subject and more attention is generally allocated to the analysis and design of main members. This is not realistic, as a structure is just as likely to fail because of insufficient strength of the connections - a fact which has occurred in many cases in practice. The detailing of connections in many design offices is allocated to those with lower academic and professional qualifications and in some cases is even left to the tracer/draughtsman.

Many universities, polytechnics and technical colleges now teach structural design but because of packed syllabuses there is often little time available to allocate to structural connections. Research into connections is not extensive and because of this the basic assumptions in the distribution of forces within connections are often not correct.

4.1 DEFINITIONS

Structural connection: A structural connection may be defined as an assembly of components which are arranged to transmit forces from one member to another. In theory, at least, a connection may be subjected to any combination of axial force, shear force and bending moment in relation to three perpendicular axes. In practice, however, the situation is generally reduced to forces in one plane. The transfer of forces through the components of a joint is often complex and must be considered in detail for each type of connection.

Movement joints: Movement joints are introduced into a structure to allow free expansion and contraction on either side of the joint due to changes in temperature, shrinkage, expansion, creep, settlement etc. These joints may be detailed to be watertight and may transmit forces.

Construction joints: Construction joints are introduced into a structure because components are manufactured to a convenient size and a joint

therefore occurs between components. In most cases these joints transmit forces, but in some cases the only requirement is that the joints should be watertight.

4.2 GENERAL

The design of connections can be approached from a number of directions: the type of structure, the type of fastener, the type of loading and the designer's special interest. The dominant concerns in the design of connections in buildings, bridges, towers such as offshore drilling platforms and ships differ. Bolts, welds and devices such as cable sockets transmit forces in different ways. Static loads, dynamic loads and the expected number of repetitions of either, pose different problems. Structural engineers and fabricators have shared interests and responsibilities but the focus of the former may be on obtaining a desired type of behaviour and that of the latter on ensuring practicable fabrication and erection.

Fundamental to the design of any connection are interrelated criteria of strength, stiffness, ductility, predictability, practicability and cost. More information on these aspects of connection design can be found in [41, 43, 46, 47, 48].

4.3 THE IDEAL STRUCTURAL CONNECTION

The ideal structural connection should be designed and manufactured to fit the practical situation. It should therefore be:

- simple to manufacture and assemble
- standardised for situations where the dimensions and loads are similar, e.g. avoid using a variety of dimensions, plate thicknesses, weld sizes and bolts

- manufactured from materials and components that are readily available
- designed and detailed so that site work is from the top of the joint, not from below where the workman's arms will be above his head. There should also be sufficient room you locate a spanner or space to weld, if required
- designed so that welding is generally confined to the workshops to ensure a good quality and reduce costs
- detailed to allow sufficient clearance and adjustment to accommodate practical imperfections
- designed to withstand not only the normal working loads but also the erection forces
- designed to avoid the use of temporary supports to the structure during its erection
- designed to develop the required load-deformation characteristics at the service load and at ultimate load
- detailed to resist corrosion and to be acceptable aesthetically
- low in cost and maintenance. Generally, for connections manufactured with an advanced technology, labour costs are high and it is therefore more economical to use more material and less labour.

4.4 STRUCTURAL CONNECTIONS IN COMPOSITE STRUCTURES

In composite (and further in sandwich) structures the weakest links and most probable sources of failure are bonded structural connections. The weakness of such connections is attributable to:

- the absence of load-bearing fibres across bonded interfaces
- the low strength under tension and shear of the thin layer of resin forming the bond
- the inevitable occurrence of stress concentrations caused by geometric irregularities and manufacturing imperfections (e.g. regions of incomplete bonding)
- the tendency of small cracks and imperfections within the bond to propagate under load, i.e. for 'peeling' to occur.

Safe and efficient design of structural connections requires a knowledge of the forces and moments to be transmitted, from which estimates may be made of direct and shear stresses acting across bonded interfaces and hence of required bond areas. Reliable estimates of such forces and moments are unlikely to be available unless finite element calculations have been carried out.

Bonded attachments may be reinforced (or replaced) by use of metal fasteners, i.e. bolts, screws or rivets. In this case care must be taken to ensure not only that fasteners are strong enough to transmit design forces and moments but also that the laminate is able to withstand concentrated bearing loads at fastener positions.

While numerical analysis of stresses at a bonded interface or in the region of metal fasteners will provide insights into joint performance and may be used as means of improving joint geometry, purely theoretical estimates of joint strength are unacceptable as a basis for design because of uncertainty about imperfections, local stress concentrations and material failure under multi-axial stresses within a connection. Reference must therefore be made to test data and development of a

new high-performance design should include a thorough programme of tests on all important joints with evaluation of static, fatigue, creep and impact strengths. Consideration should also be given to performance of joints under fire conditions.

4.4.1 BULKHEAD/SHELL CONNECTIONS

Most ship and boat hulls rely critically on transverse bulkheads to provide rigidity and strength under transverse loads: this involves transmission of direct and membrane shear stresses across the bulkhead/shell connection. An effective and economical attachment is provided by the double angle arrangement shown in Fig. 4.1. External water pressure will normally impose a favourable load condition in which the shell is pushed onto the bulkhead. Massive internal components such as machinery may, however, cause local net outward forces tending to push the shell off the bulkhead: it is important that this condition, if present, should be identified by finite element analysis, should be counteracted where necessary by local use of metal fasteners or a special bonding technique and should be represented in static and fatigue proof tests by inclusion of 'pull-off' as the much less severe 'push-on' form of loading. It will usually be worthwhile to incorporate a plug of short-strand glass/resin filler round the periphery of a bulkhead as indicated in Fig. 4.1, both in order to eliminate a potential leak-path and to transmit 'push-on' loads directly into the bulkhead rather than by shear through the boundary angles.

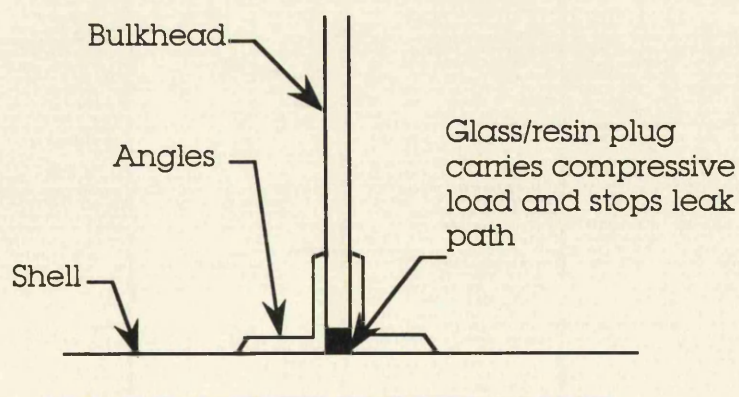


Fig. 4.1 Bulkhead/shell connection

4.4.2 STIFFENER INTERSECTIONS

At intersections between longitudinal and transverse stiffeners it is necessary to provide for

- exchange of shear forces between intersecting members;
- transmission across the intersection of direct and shear stresses in the webs and table of each stiffener.

The first requirement is readily met by provision of angles laid up on the webs of intersecting members as shown in Fig. 4.2. Maximum shear forces exchanged between intersecting members may be found from shear force distributions in longitudinal and transverse stiffeners obtained by grillage or finite element analysis. The second requirement is best satisfied by preserving as far as possible the continuity of intersecting members. The shallower stiffener will normally pass continuously through the deeper member and it is desirable that the latter should be substantially deeper than the former so that continuous material is retained in the perforated webs. Where intersections between top-hat stiffeners of nearly equal depth are unavoidable, metal brackets must be provided, built into the smaller stiffener in line with the perforated webs as shown in Fig. 4.2, to ensure transmission of direct and shear stresses: metal fasteners may be necessary to provide strength under tensile load.

4.4.3 DECK/EDGE CONNECTIONS

Knee and tee connections, which occur respectively at upper and lower deck-edges must be able to transmit shear forces associated with longitudinal bending of the hull, together with transverse bending moments and direct and shear forces transmitted primarily between deck beams and side-shell frames. Some effective deck-edge connections are shown in Fig. 4.3. Large triangular brackets, which may be susceptible to buckling, should be avoided at frame to deck-beam joints. Connections of this type can be designed, from a knowledge of the forces and moments to be transmitted, by judicious application of beam theory.

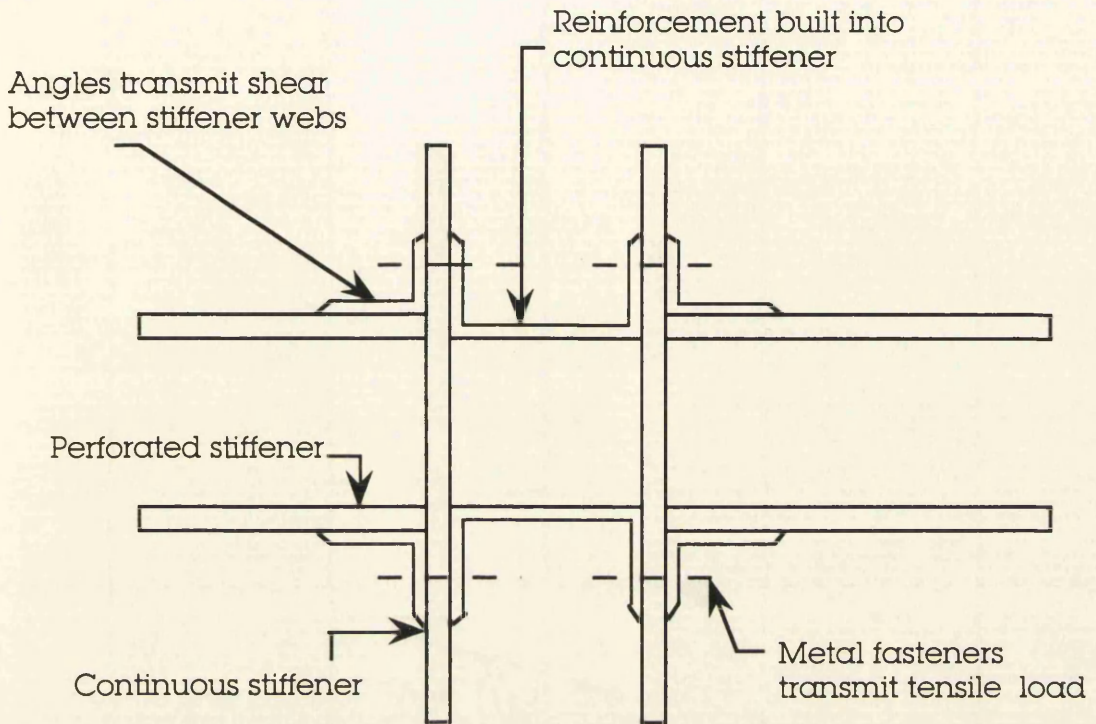


Fig. 4.2 Stiffener intersections

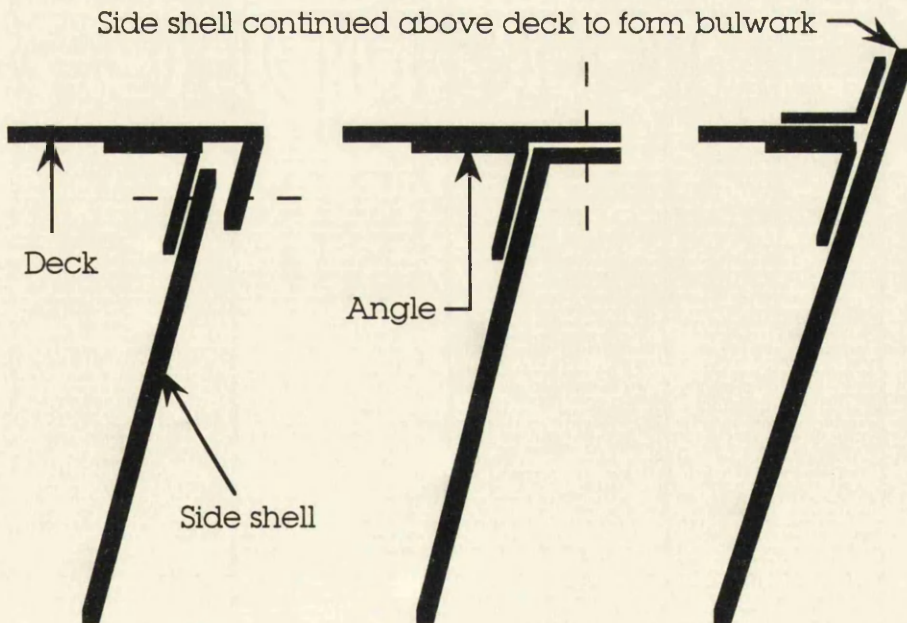


Fig. 4.3 Deck/edge connections

4.4.4 SINGLE-SKIN SHELL/SANDWICH COMPONENTS CONNECTIONS

At joints between a single-skin shell and sandwich components such as decks and bulkheads it may be desirable to taper off the core material at the boundaries of sandwich panels, as illustrated in Fig. 4.4, allowing simple, single-skin connections, possibly incorporating bolts to be made. Where transmitted loads are small, as at the boundaries of minor bulkheads, sandwich panels can be butted directly onto a single-skin deck or shell.

Design of bolted connections must be carried out with care to avoid local damage to relatively soft core material under bolt loads. Some possible arrangements are shown in Fig. 4.5, including use of rigid inserts, local reduction of a sandwich panel to a single skin and use of metal compression sleeves.

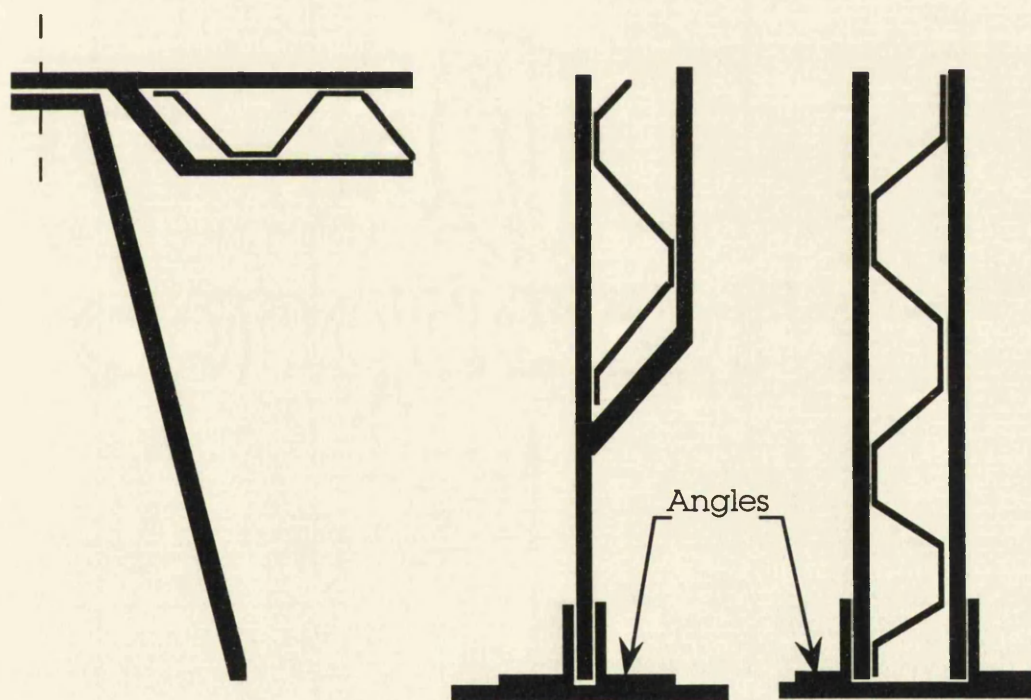


Fig. 4.4 Joints between sandwich and single skin-components

Attachment of lightweight fittings such as electrical cables to bulkheads or overhead decks can often be achieved satisfactorily by adhesive bonding. Although adhesive bonds may be strong enough to support heavier fittings, it must be ensured that such attachments do not initiate internal damage such as core-face separation. Where the position of a heavy fitting is known accurately at the design stage, local reinforcement may be incorporated during fabrication of a sandwich panel, as shown in Fig. 4.6, allowing attachment to be made by simple through-bolting or possibly by screws. Ad-hoc heavy duty attachments are likely to require metal sleeves as shown in Fig. 4.6.

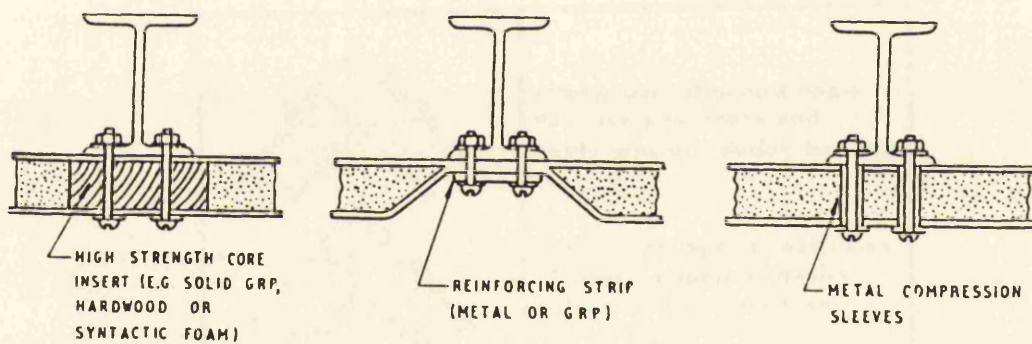


Fig. 4.5 Bolted joints in composite/sandwich structure

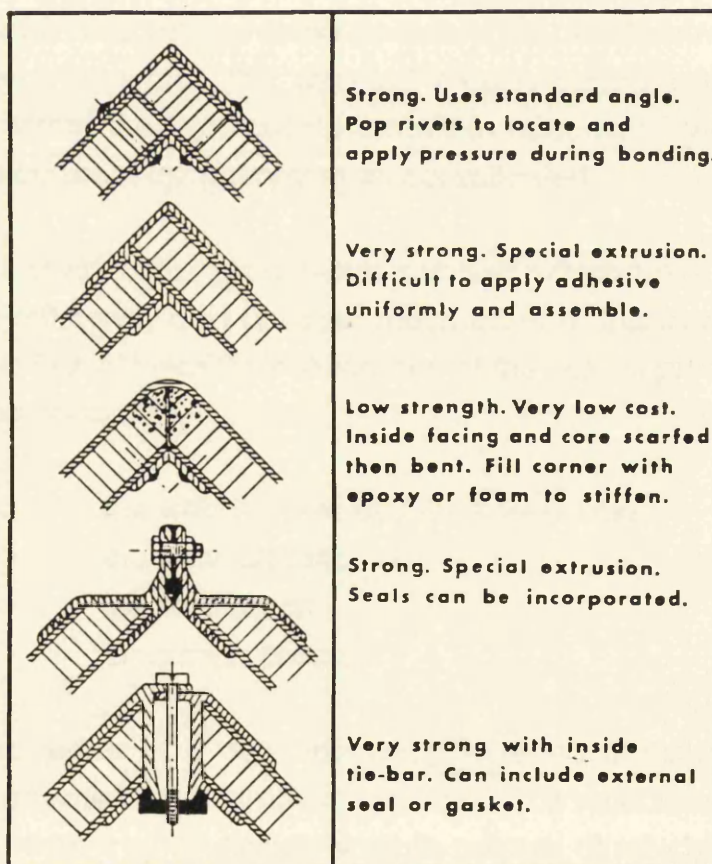
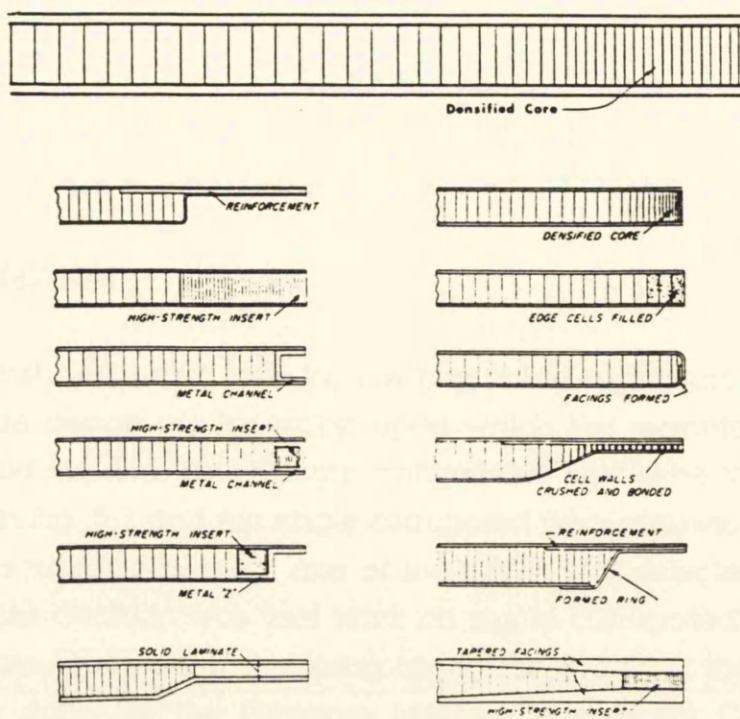


Fig. 4.6 Edge treatments and suggestions for corner designs, edge close-outs and splices

CHAPTER 5:
THE PROJECT: SELECTION AND
MANUFACTURE OF THE MODELS

5.1 INTRODUCTION

The first and basic step for the beginning of the project was the choice of the design configuration upon which the manufacture of the models would depend. That design configuration had to be one of the two appearing in Fig. 5.1 and the single corrugated core sandwich panel with corrugations running in the x axis of the panel was selected. The main reason for this decision was that work on single corrugated core panels with, this time, corrugations running along the y axis of the panel had already be done by the Glasgow Marine Technology Centre team. Therefore, useful comparisons could be drawn out. Another reason was the relative ease with which the selected design configuration could be constructed within the University premises in contrast to the second one whose manufacture is apparently more complicated.

Careful study of the parameters involved which have an important effect on the efficiency and collapse mechanism of this kind of structures and appear in Fig. 5.2 was the second step of the project procedure. These parameters include:

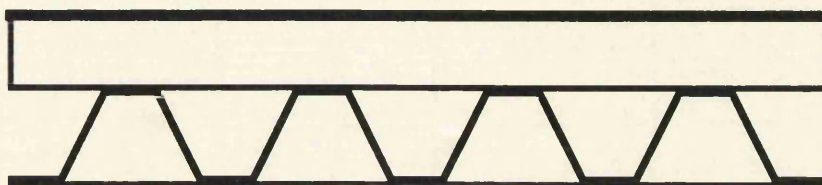
- the web B/t (breadth/ thickness) ratio
- the plate B/t ratio
- the web angle
- the flange breadth

The properties of a conventionally stiffened flat plate as well as those of a corrugated core sandwich beam can be calculated from simple beam theory with a spreadsheet, sample outputs of which are shown in Tables 5.1 and 5.2.

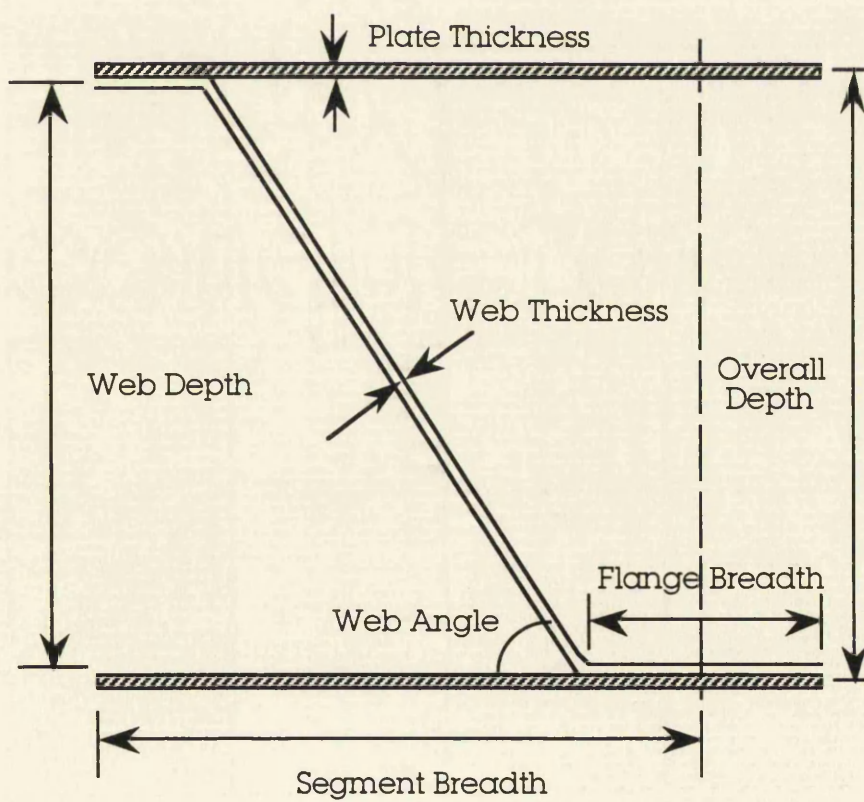
(continued on page 76)



single corrugated core



double corrugated core - orthogonal corrugations

Fig. 5.1 The design concepts of the project**Fig. 5.2** Elements of a corrugated core sandwich beam

					bp (mm)	500
					tp (mm)	10
					Ap (cm ²)	50
OBP			PLATE/STIFFENER COMBINATION			
b (mm)	t (mm)	A (cm ²)	Cent (cm)	z (cm ³ /m)	MODULUS /AREA	A (cm ² /m)
120	6.0	59.31	0.71	106.7	0.900	118.6
120	7.0	60.50	0.81	116.1	0.960	121.0
120	8.0	61.70	0.91	125.5	1.017	123.4
140	6.5	61.70	1.18	152.6	1.237	123.4
140	7.0	62.40	1.25	159.4	1.278	124.8
140	8.0	63.80	1.38	171.9	1.347	127.6
140	10.0	66.60	1.60	194.1	1.457	133.2
160	7.0	64.60	1.80	217.4	1.682	129.2
160	8.0	66.20	1.94	232.8	1.759	132.4
160	9.0	67.80	2.09	248.5	1.832	135.6
160	11.5	71.80	2.42	287.2	2.000	143.6
180	8.0	68.90	2.63	311.7	2.262	137.8
180	9.0	70.70	2.78	329.0	2.326	141.4
180	10.0	72.50	2.94	349.8	2.412	145.0
180	11.5	75.20	3.15	376.3	2.502	150.4
200	8.5	72.60	3.45	413.0	2.844	145.2
200	9.0	73.60	3.54	424.1	2.881	147.2
200	10.0	75.60	3.70	445.1	2.944	151.2
200	11.0	77.60	3.87	469.4	3.025	155.2
200	12.0	79.60	4.04	492.6	3.094	159.2
220	9.0	76.80	4.42	542.6	3.532	153.6
220	10.0	79.00	4.60	569.1	3.602	158.0
220	11.0	81.20	4.76	593.0	3.651	162.4
220	12.0	83.40	4.91	613.5	3.678	166.8
240	9.5	81.20	5.38	676.8	4.168	162.4
240	10.0	82.40	5.48	691.7	4.197	164.8
240	11.0	84.90	5.71	731.5	4.308	169.8
240	12.0	87.30	5.87	758.5	4.344	174.6
260	10.0	86.10	6.50	854.2	4.961	172.2
260	11.0	88.70	6.70	886.3	4.996	177.4
260	12.0	91.30	6.87	918.5	5.030	182.6
280	10.5	91.20	7.63	1035.5	5.677	182.4
280	11.0	92.60	7.73	1056.4	5.704	185.2
280	12.0	95.50	7.93	1098.1	5.749	191.0
280	13.0	98.40	8.11	1135.7	5.771	196.8
300	11.0	96.70	8.87	1257.1	6.500	193.4
300	12.0	99.70	9.07	1304.6	6.543	199.4
300	13.0	102.80	9.26	1349.5	6.564	205.6

Table 5.1 The properties of a range of conventionally stiffened flat plate

	1	2	3	4	5
Flange BREADTH (mm)	10.0	15.0	20.0	25.0	30.0
Web DEPTH (mm)	70.0	105.0	140.0	175.0	210.0
Web ANGLE (deg)	60.0	60.0	60.0	60.0	60.0
Web ANGLE (rad)	1.047	1.047	1.047	1.047	1.047
Web THICKNESS (mm)	1.00	1.50	2.00	2.50	3.00
Plate THICKNESS (mm)	1.250	1.875	2.500	3.125	3.750
Web B/t	80.8	80.8	80.8	80.8	80.8
Plate B/t	70.8	70.8	70.8	70.8	70.8
Overall DEPTH (mm)	72.5	108.8	145.0	181.3	217.5
Segment BREADTH (mm)	49.3	73.9	98.5	123.1	147.8
Bond WIDTH (cm/m)	20.3	20.3	20.3	20.3	20.3
Section AREA (cm ² /m)	43.0	64.5	85.9	107.4	128.9
Section MODULUS(cm³/m)	111.1	250.1	444.6	694.7	1000.3
MODULUS/AREA	2.59	3.88	5.17	6.47	7.76
Plate INERTIA (cm⁴)	15.6	79.1	250.1	610.6	1266.1
Flange INERTIA (cm ⁴)	1.2	6.0	19.0	46.5	96.4
Web INERTIA (cm⁴)	3.0	15.3	48.4	118.2	245.1
TOTAL INERTIA (cm ⁴)	19.8	100.5	317.6	775.3	1607.6
Plate AREA (cm²)	1.2	2.8	4.9	7.7	11.1
Flange AREA (cm ²)	0.1	0.2	0.4	0.6	0.9
Web AREA (cm²)	0.8	1.8	3.1	4.9	7.1
TOTAL AREA (cm ²)	2.1	4.8	8.5	13.2	19.1
y (cm)	3.6	5.4	7.3	9.1	10.9

Table 5.2 The properties of a corrugated core sandwich beam
(a general example)

The MODULUS/AREA ratio is a measure of the structural efficiency, since the section modulus and the area represent the stiffness and the weight of the structure respectively.

Fig. 5.3 compares the modulus of the steel corrugated-core sandwich structure to that of a single skin conventional stiffener arrangement. This diagram indicates the improved efficiency of the sandwich construction over conventional stiffener arrangement if a correct combination of core geometry is chosen. The curve envelope for the conventional stiffening is produced for a 10 mm plate stiffness and OBP stiffener with web depth range of 120 to 370 mm at spacing of 500 mm. The curve envelopes for the sandwich construction are based upon constant web and plate B/t ratios with differing web angles. The following points can be noted:

- As the web B/t ratio increases, the curves corresponding to the corrugated-core sandwich beam tend to lie on the left hand side of the OBP plate envelope. This means that a corrugated-core sandwich beam with less overall depth than that of a conventional OBP plate has an improved section modulus with less sectional area.
- Also, as the web angle increases, better results can be seen in terms of the section modulus and sectional area. In other words, the section modulus increases relative to the sectional area.
- For small web depths - in the range of 50-160 mm - the behaviour of the corrugated-core sandwich beams (web angle: 50°-70°) appears to be approximately the same and the gap between the corrugation envelope curve and the conventional OBP plate envelope curve is more significant. As the web depth increases, there is greater differentiation of the results among the various curve envelopes of corrugated beams.

(continued on page 78)

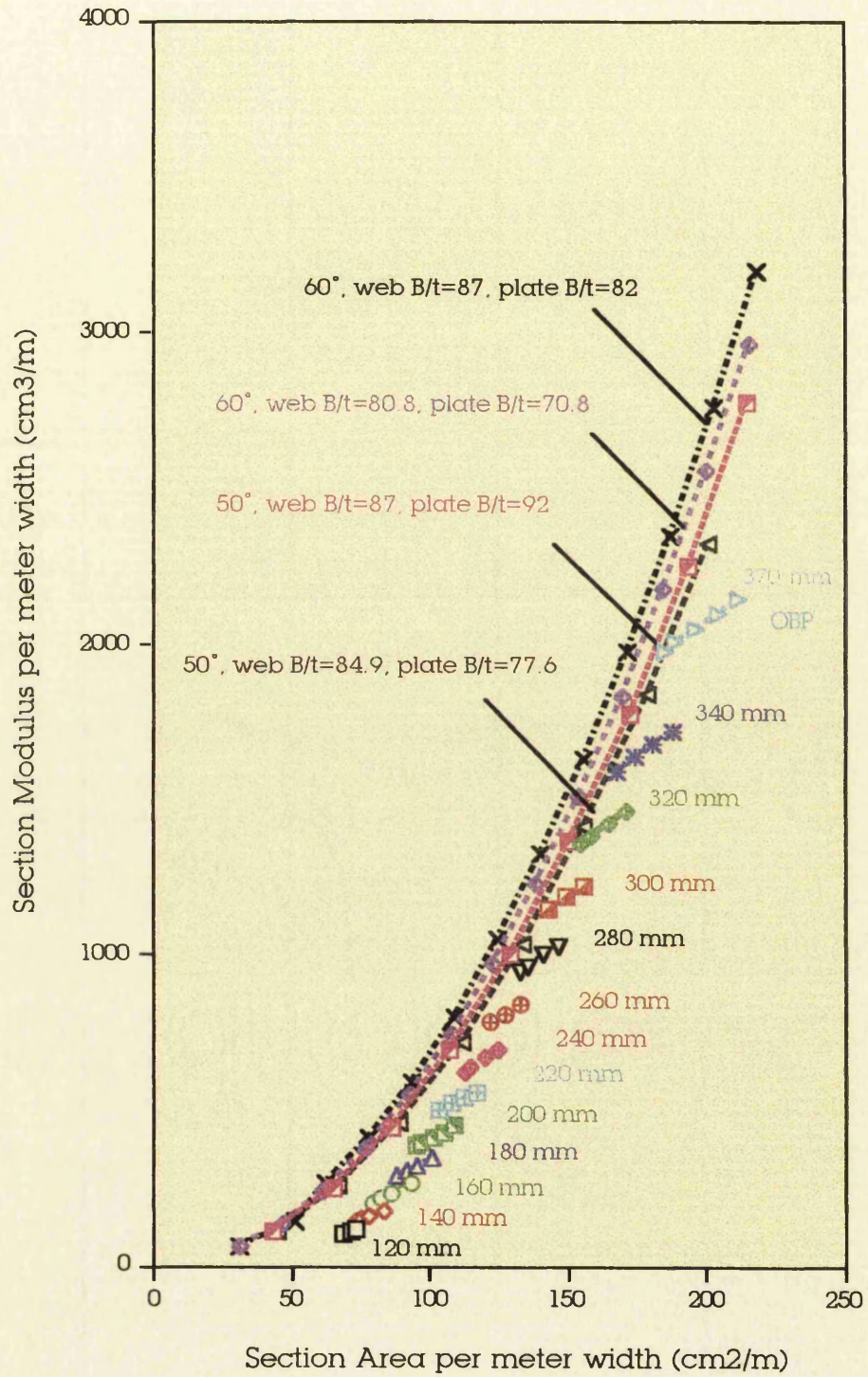


Fig. 5.3 Comparison of stiffness and section area between sandwich construction and conventionally stiffener plates

5.2 THE SELECTION OF THE MODELS

The next step appeared to be the determination of the dimensions of the models to manufacture. Those would cover a range of breadth/thickness ratios for plate and web components, so that useful comparisons could be drawn out. The main factors which influenced the selection of their dimensions was the dimensions and load capacity of the INSTRON bending machine located at the James Watt building, the dimensions of the curing oven and strength design considerations. More specifically:

- the length of the models was dictated mainly by the diagonal dimension of the testing base of the machine (the models should have been as long as possible so that they would resemble beams). Therefore, the maximum possible length was selected: 600 mm.
- the depth of the models was dictated mainly by the load capacity of the machine and secondarily by the operating space of the curing oven into which the manufacture frame would enter (oven space: 900mm*550mm*350mm). The bending machine has a maximum load capacity of 250 KN. Therefore, calculations for the required maximum section modulus of the model, which appear in Appendix D, had to be performed. Also, the B/t web and plate ratios had to be below 80-90 and 70 respectively for buckling to occur. Furthermore, the web angle should be within the range of 60°-70°, since it has been found [7] that it gives the optimum stiffness to mass ratio.
- the breadth of the models was affected by limitations on flanging capability as far as the University machinery is concerned as well as by the fact that it should not exceed 250 mm, since that was the maximum length of the weights through which the load would apply onto the models. The flange breadth was fixed to 20 mm.

Table 5.3 and Fig. 5.4 show the ten models selected for bending and compression tests.

5.3 THE MANUFACTURE OF THE MODELS

The establishment of a fabrication procedure for the chosen models formed a further step. In general, the manufacture of sandwich structures requires three conditions to be met:

- The application of pressure to effectively hold components together without deforming them
- The application of temperature (both pressure and temperature in the precise amounts required for adhesive cure)
- The provision for tooling and fixtures to hold the assembly in the desired shape and keep all the details in their proper positions during cure

A feasible way had to be found for these conditions to be met. Therefore, the manufacture of the models was accomplished with the aid of a frame which was constructed especially for this purpose, again within the University premises. The frame had to:

- provide for as high as possible quality plane surfaces
- be easy to manhandle
- provide for adequate clamp space
- be operational

(continued on page 81)

MODEL NUMBER	0-4b	1-4b	2-4b	3-4b	4-4b
	0-3b	1-c	2-c	3-3b	4-c
Web LENGTH (mm)	70.00	61.00	90.00	120.00	96.00
Flange BREADTH (mm)	20.00	20.00	20.00	20.00	20.00
Web DEPTH (mm)	65.78	55.28	81.57	112.76	87.01
Web ANGLE (deg)	70.00	65.00	65.00	70.00	65.00
Web ANGLE (rad)	1.22	1.13	1.13	1.22	1.13
Web THICKNESS (mm)	1.50	1.00	1.00	1.50	1.50
Plate THICKNESS (mm)	1.50	1.00	1.50	1.50	1.50
Web B/t	46.67	61.00	90.00	80.00	64.00
Plate B/t	43.13	69.35	62.58	65.93	65.22
Overall DEPTH (mm)	68.78	57.28	84.57	115.76	90.01
Segment BREADTH (mm)	42.35	44.68	56.93	59.45	58.92
Bond WIDTH (cm/m)	47.23	44.77	35.13	33.64	33.95
Section AREA (cm ² /m)	60.75	37.64	48.93	64.52	58.69
Section MODULUS (cm³/m)	142.62	77.69	155.13	247.29	182.08
MODULUS/AREA	2.35	2.06	3.17	3.83	3.10
Plate INERTIA (cm⁴)	14.38	7.08	29.47	58.21	34.62
Flange INERTIA (cm ⁴)	3.10	1.47	3.25	9.29	5.48
Web INERTIA (cm⁴)	3.29	1.39	4.63	17.59	8.18
TOTAL INERTIA (cm ⁴)	20.77	9.94	37.34	85.09	48.28
Plate AREA (cm²)	1.27	0.89	1.71	1.78	1.77
Flange AREA (cm ²)	0.30	0.20	0.20	0.30	0.30
Web AREA (cm²)	1.00	0.59	0.88	1.75	1.39
TOTAL AREA (cm ²)	2.57	1.68	2.79	3.84	3.46
y (cm)	3.44	2.86	4.23	5.79	4.50
Mass (kg)	5.54	3.57	6.07	8.15	3.91
Stiffness/Mass (mm³/kg)	4360.42	3889.20	5819.97	7215.04	5487.18

Table 5.3 The ten bending and compression test models

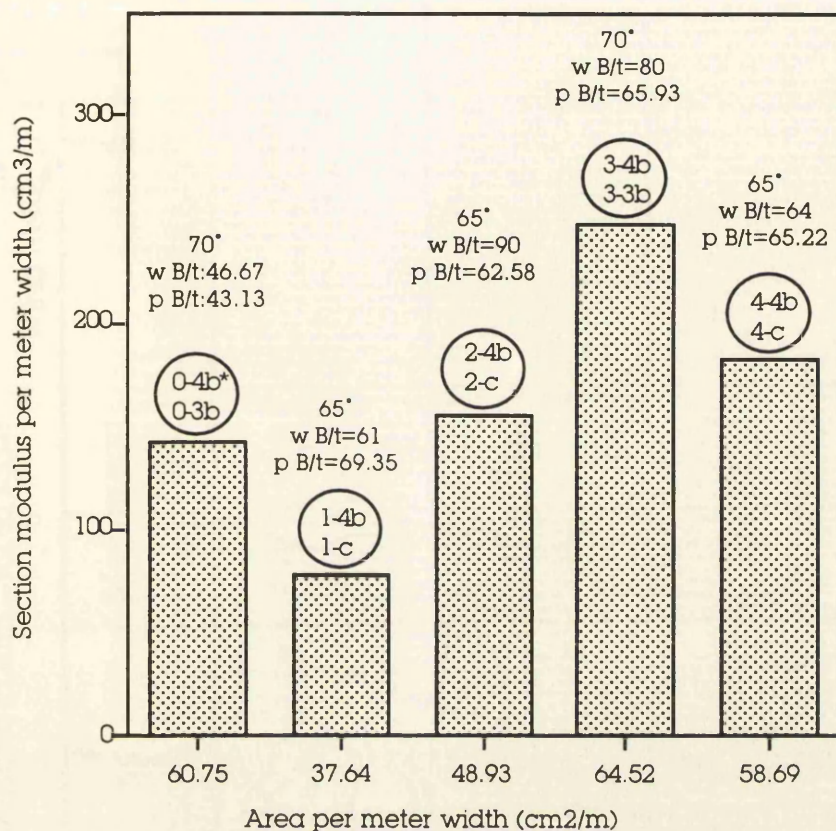


Fig. 5.4 Diagrammatic illustration of the models

Sketches of its sections and views are illustrated in Fig. 5.5-5.8. Photos 5.1-5.3 are very helpful to understand how the frame worked. At this point, it is worth mentioning that the adhesive chosen played a significant role in the manufacture and curing procedure. Araldite AV 119 (former 2007) was used, since its performance was examined by Smith et al. [7] and found satisfactory for this kind of construction. This adhesive requires a minimum temperature of 120°C to effect a cure.

(continued on page 87)

* suffix 4b after model no. denotes four point bending, suffix 3b denotes three point bending and suffix c denotes compression

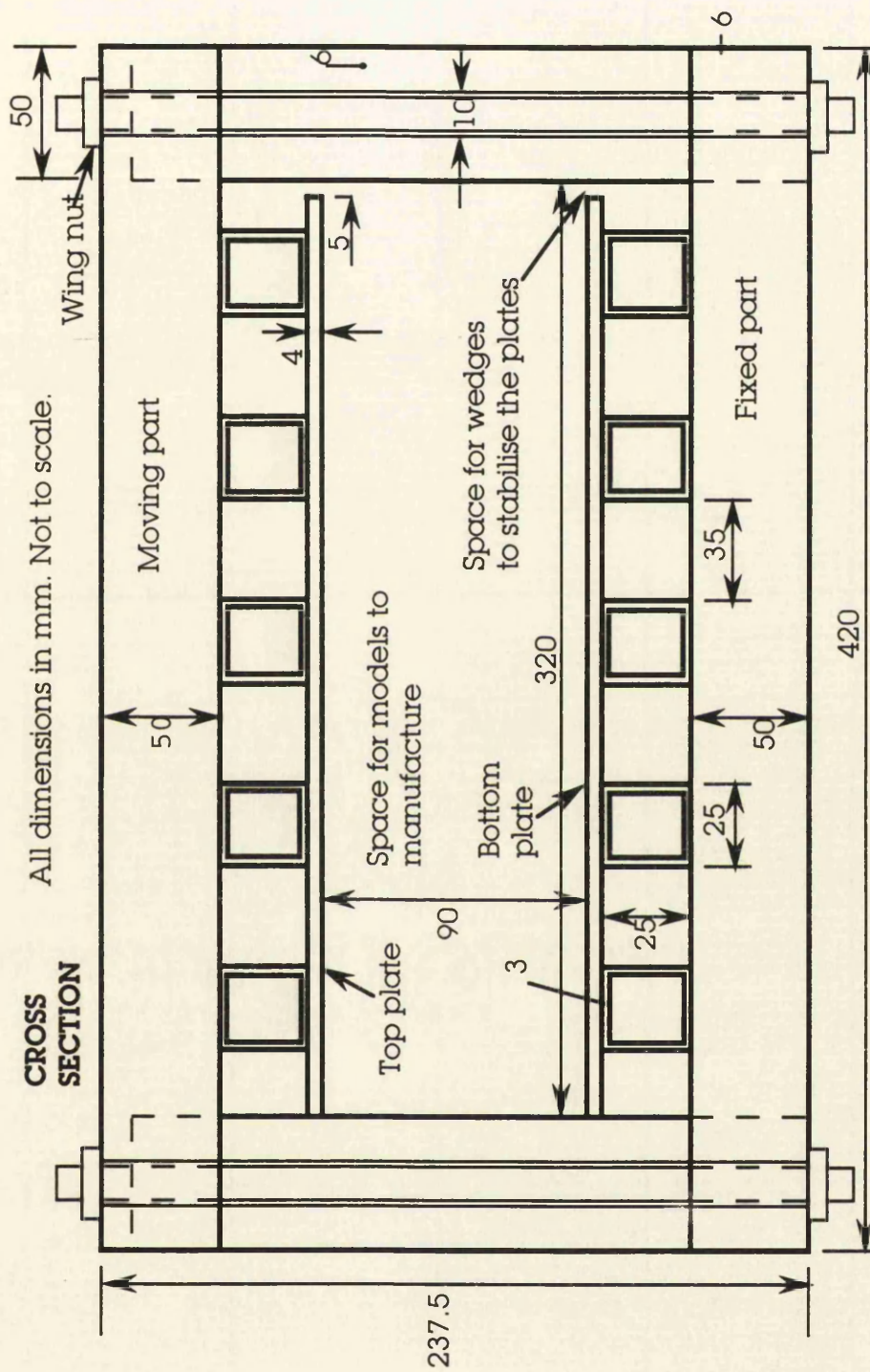
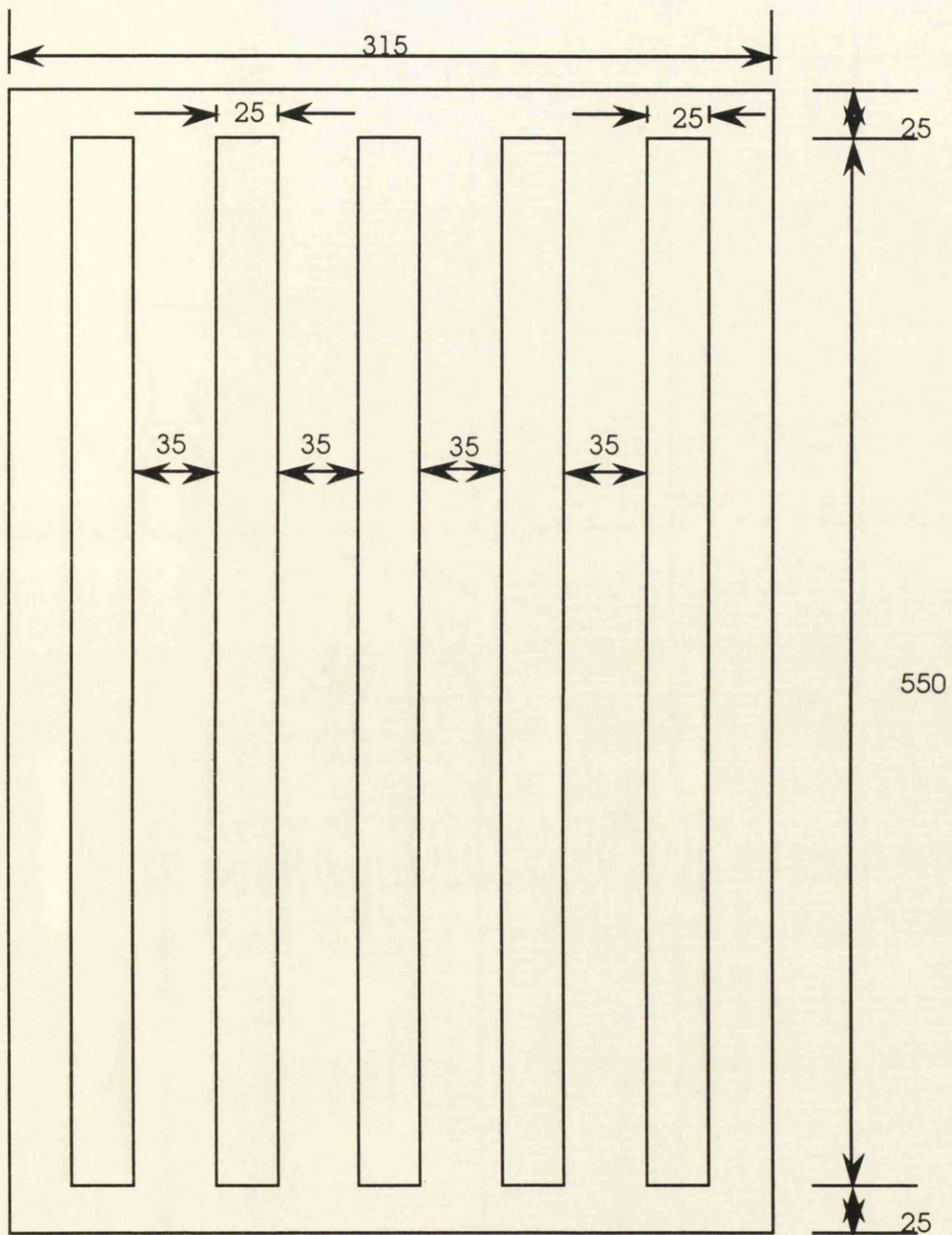


Fig. 5.5 Sketch of the cross section of the bonding frame



All dimensions in mm. Not to scale.

PLAN VIEW

Fig. 5.6 Sketch of the plan view of the top and bottom plates

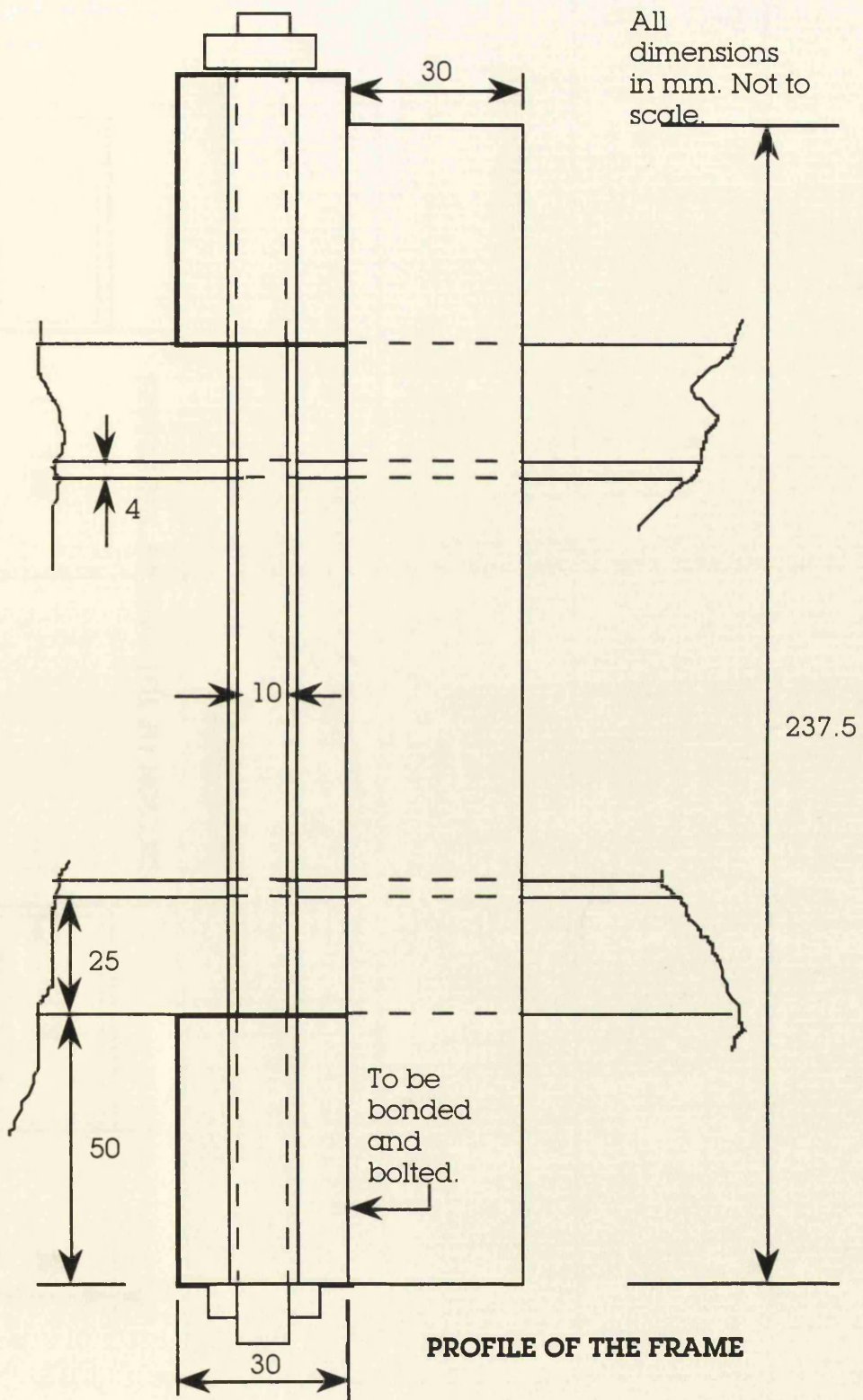


Fig. 5.7 Sketch of the profile of a clamp

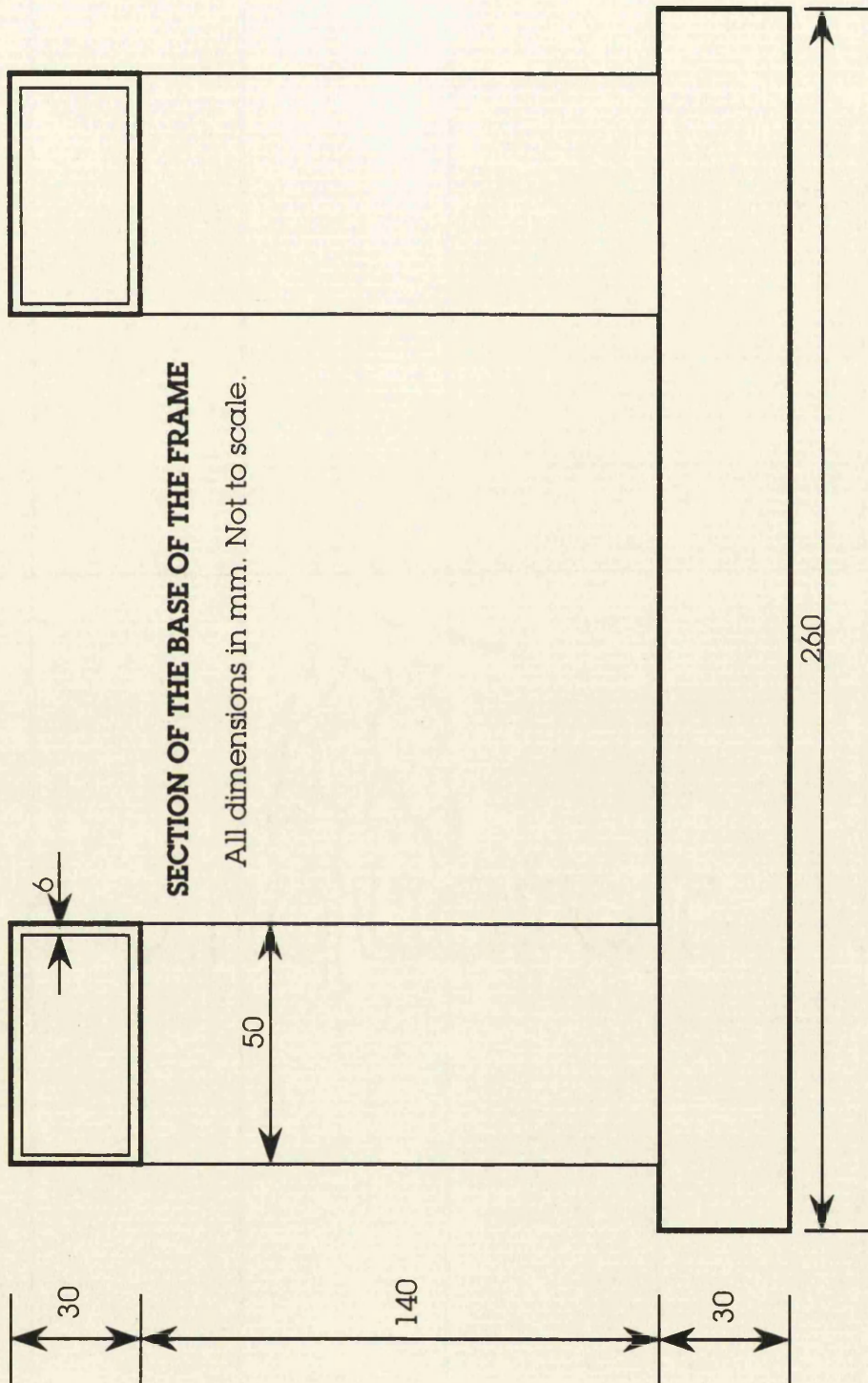


Fig. 5.8 Sketch of the section of the frame base

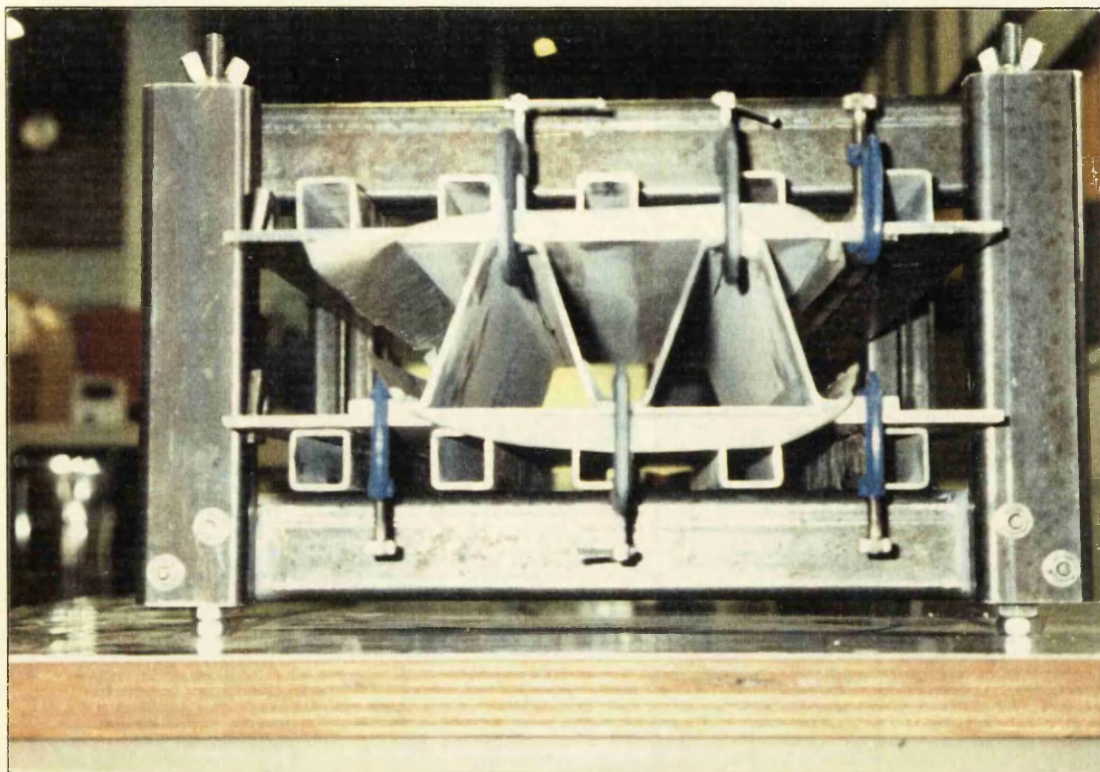


Photo 5.1 Cross section of model 0-4b and frame

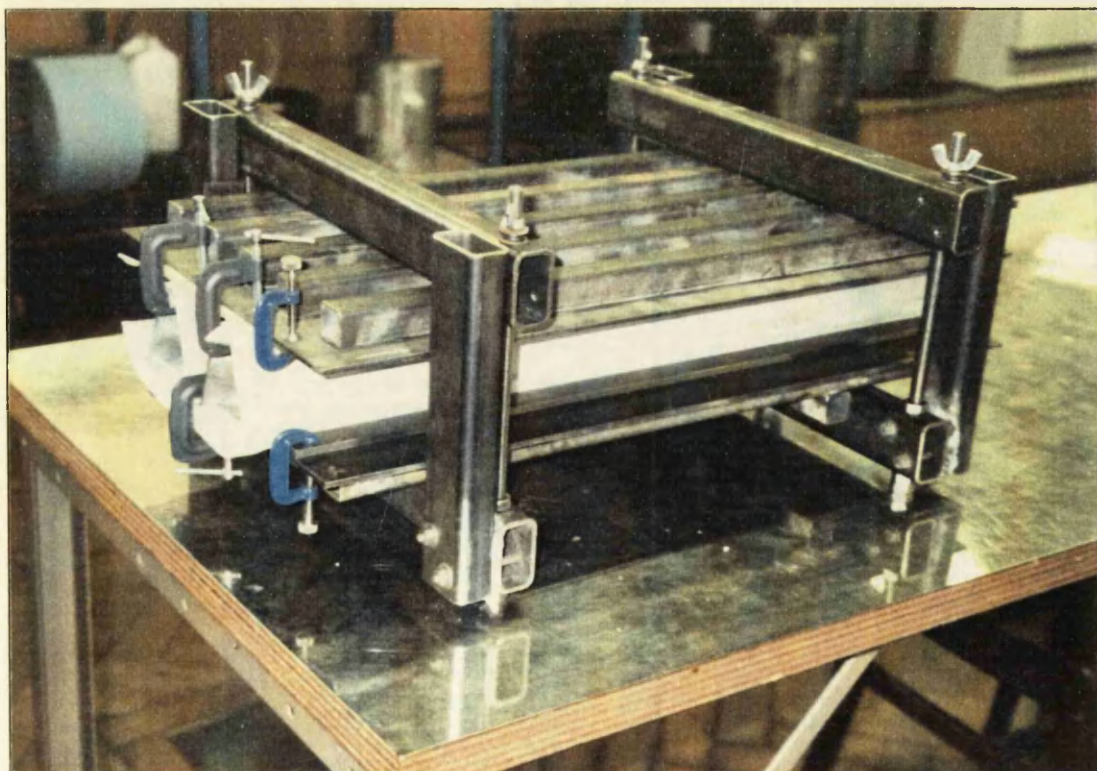


Photo 5.2 View of model 0-4b and frame

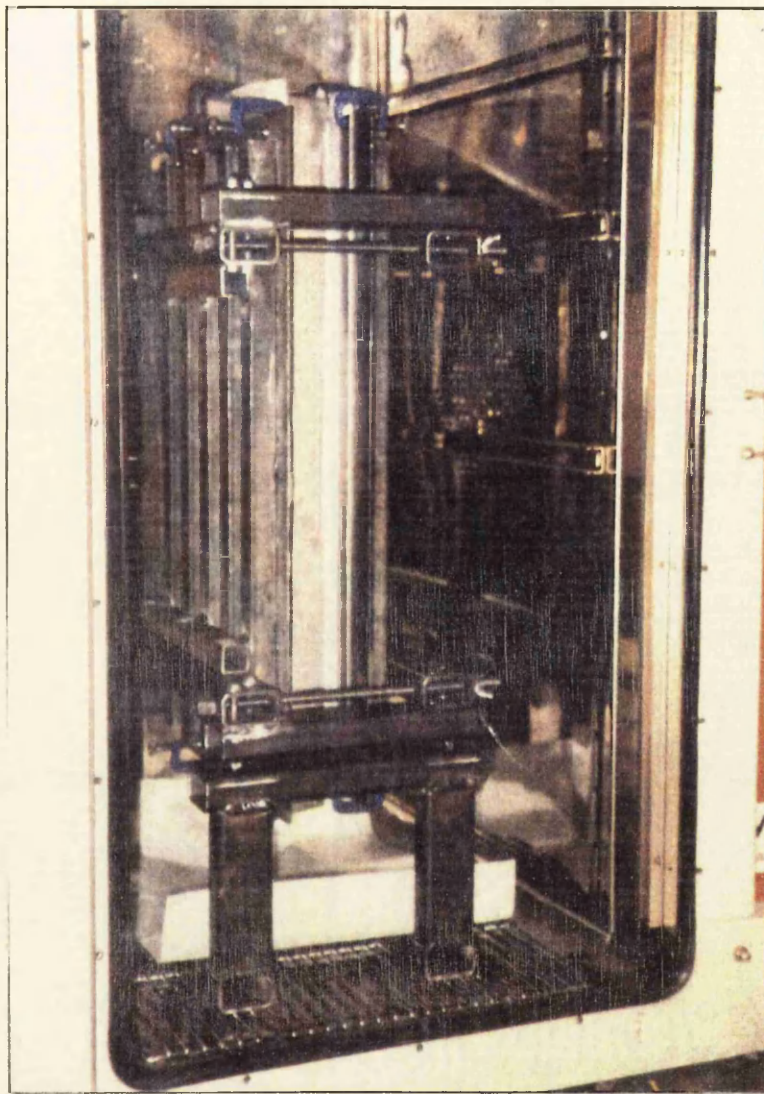



Photo 5.3 Model 0-4b in the oven

Another very important point to mention is that the core of the models had to be manufactured with the joining of half corrugations, i.e.

 This was done firstly due to the fact that facilities within the University premises could not provide for a continuous corrugated core and secondly that the behaviour of that special corrugation joining could be examined during the experiments so that suggestions for the manufacture of large (real size) scale corrugated-core sandwich structures could be done to the marine industry. It is worth mentioning that the web depth in real size sandwich structures can reach 1 m (SWATH).

A few suggestions are offered by Marshall [24] to aid in living with the problems of sandwich bonding and more general information is also provided in [24]:

- Make sure the core is properly sized to fit the space it is intended to occupy.
- The elevated temperatures which most core-to-facing adhesives require for curing are often inaccurately measured.
- Most adhesives flow at an early point in the cure cycle.
- Inserts or heavy members being cured as a part of a very light assembly will heat up much more slowly, giving rise to warpage problems on cool-down.
- Be sure to provide a route for the escape of trapped air and gases from a totally enclosed part while it is being cured.
- Caul plates should be carefully matched to the job they are expected to perform.
- Make sure that core, pre-cured or rigid edges, inserts, skins and other relatively unyielding details assembled in the lay-up have close enough dimensional control to allow adhesives or resins to achieve the target strengths.

The fabrication procedure developed on the first of the five bending specimens, and retained for the remaining, is as follows:

- Marking of the top and bottom face plate to indicate the areas where shot-blasting should take place.
- Shot-blasting of the marked areas of facings and flanges at over the joint areas takes place as it was found [7] that gives

improved short term strength.

- All shot-blasted surfaces are degreased with acetone.
- Webs are assembled first with the aid of clamps bearing in mind that the end corrugated core should be as flat as possible. (This is mentioned because the final web components coming from the bending machine have a lot of imperfections as far as web angle is concerned, i.e. it is quite difficult to get a perfect specimen.)
- Greaseproof paper is put between the plate of the frame and the face plate of the model to prevent adhesive getting in contact with both these metal surfaces.
- Adhesive is applied with the aid of a gun, first at the bottom flanges of the corrugated core.
- The corrugated core is then positioned on the bottom face plate - one edge first and the other is pushed slightly within the space provided by the bottom plate.
- Adhesive is applied at the top flanges of the corrugated core.
- The top plate is then positioned on the corrugated core. Markings on the corrugated core show where exactly the top plate should be positioned. These markings have been put when the model was dry.
- After that, a check of the dimensions should be performed.
- The whole model is put on the top of a metal base especially designed for this purpose, drawing of which can be found in Fig. 5.8. In order to do that, the clamps, which previously held the flanges of the corrugated core only, are now holding

simultaneously both the flanges and the plates at the top of the model. The clamps at the bottom of the model are removed.

- The final step of the manufacture process is to put the model in the curing oven at 125°C for approximately four and a half hours.

The five models which were used during the four point bending tests are shown in Photos 5.4 - 5.8.



Photo 5.4 Model 0-4b

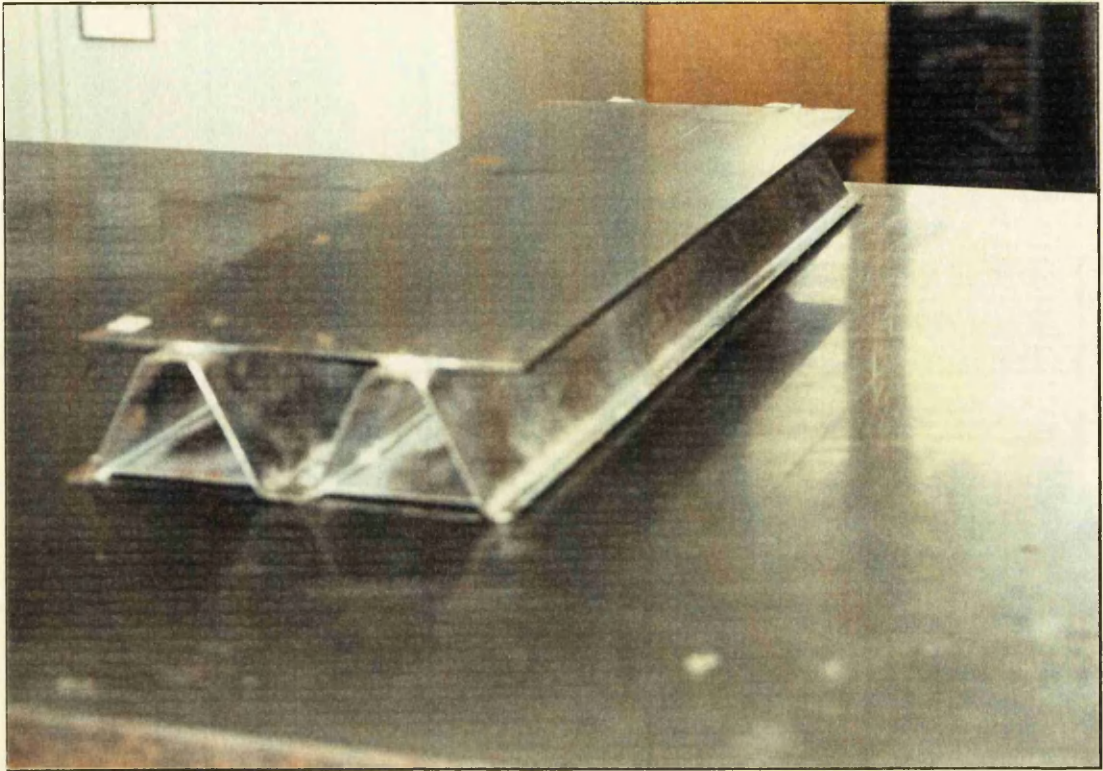


Photo 5.5 Model 1-4b

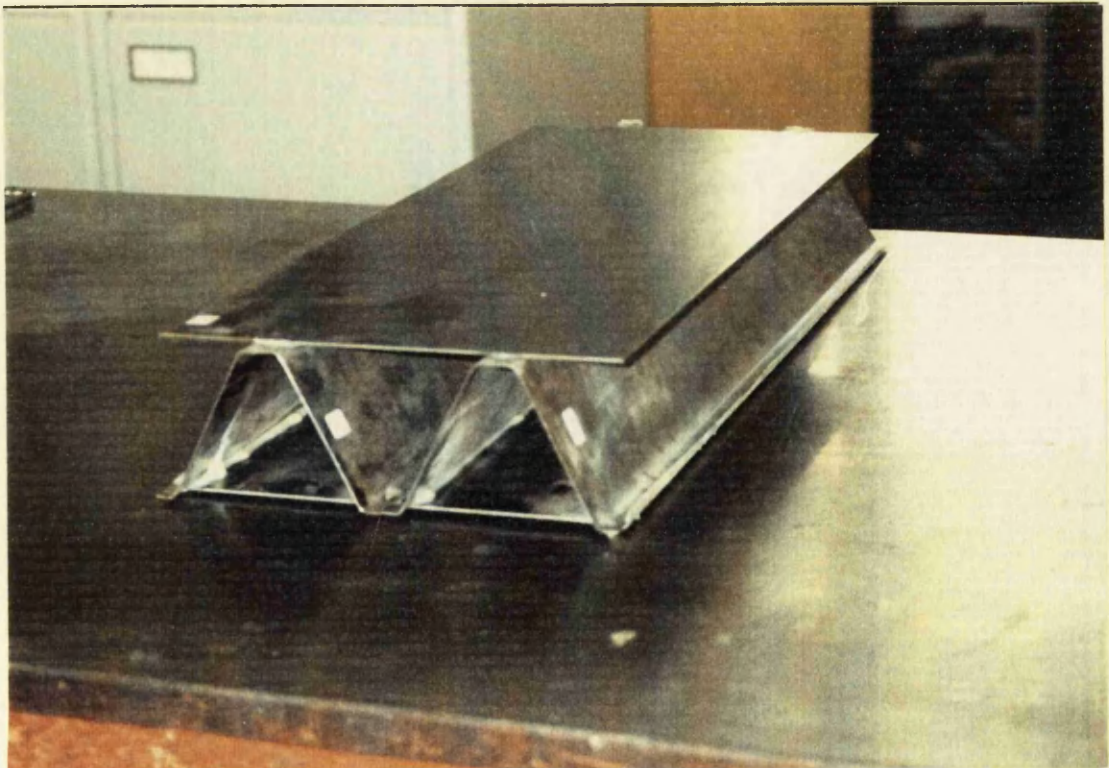


Photo 5.6 Model 2-4b

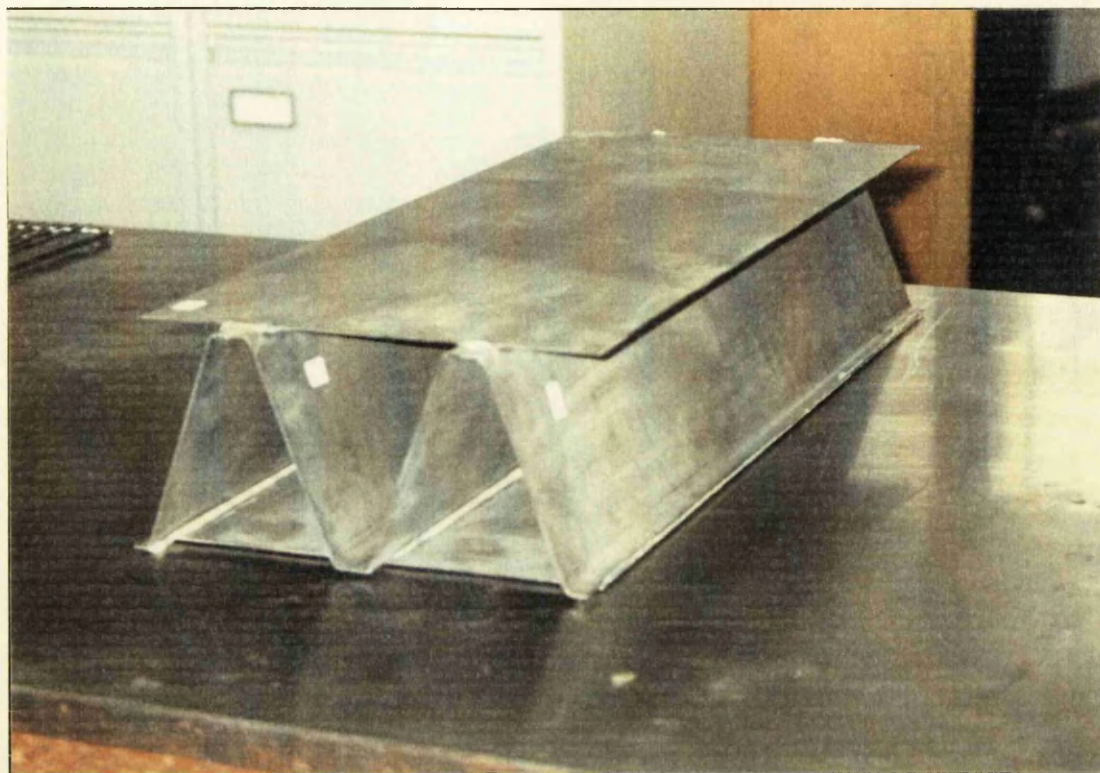


Photo 5.7 Model 3-4b



Photo 5.8 Model 4-4b

5.4 THE TENSILE TESTS

Tensile tests were also performed to evaluate any variations in Young's modulus of elasticity for each part of the model. These tensile tests were essential for this project since the models were constructed from cold rolled steel plates cut in different directions. A number of 'strange' first results were found which could be corrected and explained with the aid of those tensile tests. Fifteen specimens, like that appearing in Fig. 5.9, were cut with a hacksaw from the top, bottom and web (*mid* at the table of the results) plate away from the deformed region of each model after their four point bending tests. The dimensions of the specimens were dictated by the size of the models and those recommended at the British Standard (BS 18:1987) for tensile tests. The results of the tensile tests appear in Table 5.4 and Fig. 5.10. All further calculations of bending and axial compression strength and all diagrams of Chapter 6 are based on those values of Young's modulus. More specifically, during the calculations, the core Young's modulus was fixed as the rounded up value corresponding to the midplate specimen, while for the face modulus of elasticity, the least conservative value between the top and bottom plate specimens was selected as shown in Table 5.5.

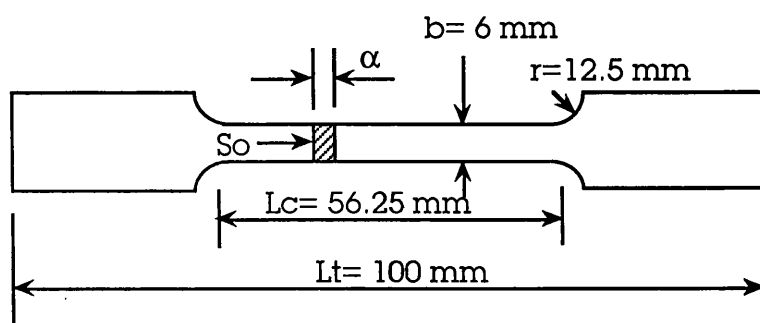


Fig. 5.9 The dimensions of each tensile test specimen

Specimen	So(mm ²)	Force(N)	Lf(mm)	Lo(mm)	e	E(KN/mm ²)
O1 (BOT)	9	3375	25.04	25	1.60E-03	234
O2 (MID)	9	3275	25.042	25	1.68E-03	217
O3 (TOP)	9	3200	25.04	25	1.60E-03	222
11 (BOT)	6	800	25.015	25	6.00E-04	222
12 (MID)	6	800	25.015	25	6.00E-04	222
13 (TOP)	6	625	25.012	25	4.80E-04	217
21 (BOT)	9	2725	25.034	25	1.36E-03	223
22 (MID)	6	750	25.015	25	6.00E-04	208
23 (TOP)	9	1660	25.02	25	8.00E-04	231
31 (BOT)	9	2750	25.036	25	1.44E-03	212
32 (MID)	9	3500	25.044	25	1.76E-03	221
33 (TOP)	9	3150	25.036	25	1.44E-03	243
41 (BOT)	9	2000	25.025	25	1.00E-03	222
42 (MID)	9	3000	25.04	25	1.60E-03	208
43 (TOP)	9	2300	25.028	25	1.12E-03	228

Table 5.4 The results of the tensile tests

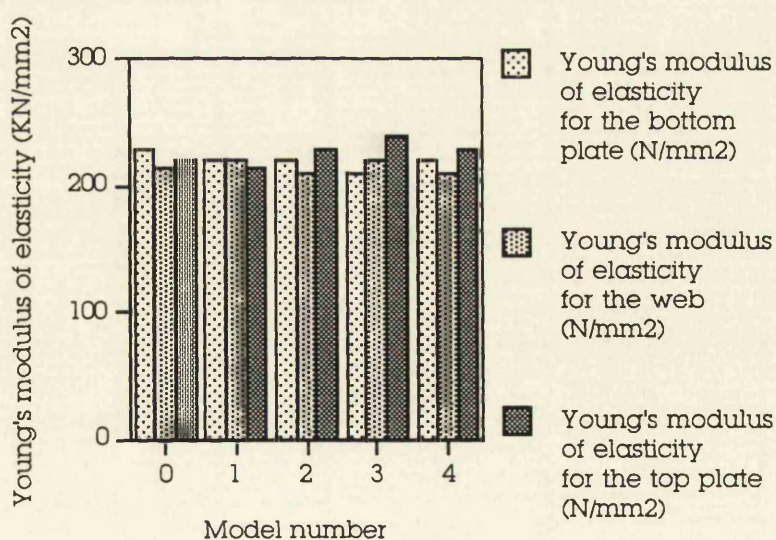


Fig. 5.10 Diagrammatic illustration of E variation

MODEL NUMBER	0-4b 0-3b	1-4b 1-c	2-4b 2-c	3-4b 3-3b	4-4b 4-c
E _{core} (KN/mm ²)	220	220	210	220	210
E _{face} (KN/mm ²)	230	220	230	230	230

Table 5.5 The final values of E for all models

CHAPTER 6

THE PROJECT: THE MODELS TESTS AND FINAL RESULTS

6.1 INTRODUCTION

The next phase of the project involved development of an understanding of the typical overall modes of failure (i.e. the failure mechanisms), the areas of the structure in which these dominate and their relationship to dimensional variables. That was done through experimentation, supported by theoretical analysis. More specifically, simple beam theory was applied in the four and three point bending tests for the calculation of bending stresses in the longitudinal direction and theory of Chapter 3 (which indicates the present standing of theoretical work) for the compression tests, for the calculation of the compressive stresses in the longitudinal direction of the panel.

As it is pointed out by Smith et al. [7], the corrugated core is highly directional and is generally stiff enough to make a distinct contribution to the flexural rigidity in the longitudinal direction but is more compliant in the transverse direction. Also, the core structure is a series of plate elements and as such permits local instabilities. In other words, there are many interactions among the webs, the top and bottom plates and the flanges which result in a non-uniform stress behaviour. For this reason, finite element analysis is quite useful, otherwise, much information data has to be drawn out during the experiments with the use of numerous strain gauges.

6.2 STRAIN GAUGES INSTALLATION

To measure the microstrains created during the experiments, rosette strain gauges (EA-06-060RZ-120 with 1.5 mm active length) were installed at certain points on each model that can be seen specifically for model 0-4b in Fig. 6.1 (the strain gauge installation points for the rest of the models are shown in Section 6.6). Appendix C shows the procedure for that installation. As it is shown in Photo 6.1, a large number of strain gauges were first put on model 0-4b to have a better visualisation of the strain-stress distribution of this model, which for this kind of construction is rather complicated as pointed out above. From simple beam theory, the maximum bending stress in the longitudinal direction occurs at mid span and therefore, all strain gauges were positioned at midlength of the model.

Installation of strain gauges on the outer web faces of the rest of the models was avoided due to irregular and local performance of this part of the sandwich construction detected mainly with the aid of graphs taken during some preliminary tests. This irregular performance can be explained, again, mainly due to the interaction between the top - bottom plates and the web. The web is influenced by the deformation of both top and bottom plates through its flanges and, therefore, the strains measured on it do not have a normal linear behaviour (at least up to the elastic point).

The values of the microstrains were recorded by an ORION data logger using the program appearing in Appendix E. The type of 1/4 bridge wiring was used in this case. Afterwards, the microstrains were translated into principal strains and stresses using spreadsheets based on the formulae of Appendix F.

(continued on page 100)

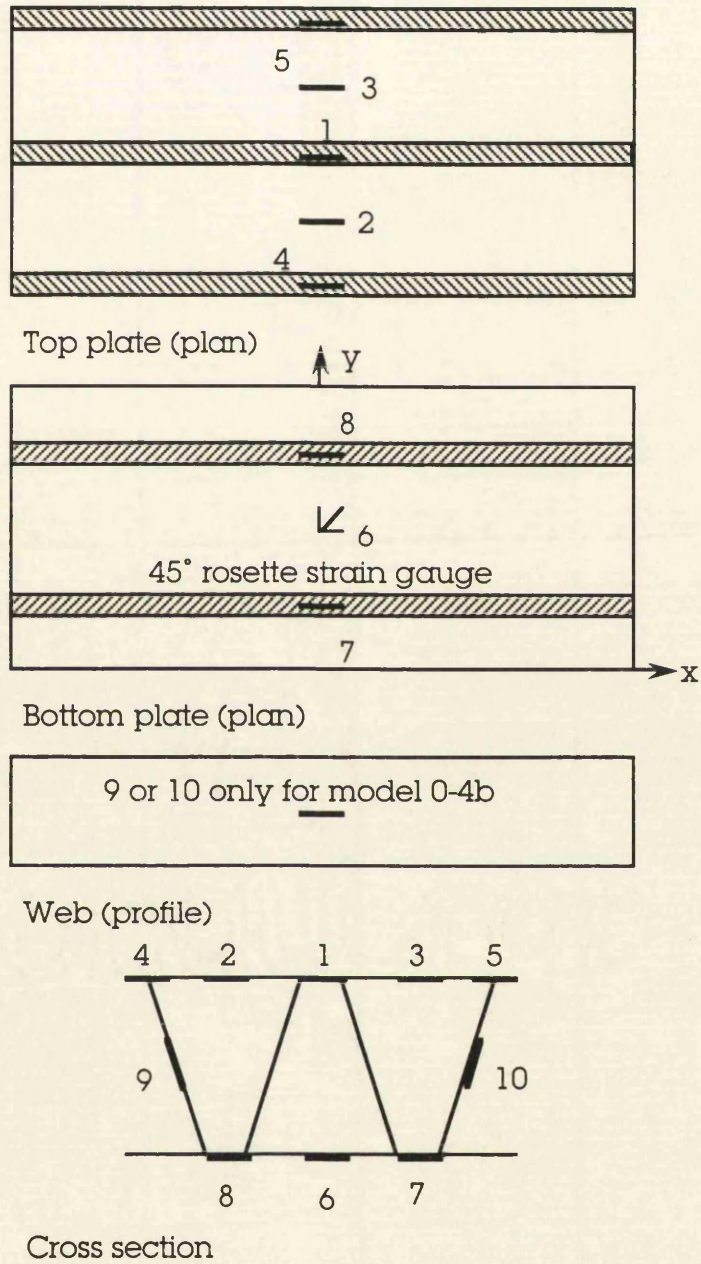


Fig. 6.1 The points where strain gauges were installed



Photo 6.1 Model 0-4b after the strain gauges installation and wiring

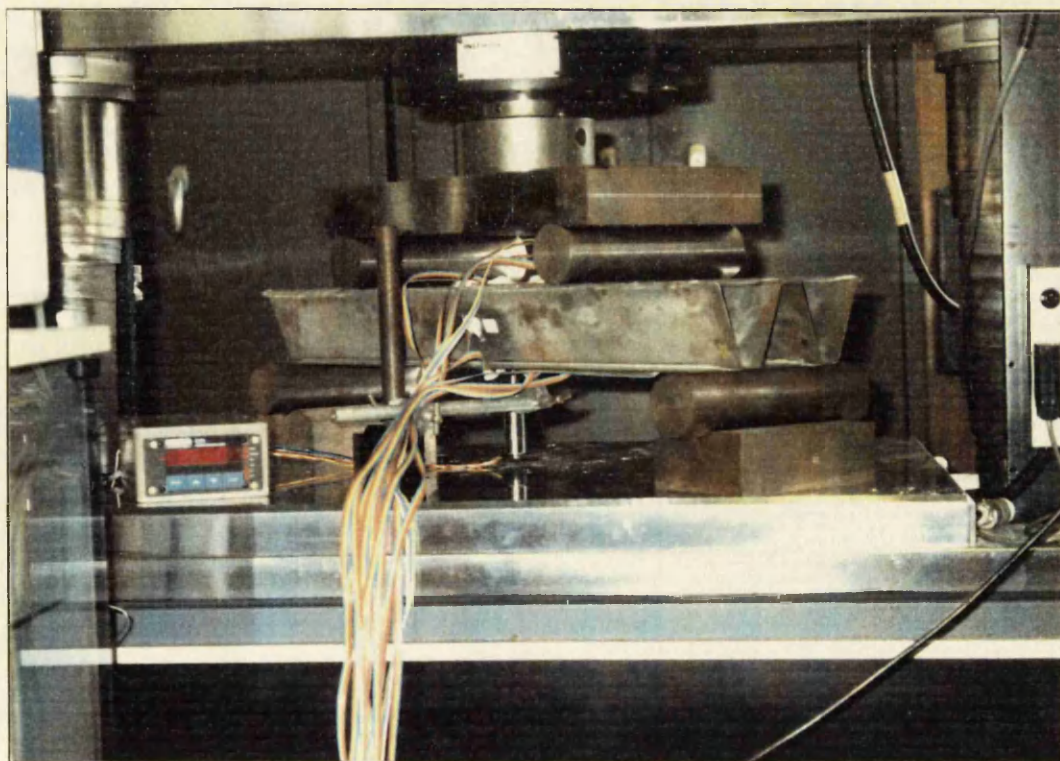


Photo 6.2 Model 0-4b at INSTRON machine before the four point bending test

6.3 THE FOUR POINT BENDING TESTS

The four point bending tests were performed with the aid of a 250 KN INSTRON machine. Photo 6.2 shows model 0-4b at INSTRON machine. A linear voltage displacement transducer (LVDT) was positioned directly beneath the lower plate of the model at midlength to measure maximum beam deflection - especially the bottom plate deflection - as illustrated in Photo 6.2. A calibration procedure had to be followed for it before each test. Measurements of the top plate deflection were taken through the graph of INSTRON plotter, giving the load vs deflection.

Six tests preceded the main four point bending tests in order to draw out as much information about the behaviour of the model within the elastic region as it was possible. More specifically during:

- **Test 1:** Model 0-4b was loaded up to 10 KN with increments of 1 KN.
- **Test 2:** Model 0-4b was loaded up to 20 KN with increments of 2.5 KN.
- **Test 3:** A constant load of 20 KN was applied to model 0-4b for 6 hours. First indications of creep appeared to take place.
- **Test 4:** Model 0-4b was loaded up to 25 KN.
- **Test 5:** A constant load of 20 KN was applied to model 0-4b which, this time, was overturned upside down.
- **Test 6:** Model 0-4b was loaded up to 30 KN.

From these preliminary tests, an observation of possible creep effects in the adhesive was apparent. Therefore, a creep test was proposed for each model. The constant load which would apply had to be well below the load corresponding to the elastic limit of each model, so that no plastic deformation would occur before the tests to determine the yield point and the progressive plastic collapse behaviour. Some special points that we have to mention about creep tests are:

- The maximum time of creep load application was seven hours and a half since the machine could not be left safely

unattended under load for longer.

- Sometimes INSTRON machine had problems in maintaining the creep load level constant and certain adjustments had to be made at certain time intervals.
- Measurements concerning microstrains and deflection from LVDT were logged on special roll paper and were taken one each half an hour at the beginning and throughout the test, and one every quarter of hour at the end of the test, so that enough data would be available for plotting the graph.
- It may be possible that the four point bending tests following the creep ones were affected, in a way, by them and variations on bending stresses could have been occurred because of them.
- The deflection of the model right after the creep tests had increased in relation to that before them, but before the four bending tests it was maintained at its initial levels.

Ten four point bending tests took place, two for each model, which can be summarised as follows:

- **Test 7:** A constant load of 25 KN was applied to model 0-4b for seven and a half hours.
- **Test 8:** Model 0-4b was loaded up to and beyond its yield point with 0.5 mm/min rate
- **Test 9:** A constant load of 10 KN was applied to model 1-4b for seven hours.
- **Test 10:** Model 1-4b was loaded up to and beyond its yield point with 0.5 mm/min rate.
- **Test 11:** A constant load of 35 KN was applied to model 2-4b for seven hours.
- **Test 12:** Model 2-4b was loaded up to and beyond its yield point with 0.5 mm/min rate.

- **Test 13:** A constant load of 15 kN was applied to model 4-4b for seven hours.
- **Test 14:** Model 4-4b was loaded up to and beyond its yield point with 0.5 mm/min rate.
- **Test 15:** A constant load of 35 kN was applied to model 3-4b for seven hours.
- **Test 16:** Model 3-4b was loaded up to and beyond its yield point with 0.5 mm/min rate.

Initially, the span between load points was 590 mm but when edge failure appeared during Test 8, as illustrated in Photo 6.3, the span was reduced to 490 mm. That edge failure was largely expected due to the way the corrugated core had been constructed.

Photos 6.4-6.10 show the local deformations of most models during the tests and their final shape and condition after them. It can easily be observed that buckling of the webs and any other deformation occurred only adjacent to the points of load application causing some local but not global adhesive damage.

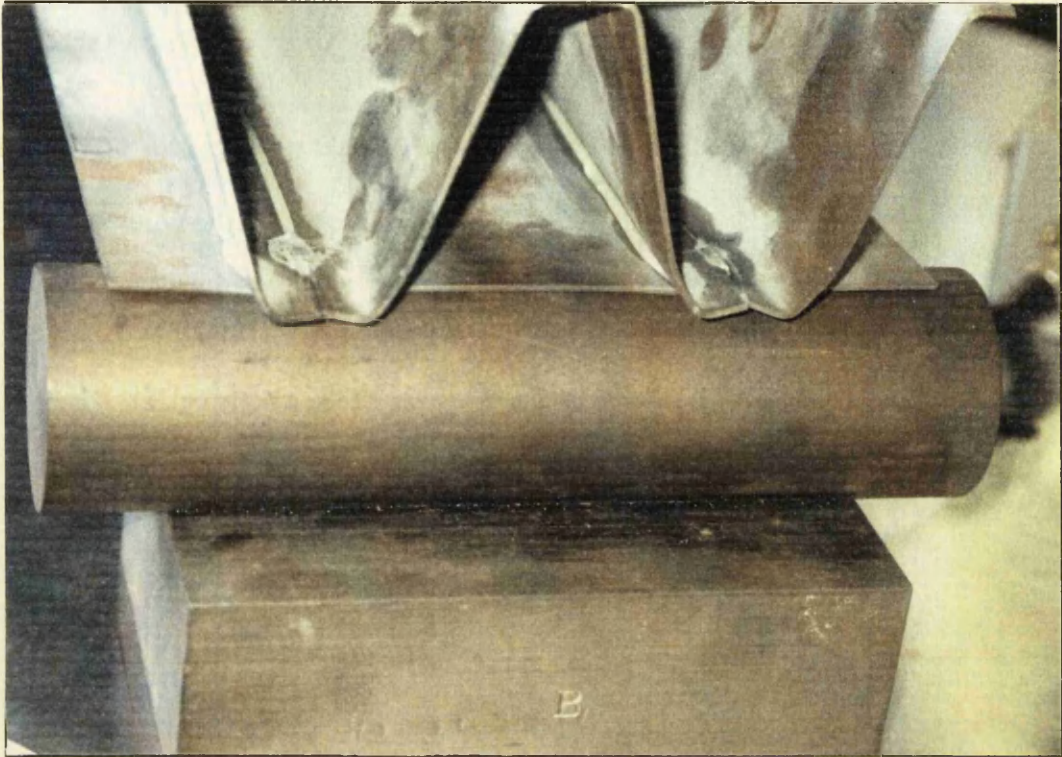


Photo 6.3 Model 0-4b: the edge failure during the bending test

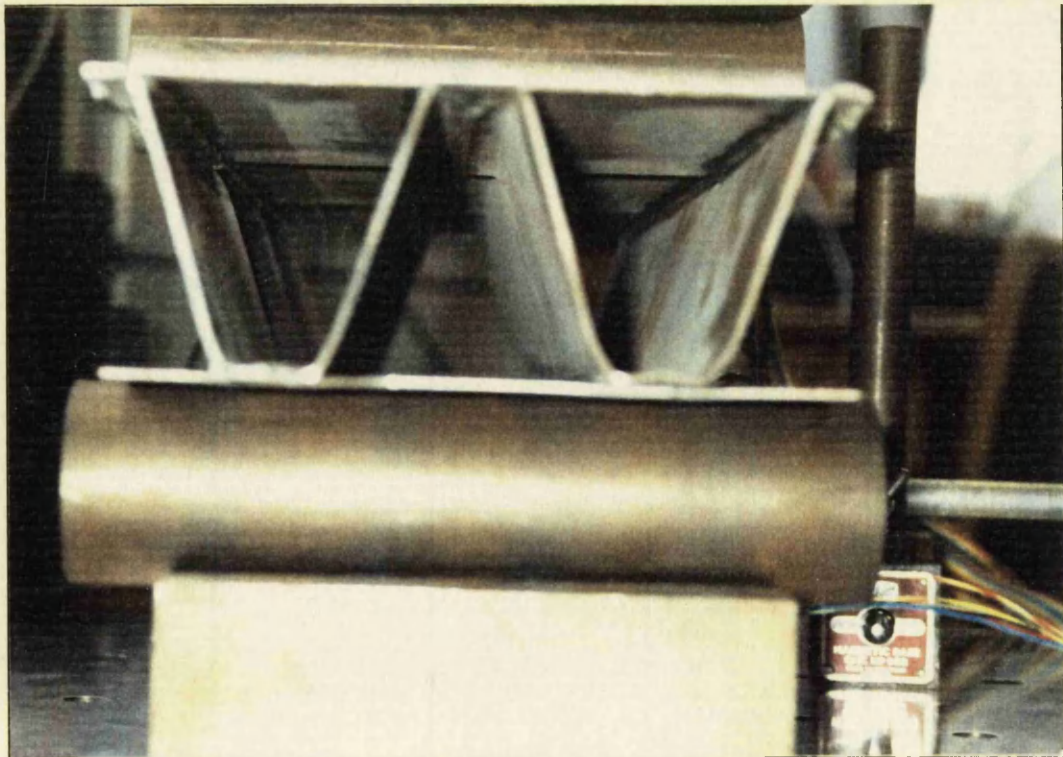


Photo 6.4 Model 0-4b: the buckling of the webs is apparent

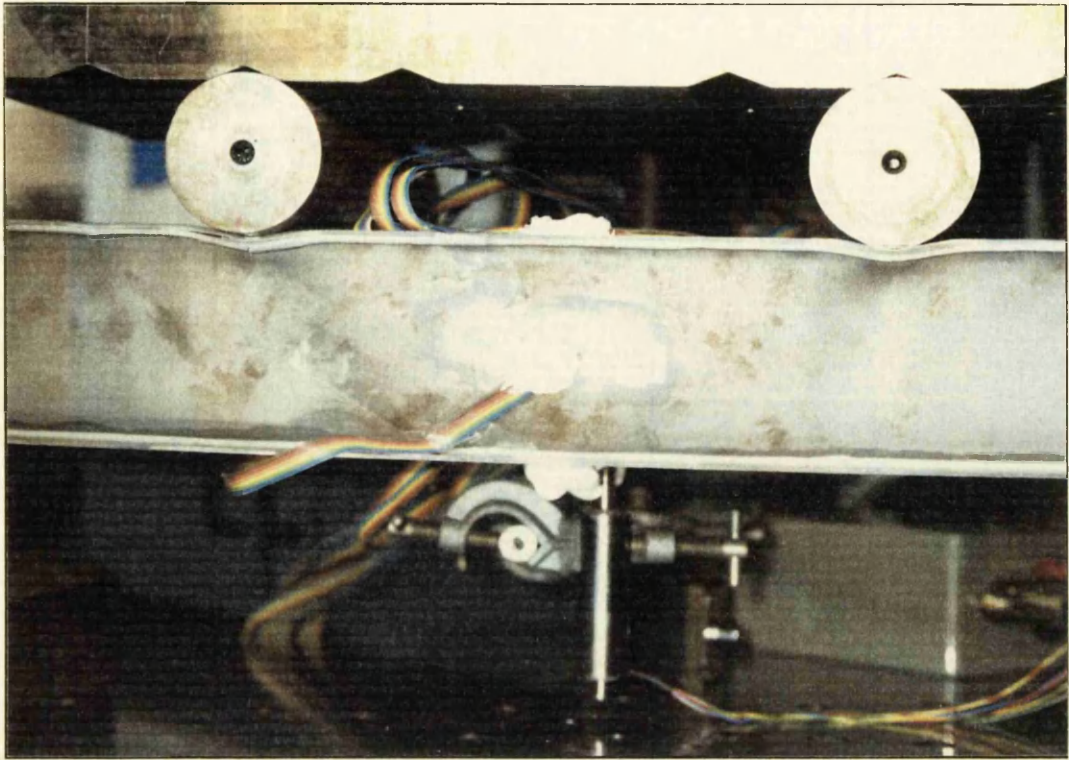


Photo 6.5 Model 0-4b: the local deformation of the top plate

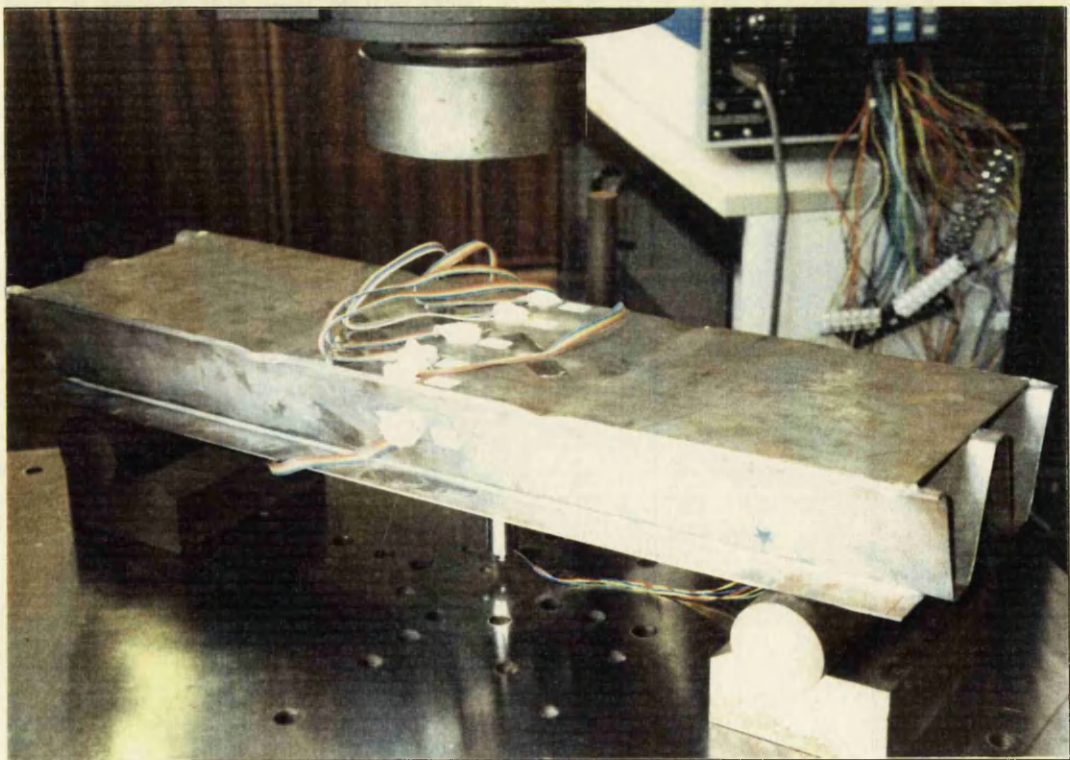


Photo 6.6 Model 0-4b after the four point bending test



Photo 6.7 Model 2-4b after the four point bending test

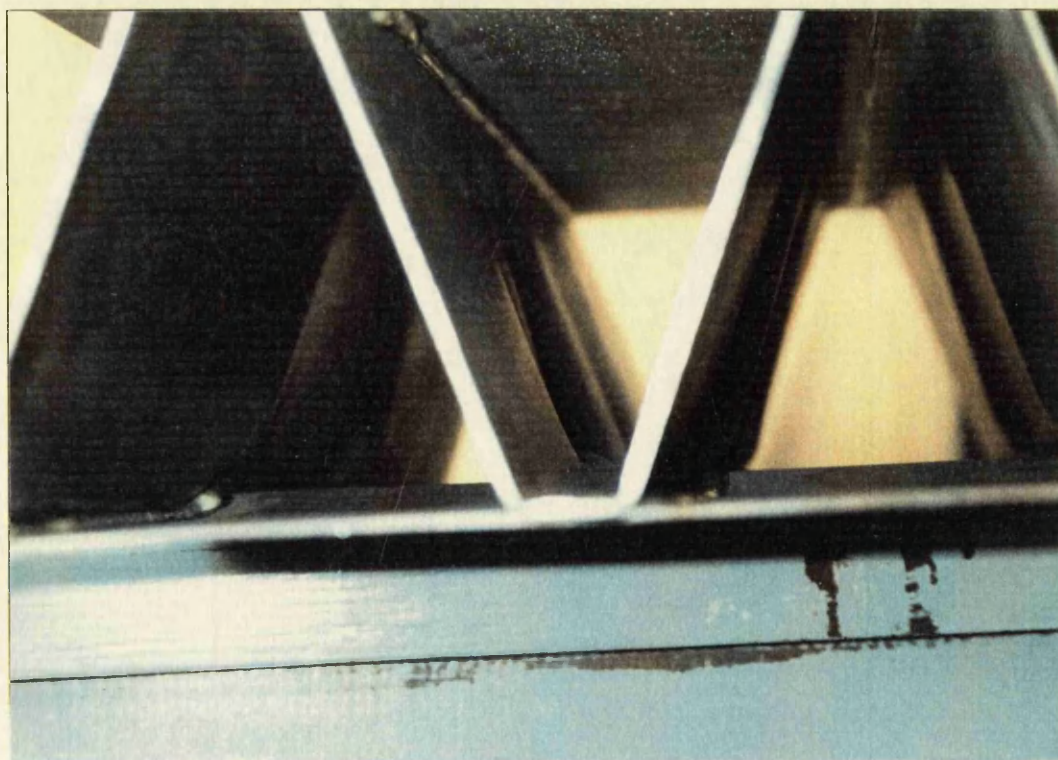


Photo 6.8 Model 3-4b: detail of the buckling of the webs

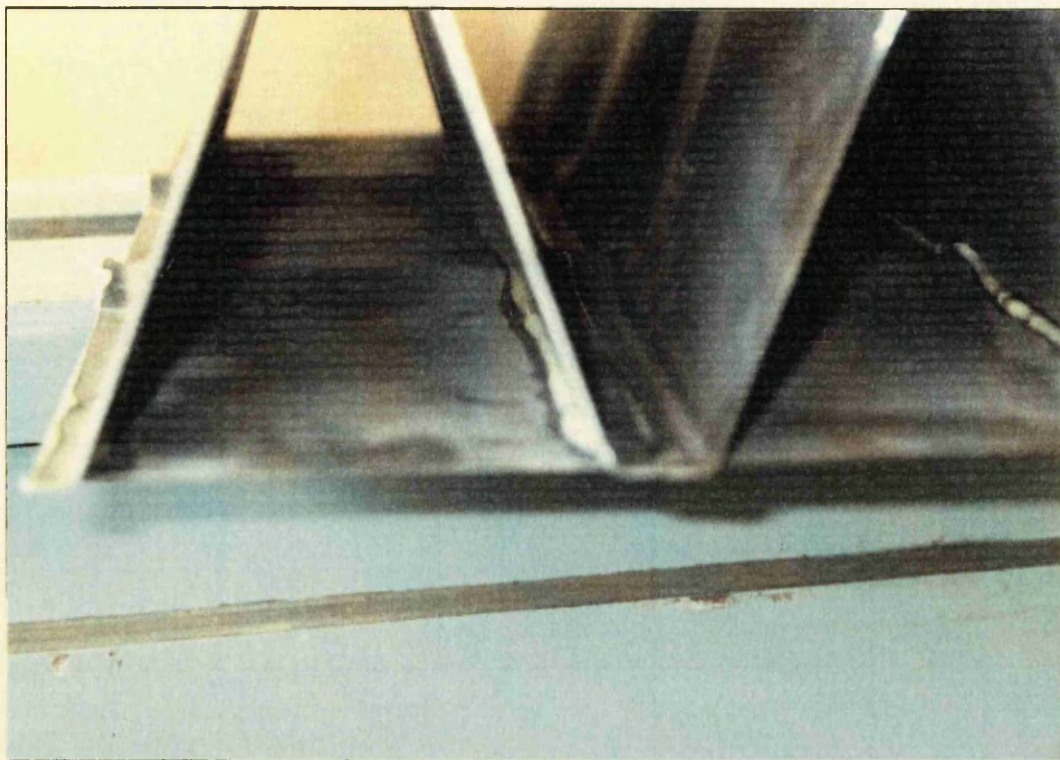


Photo 6.9 Model 3-4b: internal detail of the local deformation of the top plate

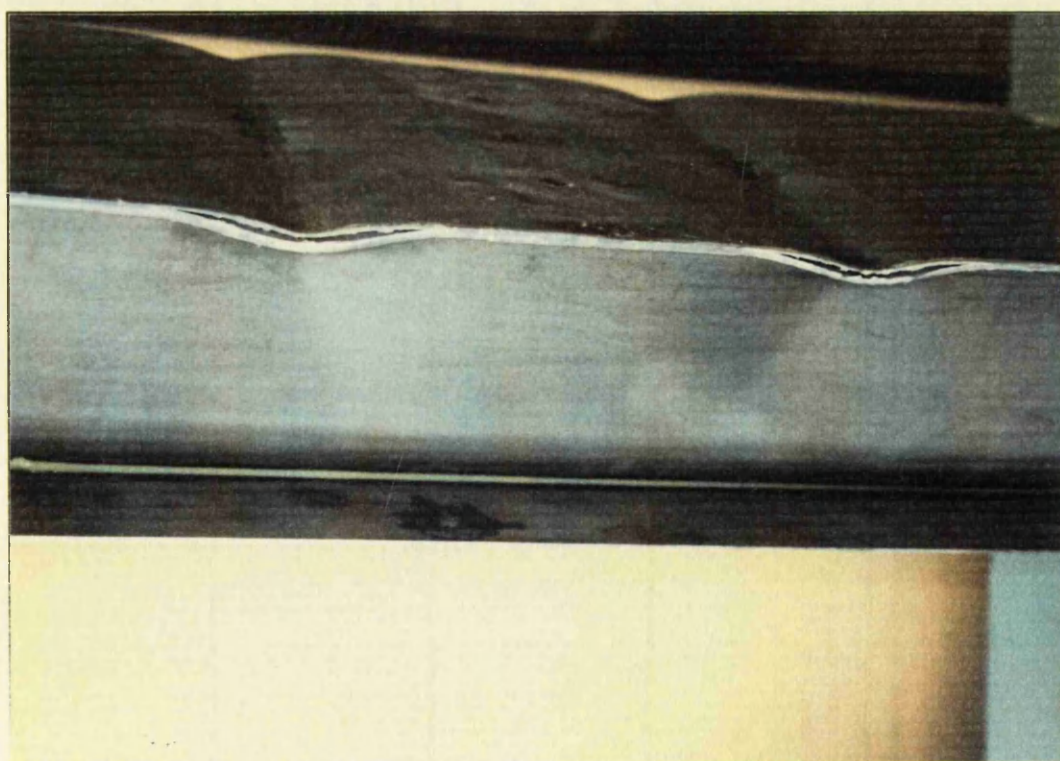


Photo 6.10 Model 3-4b: detail of the local deformation of the top plate

6.4 THE AXIAL COMPRESSION TESTS

The compression tests were also performed in the same INSTRON machine as the bending tests. In reality, the so called compression tests were column buckling experiments with clamped edges as shown in Photo 6.11. The compressive strength of the models should have been evaluated experimentally using a compressive test rig like that illustrated in Fig. 6.2.

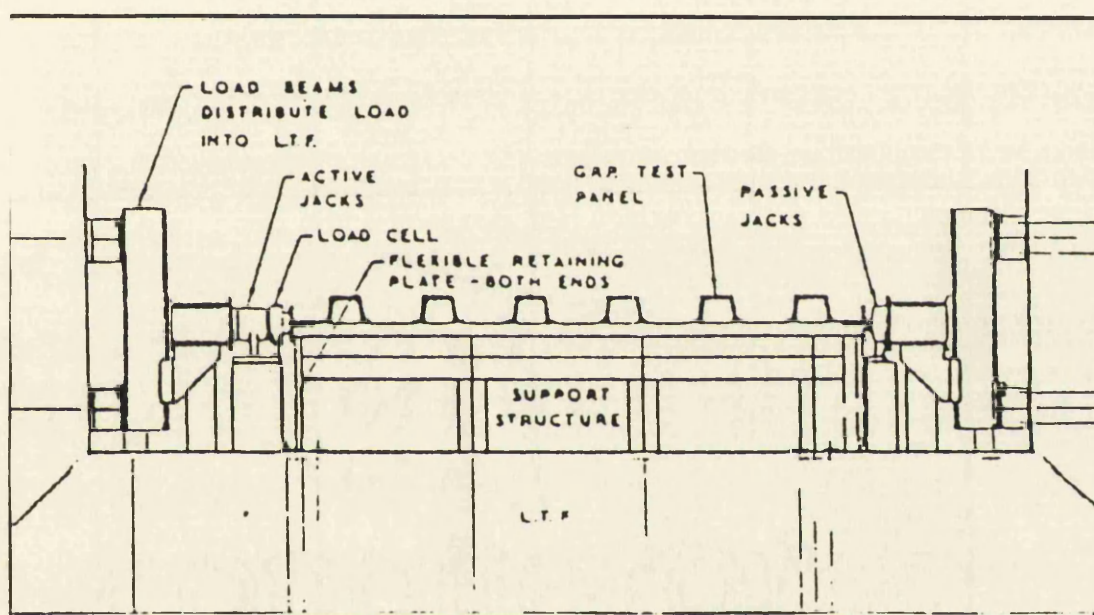


Fig. 6.2 Compression test rig [18]

Furthermore, conditions of simple or clamped support at the ends of test models should have had to be imposed with the aid of mechanisms carefully designed for this purpose, but there is no provision for this kind of equipment and facilities within the University premises.

All models which had previously been tested for bending were tested (duplicate models, of course) for column buckling but only three of them collapsed.

Three axial compression tests took place which can be summarised as follows:

- **Test 17:** Model 2-c was loaded up to a severe buckled shape with 0.5 mm/min rate.
- **Test 18:** Model 1-c was loaded up to a severe buckled shape with 0.5 mm/min rate.
- **Test 19:** Model 4-c was loaded up to a severe buckled shape with 0.5 mm/min rate.

Before the tests models edges were squared off gradually by means of a hacksaw, which resulted in a reduction of their length. Photos 6.12-6.21 show the modes of failure of models 2-c, 1-c and 4-c. All three models collapsed only at their upper part at quarter or less than quarter length where the load was applied, probably because both edges of the models were restrained and, having been not able to rotate, produced the prementioned type of deformed shape. It is easy to observe the development of plate buckling which was followed by adhesive debonding. The most symmetrical failure occurred at model 1-c, probably because it was the slenderest of the three and most suitable for (compression) column buckling test at INSTRON machine. This could imply that a longer and smaller in its cross section model with simply supported edges should have had to be manufactured if we had wished to see an S buckled shape throughout the whole length.

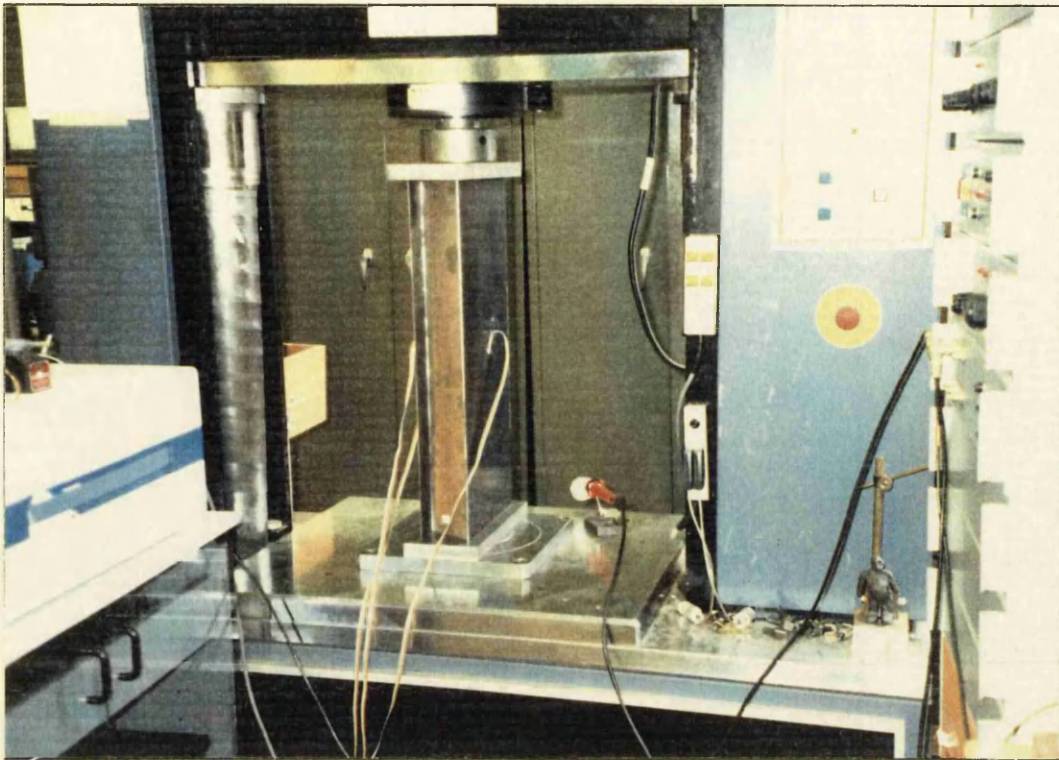


Photo 6.11 Model 2-c before the axial compression test

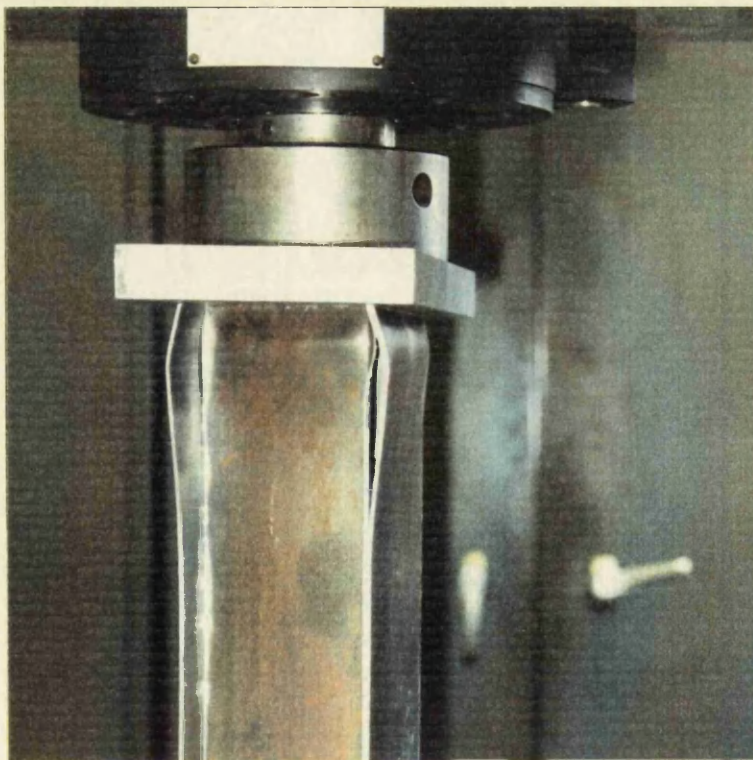


Photo 6.12 Model 2-c: the beginning of adhesive debonding and local buckling of the upper edge

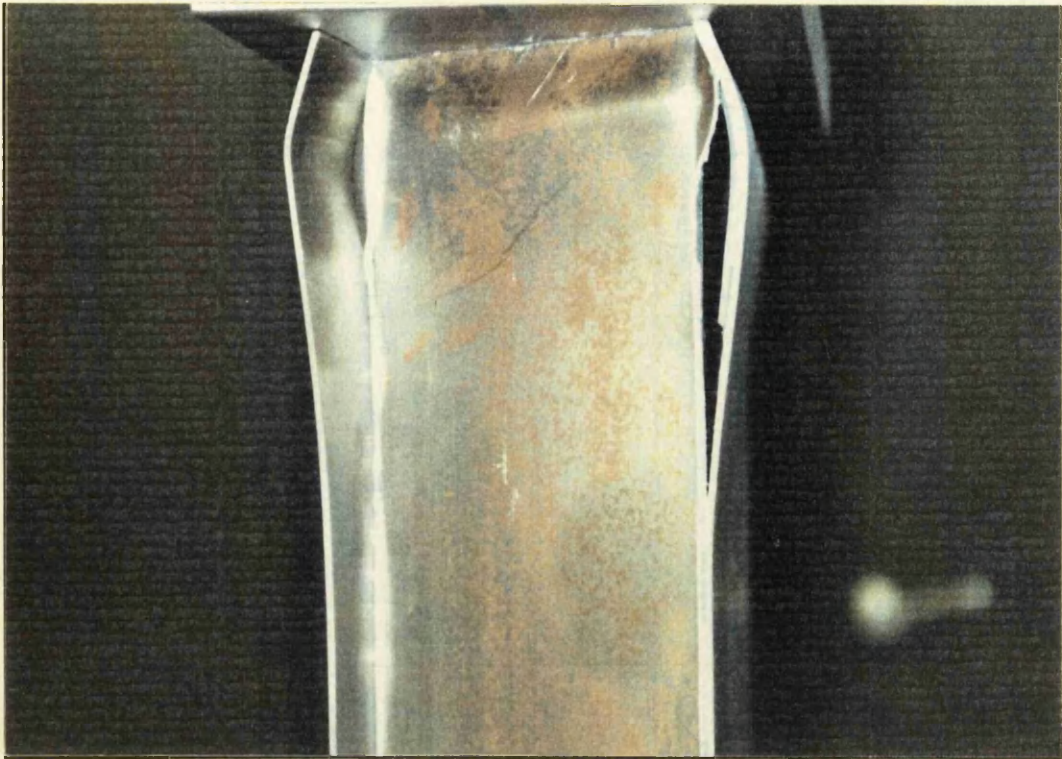


Photo 6.13 Model 2-c: the adhesive debonding and local deformation become more severe



Photo 6.14 Model 2-c after the axial compression test

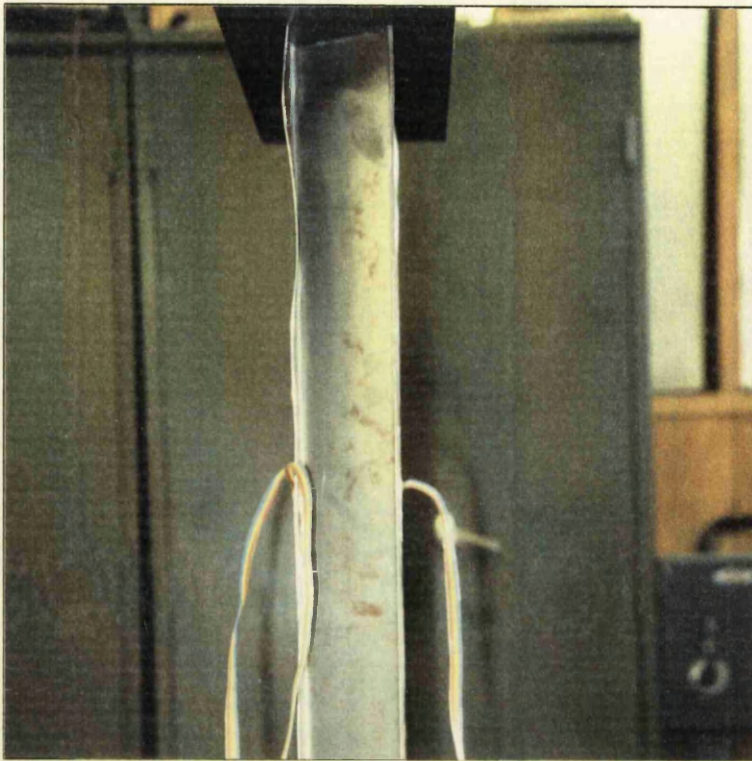


Photo 6.15 Model 1-c: the first signs of buckling



Photo 6.16 Model 1-c: local buckling continues



Photo 6.17 Model 1-c: a characteristic view of the continuing deformation

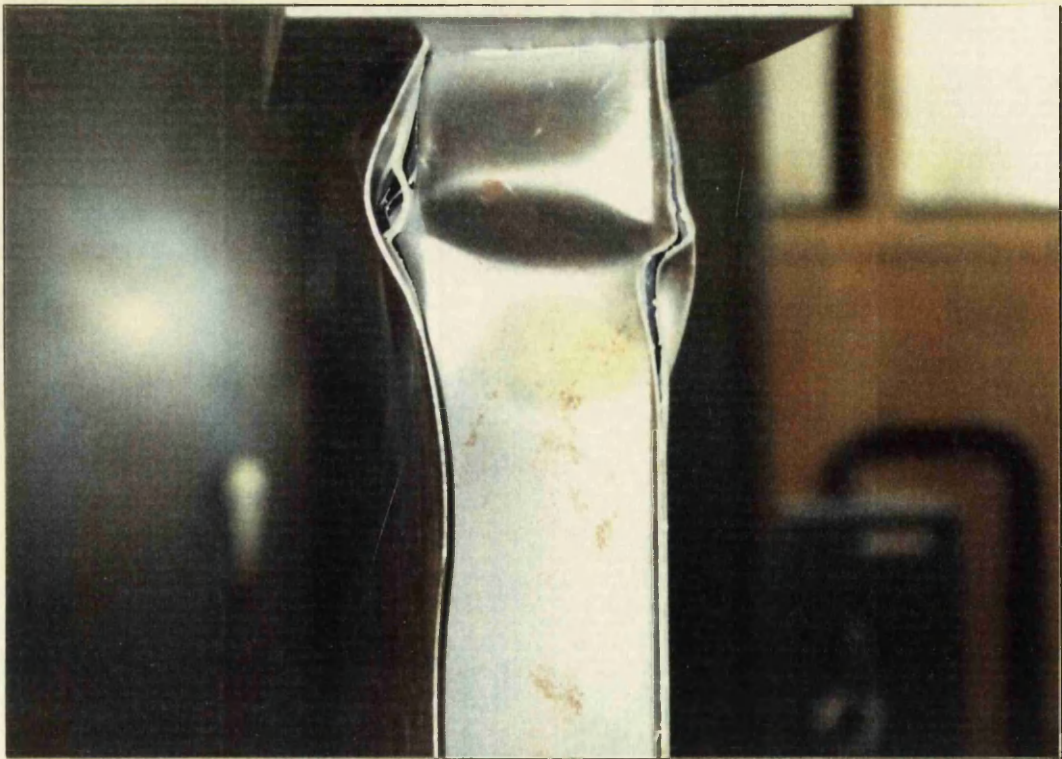


Photo 6.18 Model 1-c: adhesive debonding

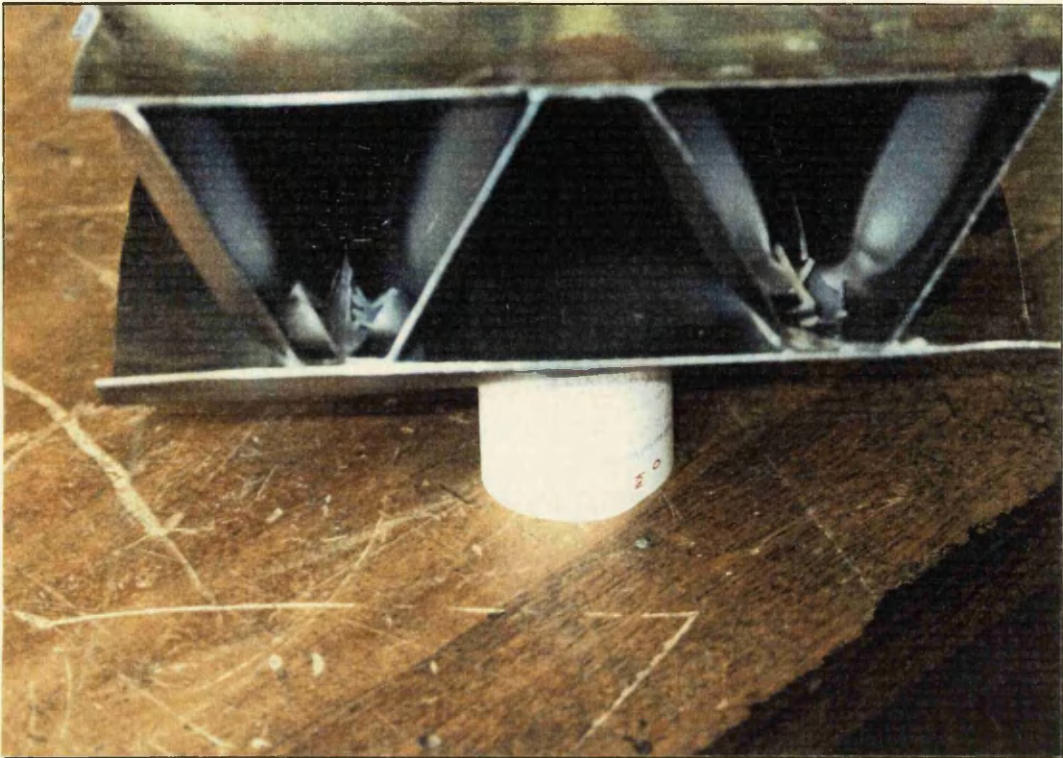


Photo 6.19 Model 1-c after the axial compression test

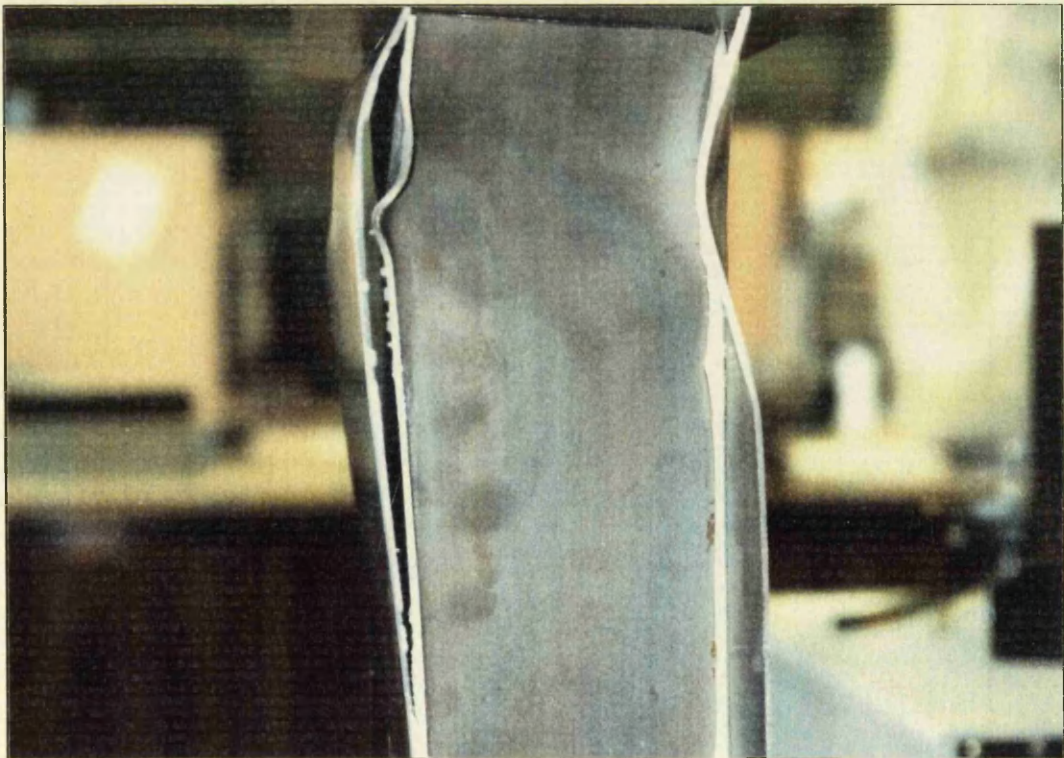


Photo 6.20 Model 4-c: adhesive debonding and local deformation

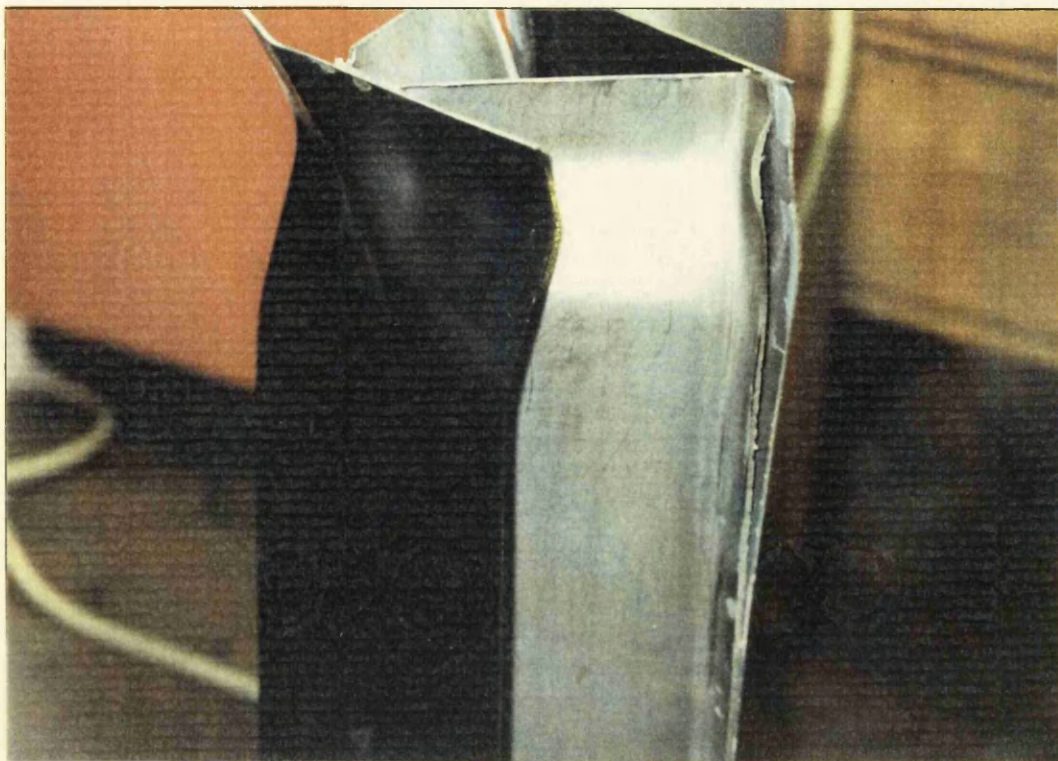


Photo 6.21 Model 4-c after the axial compression test

6.5 ADDITIONAL THREE POINT BENDING TESTS

Former models 0-c and 3-c, namely models 0-3b and 3-3b, which did not buckle during the column buckling tests, were tested in three point bending tests in INSTRON machine. These tests were performed mainly in order to cross check the results obtained from the four point bending tests. This time the load was applied at midlength and therefore the strain gauges had to be installed at points corresponding to a quarter of model length away from both its edges. The span between load points was fixed at 490 mm.

Two three point bending tests took place which can be summarised as follows:

- **Test 20:** Model 0-3b was loaded up and beyond its yield point with 0.5 mm/min rate.

- **Test 21:** Model 3-3b was loaded up and beyond its yield point with 0.5 mm/min rate.

Photos 6.22-6.24 show the position of model 0-3b at the machine and the final condition of both models after the experiments. Again, it can easily be observed that buckling of the webs and any other deformation occurred only adjacent to the points of load application causing some local but not global adhesive damage.



Photo 6.22 Model 0-3b before the three point bending test

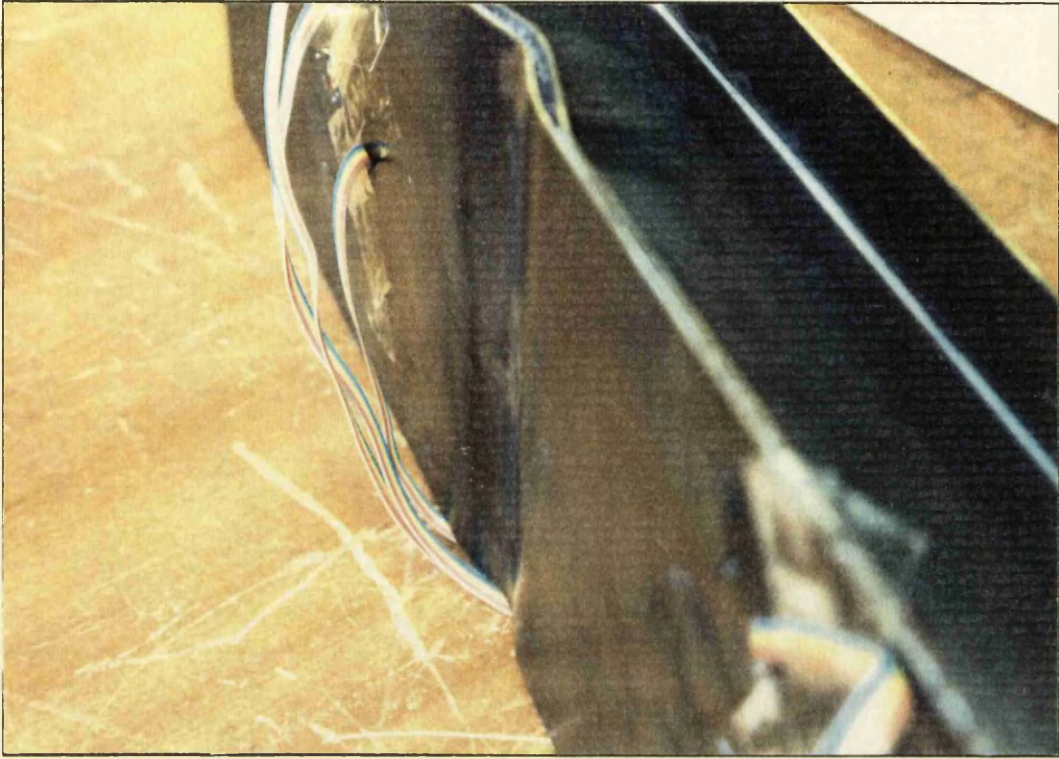


Photo 6.23 Model 0-3b after the three point bending test

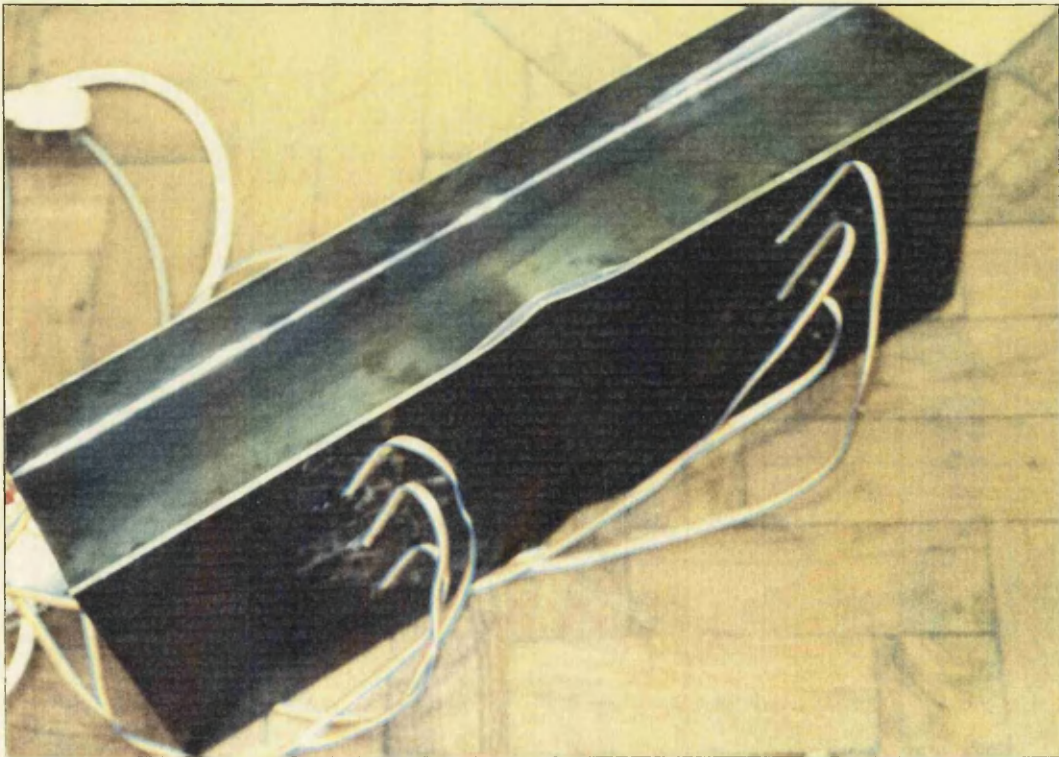


Photo 6.24 Model 3-3b after the three point bending test

6.6 THE RESULTS

To evaluate the bending and column buckling strength of the models, calculations had to be performed to translate the experimentally obtained strains of the rosettes into stresses along the x (longitudinal) and y (transverse) axes. This was done using a computer program based on the theory and formulae appearing in Appendix F.

For comparison, theoretical values of the bending and axial compression (column buckling) strength were also obtained using programs based on simple beam theory and formulae for bending and column buckling theory appearing in Appendix B.

Appendix D contains the basic Excel spreadsheets used to make calculations for the determination of the bending and compression stresses.

A better visualisation of the results is obtained through stress-strain-deflection diagrams. These were prepared for each test and appear as Fig. 6.8-6.38. The position and numbering of the strain gauges on each model is shown in Fig. 6.3-6.7.

(continued on page 123)

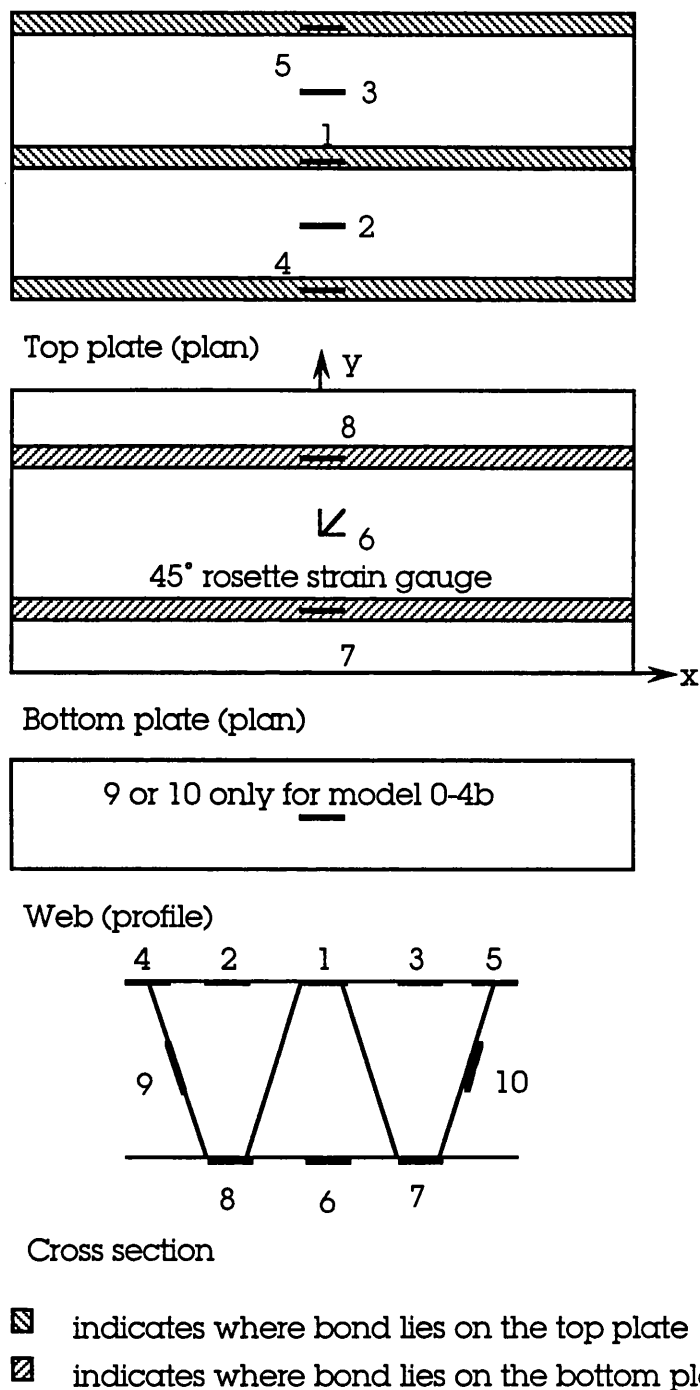


Fig. 6.3 The position and numbering of strain gauges on models 0-4b, 1-4b, 2-4b and 3-4b

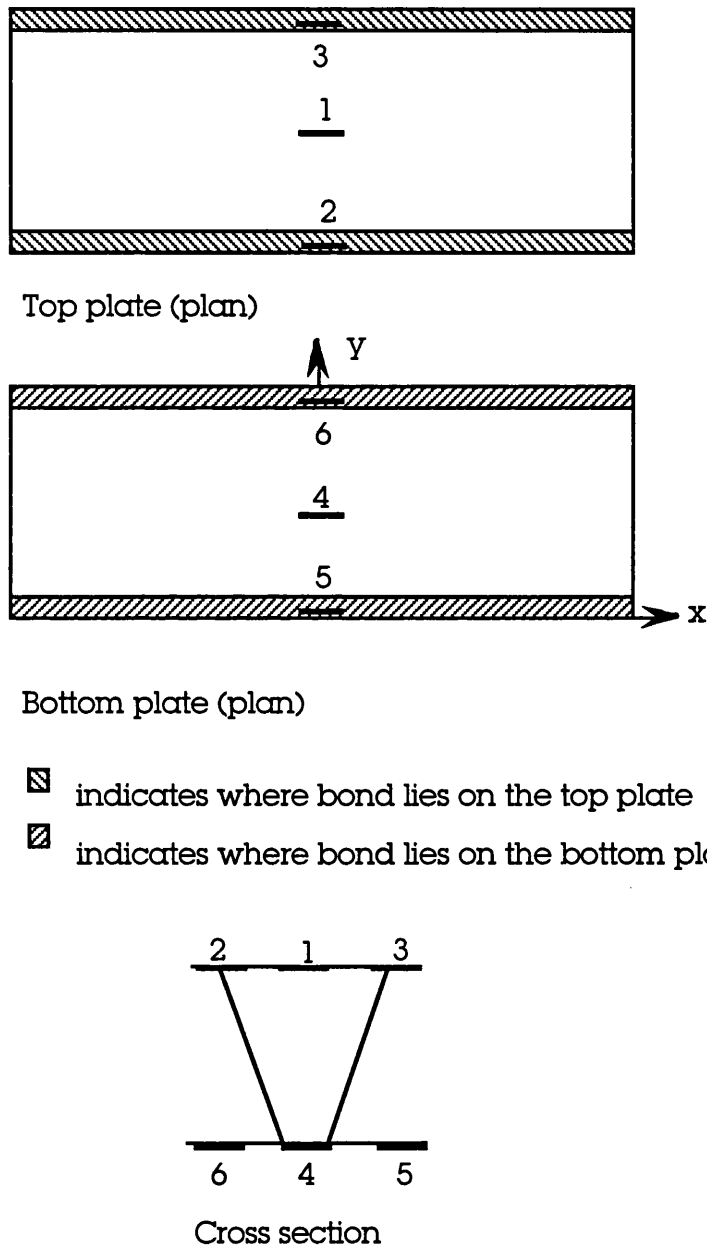


Fig. 6.4 The position and numbering of strain gauges on model 4-4b

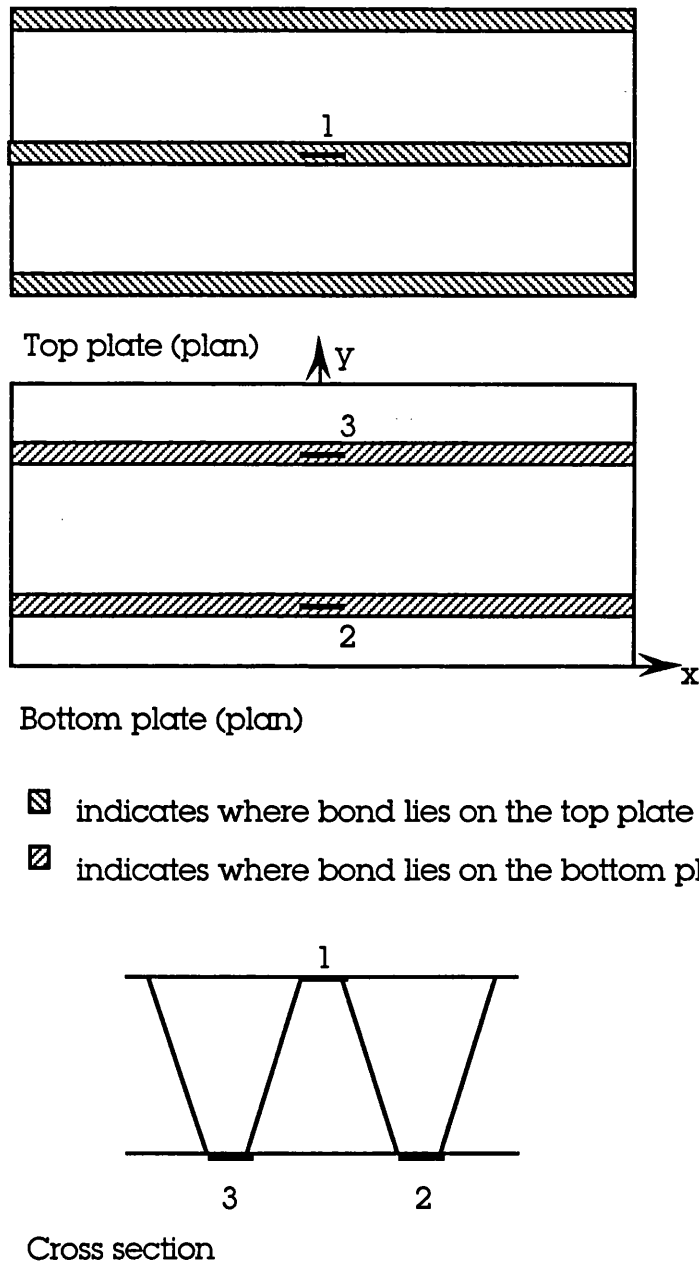
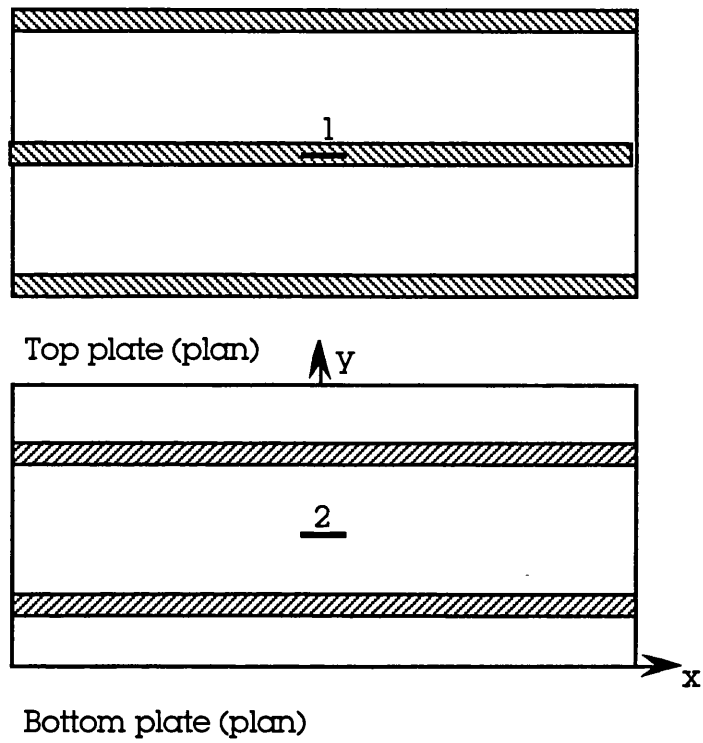


Fig. 6.5 The position and numbering of strain gauges on models 2-c and 1-c



- ▣ indicates where bond lies on the top plate
- ▤ indicates where bond lies on the bottom plate

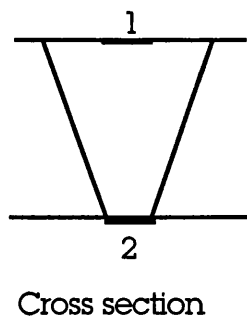


Fig. 6.6 The position and numbering of strain gauges on model 4-c

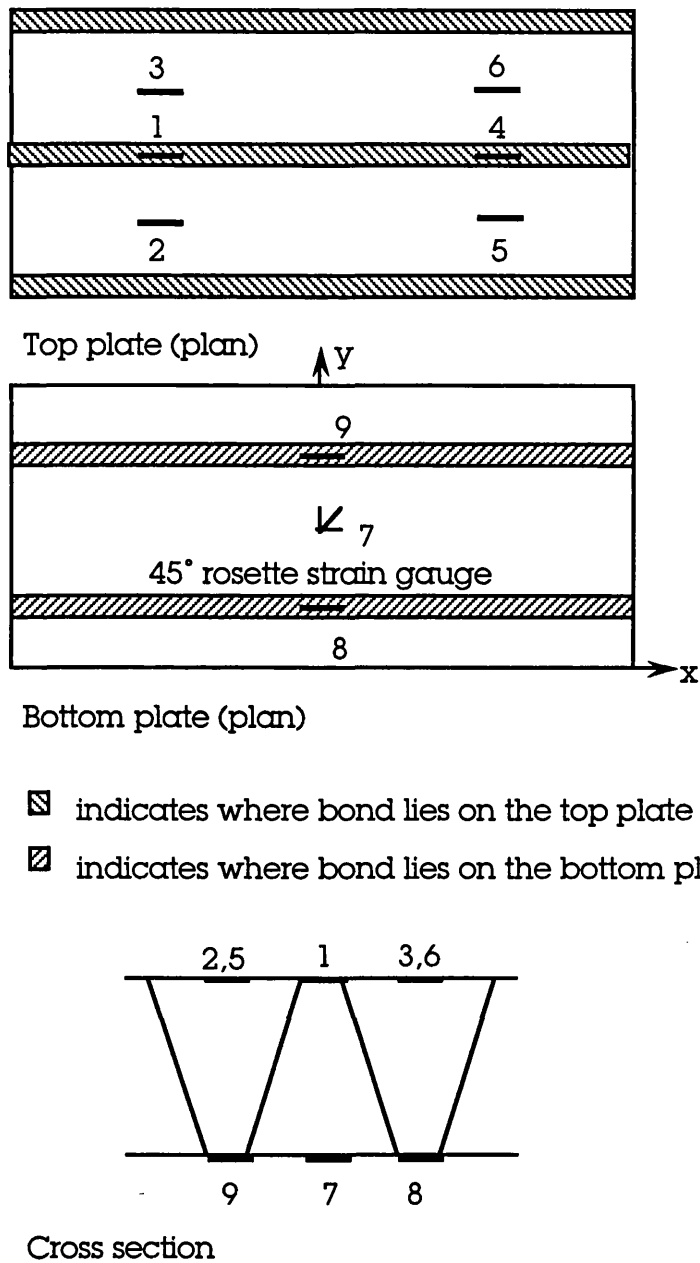


Fig. 6.7 The position and numbering of strain gauges on models 0-3b and 3-3b

The results of the four point bending tests appear in Fig. 6.8-6.19. All values of deflections and stresses are differences from initial 'zero' values taken with an unloaded model at the start of the experiments. The longitudinal bending stress is the stress along the x axis of the model while the transverse one is along the y axis. The diagrams contain those points which describe the behaviour of the model up to and including the maximum registered bending load point. In the legend accompanying the diagrams, s stands for stress while the number denotes the particular point of the model, having been defined previously in Fig. 6.3-6.4, where that strain gauge is available. SBT stands for the value estimated using Simple Beam Theory. During test 8 there was a malfunction of the strain gauges at points 3, 4 and 8; therefore their recordings have been omitted from the diagrams.

In Fig. 6.11, 6.13, 6.15, 6.17 and 6.19 a curve fit - in order to determine the gradient of the corresponding curves - was applied just to the linear part of the curves describing the relationship between the experimental longitudinal bending stress and the bottom plate deflection. For reasons of comparison, the models and their corresponding diagrams have been grouped according to the similarity of their structural arrangements and their performance during the tests which is clearly illustrated in Fig. 6.8, which forms a sketch of the diagrams made by the plotter of the bending machine, and Fig. 6.9. More specifically, some important observations are made here; while model's 3-4b total moment of inertia is approximately four times that of model's 0-4b and model's 4-4b is one point three times that of model's 2-4b, the registered bending load curves do not follow these proportionalities. In other words, the potential strength of models is not demonstrated by Fig. 6.8; instead, it is an indication of local rather than global failure.

Bearing those in mind, models 0-4b and 3-4b form one group (A), models 2-4b and 4-4b form a second group (B) and model 1-4b alone forms a final third group (C). It is also worth mentioning that the models of group (A) have the same plate and web thicknesses (1.5 mm) and the same number of half corrugations (4), the models of group (B) have the same plate thicknesses (1.5 mm) but different web thicknesses (1 and 1.5

mm) as well as different numbers of half corrugations (4 and 2).

Before mentioning some observations concerning the set of diagrams, a very important point should be highlighted and commented. The tests and especially the relevant diagrams describe mainly the behaviour of that part of the models which resisted the bending load application, namely the upper part, and **not** the behaviour of each model as a whole unit. This explains why a global failure of the models did not occur but just a local one. Also, it explains why models of the same group, though they are of completely different sectional stiffness level (see Table 5.3), appear to collapse in such a similar manner; i.e. their behaviour during the tests is not proportional to their strength. Finally, it explains why the value of yield stress expected from simple beam theory calculations does not coincide with the experimental values. In other words, as far as the tests of the present project are concerned, the strength of the models was dictated by the local strength of their top plate together with some part of their upper region (i.e. a part of the upper web plating too) with the neutral axis of the structure not lying at half depth but having moved upwards. This simply implies that the models have been too stiff to bend within the available machine. However, it has to be mentioned that at least as far as the web length, and in consequence the web depths, are concerned, they could not be made smaller than that of model 1-4b, because of the unavailability of suitable manufacturing equipment within the University premises. Therefore, the only parameter that could change is the model width reducing, in this way, the number of alternative design options. So, a suggestion that could be made for possible future work concerning corrugated core sandwich models is that the models should be tested over large spans in a larger testing machine.

Now, some observations regarding Fig. 6.10-6.19 are as follows:

- As far as the longitudinal bending stress diagrams, that is Fig. 6.10, 6.12, 6.14, 6.16 and 6.18, are concerned, the stress distribution at the different points on both plates of each model is not uniform. There is certain variation, that is the stress level is not the same at all points of either the top or bottom plate, but it

is not large and the pattern is linear (at least within the elastic region). In contrast, at the transverse bending stress diagrams, not only does a non-uniform pattern exist but a non-linearity as well. However, the stress level in the y direction is low and therefore the transverse stresses do not have an important effect in this kind of structures.

- The stress level at points where bond lies, as shown in Fig. 6.3 and 6.4, (points 1, 4, 5, 7 and 8 for all models except 4-4b; for this model the points are 2, 3, 5 and 6) is somewhat greater than that at interflange points (points 2, 3 and 6; for 4-4b: 1 and 4). This can also be seen clearly in Fig. 6.11, 6.13, 6.15, 6.17 and 6.19 with a few exceptions. This may suggest that the region along the bond area contributes to the local stiffening of the structure which should be expected and exploited.
- As mentioned before, simple beam theory values for stresses and deflections does not seem to agree with the experimental ones for all cases of the models tested. There seem to be some discrepancies between them which could also be attributed to imperfections occurring during the manufacture of the models, the material properties from which they were constructed, the installation of the strain gauges, the measuring of the strain gauge values and the important fact that these tests followed the creep ones. Especially for model 0-4b, we have to mention that not only was it subjected to creep tests but preliminary tests 1-6 as well, having been overturned twice. Also, it is important to mention that this particular model was loaded during the tests 1-7 with an l value (see Appendix D) of 590 mm. From Test 8 and on l changed to 490 mm for reasons mentioned in Chapter 5. All these conditions might have contributed to an increase of its strength, having made it more 'flexible'. However, from Fig. 6.13, 6.15, 6.17 and 6.19, it can easily be observed that there is a relative consistency between theory and experiments with deviations below 42%, even under the

conditions they were performed. Besides this consistency seems to be better at the points of the bottom plate with deviations below 24.5%. For model 0-4b, these deviations are approximately 50%, a fact which cannot be explained seriously, apart from the statements made before.

- The stress values at antisymmetric points (points 2 and 3, 4 and 5, 7 and 8) on the top or bottom plate of each model of groups (A) and (B), are more or less the same or very near to one another. Good examples are Fig. 6.12 and 6.14. Furthermore, the position of the curves characterising the stress level of each point in relation to the curve of the middle point of either the top or the bottom plate is more or less the same. For example as far as the top plate is concerned, in Fig. 6.12, both red and green curves lie above the black one whereas both blue and cyan curves lie below it. The same happens in Fig. 6.14.
- As mentioned in Chapter 5, there were two measurements of deflection taken and the top plate deflection values were greater than the bottom plate ones. That can be explained by the fact that deflection level at that part of model is greatly influenced by the indentation of the top plate and does not represent a true value. Therefore, only the lower plate deflection values were used in analysis.
- As already mentioned in Chapter 5, the fact that the four point bending tests followed the creep tests may imply that the stress level might have been influenced in a way by them. In other words, creep of the adhesive may play a significant role in the bending behaviour and lifetime performance of such type of structures. More comments about this matter can be found in the analysis of creep data.
- Any non-linearity occurring between the first (zero) and the second point of each curve of the longitudinal bending stress vs

bottom plate deflection diagrams of Fig. 6.10, 6.12, 6.14, 6.16 and 6.18, may be attributed to a first 'bending in' of each model, i.e. a possible initial torsion before the model was stabilised under the bending load application.

- Model 1-4b, as the most slender, appears to behave as expected, matching beam theory predictions quite well within the linear region. In other words, its ultimate strength and plastic failure appear to follow closely that of beam theory.
- Local indentation is evident in the plastic region.
- There seems to be no evidence of adhesive failure or element failure, except in way of distortions under load points, a fact which applies to all specimens.
- Unfortunately, the absence of a standard test (a test that could be used as a 'guide') cannot give the opportunity of making more reliable comparisons among the models.

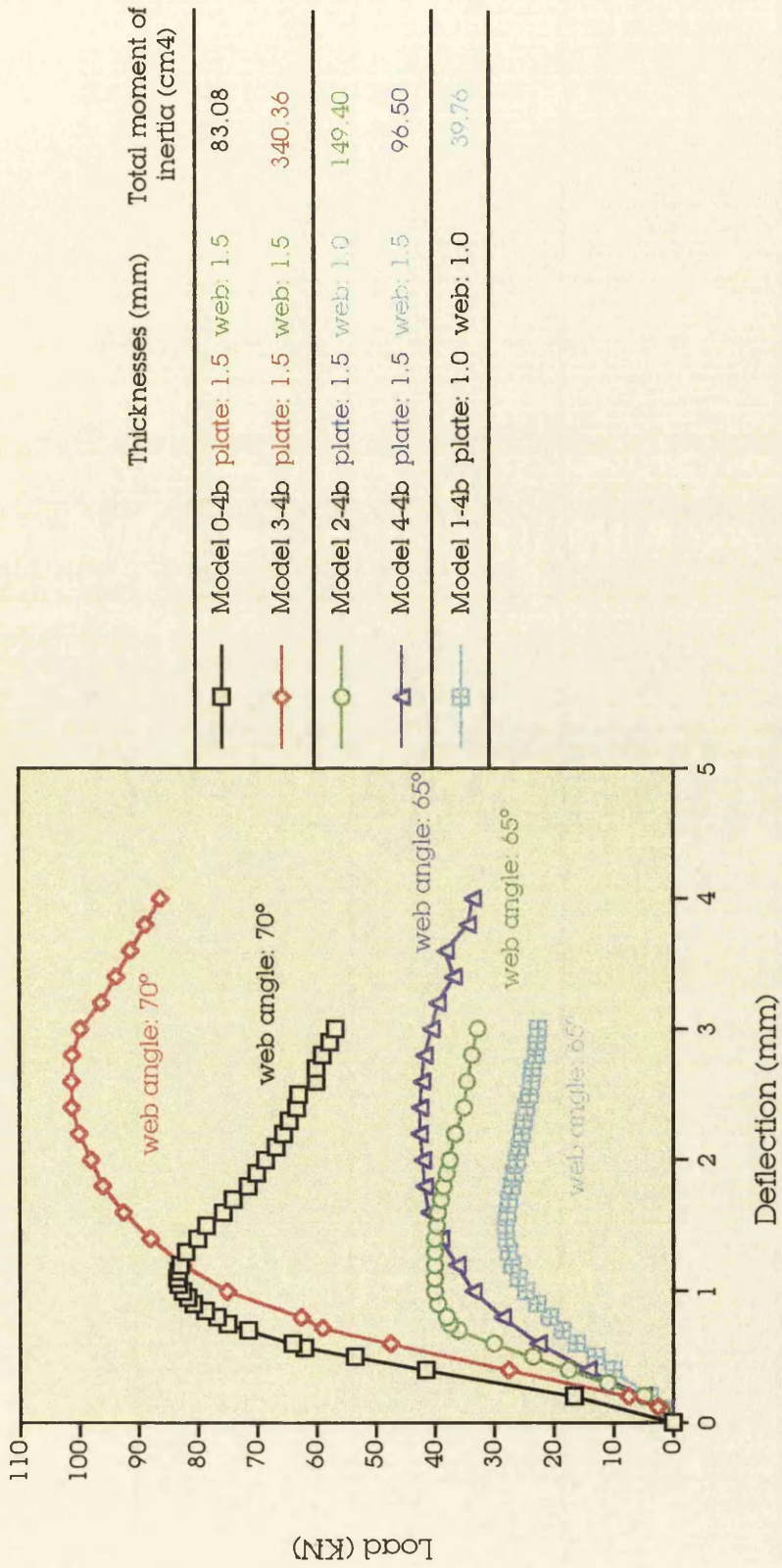


Fig. 6.8 Records of the load vs deflection relationship of all four point bending tests

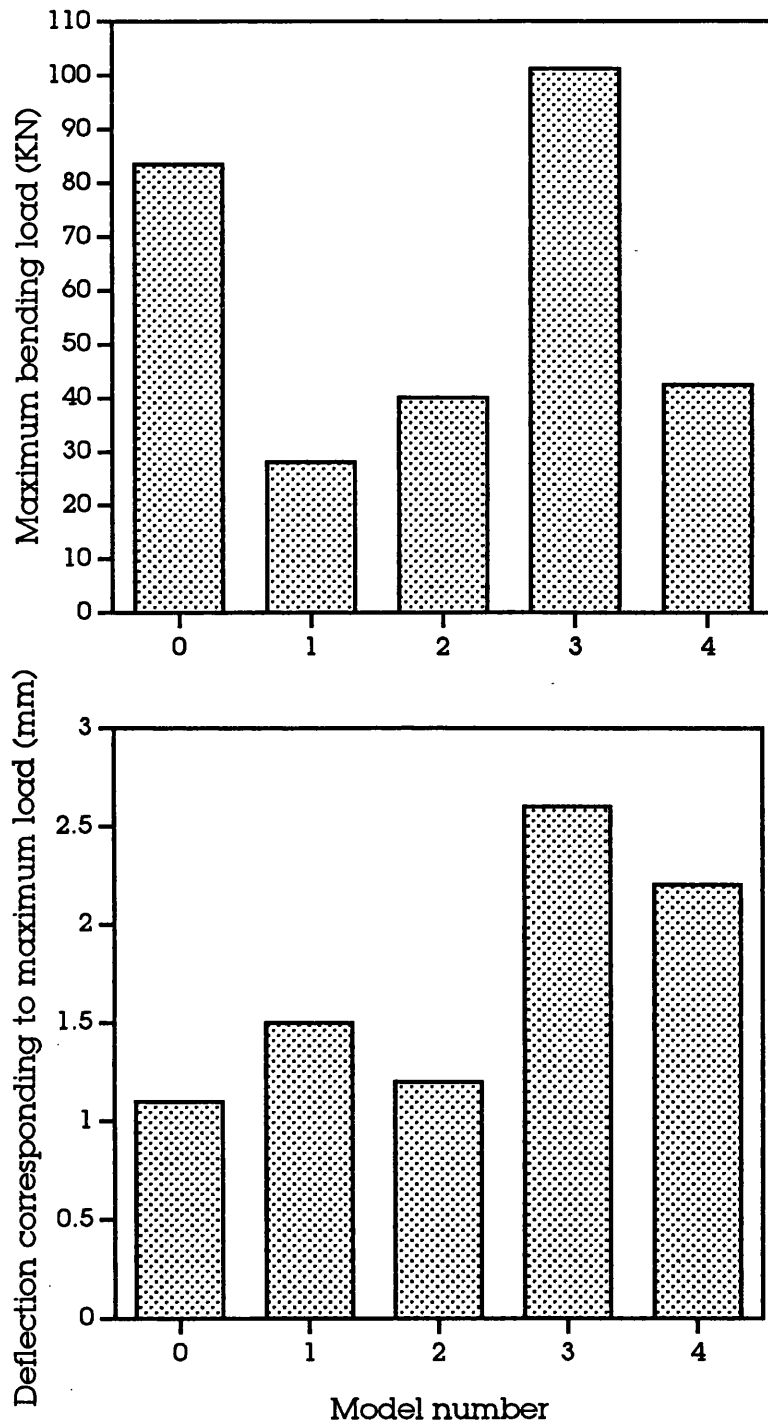


Fig. 6.9 Diagrams showing the maximum bending load and deflection levels for each model of the four point bending tests

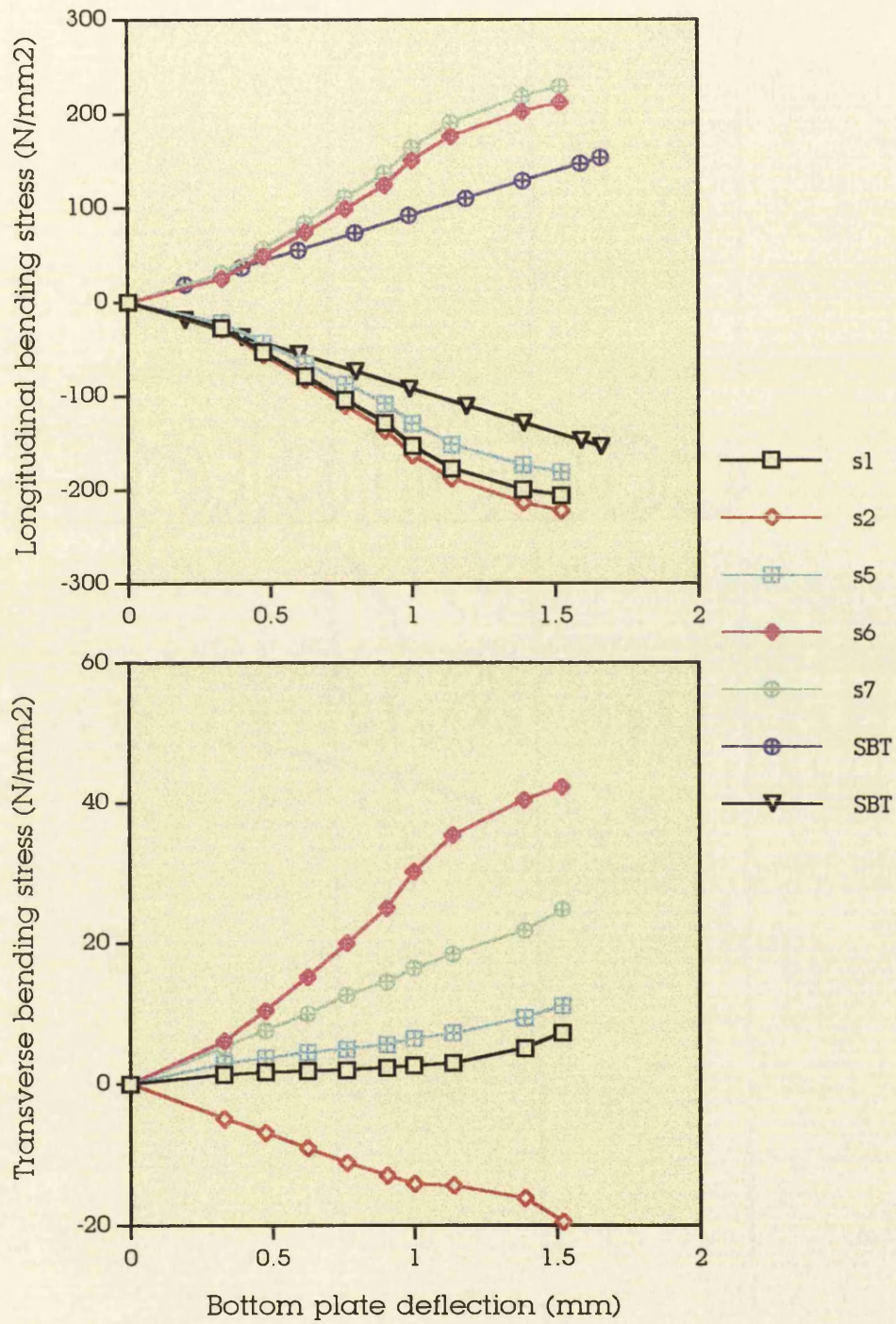


Fig. 6.10 Test 8: four point bending test of model 0-4b
Diagrams of bending stresses vs deflection

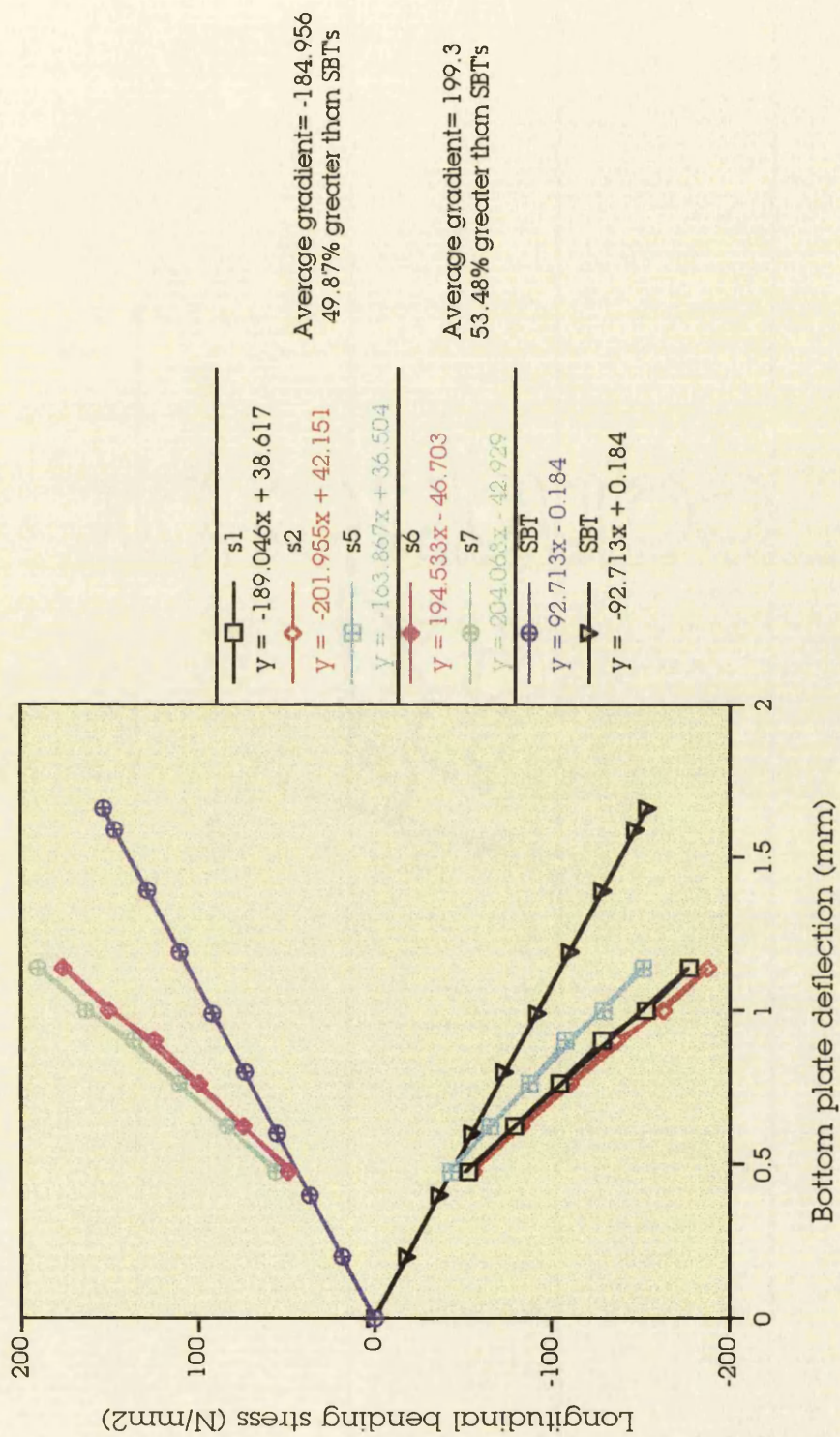


Fig. 6.11 Test 8: Comparison between the gradients of the experimentally obtained curves and the SBT ones

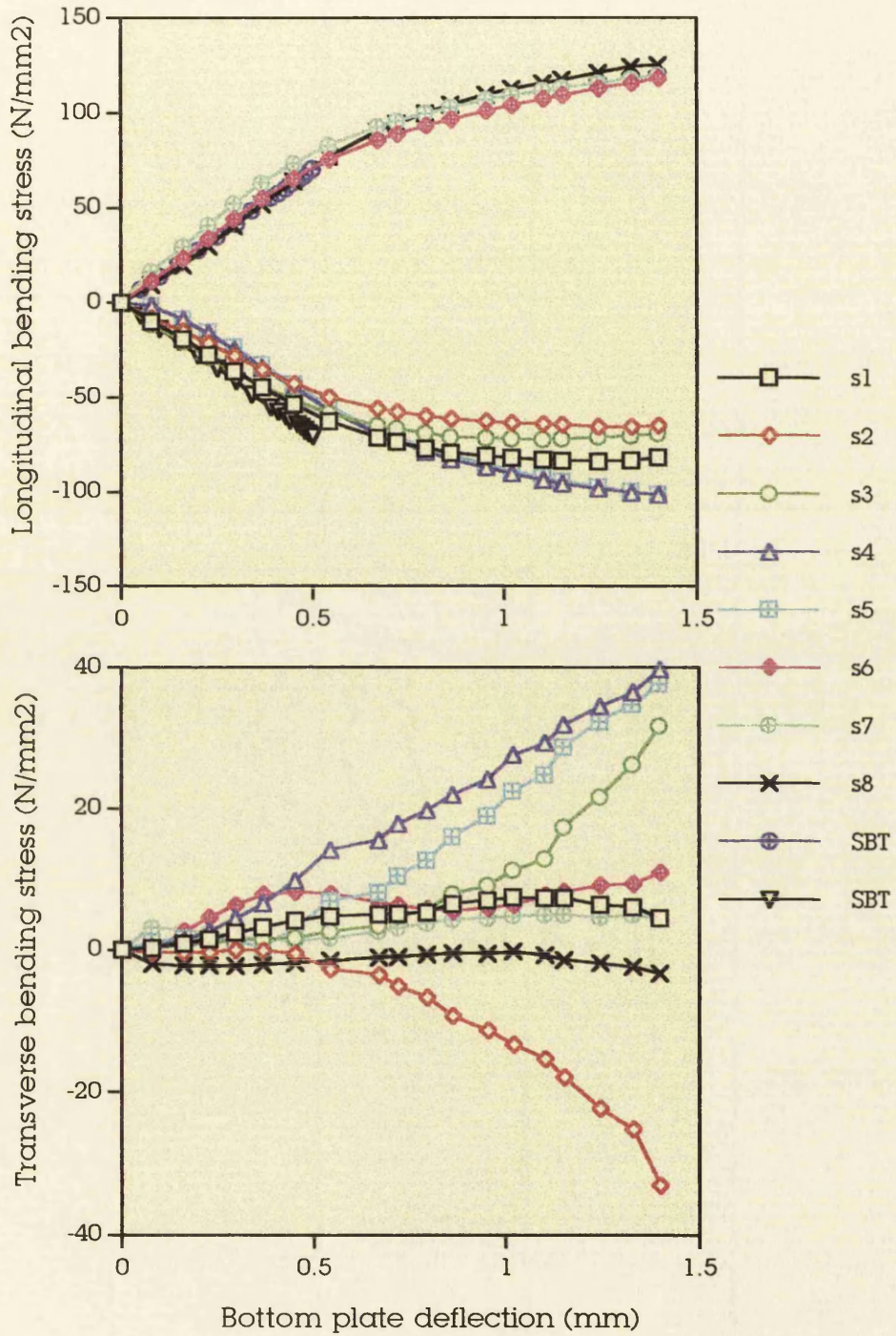


Fig. 6.12 Test 16: four point bending test of model 3-4b
Diagrams of bending stresses vs deflection

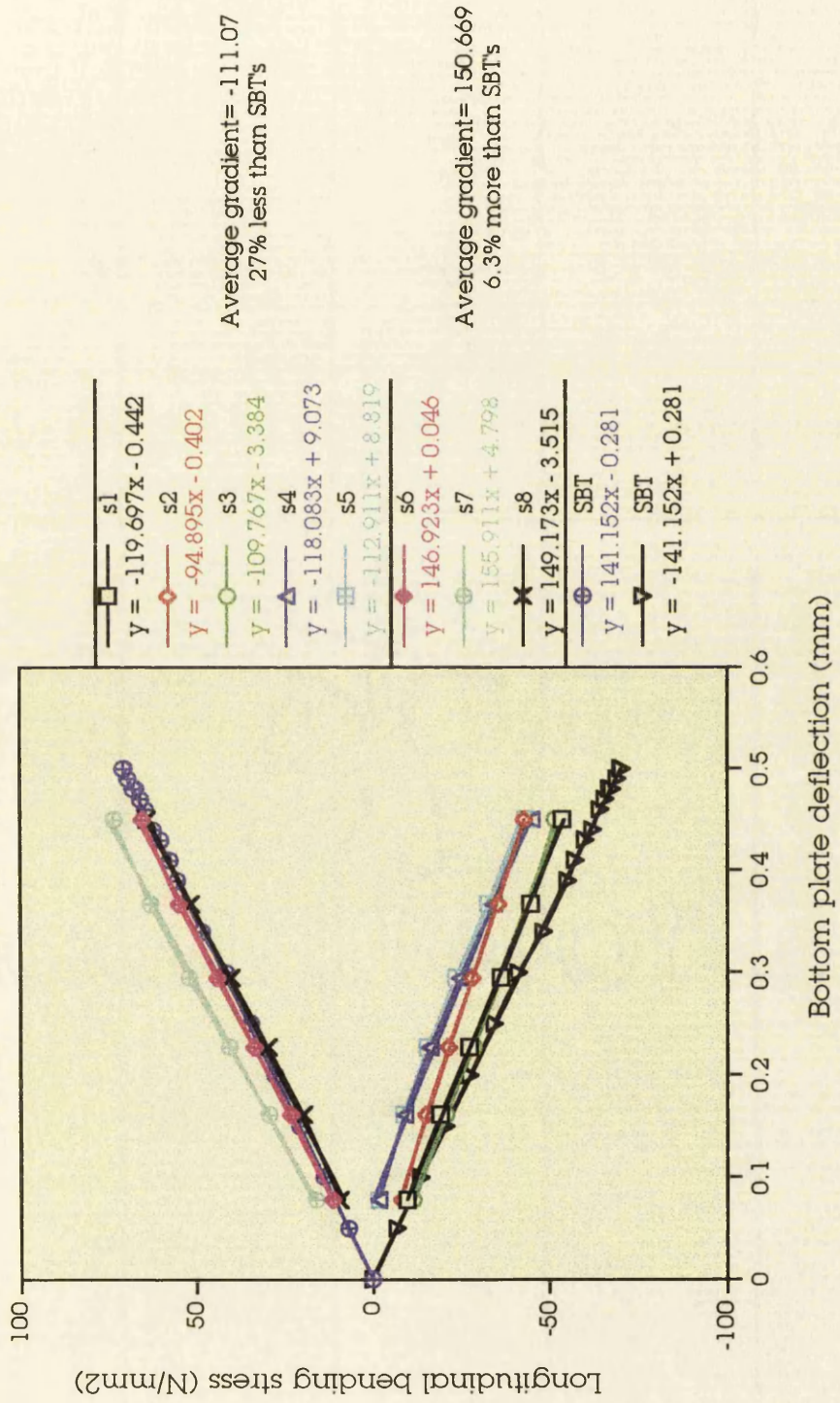


Fig. 6.13 Test 16: Comparison between the gradients of the experimentally obtained curves and the SBT ones

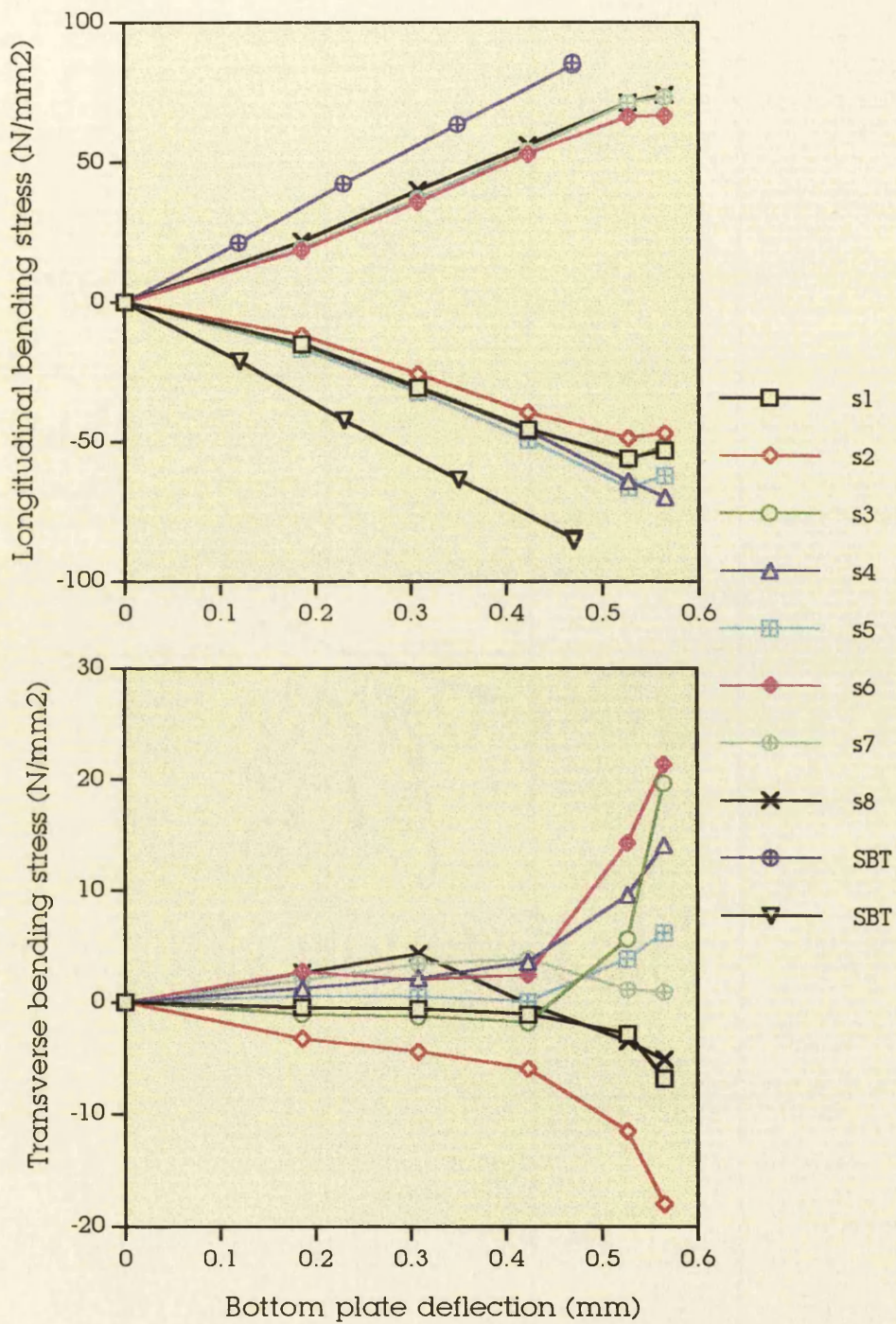


Fig. 6.14 Test 12: four point bending test of model 2-4b
Diagrams of bending stresses vs deflection

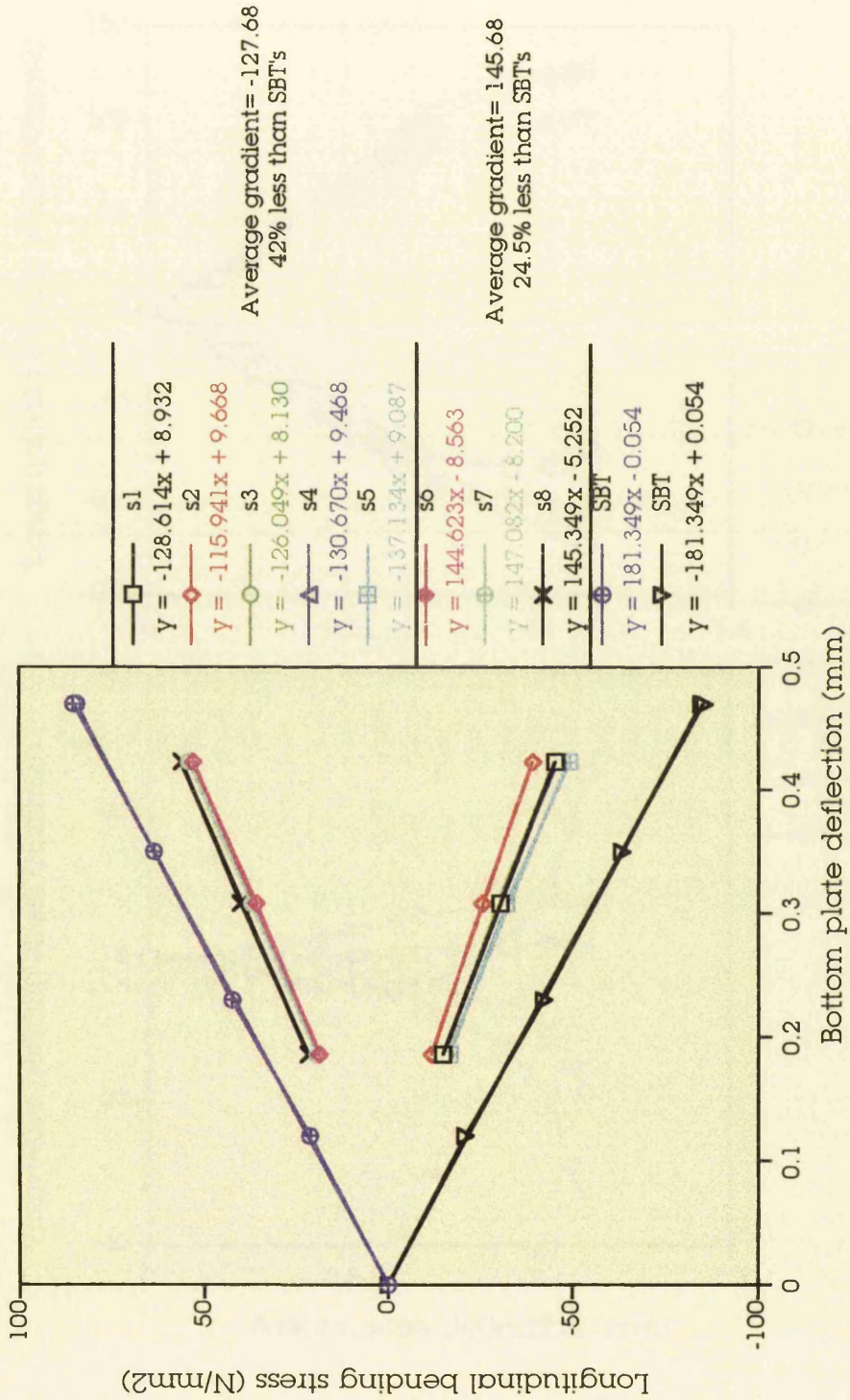


Fig. 6.15 Test 12: Comparison between the gradients of the experimentally obtained curves and the SBT ones

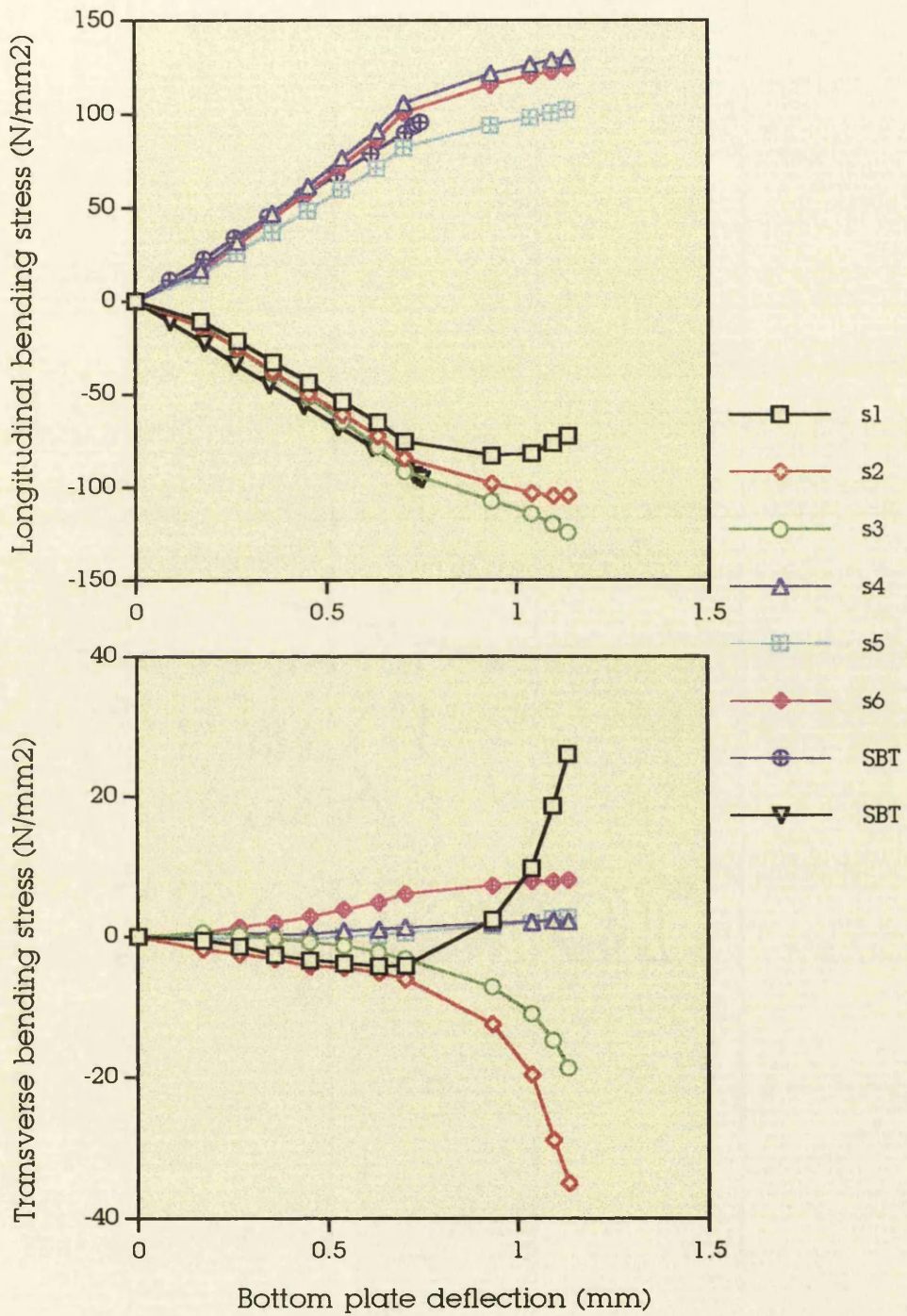


Fig. 6.16 Test 14: four point bending test of model 4-4b
Diagrams of bending stresses vs deflection

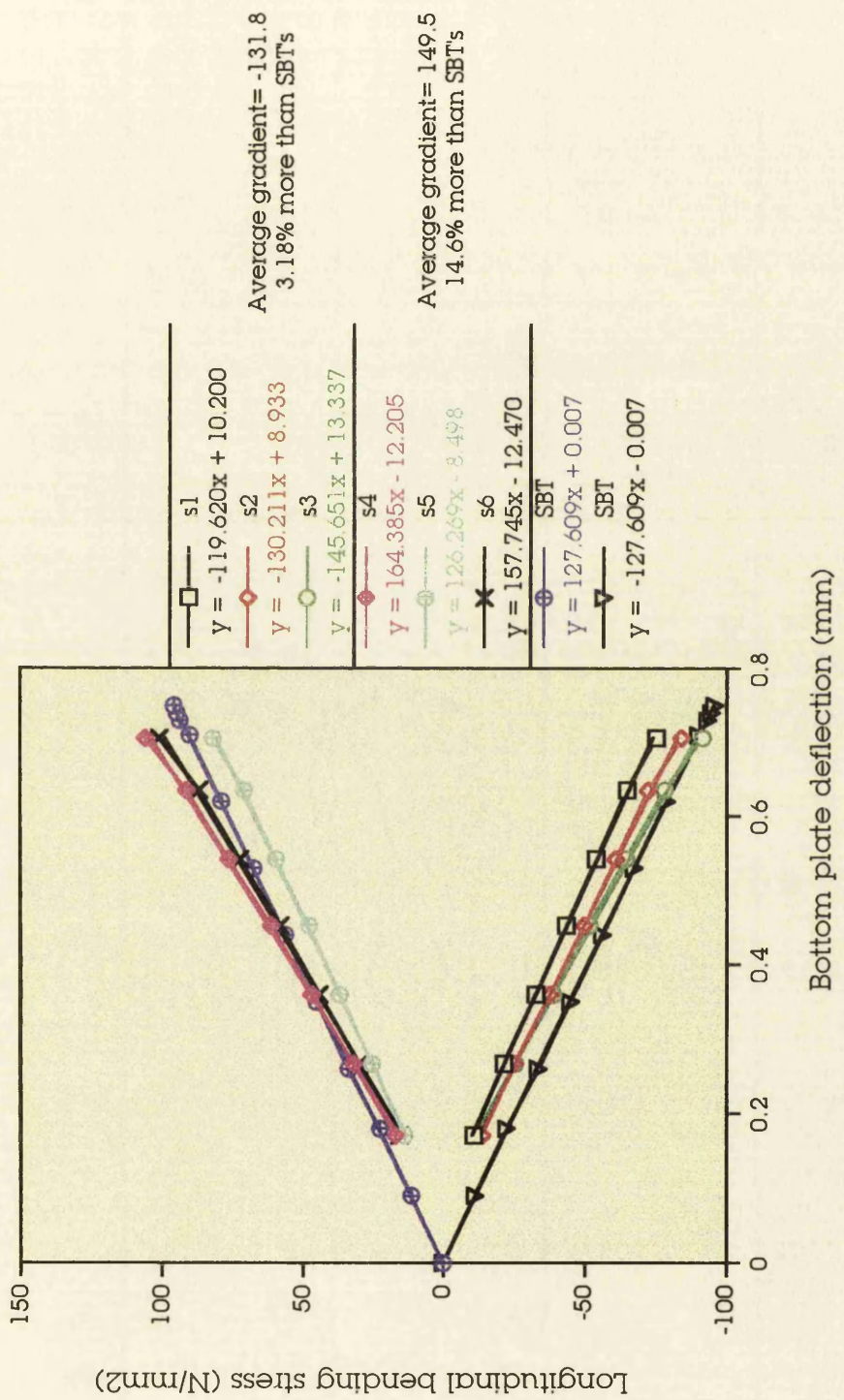


Fig. 6.17 Test 14: Comparison between the gradients of the experimentally obtained curves and the SBT ones

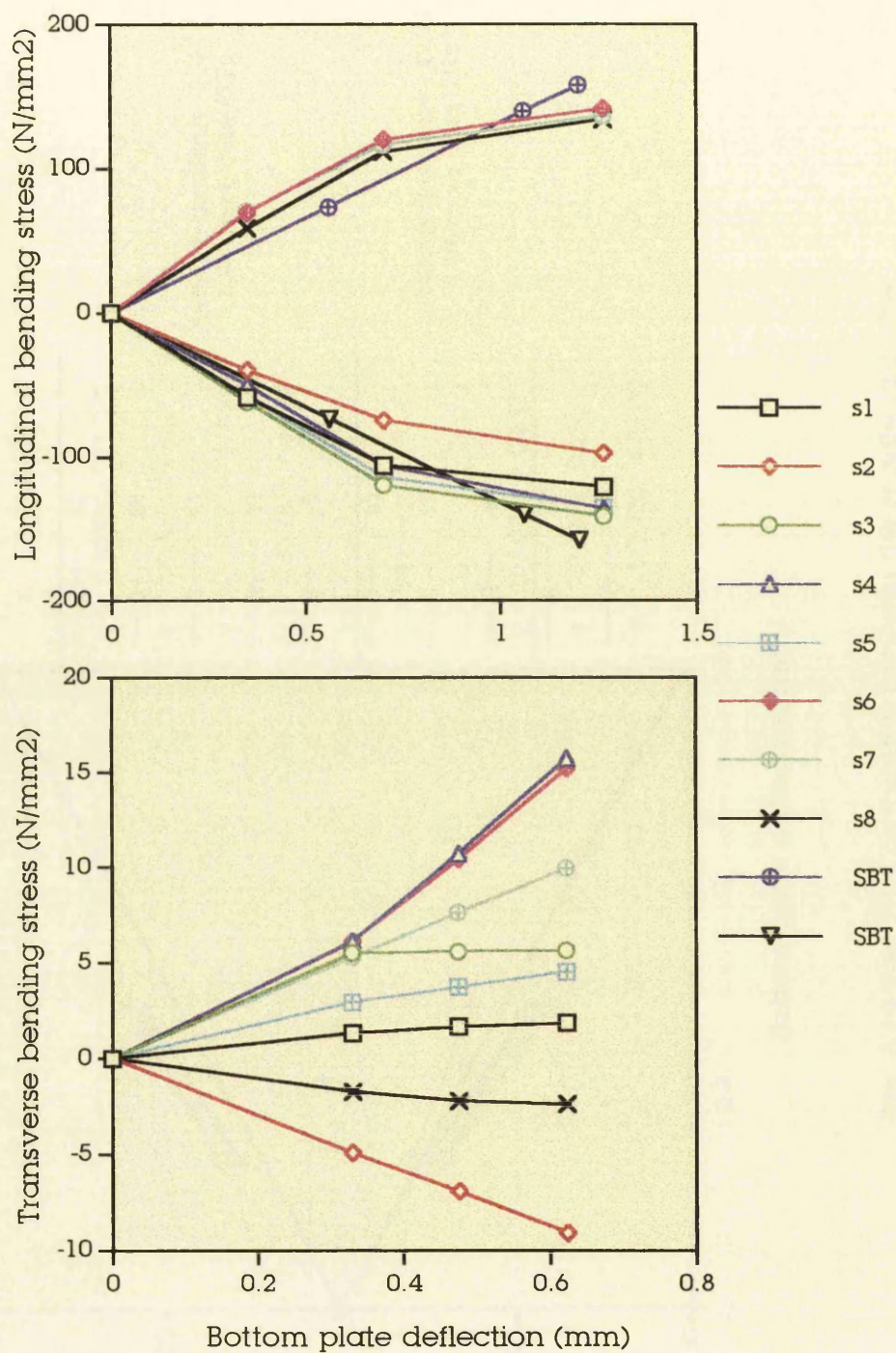


Fig. 6.18 Test 10: four point bending test of model 1-4b
Diagrams of bending stresses vs deflection

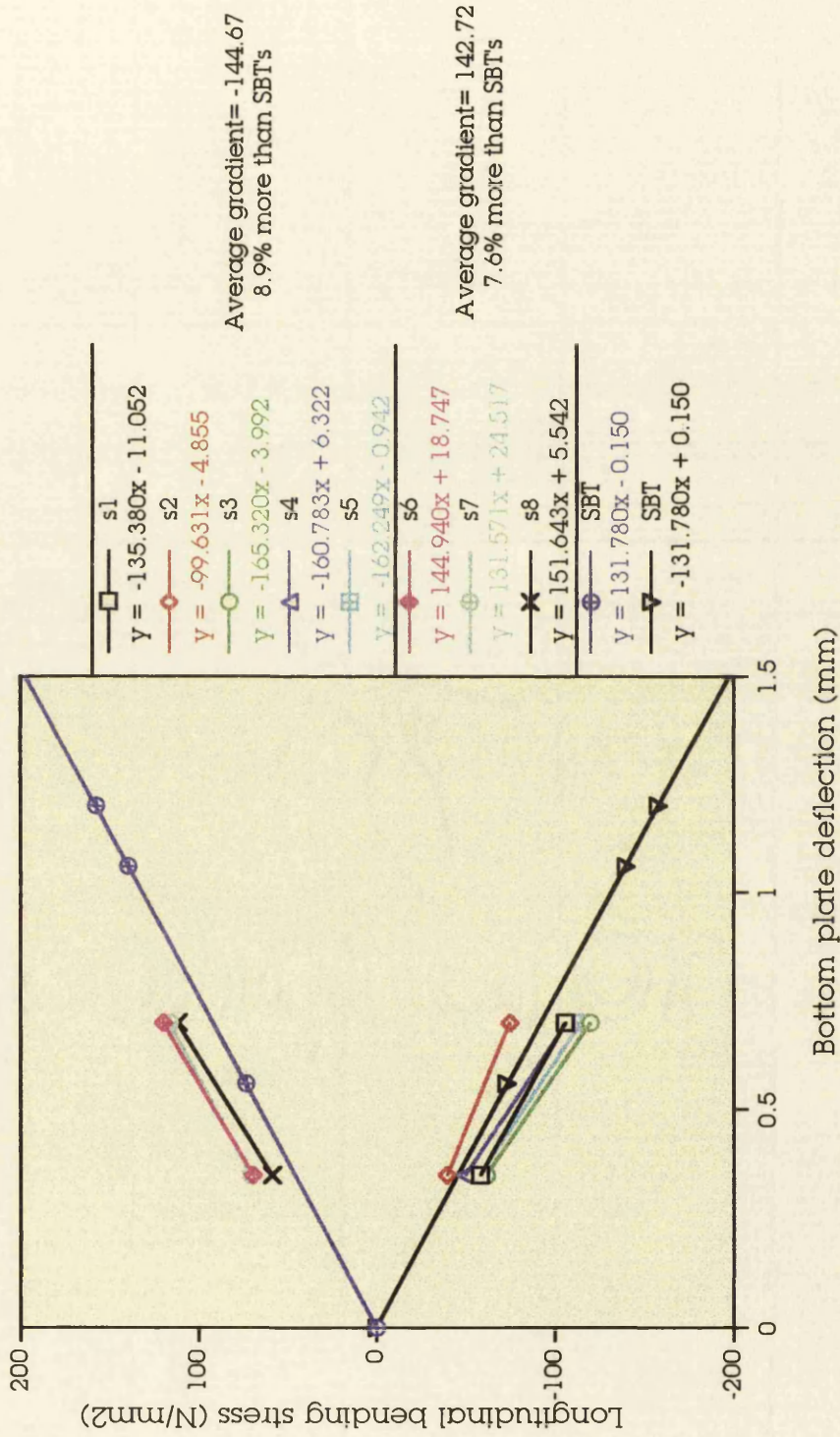


Fig. 6.19 Test 10: Comparison between the gradients of the experimentally obtained curves and the SBT ones

The creep tests results appear in Fig. 6.20-6.32. All values of deflections, strains and stresses are differences from initial 'zero' values taken with an unloaded model at start of the experiments. The longitudinal bending strain and stress is the strain and stress along the x axis of the model. In the legend accompanying the diagrams, e stands for strain while the number denotes the particular point of the model, having been defined previously in Fig. 6.3-6.4, where that strain gauge is available.

In Fig. 6.20 the load referred to at the legend is the one that was determined to apply constantly for a certain period of time but this does not mean that the machine managed to keep it constant. This can be observed in some of the creep tests diagrams, taken from the plotter of the machine, where there is a trembling line instead of a straight one. Also, it must be noted that this trembling line took a severe shape during model 4-4b's creep test, a less severe shape during 1-4b's, 2-4b's and 3-4b's tests. Finally, during the 2-4b's test, a malfunction of the data logger machine took place and the model had to be unloaded and loaded again at the same level. Again, a question should be put as far as the suitability of the existing equipment within the University premises is concerned for this type of tests.

At the curve fit diagrams for both deflection and strain, the equation describing the linear curve fit has been written in the legend. Curve fit was applied just to the linear part of the creep tests curves and its aim is to make the analysis of this part of results easier. At the longitudinal strain-stress vs time diagrams the number near each curve denotes the particular point of the model, having been defined previously in Fig. 6.3-6.4, where that strain gauge is available. In the analysis of these creep results a useful factor is introduced to have a better visualisation of the efficiency of models during these tests. In other words, the load applied to each model was divided by the model section modulus and the factors obtained are as follows:

Model 0-4b	Model 3-4b	Model 2-4b	Model 4-4b	Model 1-4b
1.035	0.595	0.99	0.699	0.72

Finally, the same grouping as that appeared in the analysis of the four point bending tests is followed here as well, for reasons of comparison.

Some observations regarding Fig. 6.20-6.32 are as follows:

- There does exist a creep of the adhesive which can affect the performance of the models. Here, it is worth mentioning that, taking into account the important observation made during the four point bending test analysis, it is very difficult or even impossible to know whether the present creep tests describe the behaviour of the adhesive in conjunction with the members of the 'model' structure as a whole unit or they just describe the adhesive behaviour within the upper region of the structure.
- As mentioned in a previous section, the constant load which applied had to be well below the load corresponding to the elastic limit of each model, so that no plastic deformation would occur before the four point bending tests. If a comparison was made among the values of the constant load applied and the final values of the maximum bending load occurring after the four point bending tests, it would be noted that this is really within the elastic region and forms approximately the one third of the maximum bending load. There is, of course, the exception of model 2-4b which was loaded at 35 KN and its maximum bending load was 40.5 KN, which might have an effect in its creep test results.
- There is a common behaviour of all models tested for creep as far as the deflection is concerned, except for model 4-4b, as observed in Fig. 6.21, taking into account the gradient of the equation describing the curve fit. This together with the results appearing in Fig. 6.28 and 6.29 could be attributed to the observation made at the beginning of the analysis concerning the equipment used for the test.
- For models 0-4b and 2-4b, both compressive and tensile strains

and stresses increase with respect to time which may imply that a redistribution of strains and stresses takes place. Model 1-4b seems to have the same behaviour at least as far as the tensile strains and stresses are concerned. The results of Fig. 6.24 seem to be a little strange in relation to the rest, but there does exist a strange 'jump' in the recorded data as well; therefore, a malfunction of some kind must have taken place. In addition, the grouping suggested at the beginning of the analysis does not seem to work here. Finally, tests no. 13 and 15 should not be considered reliable.

- It is worth mentioning the variation (i.e. the curves corresponding to the various points across the top and bottom plate of the model do not overlay) in strain and stress values at the different points of the models. Again, at the points where the bond lies the strain and stress values seem to be higher than those concerning the interflange points. Antisymmetric points on both top and bottom plate of the models (i.e. 2-3, 4-5 and 7-8) do not behave in the same way (there is a gap) and besides there seems to be a kind of destabilisation of the structure during the application of the same or approximately the same amount of load (e.g. points 7-8 during tests 9 and 11).
- Another observation that can be made is that at a certain time point the creep curve of all points of the models follows the opposite direction from the initial one going towards the initial condition. Unfortunately, this takes place at a point near the end of each creep test and it would have been useful if much more information had been available for this point of the creep tests. This means that maybe longer creep tests should take place in the future.
- Again, there can be observed a common behaviour of the models tested for creep as far as the strains are concerned, as observed in Fig. 6.23, 6.27 and 6.31, taking into account the

gradient of the equation describing the curve fit.

- Fig. 6.32 consists of two synoptic diagrams containing all information provided by Fig. 6.21, 6.23, 6.25, 6.27 and 6.31. The first diagram illustrates the relationship between Load/Section modulus factor and the change in strain gradient. Each white square point in the different groups - each group corresponding to one model, therefore same load/section modulus factor - represents the value of each strain gradient of the curve fits in Fig. 6.23, 6.25, 6.27 and 6.31. The red square points represent the average value of each group of the white ones. Therefore, it can be seen that as the load increases there is also an increase in strains, as it should be expected. Normally, the line of the curve fit should pass through 0 (as no load results in no strain and deflection) but it does not. The reason this happens is a little difficult to explain.

In contrast, the line of the curve fit of the second diagram, which describes the relationship between the Load/Section modulus factor and the change in deflection, passes through 0 and this diagram seems to be more reliable. Again this relationship is an expectable one and proves the existence of the creep effect of the adhesive. Although there must be a law underlying these relationships, it cannot be presented in this thesis, but a future attempt to discover it could be possible and necessary.

- Of course, if the factor described at the beginning of the creep tests analysis had been the same for all models - basically that could be done by applying special chosen load amounts - the comparison between the models could have been easier and probably more useful information would have been drawn out.

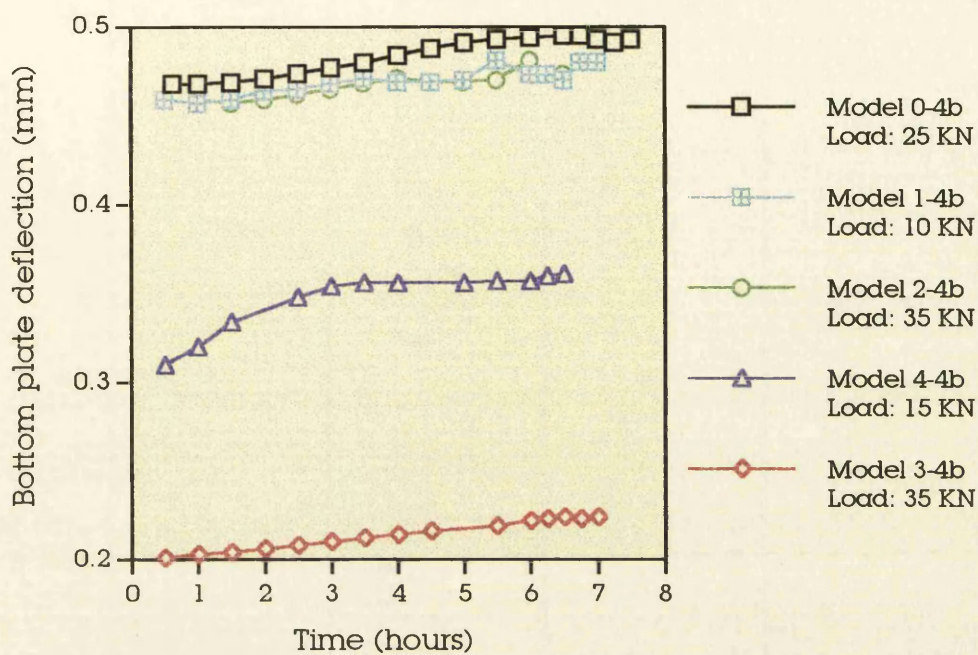


Fig. 6.20 Creep tests of all models
Diagram of bottom plate deflection vs time

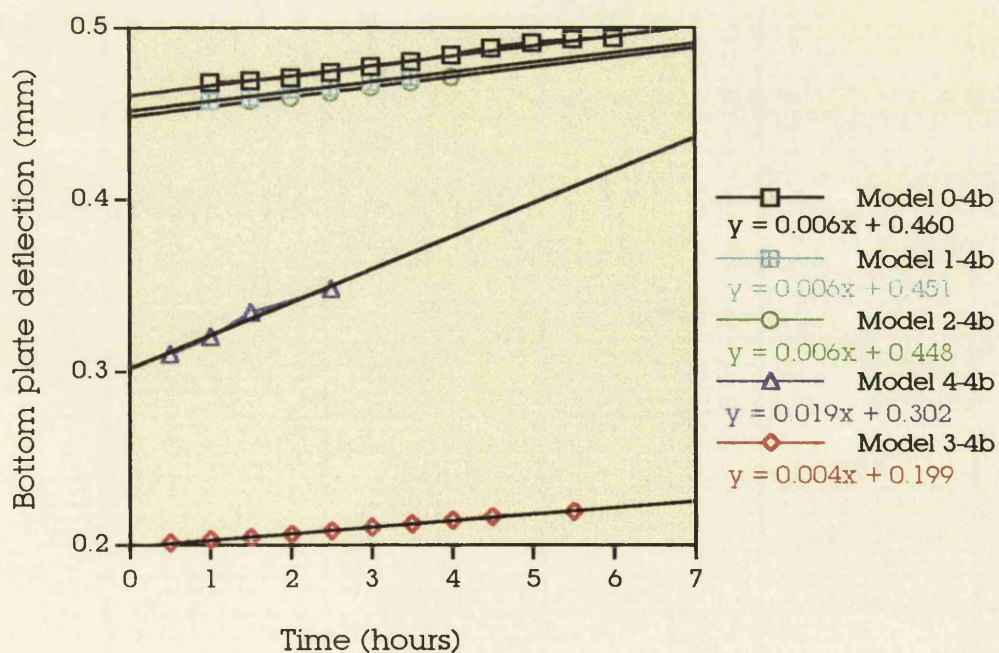


Fig. 6.21 Curve fit of the linear part of creep curves of all models

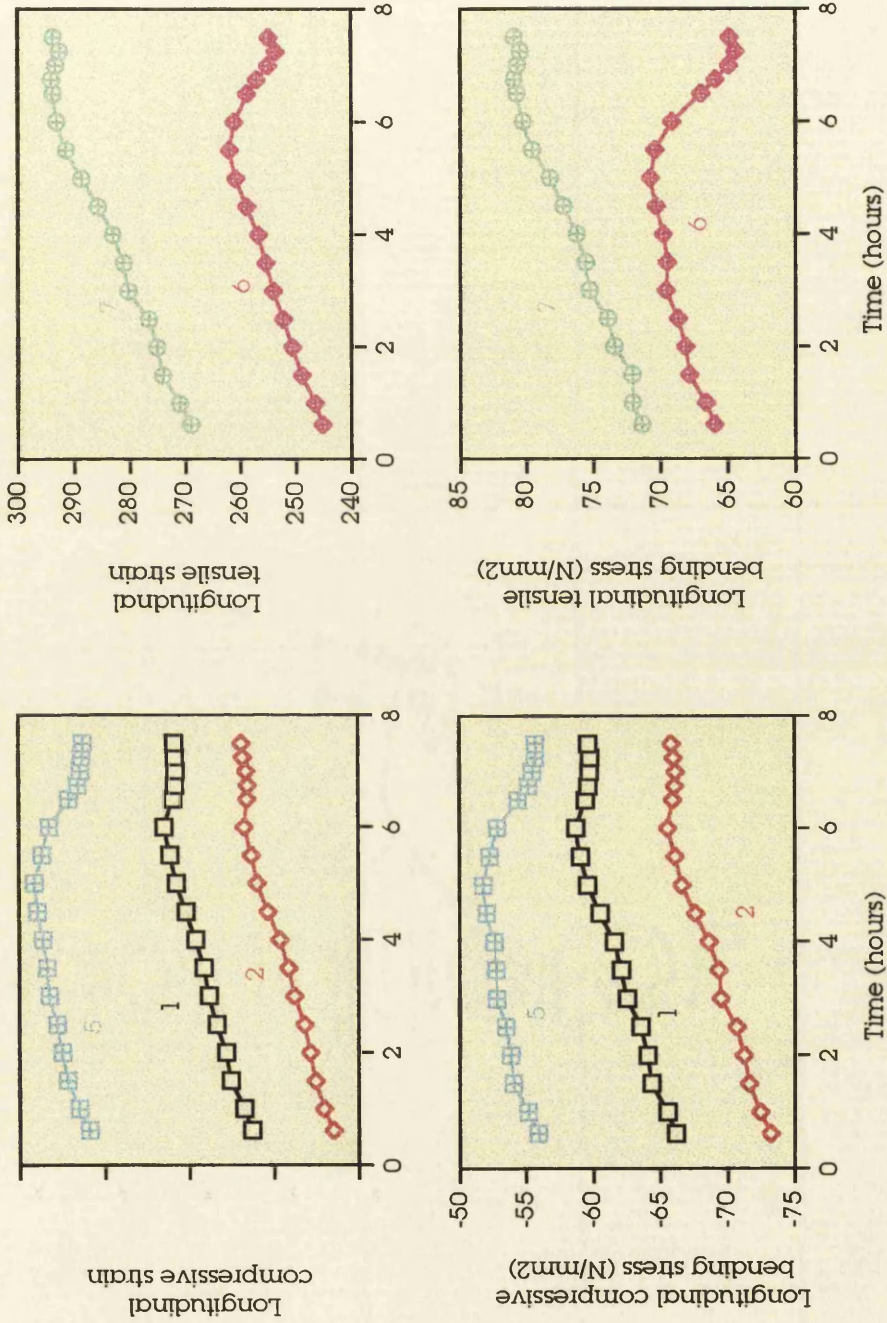


Fig. 6.22 Test 7: creep test of model 0-4b
Diagrams of longitudinal strains and stresses vs time

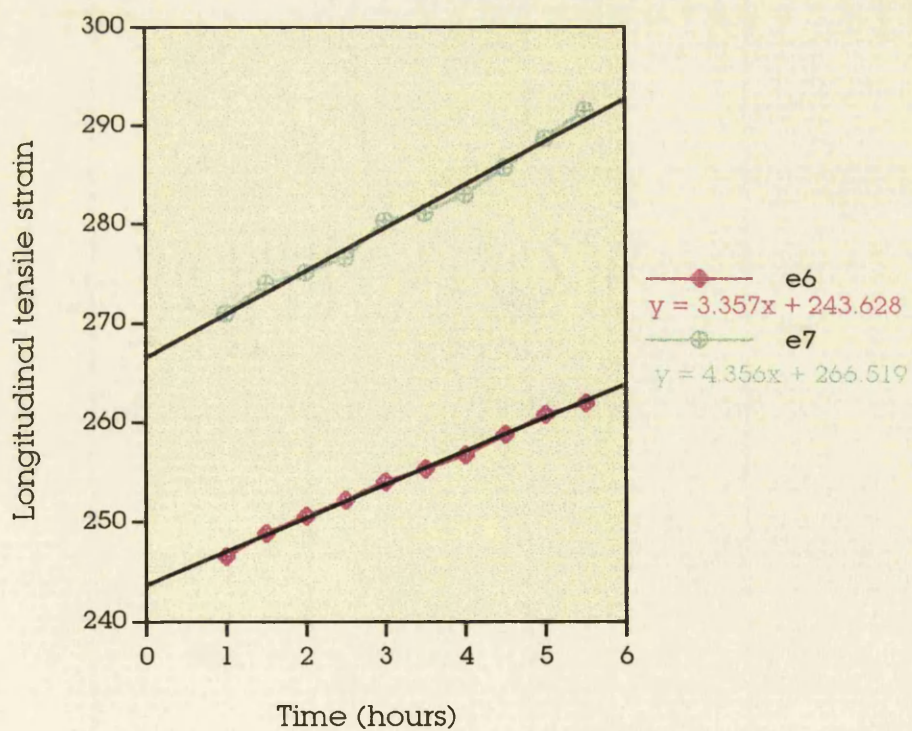
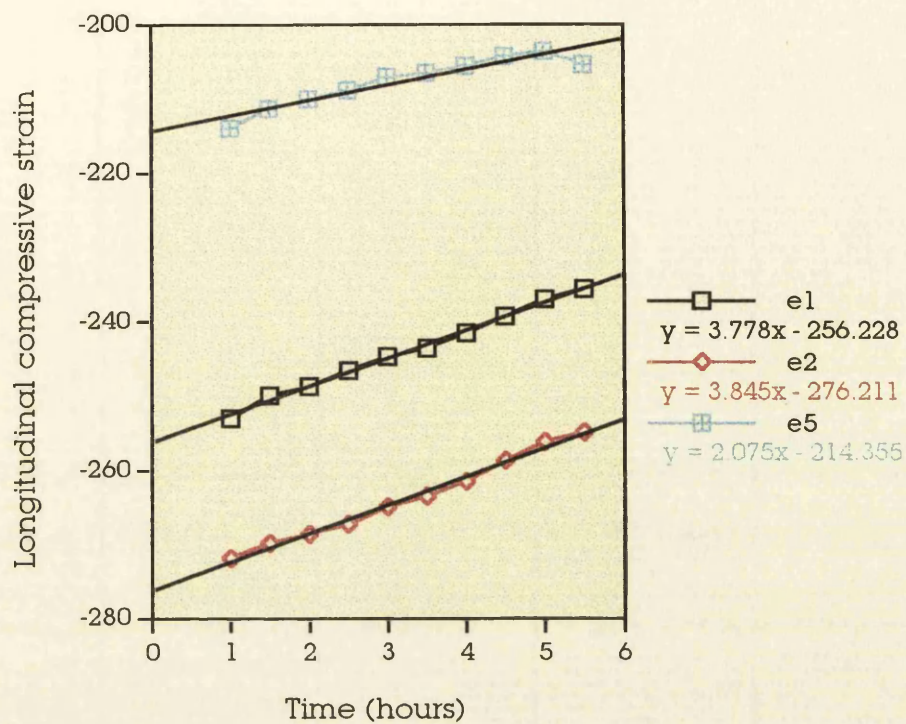


Fig. 6.23 Curve fit of the linear part of strain creep curves of model 0-4b

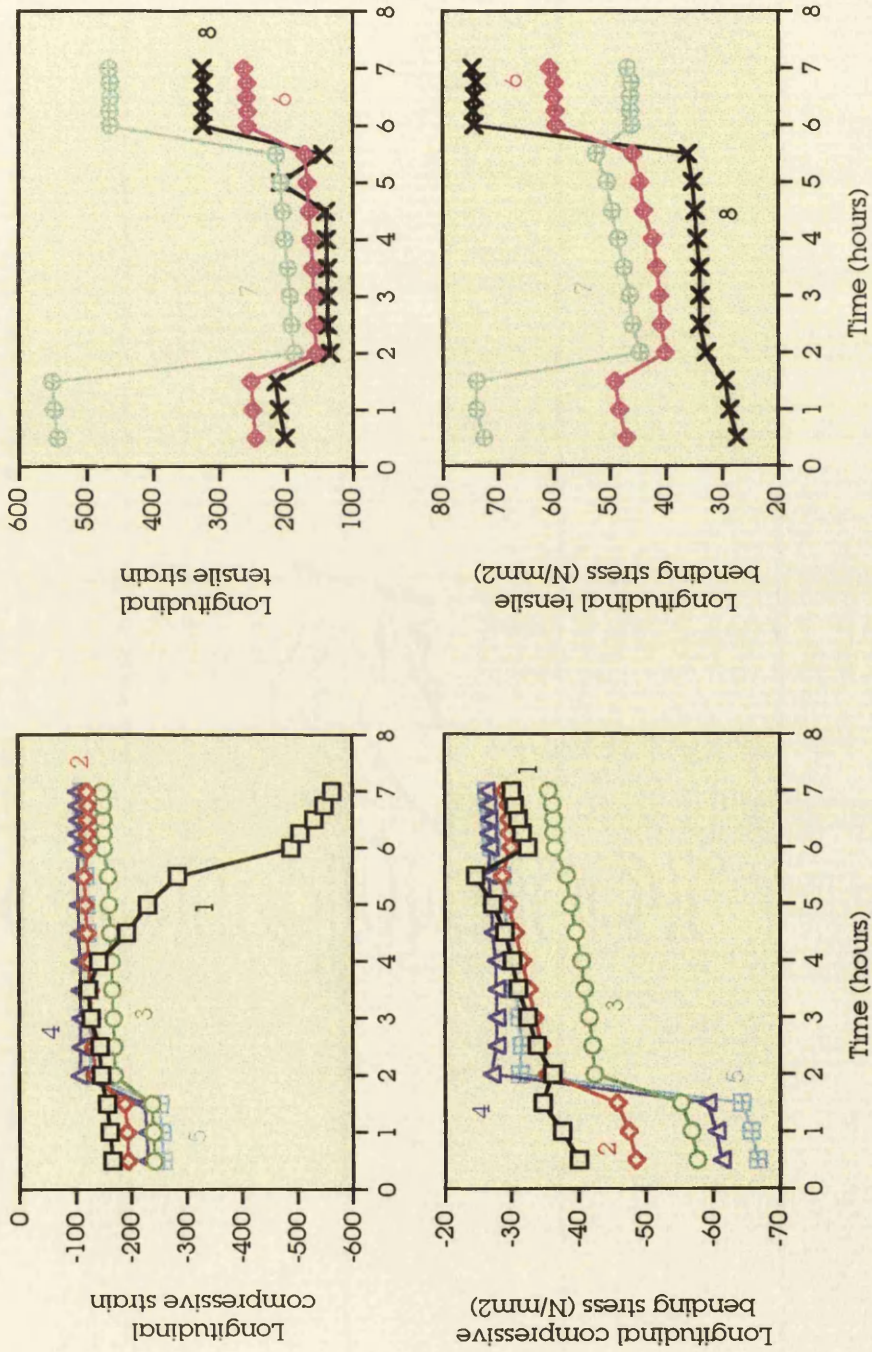


Fig. 6.24 Test 15: creep test of model 3-4b
Diagrams of longitudinal strains and stresses vs time

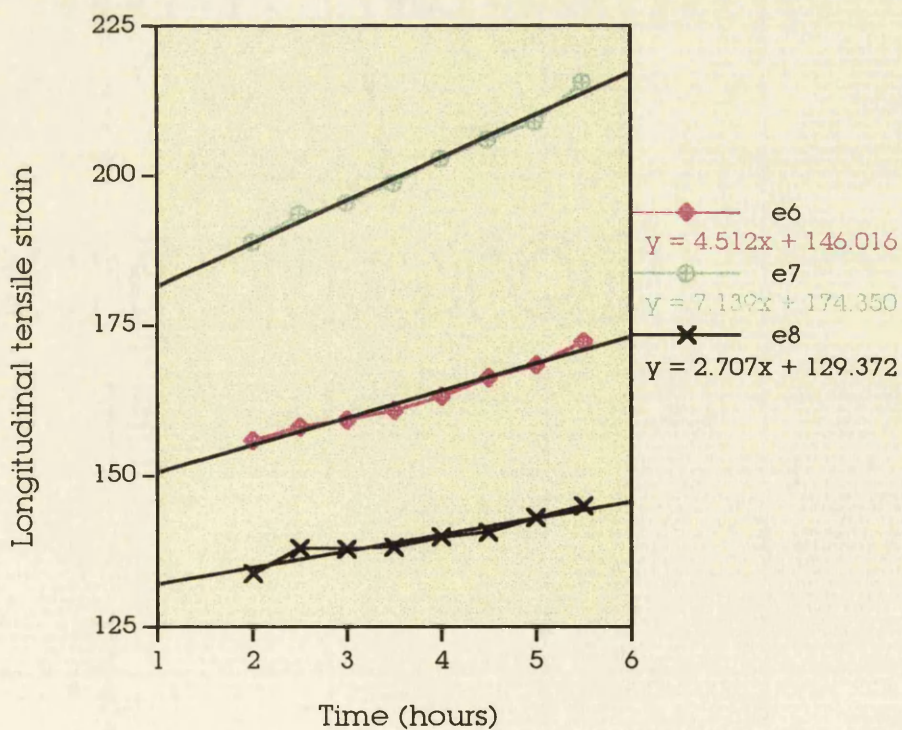
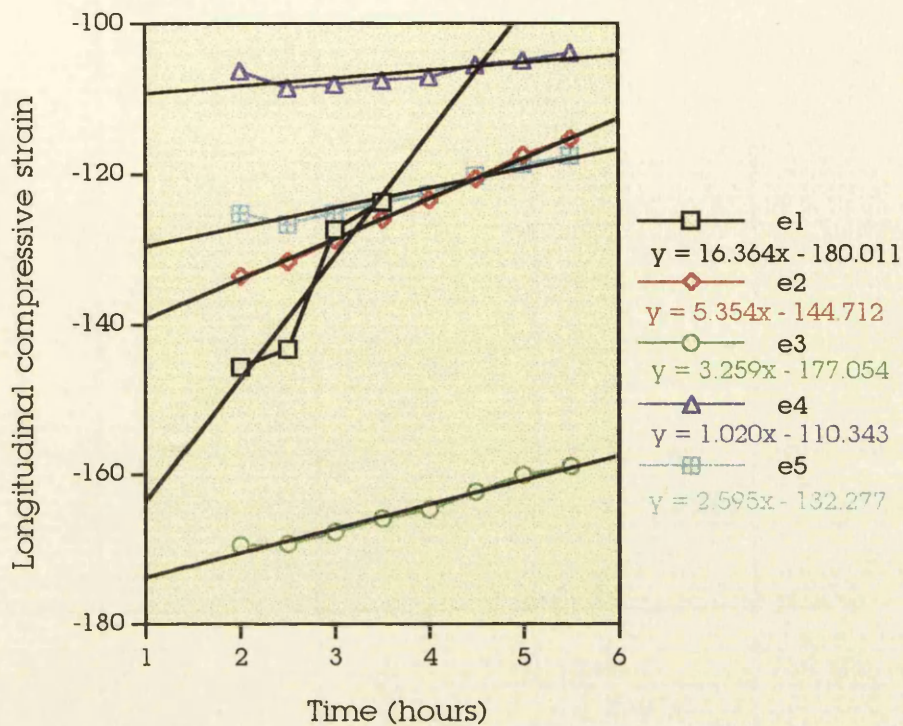


Fig. 6.25 Curve fit of the linear part of strain creep curves of model 3-4b

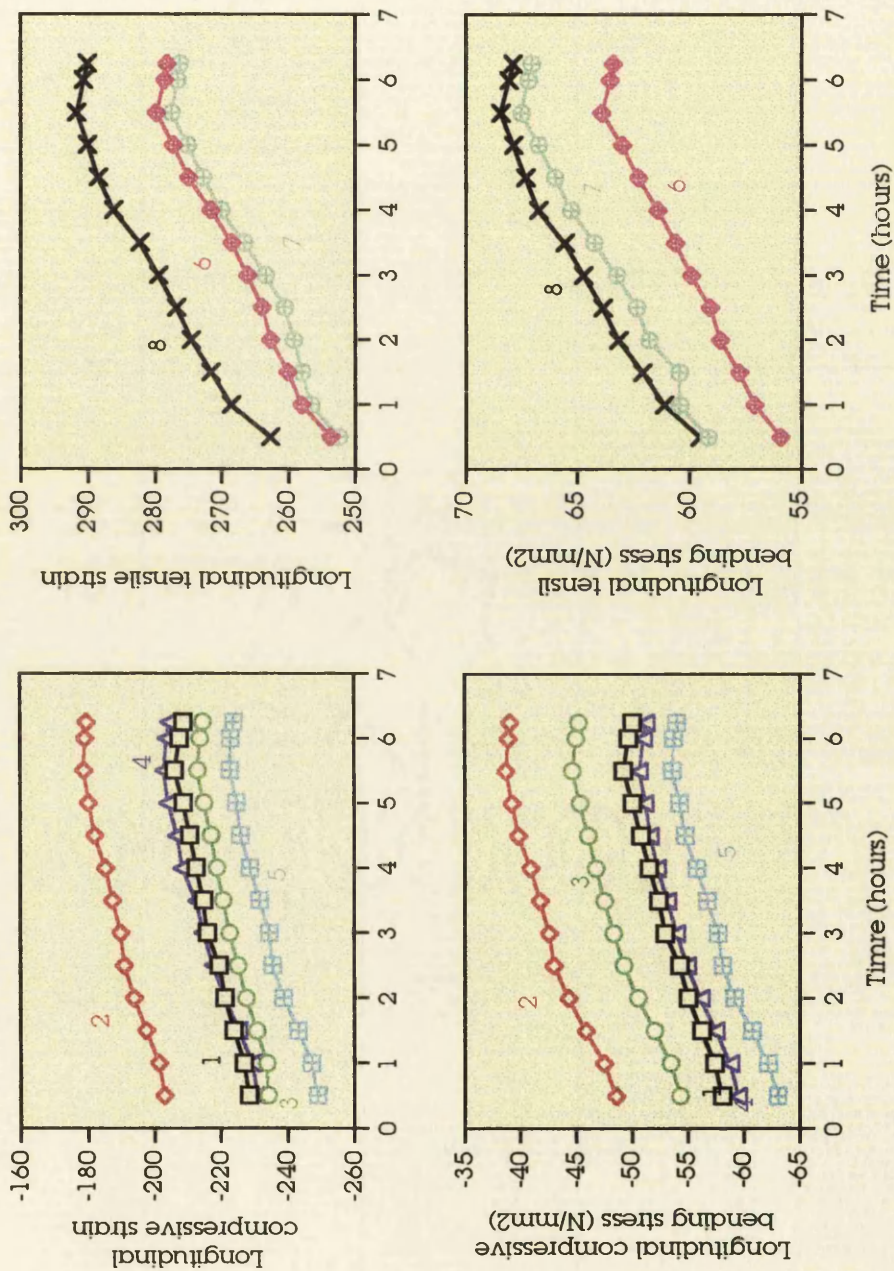


Fig. 6.26 Test 11: creep test of model 2-4b
Diagrams of longitudinal strains and stresses vs time

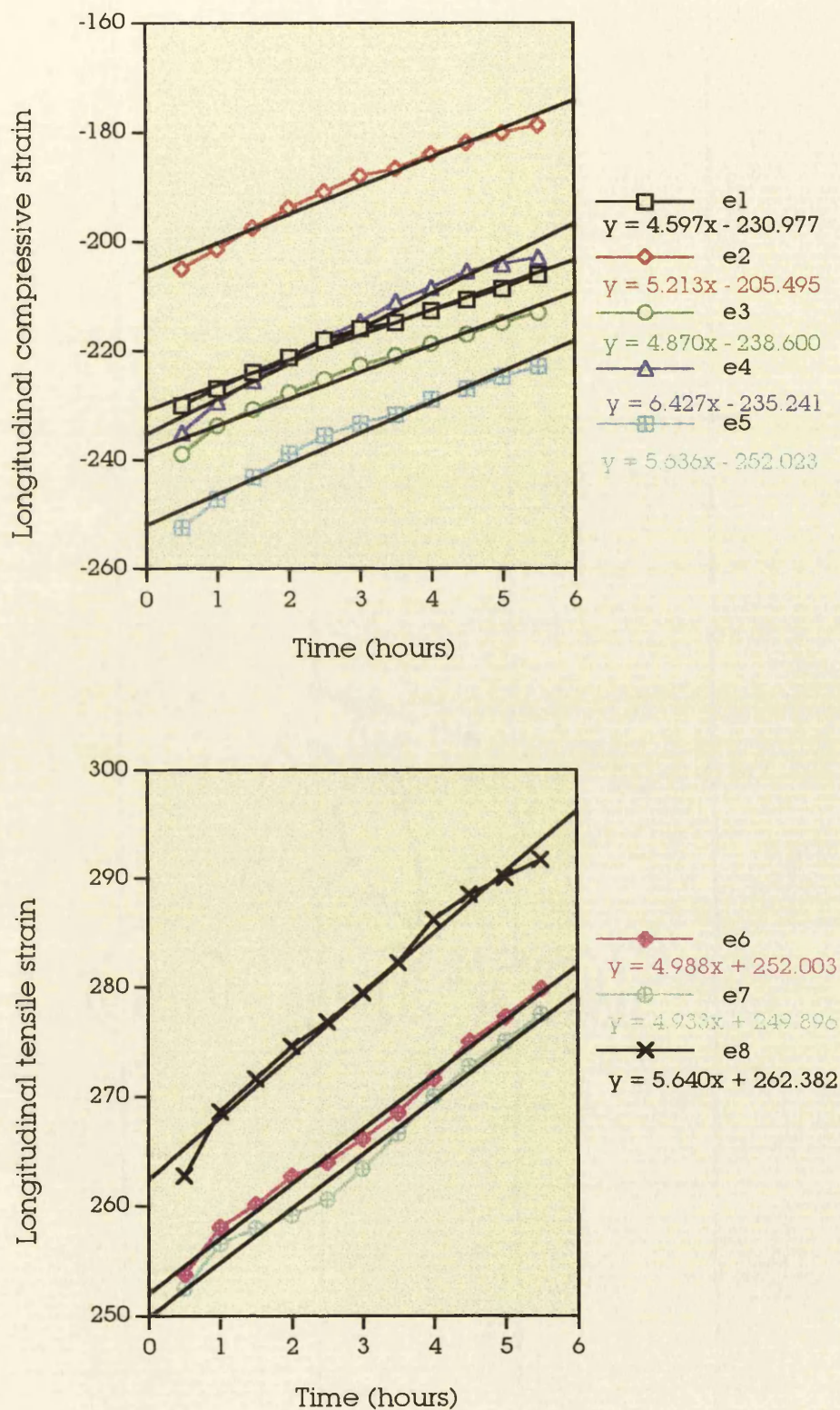


Fig. 6.27 Curve fit for the linear part of strain creep curves of model 2-4b

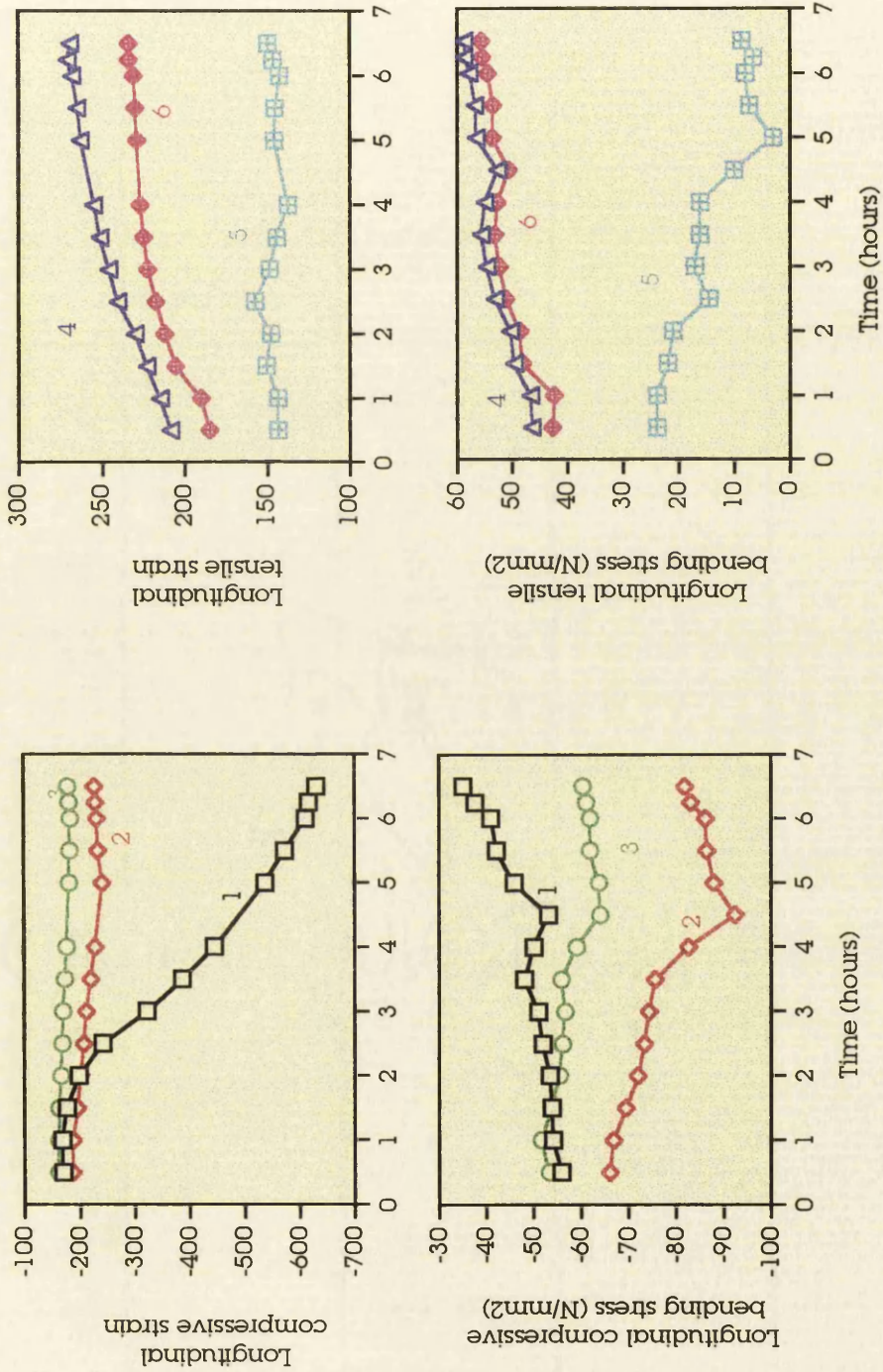


Fig. 6.28 Test 13: creep test of model 4-4b
Diagrams of longitudinal strains and stresses vs time

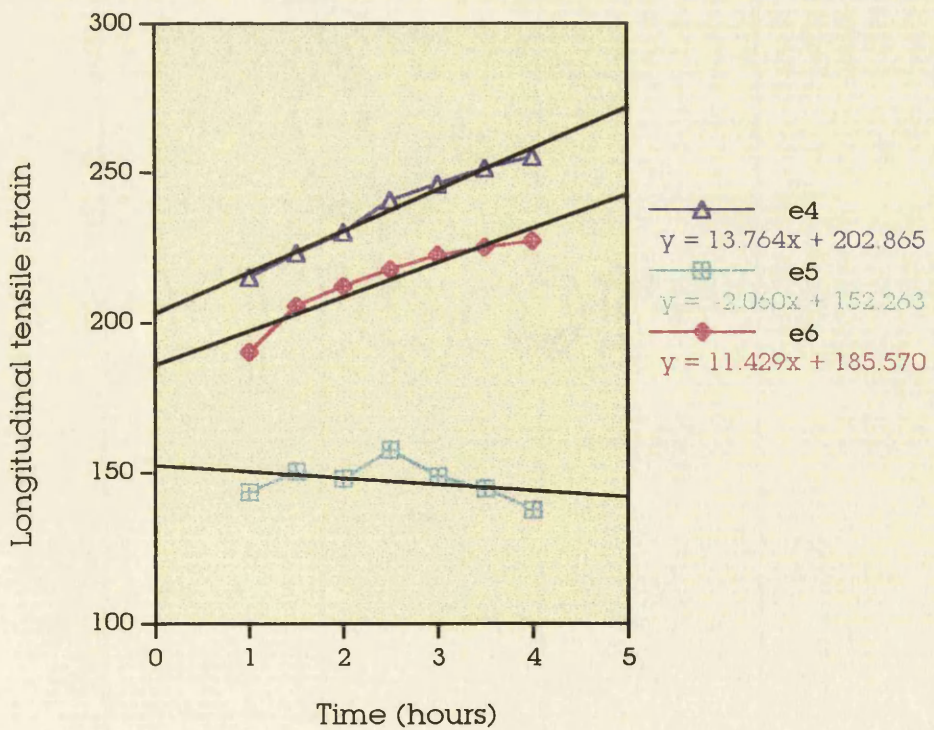
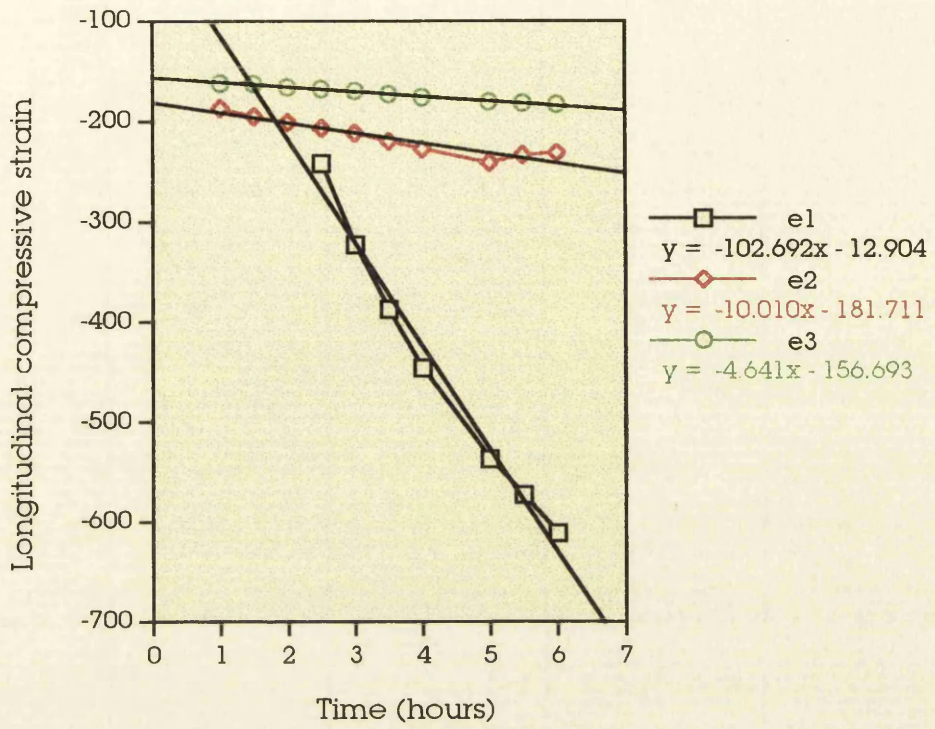


Fig. 6.29 Curve fit of the linear part of strain creep curves of model 4-4b

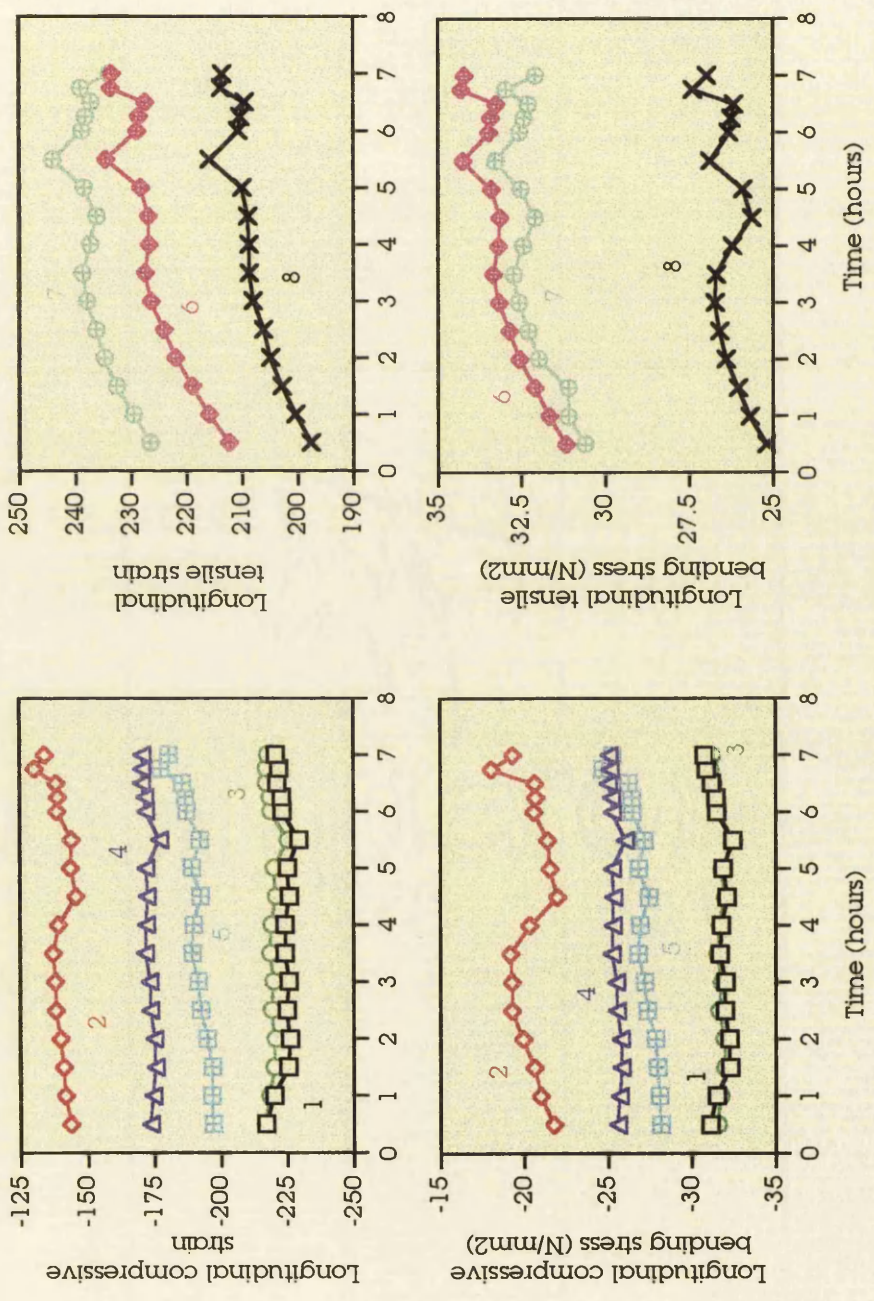


Fig. 6.30 Test 9: creep test of model 1-4b
Diagrams of longitudinal strains and stresses vs time

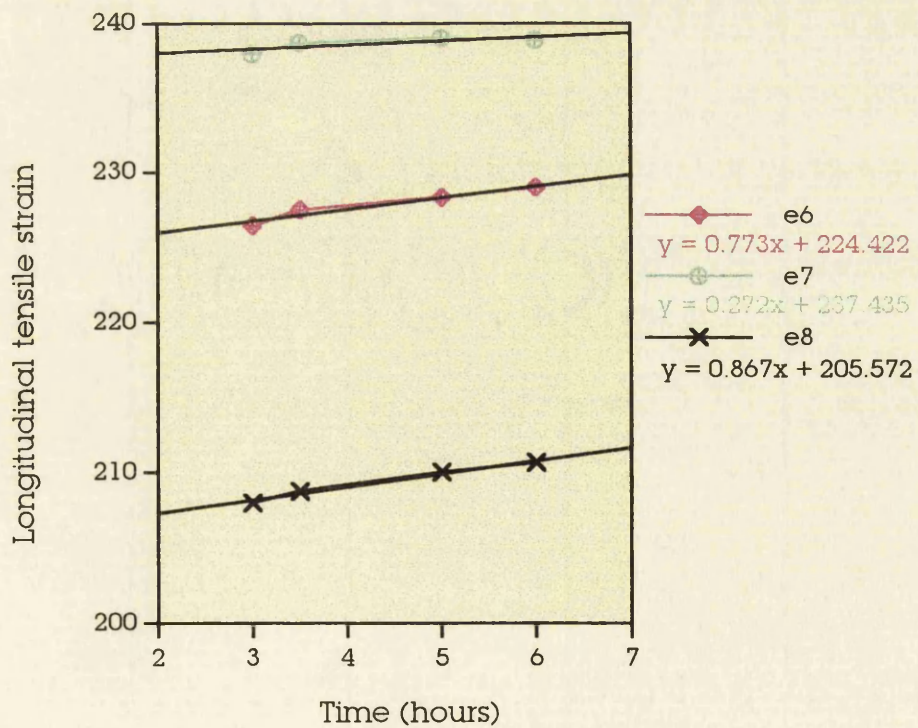
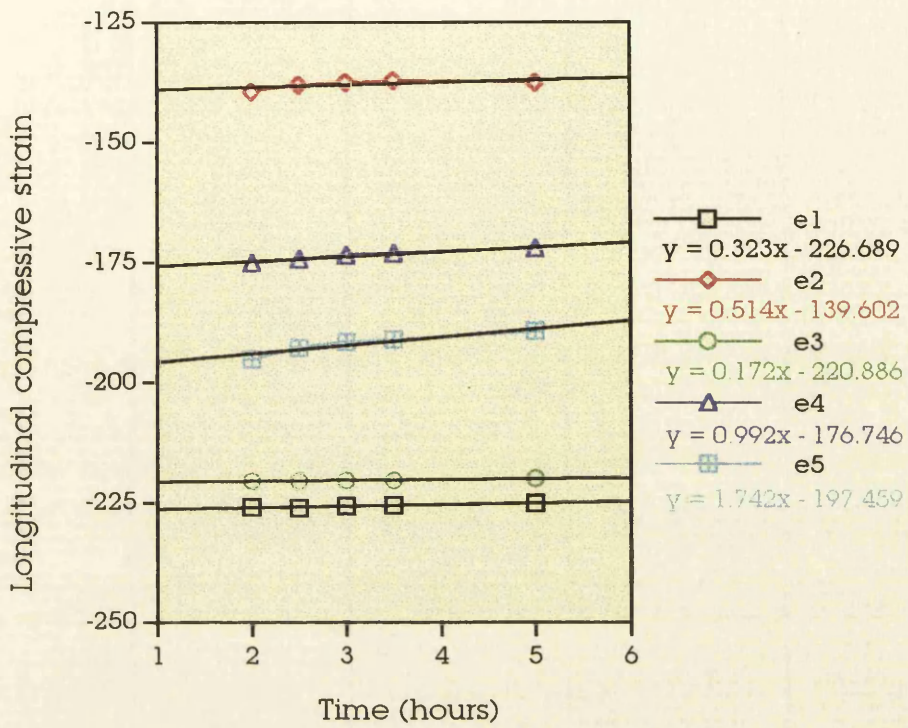


Fig. 6.31 Curve fit of the linear part of strain creep curves of model 1-4b

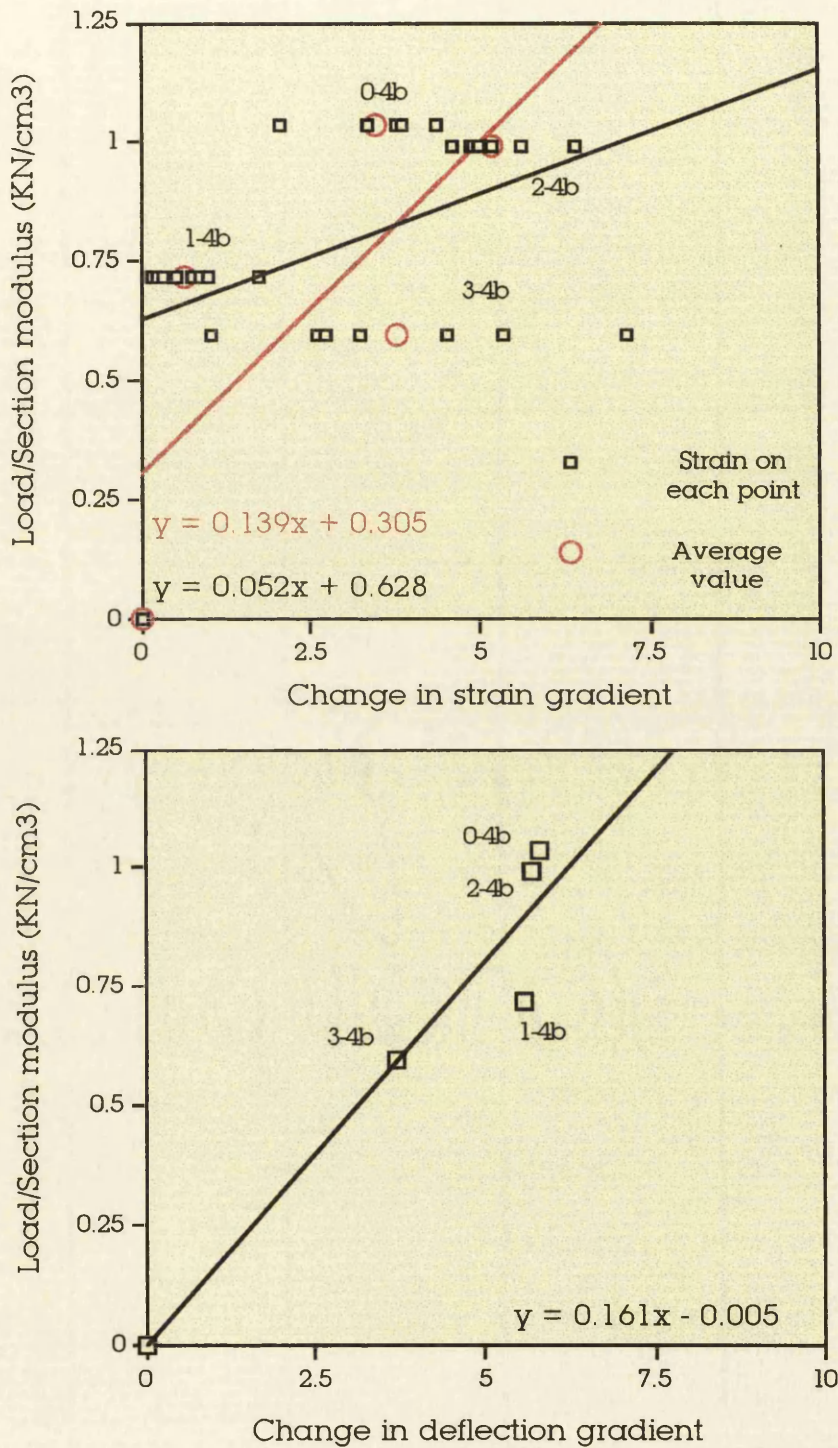


Fig. 6.32 Diagrams showing the relationship between Load/Section modulus factor and strain or deflection gradient

The axial compression tests results appear in Fig. 6.33-6.36. All values of deflections and stresses are differences from initial 'zero' values taken with an unloaded model at the start of the experiments. The longitudinal bending stress is the stress along the x axis of the model while the transverse one is along the y axis. The diagrams contain those points which describe the behaviour of the model up to and including the maximum registered compression load point. In the legend accompanying the diagrams, s stands for stress while the number denotes the particular point of the model, having been defined previously in Fig. 6.5-6.6, where that strain gauge is available.

Here again, before mentioning some observations concerning the diagrams which follow, a very important point should be highlighted and commented. The tests and especially the relevant diagrams describe mainly the behaviour of that part of the models which resisted the compression load application, namely the upper part, and **not** the behaviour of each model as a whole unit. This explains why a global failure of the models did not occur but just a local one. Also, it explains why models of completely different sectional stiffness level (see Table 5.3), appear to collapse in such a similar manner; i.e. their behaviour during the tests is not proportional to their strength. Here, however, the value of compression stress expected from theory calculations does not differ very much from the experimental values, **taking of course into account** that the value of m has been selected quite arbitrarily (see Appendix D). In other words, during these tests happened the same thing as in the four point bending ones: the strength of the models was dictated by the local strength of their upper part. This simply implies that the models have been too stiff to compress within the available machine. However, it has to be mentioned that at least as far as the web length, and in consequence the web depths, are concerned, they could not be made smaller than that of model 1-4b, because of the unavailability of suitable manufacturing equipment within the University premises. Therefore, the only parameter that could change is the model width reducing, in this way, the number of alternative design options.

Now, some observations regarding Fig. 6.33-6.36 are as follows:

- As far as the longitudinal compression stress diagrams, that is Fig. 6.33, 6.34 and 6.35, are concerned, the stress distribution at the different points on both plates of each model is not uniform. There is certain variation, that is the stress level is not the same at all points of either the top or bottom plate, but it is not large. In contrast to the bending tests, at the transverse compression stress diagrams, the stresses behave in a more consistent way. Furthermore, the stress level in the y direction is not so low as in the bending tests and therefore in this case the transverse stresses may have an important effect for this kind of structures.
- Again, the stress level at the point where bond lies, as shown in Fig. 6.6, (point 1 for model 4-c) is somewhat greater than that at the interflange point (point 2). This may suggest that the region along the bond area contributes to the local stiffening of the structure which should be expected and exploited.
- There seems to be no evidence of adhesive failure or element failure, except in way of distortions under load application, a fact which applies to all specimens.
- Fig. 6.36 shows quite clearly how theory coincides with experiments and this happens mainly because a lot of serious studies have been done in the past by a number of scientists as far as compression in sandwich, and especially corrugated core sandwich, structures is concerned which results in small deviations to exist. Of course here it has to be repeated that the theoretical values have been calculated based on an arbitrarily chosen m .

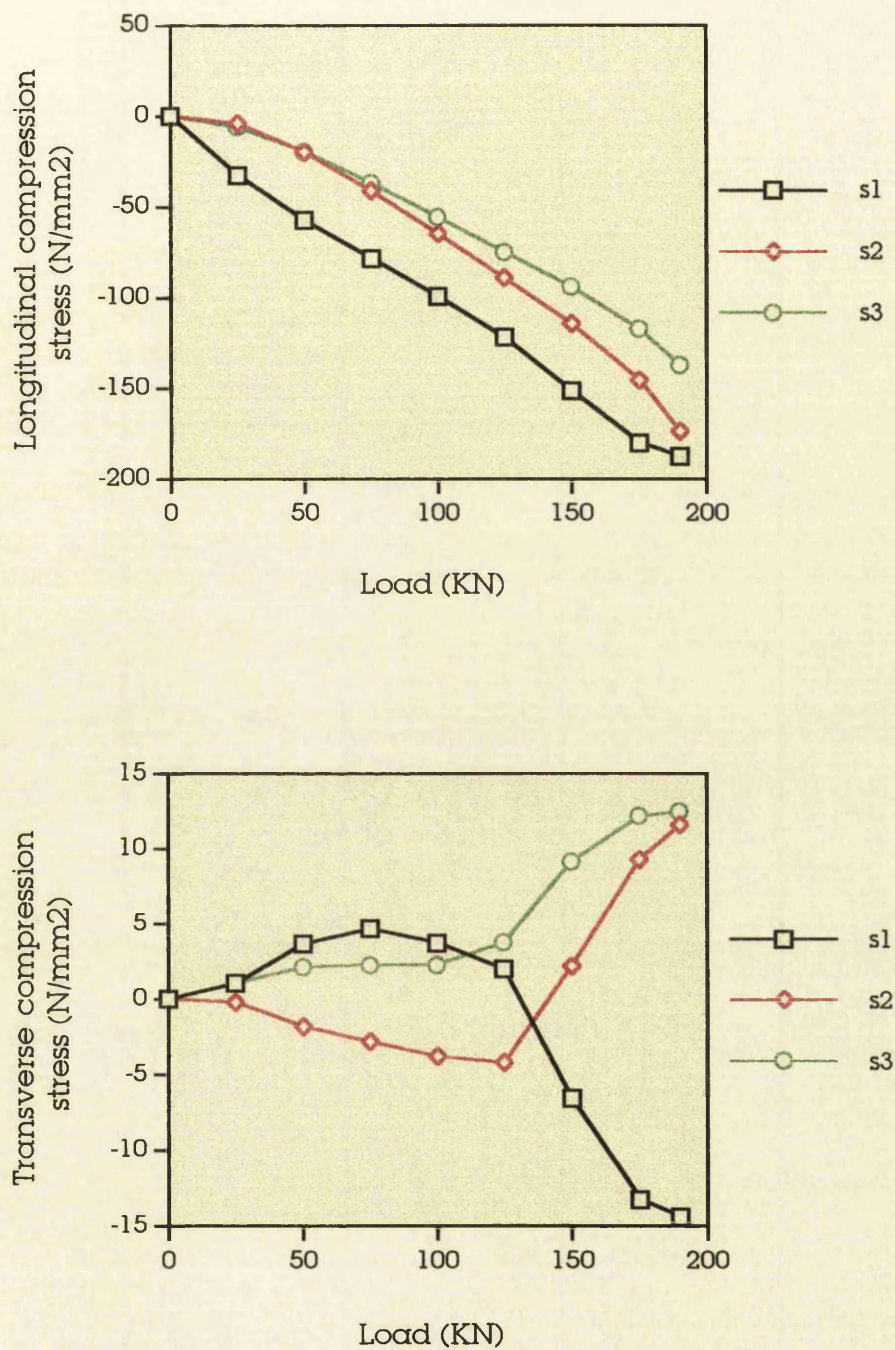


Fig. 6.33 Test 17: axial compression test of model 2-c

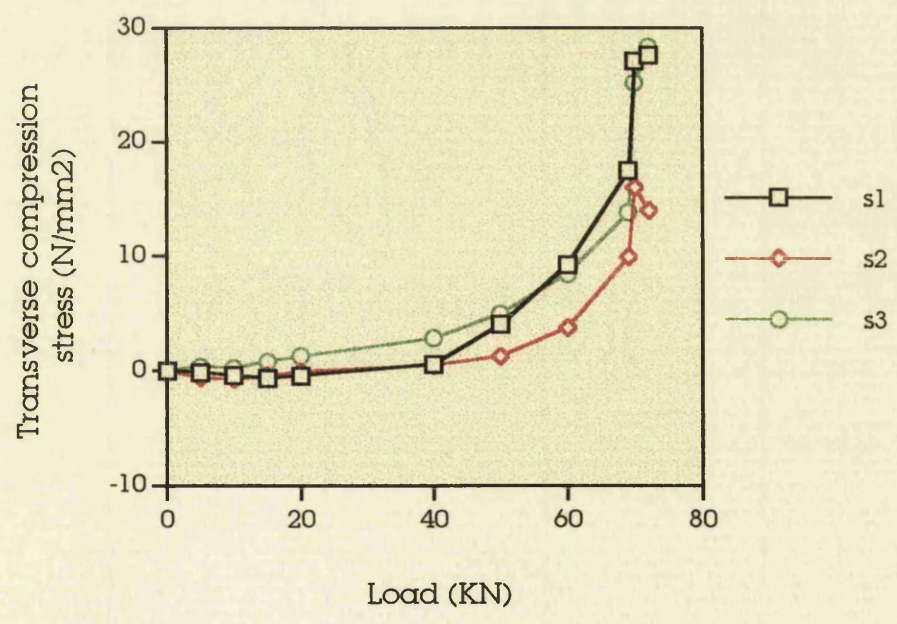
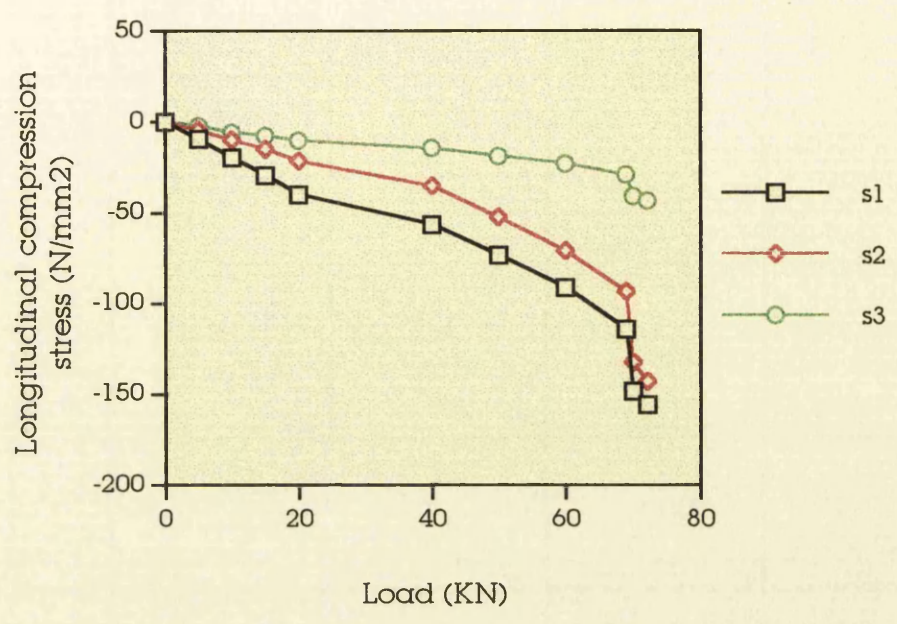


Fig. 6.34 Test 18: axial compression test of model 1-c

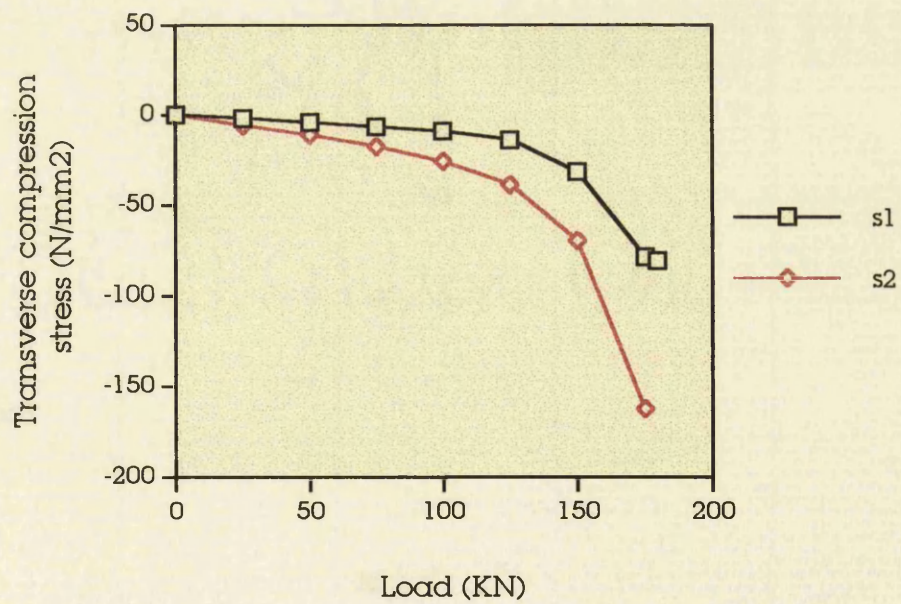
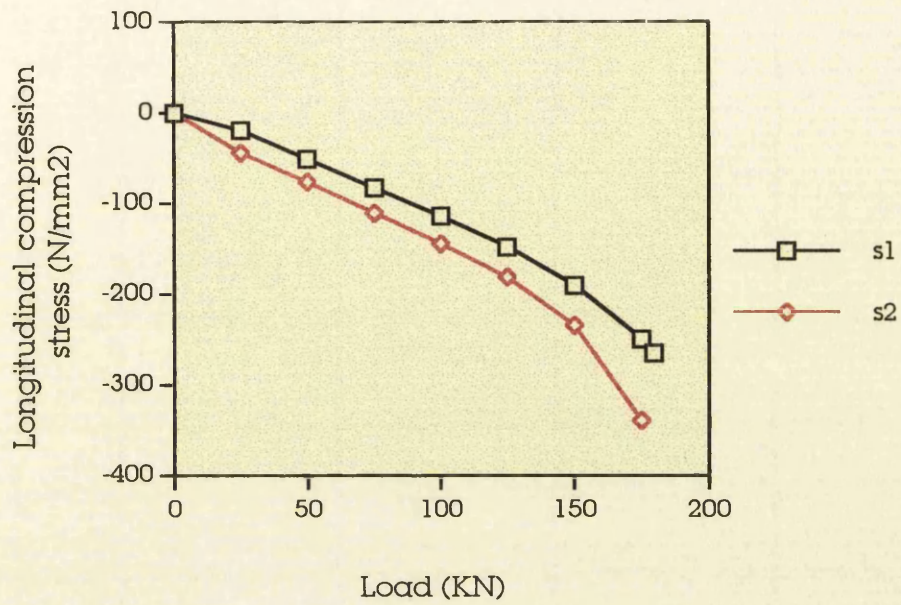


Fig. 6.35 Test 19: axial compression test of model 4-c

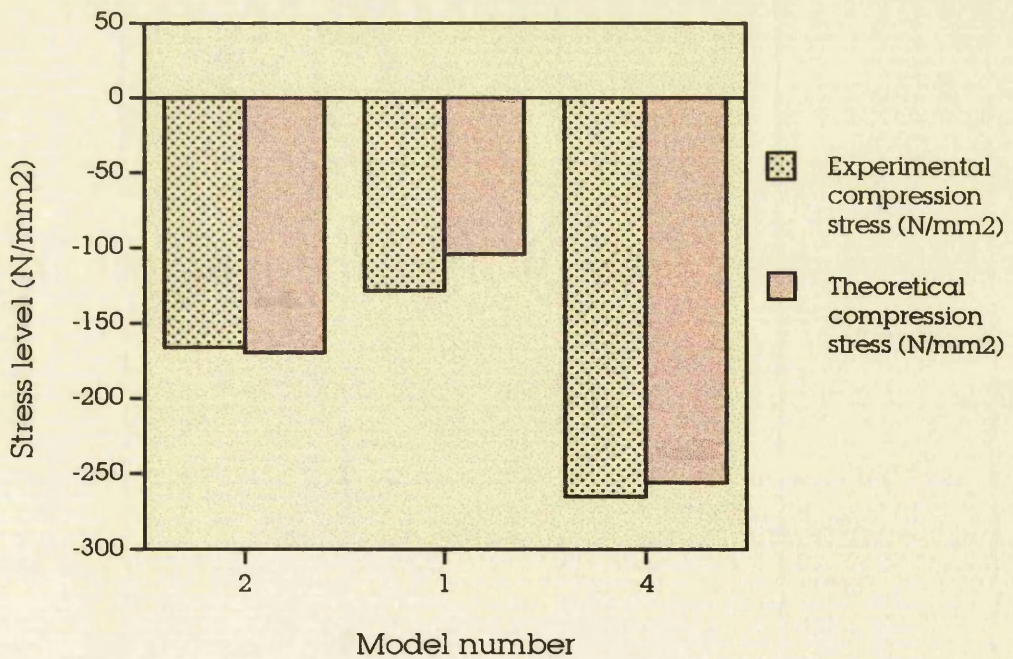
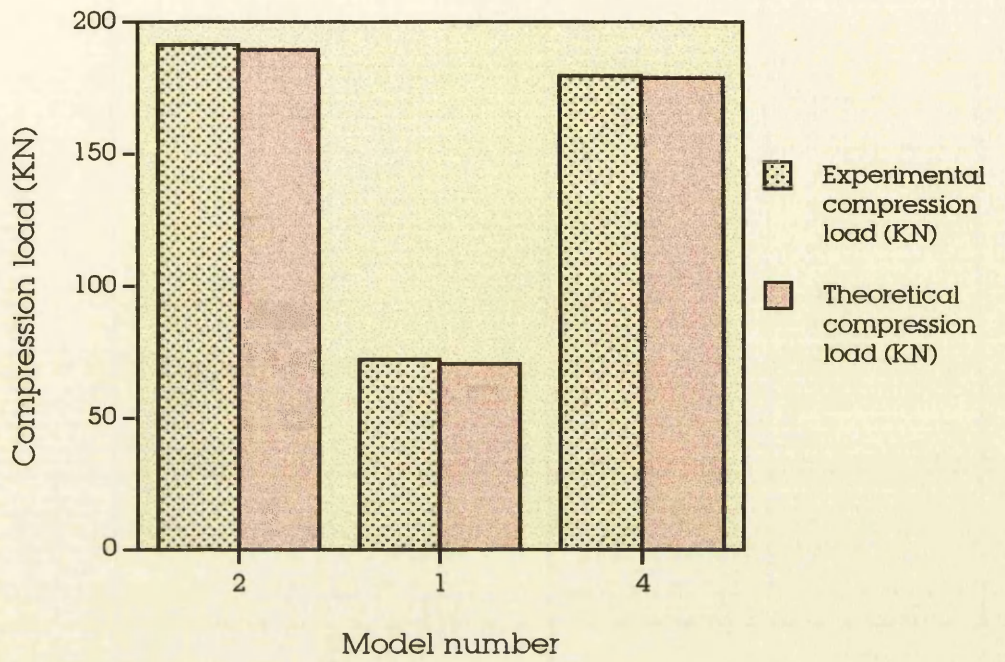


Fig. 6.36 Axial compression tests of models 2-c, 1-c and 4-c
Diagrams of compression load and stress levels for all models

The three point bending tests results appear in Fig. 6.37-6.38. What should be repeated here is that models 0-3b and 3-3b had been previously tested for axial compression, which implies that they were not intact. Furthermore, creep tests were not performed for these models. All values of deflections and stresses are differences from initial 'zero' values taken with an unloaded model at the start of the experiments. The longitudinal bending stress is the stress along the x axis of the model while the transverse one is along the y axis. The diagrams contain those points which describe the behaviour of the model up to and including the maximum registered bending load point. In the legend accompanying the diagrams, s stands for stress while the number denotes the particular point of the model, having been defined previously in Fig. 6.7, where that strain gauge is available. SBT stands for the value estimated using Simple Beam Theory.

Before mentioning some observations concerning the diagrams which follow, it must be noted that the same important point highlighted and commented during the four point bending tests discussion is still valid here. To prove that, it is worth mentioning that the maximum bending load for model 0-3b was 44.6 KN while for model 3-3b was just 49.45 KN.

Now, some observations regarding Fig. 6.37-6.38 are as follows:

- As far as the longitudinal bending stress diagrams are concerned, the stress distribution at the different points on both plates of each model again is not uniform. There is certain variation, that is the stress level is not the same at all points of either the top or bottom plate, but it is not large - in fact, it is smaller than the four point bending tests - and the pattern is linear (at least within the elastic region). In contrast, at the transverse bending stress diagrams, not only does a non-uniform pattern exist but a non-linearity as well. However, the stress level in the y direction is low and therefore the transverse stresses do not have an important effect in this kind of structures.
- The stress level at points where bond lies (points 1, 4, 8 and 9) is

somewhat greater than that at interflange points (points 2, 3, 5, 6 and 7).

- As mentioned in the four point bending tests discussion, simple beam theory values for stresses and deflections does not seem to agree with the experimental ones, especially for model 3-3b. For model 0-3b, the situation is somewhat better. Here it should be mentioned that comparing Fig. 6.30 with Fig. 6.8, it can be seen clearly that model 0-3b, which was not tested for creep, behaves in a more consistent way. There seem to be some discrepancies between theory and experiments which could also be attributed to imperfections occurring during the manufacture of the models, the material properties from which they were constructed, the installation of the strain gauges, the measuring of the strain gauge values and the important fact that before these tests the models were tested in column buckling tests as well. Here we have to mention that only the SBT curve corresponding to the tensile stress level has been plotted, since only that should be compared to the curves corresponding to stress values at points 7, 8 and 9, lying at midlength of the model (see Fig. 6.7).
- The stress values at antisymmetric points (points 2 and 3, 5 and 6, 8 and 9) on the top or bottom plate of each model, are more or less the same or very near the one to another.
- As already mentioned, the models had previously been used in axial compression tests and this may imply that the stress level appearing in the diagrams might have been influenced somehow.
- There seems to be no evidence of adhesive failure or element failure, except in way of distortions under load application, a fact which applies to all specimens.

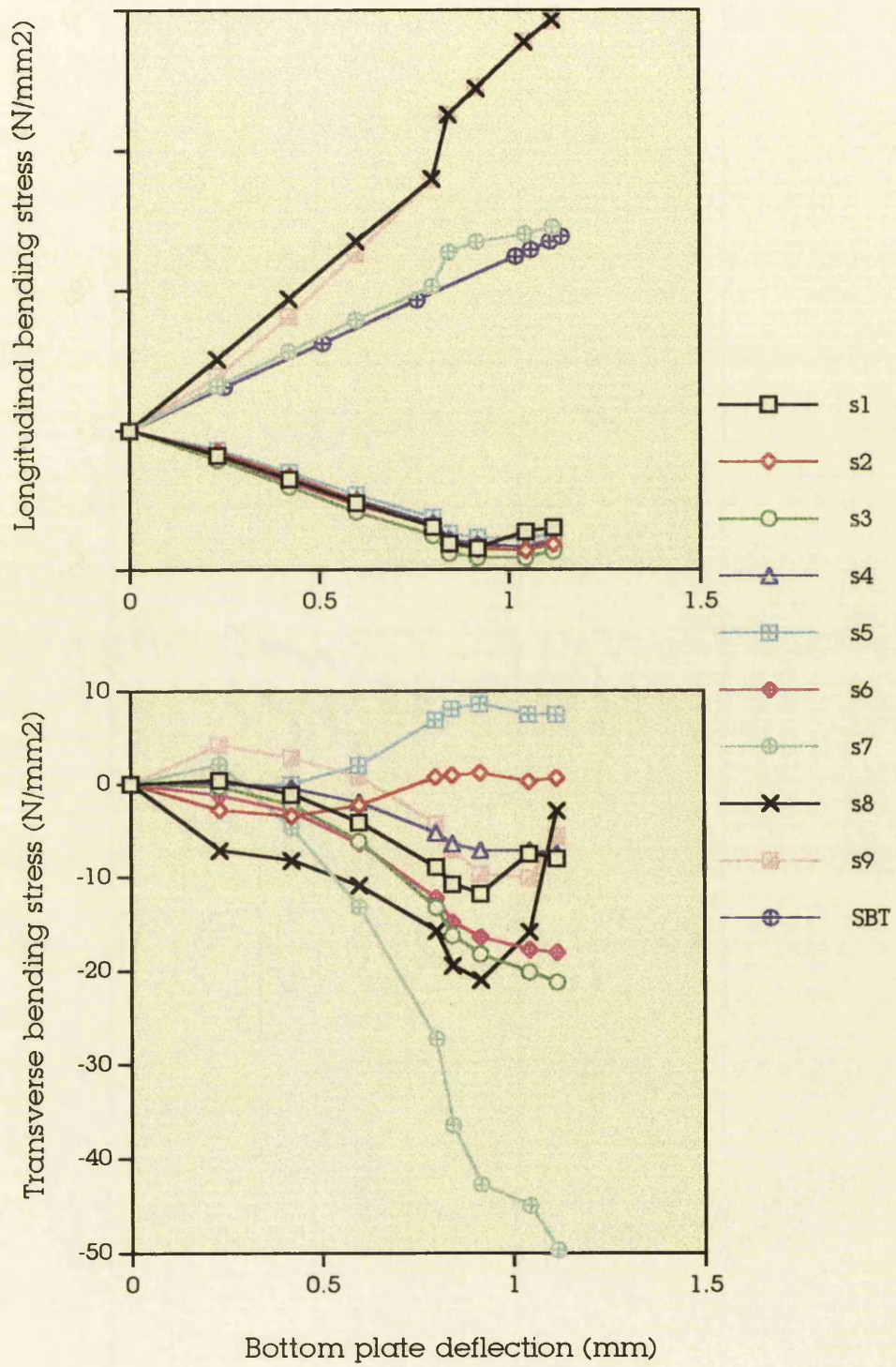


Fig. 6.37 Test 20: three point bending test of model 0-3b
Diagrams of bending stresses vs deflection

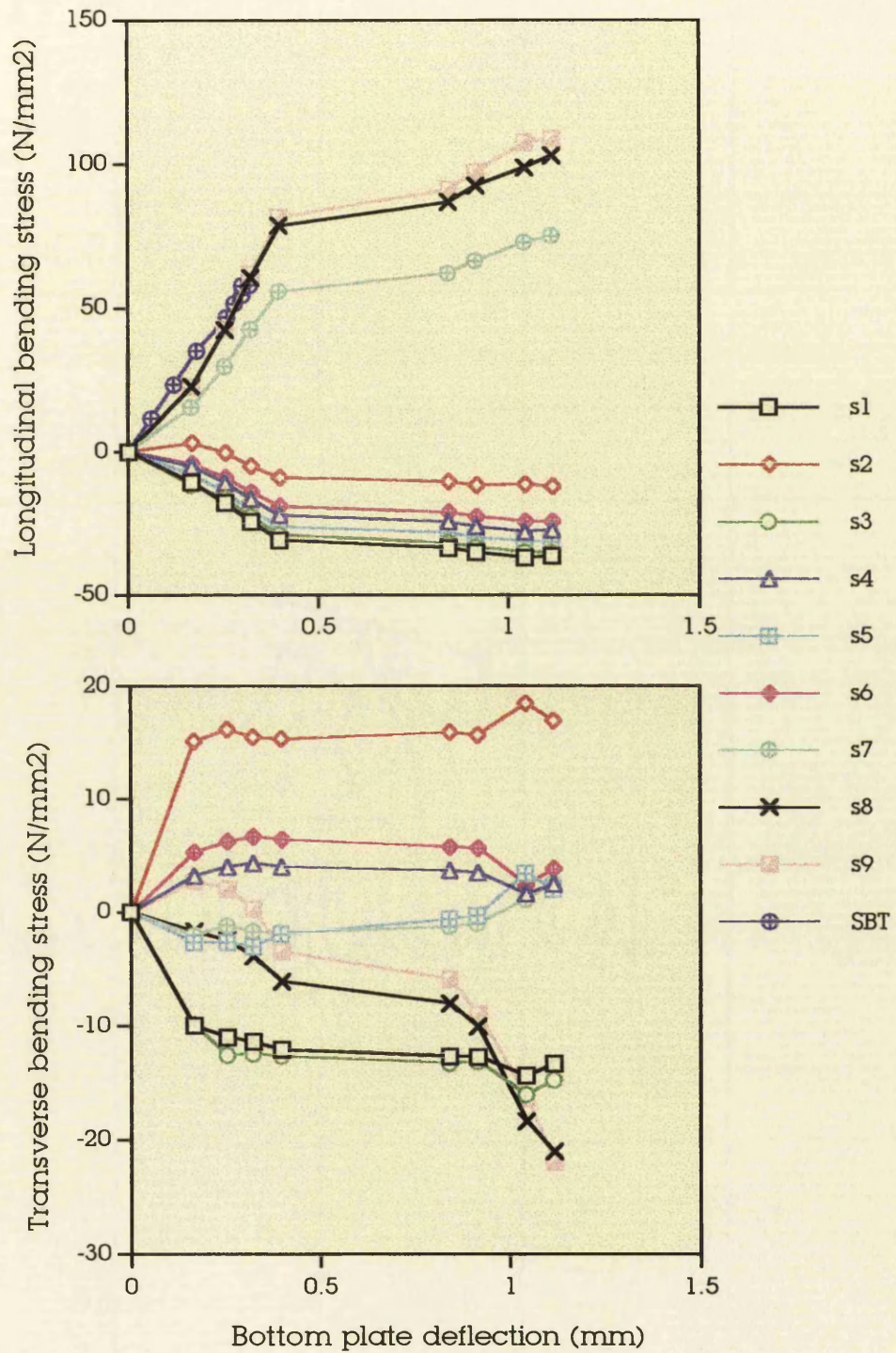


Fig. 6.38 Test 21: three point bending test of model 3-3b
Diagrams of bending stresses vs deflection

CHAPTER 7

DISCUSSION

"In fact we have to give up taking things for granted, even the apparently simple things. We have to learn to understand nature and not merely to observe it and endure what it imposes on us. Stupidity, from being an amiable individual defect, has become a social vice."

J.D.Bernal, *New Scientist*, 5-1-67. [55]

7.1 GENERAL

The problem studied in this MSc thesis is concerned with understanding the performance of adhesively bonded steel corrugated core sandwich structures used for marine applications under realistic loading, namely bending and axial compression. This has been accomplished through experimentation on models manufactured especially for this purpose and represents a development of research at Glasgow undertaken within SERC/MoD contract GR/E96832, entitled "Adhesively Bonded Sandwich Structures in Marine Technology" [7], which investigated the feasibility of bonding corrugated steel cores into steel sandwich beams typical of potential bulkhead and deck structures for ships. The findings of the work can be stated as follows:

Prediction of the stresses in a corrugated core sandwich structure with corrugations running along the x axis when it is subject to bending (either four or three point bending) appears to conform to simple beam theory, although there seem to be some discrepancies between theoretical and experimental values. These could be attributed to imperfections occurring during the manufacture of the models, the material properties from which they are constructed, the installation of the strain gauges, the measuring of the strain gauge values and the important fact that **both kinds of bending tests followed either the creep or compression tests**. One should expect a different set of results from completely intact models, but earlier tests [3] had indicated that repeated loading to such beams did not

compromise failure strength or stiffness.

Here a very important point should be highlighted and commented. The tests and related results appear to be limited mainly by the behaviour of that part of the models which resisted the localised bending load application, namely the upper flange, and **not** the behaviour of each model as a whole unit. This explains why no global failure of the models could be produced but just a local one. Also, it explains why models of the same group, (see Section 6.6) though they are of completely different sectional stiffness level, appear to collapse in such a similar manner; i.e. their behaviour during the tests is proportional to their local upper flange strength. Finally, it explains why the value of yield stress expected from simple beam theory calculations does not coincide with the experimental values. In other words, as far as the tests of the present project are concerned, the strength of the models was dictated by the local strength of their top plate together with a part of the upper web plating, with the neutral axis of the structure not lying at half depth but having moved upwards. This simply implies that the models have been too stiff to bend within the available machine. However, it has to be mentioned that at least as far as the web length, and in consequence the web depths, are concerned, they could not be made smaller than that of model 1-4b, because of the unavailability of suitable manufacturing equipment within the University premises. Therefore, the only parameter that could change is the model width reducing, in this way, the number of alternative design options. So, a suggestion that could be made for possible future work concerning corrugated core sandwich models is that the models should be tested over large spans in a larger testing machine.

7.2 BENDING TESTS

As far as the longitudinal bending stress is concerned, the stress distribution across each model is not uniform either between or within the flange plate. More specifically, the stress level at points where the bond lies is somewhat greater than that at interflange points which means that the adhesive helps for the 'concentration' and rigidity of the structure at the


aforementioned points. Furthermore, the stress values at antisymmetric points on the top or bottom plate of each model are more or less the same or very close to one another. However, this variation is not large and the pattern is linear (at least within the elastic region, see Fig. 6.10). In contrast, for the transverse bending stress, not only does a non-uniform pattern exist but a non-linearity as well (see Fig. 6.10). However, the stress level in the y direction is low (approximately 10% of that in the x direction) and therefore the transverse stresses do not have an important effect in this kind of structures irrespective of the web angle under which they have been constructed.

As far as the deflection levels are concerned, the top plate deflection values are greater than the bottom plate ones which can be explained by the fact that the measured deflection at that part of model is significantly increased by the local indentation of the top plate at load application points. These local deflection readings cannot therefore be used to represent overall beam deflection.

This type of corrugated core (with corrugations running along the x axis) is highly directional, its rigidity in the longitudinal direction being many times greater than that in the transverse direction, as shown by the results of the panels studied by Smith et al. [7], where the core structure runs in the y direction. From that it could be concluded that to utilise a panel to its best advantage the core should be oriented such that the predominant load is carried in the longitudinal direction. Buckling of the webs and any other deformation occurred only adjacent to the points of load application causing some local, but no global, adhesive damage. In this type of structures the core consists of a series of plate elements which may permit local instabilities. In other words, there are many interactions among the webs, the top and bottom plates and the flanges which may result in a non-uniform and complicated but linear stress behaviour along the x axis of the faces of the sandwich and a non-uniform, complicated and non-linear stress behaviour along the y axis of the faces (see, for example, Fig. 6.12).

For this reason, to fully evaluate the aforementioned effects, extensive finite element analysis would be required, otherwise, much data has to be drawn out during experiments with the use of numerous strain

gauges. This could form the subject of a future study since the present one did not have this as an objective. So, one should expect that - as discussed in Chapter 2 (2.8), and pointed out in [7] - the mode of failure of the corrugated-core sandwich panel is governed by the combination of face and core geometry. There is no single predominant factor. Core and face plate failures are mutually exclusive since the mechanism of face failure requires core integrity to develop very high axial stresses in the faces. This can only occur at moderate curvatures provided the skins remain a large distance from the neutral axis. The switch between the two failure types is subtle and thus a detailed understanding of the core geometry and localised deformation effects is necessary to permit design for a specific mode of failure. In addition, because of the fact that for marine applications the skin thickness will generally be kept high to allow for corrosion and guard against accidental penetration damage from local impact, failure of the skins is relatively unlikely and the geometry of the core will be the important design parameter. More specifically, the web angle must be considered to be the more serious and critical design parameter due mainly to the great accuracy which is required to manufacture it.

The idea of manufacturing the core of the models by joining half corrugations, i.e. , seems to work satisfactorily especially since in the real life of marine industry high core depths are required (approximately 0.3-1 m in SWATHs) and fabrication of a continuously corrugated core is very difficult, if not impossible in such cases. However, further investigation has to be undertaken on this concept, since the areas of both half flanges along the whole length of the model form the bond area and, as pointed out in [7], finite element analysis has highlighted the bond area as a critical design feature of the core geometry which in turn is the most important design parameter for marine applications. But, in general, we have to mention that accuracy within predetermined tolerances during construction is an effective way to prevent operational anomalies during the time this specialised structure is under service.

As a conclusion for the bending tests, it can be pointed out that the performance of the models was more than satisfying as far as their design

is concerned in combination to the adhesive performance. It should be remembered (see Chapter 5) that the models were designed to their buckling limits. However, buckling of the webs and any other deformation occurred only adjacent to the points of load application causing some local but no global adhesive failure and premature model damage. Besides, none of the models collapsed due to the fact that their strength was dictated by the local strength of their top plate together with a part of the upper web plating and therefore have been too stiff to collapse through overall bending failure within the available machine.

7.3 CREEP TESTS

The creep tests go some way towards a better understanding of the adhesive performance under constant load and its effect on the corrugated core steel sandwich structures. Creep of the adhesive can affect the performance of the models. This is shown by taking into consideration the common behaviour of all models tested for creep as far as variations in strains and deflection are concerned (as discussed in Chapter 6). Here, it is worth mentioning that, taking into account the fact that the strength of the models was dictated by the local strength of their top plate together with a part of the upper web plating, it is very difficult or even impossible to know whether the present creep tests describe the behaviour of the adhesive in conjunction with the members of the 'model' structure as a whole unit or they just describe the adhesive behaviour within the upper region of the structure. At this point, it is worth noting that sometimes during the creep of the adhesive both compressive and tensile strains and stresses may increase with respect to time which implies that a redistribution of strains and stresses is taking place.

Similar variations in strain and stress values occur at different points across the section as in the bending tests. Furthermore, at the points where the bond lies the strain and stress values seem to be higher than those concerning the interflange points. In addition to that, symmetrical points on both top and bottom faces do not seem to behave in the same way and besides there seems to occur a slight twist of the structure during the

application of the same or approximately the same amount of load for a long time (see Fig. 6.30). This slight twist may have occurred due to minor adhesive slippage or due to the fact that the upper plate of the model was not perfectly parallel to the bottom one. Finally, as discussed in Chapter 6, at a certain time point the creep curve of all points of the models starts to move in the opposite direction returning towards the initial condition. Unfortunately, this takes place towards the end of each creep test and it would have been useful if much more information had been available for this point of the creep tests. However, it should be noted that the maximum time of creep load application during the creep tests of this study was seven and a half hours since the machine could not be left safely unattended under load for a longer period. Longer creep tests with the load maintaining as constant as possible throughout the experiments should take place in the future. Furthermore, the testing machine could barely maintain the required constant load constantly (certain adjustments had to be made at certain time intervals and in one experiment it completely failed) and results cannot be considered as reliable. In the analysis of the creep results a useful factor is introduced to have a better visualisation of the efficiency of models during these tests and furthermore useful information can be drawn out. In other words, the load applied to each model can be divided by the model section modulus. Using this, it can be seen that as the load increases there is also an increase in strains and deflection, as should be expected. Furthermore, from this, the most applicable and appropriate for comparison constant creep load for any model could be calculated. In this project this was done after the creep tests and therefore the comparison has become relatively difficult but not impossible. However, the use of the prementioned factor could be recommended for future use. Finally, although there must be a law underlying the predetermined relationships (Load/Section modulus vs strains or deflection), it cannot be presented in this thesis, but a future attempt to discover it should be possible and worthwhile.

In a few words, in terms of real life performance, the strength of the adhesively bonded corrugated core sandwich structures can be seriously affected by the creep of the adhesive. This performance seems to be common for any corrugated core structure irrespective of the combination

of face and core geometry. This would seem to preclude use of such structures where significant continuous loading is concerned (for example, heavy weights on deck structure).

7.4 TENSILE TESTS

The tensile tests proved the importance of the role the manufacture material plays in this type of construction having a core with orthotropic flexural (bending) and transverse shear properties. If the material is orthotropic as well, the overall performance of this structure is far more complicated than if the material were isotropic. In the present project the tensile tests were performed after all main tests because they were essential for this project since the models were constructed from cold rolled steel plates cut in different directions from the parent plates. As a result, a number of 'strange' initial results could be corrected and explained with the aid of these tensile tests. This approach cannot be recommended for future work or for real life design of this kind of structures. Tensile tests should have been performed before any action.

7.5 COMPRESSION TESTS

In contrast to what happens in bending, in compression of this type of structures theory agrees almost perfectly with experiments and this happens mainly because a lot of serious studies [25, 27, 28, 30, 31] have been done in the past by a number of scientists as far as this matter is concerned which results in small deviations to exist. Therefore, prediction of the stresses in compression is possible and can be done very accurately. However, in the present project, the expression 'axial compression tests' should be replaced by column buckling experiments with clamped edges. The compressive strength of the models should have been evaluated experimentally using a compressive test rig like that illustrated in Fig. 6.2. Furthermore, conditions of simple or clamped support at the ends of test models should have had to be imposed with the aid of mechanisms

carefully designed for this purpose, but there was no suitable equipment available or provision to manufacture it within the project's objectives; also, there were practical limits on the length and slenderness of models which could be manufactured. Therefore, the dimensions of the compression models should have been somewhat different. In other words, longer and smaller in their cross section models should have had to be manufactured if we had wished to see an S buckled shape throughout the whole length (of course this is stated taking into consideration the capacity of the existing machine within the University premises). This resulted in the plate aspect ratio of the models of the present project not to be within the range in which the various authors of axial compression of corrugated core sandwich panels have made calculations and plotted graphs of relevant contents (for example the buckling coefficient for compression k vs plate aspect ratio β graphs), and therefore detailed comparisons cannot be done. So, the study from this point of view cannot be considered complete or successful. Here again it is important to note that the tests and especially relevant diagrams (Fig. 6.33-6.35) mainly describe the behaviour of the portion of the models which resisted the compression load application, namely the upper part, and **not** the behaviour of each model as a whole unit. This explains why a global failure of the models did not occur but just a local one. This also explains why models of completely different sectional stiffness level, appear to collapse in such a similar manner; i.e. their behaviour during the tests is not proportional to their strength. Here, however, the value of compression stress expected from theory calculations does not differ very much from the experimental values, **taking of course into account** that the value of m has been selected quite arbitrarily (see Appendix D, Table 2). In other words, the same thing happened in these tests as in the four point bending tests: the strength of the models was dictated by the local strength of their end faces. This simply implies that the models have been too stiff to compress within the available machine. However, it has to be mentioned that at least as far as the web length, and in consequence the web depths, are concerned, they could not be made smaller than that of model 1-4b, because of the unavailability of suitable manufacturing equipment within the University premises. Therefore, the only parameter that could change is the model

width reducing, in this way, the number of alternative design options.

However, some general statements as far as the column buckling tests are concerned can have as follows:

- The stress distribution at the different points on both faces is not uniform. There is certain variation, but it is not large. In contrast to bending, the transverse stresses behave in a more consistent way.
- The stress level in the y direction is not so low as in bending and therefore in this case the transverse stresses may have an important effect for this kind of structures.
- The stress level at points where bond lies is somewhat greater than that at interflange points.
- Buckling of the faces and any other deformation occurred only adjacent to the points of load application causing some local but not global adhesive debonding.

7.6 CONCLUSION

In conclusion, all objectives of the present work, as were clearly defined in Preface, have been achieved except for the fact that the models did not reach their ultimate strength so that a complete analysis could take place. However, the model structures designed for the purposes of the present project proved to be stable and strong; of course, in order to design and manufacture real life marine structures according to them, one should also take into consideration a number of additional parameters which have special importance for the kind of sandwich structures, namely marine environment characteristics, fatigue performance, the type and amount of loads imposed on them during their lifetime, construction and others. The way has been opened and further research work is expected to take place in the future.


CHAPTER 8
CONCLUSIONS
PROPOSED FUTURE WORK

8.1 CONCLUSIONS

The work and research done so far on the topic of the present thesis draw out some conclusions which are as follows:

- Corrugated core sandwich steel construction generates opportunities in the marine industry for lighter, high strength, stiff structures.
- Any experimental research concerning this kind of structures has to be designed very carefully taking into consideration factors such as: capability of construction facilities, availability of testing facilities, capabilities of testing equipment, properties of available material before any testing takes place, careful design of models and continuous attention before, during and after the testing in search of unusual phenomena.
- Prediction of the stresses in a bonded corrugated core sandwich structure with corrugations running along the x axis when it is subject to bending (either four or three point bending) conforms generally to simple beam theory, although there seem to be some discrepancies between theoretical and experimental values. These could be attributed to imperfections occurring either during the manufacturing process or during the whole experimental procedure.
- Local deformation of the plate and web at the point where the load is applied seems to be the main mode of failure in the tests used. The behaviour of the adhesive is excellent and failure of the structure occurs due to local effects rather than adhesive failure. Where adhesive failure does occur in way of point loads

on local structural deformation, it does not readily propagate along the joints maintaining an ability to transmit bending shear.

- In this type of structures the core consists of a series of plate elements each of which may permit local instabilities. In other words, there are many interactions among the webs, the top and bottom plates and the flanges which may result in non-uniform but linear stress behaviour along the x axis of the faces of the sandwich and a non-uniform, complicated and non-linear stress behaviour along the y axis of the faces, accompanied by many local instabilities. However, the stress pattern on the web plates, which are highly influenced by the deformation of both top and bottom plates through their flanges, is quite irregular and localised without showing a normal linear behaviour (even up to the elastic limit). For this reason, finite element analysis would be quite useful, otherwise, much information has to be drawn from experiments with the use of numerous strain gauges.
- It is worth noting that the stress level at points where the bond lies is somewhat greater than that at interflange points which implies that the adhesive contributes to the transmission of stress. Furthermore, the stress values at antisymmetric points of the top or bottom plate of each model are more or less the same.
- In addition, the idea of manufacturing the core of the models with the joining of half corrugations, i.e. , seems to work sufficiently (within the scope of this project), especially since in the real life of marine industry high core depths may be required up to 1 m (in SWATHs) and fabrication of continuous corrugations is impractical in such cases.
- The creep tests, however, reveal a serious potential disadvantage of adhesives, which can influence the strength of the structure during its operational lifetime. Physical laws

underlying adhesive creep performance are not fully evaluated in this thesis, but future work to discover them would be worthwhile. In terms of real life performance, the long term strength of adhesively bonded corrugated core sandwich structures can be seriously affected by the creep performance of the adhesive. That performance seems to be consistent for a range of corrugated core geometry. For marine applications this may be a serious limitation to use of adhesives where continuous high loading is present (for example, heavy weights on deck structure).

- In contrast to what happens in bending, the evaluation of compression strength for this type of corrugated core sandwich structure has been dealt with in detail by a large number of scientists [25, 27, 28, 30, 31] and therefore the difference between the theoretical and experimental results is quite small. Unfortunately, the present project has not been able to confirm this for reasons explained in the discussion, but it gives the stimulus to confirm this in a future work.
- The distribution of stress across the faces should be uniform for a well constructed model (with perfect installation of strain gauges and accurate measurements). In practice this does not appear to happen. So, bearing in mind that the behaviour of the models during the experiment programme gives an indication of how large scale real panels would behave, great attention should be paid to their design and incorporation in any marine structure. That attention should include knowledge of the whole system of the manufacturing process, the conditions present at the time of experimentation, how and to what extent should one make a serious interpretation and exploitation of the results and the conditions present in real life operation.

8.2 PROPOSED FUTURE WORK

In the author's opinion, the concept of adhesively bonded steel corrugated core sandwich structures specifically designed for marine applications is still new and is worth developing much further by encouraging further research.

Such research work would concentrate on making further investigations and comparisons into the behaviour of this kind of structures under not only bending and compression but combinations of loading conditions as well (e.g. bending and compression, uniaxial compression, transverse pressure and compression). The structural configurations would be again simple or more complicated. In the latter case, one should examine very carefully whether the configuration can be structurally viable and used as a structural member in any marine application. In fact, simplicity has always been regarded as a positive factor and prevents many problems from occurring. The present project proves quite clearly that adhesives, when used in this type of structures, are not the ultimate problem but rather the manufacturing technology and the detailed design of connections.

Furthermore, design of inter-frame panels (steel frames supporting GRP or aluminium skins) essentially to carry transverse pressures or any other type of loading would form an interesting topic for research work. These type of alternative configurations may be quite attractive and could be used widely in the construction of superstructures for any type of marine structures.

An understanding of the stress distribution within the adhesive bondlines using finite element analysis would be very useful for the future design of this type of structures since the present project proved clearly that there exists a differentiation. As a result, a logical and physical explanation, i.e. an underlying law, would perhaps be revealed to facilitate the future design.

The creep effect in the adhesives and how it can be reduced it would form another idea for future research work. More specifically, not only could the underlying physical laws be confirmed but methods to minimise the effects could be devised as well. Creep is a time dependent

phenomenon which also depends on magnitude of loading. In addition, the varying material properties of the adhesives under consideration are likely to have an effect on the physical laws so that the resulting deformation or displacement should result from a combination of these two parameters (adhesive properties and time). However, such research would demand long experimentation times and suitable testing equipment.

One of the main reasons for considering the type of structures studied in this project is that they possess high strength and high stiffness to weight ratios. This form of construction is appropriate for structures where the self weight is one of the governing design criteria. This is particularly applicable in cases where the self weight should be reduced while the strength is maintained. So, another interesting topic for future work would be the design of a sandwich panel with absolute minimum weight, yet retaining structural integrity (i.e., structurally optimum) for a given load index, panel geometry and face and core materials. All necessary rational methods concerning this very interesting topic have already been developed and can be found in [58]. Here, it should be highlighted that the methods developed in [58] have to do with triangulated core (truss-core), web-core and 'hat-shaped' core (corrugated-core) constructions subjected to uniaxial compressive loads. Nevertheless, comparisons could be made among those configurations in marine structures and useful conclusions drawn.

Finally, the manufacturing and testing of full scale models of sandwich panels should be an objective of any future research work. Such tests would allow everyone to get a better understanding of how this type of structures behaves under conditions approximately close to real life's ones and what the differences are from small scale model tests. Of course, such an action requires the support of a large constructional unit, such as a shipyard.

REFERENCES

1. J.M.Christie, SHIPYARD APPLICATIONS OF ADHESIVES, NAOE Final Year Project, 1984-1985
2. R.K.Macleod, ADHESIVELY BONDED STEEL SANDWICH BULKHEADS, NAOE Final Year Project 89-06
3. R.L.Johansen, BONDED SPACE FRAME SANDWICH CORES FOR SHIP CONSTRUCTIONS, NAOE Final Year Project 91-05
4. H.G.Allen, ANALYSIS AND DESIGN OF STRUCTURAL SANDWICH PANELS, Commonwealth and International Library of Science Technology Engineering and Liberal Studies
5. F.J.Plantema, SANDWICH CONSTRUCTION, John Wiley & Sons, Inc., N.Y.* London * Sydney
6. I.E.Winkle, M.J.Cowling, S.A.Hashim, E.M.Smith, WHAT CAN ADHESIVES OFFER TO SHIPBUILDING?, Journal of Ship Production, Vol. 7, No 3, Aug. 1991, pp. 137-152
7. I.E.Winkle, M.J.Cowling, E.M.Smith, ADHESIVELY BONDED SANDWICH STRUCTURES IN MARINE TECHNOLOGY, Final Report, October 1991, Joint SERC/MoD Project GR/E96832
8. I.E.Winkle, M.J.Cowling, S.A.Hashim, A STRUCTURAL ROLE FOR ADHESIVES IN SHIPBUILDING? in Proceedings, RINA, Spring Meetings, London, 1989
9. W.A.Lees, ADHESIVES IN ENGINEERING DESIGN, The Design Council, London, 1984
10. C.V.Horie, MATERIALS FOR CONSERVATION (Organic

consolidants, adhesives & coatings), Butterworths (pp. 71-75)

11. Edited by D.M.Brewis, D.Briggs, INDUSTRIAL ADHESION PROBLEMS, Orbital Press * Oxford

12. Edited by D.F.Aitken, ENGINEER'S HANDBOOK OF ADHESIVES, The Machinery publishing Co. Ltd

13. Edited by R.K.Penny, THE EXPERIMENTAL METHOD, Longman

14. M.J.Cowling, S.A.Hashim, E.M.Smith and I.E.Winkle, ADHESIVE BONDING FOR MARINE STRUCTURAL APPLICATIONS, Paper 7, Reprint of Polymers in a Marine Environment, London, 23-24 October 1991, organised by the Institution of Marine Engineers

15. W.Brockmann, STEEL ADHERENDS, Chapter 7: 'Durability of Structural Adhesives', Fraunhofer, Institut fur Angewandte Materialforschung, Bremen, Federal Republic of Germany

16. I.J.McGregor and D.Nardini, MODELLING AND TESTING OF ALUMINIUM BONDED STRUCTURAL COMPONENTS, Alcan International Ltd, Banbury Laboratories, Oxon, UK

17. R.N.Swamy, R.Jones, J.W.Bloxham, STRUCTURAL BEHAVIOUR OF REINFORCED CONCRETE BEAMS STRENGTHENED BY EPOXY-BONDED STEEL PLATES, The Structural Engineer, Vol. 65A, No. 2, February 1987

18. C.S.Smith, DESIGN OF MARINE STRUCTURES IN COMPOSITE MATERIALS, Elsevier Applied Science, 1990

19. RINA, SYMPOSIUM ON GRP SHIP CONSTRUCTION, London, October 1972

20. D.A.Taylor, MERCHANT SHIP CONSTRUCTION, Second edition, Butterworths, 1985

21. W.Muckle, THE DESIGN OF ALUMINIUM ALLOY SHIPS' STRUCTURES, Hutchinson of London, 1963
22. I.E.Winkle, THE ROLE OF ADHESIVES, Chapter 4 (pp. 43-62) of Composite Materials in Marines Structures, Vol. 2 Practical consideration, Shenoi R.A. and Wellicome, J.F. (eds), Cambridge University Press, Contribution to the 18th WEGEMT Graduate school (University of Southampton - March 1993) on "FRP Composite materials and their Marine Applications"
23. W.R.Graner, MARINE APPLICATIONS, Handbook of composites edited by G.Lubin, 1982
24. A.Marshall, SANDWICH CONSTRUCTION, Handbook of composites edited by G.Lubin, 1982
25. L.A.Harris and R.A.Auelmann, STABILITY OF FLAT SIMPLY-SUPPORTED CORRUGATED-CORE SANDWICH PLATES UNDER COMBINED LOADS, Journal of the Aero/space Sciences **27**, 7 July 1960, pp. 525-534
26. Published by the American Society For Testing Materials (A.S.T.M.), SYMPOSIUM ON STRUCTURAL SANDWICH CONSTRUCTIONS, Special Technical Publication No. 201, 1956, [papers related to constructional details]
27. P.Seide, THE STABILITY UNDER LONGITUDINAL COMPRESSION OF FLAT SYMMETRIC CORRUGATED-CORE SANDWICH PLATES WITH SIMPLY-SUPPORTED LOADED EDGES & SIMPLY-SUPPORTED OR CLAMPED UNLOADED EDGES, NACA TN 2679, 1952
28. C.Libove and R.E.Hubka, ELASTIC CONSTANTS FOR CORRUGATED CORE SANDWICH PLATES, NACA TN 2289 ,1951
29. Published by the American Society For Testing Materials (A.S.T.M.), SYMPOSIUM ON STRUCTURAL SANDWICH CONSTRUCTIONS, Special

Technical Publication No. 118, 21-6-1951, [reviews by various authors]

30. J.R.Robinson, THE BUCKLING AND BENDING OF ORTHOTROPIC SANDWICH PANELS WITH ALL EDGES SIMPLY-SUPPORTED, The Aeronautical Quarterly **6**, 2 May 1955, pp. 125-148

31. C.Libove and S.B.Batdorf, A SMALL DEFLECTION THEORY FOR FLAT SANDWICH PLATES, NACA Report No. 899, 1948

32. Edited by R.A.Shenoi and J.F.Wellicome, COMPOSITE MATERIALS IN MARINE STRUCTURES, Cambridge Ocean Technology Series 4&5, Volume 1: Fundamental aspects, Volume 2: Practical considerations, 1993

33. A.J.Kinloch, ADHESION AND ADHESIVES, Chapman and Hall, 1987

34. W.A.Lees and T.R.Baldwin, ADHESIVES FOR THE STRUCTURAL AND MECHANICAL ENGINEER, Chapter 7 of Industrial applications of Adhesive bonding, edited by M.M.Sadek, Elsevier Applied Science, 1987

35. G.C.Mays and A.R. Hutchinson, ADHESIVES IN CIVIL ENGINEERING, Cambridge University Press, 1992

36. O.F.Hughes, SHIP STRUCTURAL DESIGN, edited by John Wiley and Sons, 1983

37. Edited by R.Taggart, SHIP DESIGN AND CONSTRUCTION, Society of Naval Architects and Marine Engineers (SNAME), New York, 1980

38. E.M.Knox, S.A.Hashim, M.J.Cowling, I.E.Winkle, PERFORMANCE OF ADHESIVELY BONDED STRUCTURAL COMPONENTS FOR MARINE STRUCTURES, Conference on Structural Materials in Marine Environments, London, 11-12th May 1994

39. C.M.Davies, A.J.Stevens and A.F.Turner, STEEL BASED COMPOSITES FOR BRIDGE ENCLOSURE PANELS, Conference on Structural Materials in

Marine Environments, London, 11-12th May 1994

40. Edited by CONSTRADO, STEEL DESIGNER'S MANUAL, 4th edition, prepared for the Constructional steel research and development organisation, Oxford, 1972

41. B.Cheal, DESIGN OF CONNECTIONS, Chapter 26 of Steel Designers' Manual, edited by G.W.Owens and P.R.Knowles, 5th edition, The Steel Construction Institute, Blackwell Scientific Publications, Oxford, 1992

42. J.Robinson, FIRE PROTECTION AND FIRE ENGINEERING, Chapter 34 of Steel Designers' Manual, edited by G.W.Owens and P.R.Knowles, 5th edition, The Steel Construction Institute, Blackwell Scientific Publications, Oxford, 1992

43. W.McGuire, INTRODUCTION TO CONNECTION DESIGN, from Constructional Steel Design / An International guide, edited by P.J.Dowling, J.E.Harding and R.Bjorhovde, Elsevier Applied Science, London and New York, 1992

44. G.M.Newman and H.B.Walker, STEEL FRAMED MULTI-STOREY BUILDINGS. DESIGN RECOMMENDATIONS FOR COMPOSITE FLOORS AND BEAMS USING STEEL DECKS. SECTION 2: FIRE RESISTANCE, edited by CONSTRADO, 1983

45. B.O.Kuzmanovic and M.R.Sanchez, GIRDERS COMPOSED OF CORRUGATED METAL SHEETS, from Constructional Steel Design / World developments, edited by P.J.Dowling, J.E.Harding, R.Bjorhovde and E.Martinez-Romero, Elsevier Applied Science, London and new York, 1992

46. Edited by J.H.Howlett, W.M.Jenkins and R.Stainsby, JOINTS IN STRUCTURAL STEELWORK, The design and performance of semi-rigid and rigid joints in steel and composite structures and their influence on structural behaviour, Proc. of the Intl Conf. held at Teesside Polytechnic, Middlesbrough, Cleveland, 6-9th April 1981, Pentech Press

47. M.Holmes and L.H.Martin, ANALYSIS AND DESIGN OF STRUCTURAL CONNECTIONS: REINFORCED CONCRETE AND STEEL, published by Ellis Horwood Ltd, 1983
48. Edited by R.Narayanan, STRUCTURAL CONNECTIONS. STABILITY AND STRENGTH, Elsevier Applied Science, London and New York, 1989
49. G.P.Anderson, S.J.Bennett and K.L.DeVries, ANALYSIS AND TESTING OF ADHESIVE BONDS, Academic Press, New York - San Francisco - London, 1977
50. R.M.Hussein, COMPOSITE PANELS/PLATES: ANALYSIS AND DESIGN, Technomic Publishing Co., 1986
51. T.C.Fung, K.H.Tan and T.S.Lok, ANALYSIS OF CORRUGATED-CORE SANDWICH PLATE DECKING, ISOPE 93, 3rd Intl. Offshore & Polar Engng. Conf./Singapore, 6-11 June 1993, BMT ICONS, Vol. IV
52. E.P.Popov, ENGINEERING MECHANICS OF SOLIDS, Prentice Hall, Englewood Cliffs, New Jersey 07632, 1990
53. Edited by G.Weidmann, P.Lewis and N. Reid, STRUCTURAL MATERIALS, The Open University, Materials Department, Butterworths, UK, 1990
54. R.Hussein and M.Morsi, COMPOSITES, Chapter 31 of STRUCTURES, edited by P.N.Cheremisinoff, N.P.Cheremisinoff and S.L.Cheng, Technomic Publishing Company Inc., 1987
55. J.E.Gordon, THE NEW SCIENCE OF STRONG MATERIALS or WHY YOU DON'T FALL THROUGH THE FLOOR, Penguin Books, 1968
56. J.R.Vinson and R.L.Sierakowski, THE BEHAVIOUR OF STRUCTURES COMPOSED OF COMPOSITE MATERIALS, Martinus Nijhoff Publishers, 1986

57. Edited by A.G.H.Dietz, COMPOSITE ENGINEERING LAMINATES, The MIT Press, 1969

58. J.R.Vinson et al., STRUCTURAL OPTIMIZATION OF CORRUGATED CORE AND WEB CORE SANDWICH PANELS SUBJECTED TO UNIAXIAL COMPRESSION, Structural Mechanics associates, Narberth, PA, NAEC ASL 1109, N156 46654, 109 P, 15 May 1967

59. CODE OF PRACTICE FOR RESISTANT DESIGN, BS 5950, Part 8

APPENDIX A
STEELWORK IN FIRE
INFORMATION SHEET

The following pages have been taken from [40].

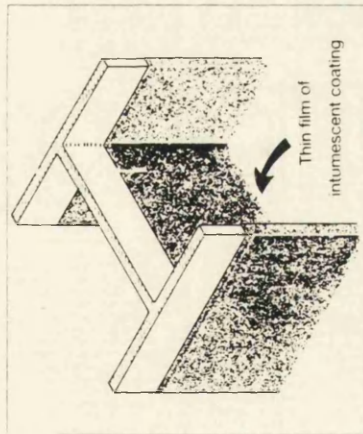
STEELWORK IN FIRE INFORMATION SHEET

This series of information sheets is intended to illustrate methods of achieving fire resistance in steel structures. It should not be used for design without consulting detailed design guidance referenced below.

MO3

INTUMESCENT COATINGS

UP TO 2 HRS



METHOD

Most intumescent coatings can be applied by spray, brush or roller and can achieve up to 1 hour fire resistance on fully exposed steel members. Some thick film products can achieve up to 2 hours fire resistance on some section sizes.

PRINCIPLE

Insulation is created by swelling of the coating at elevated temperatures to generate a foam like char. This reduces the heating rate so that the limiting temperature of the steel member is not exceeded during the required fire resistance period. The coating thickness necessary depends on the section factor (Hp/A) and the fire rating required.

ADVANTAGES

- a) Decorative finish
- b) Rapid application
- c) Easy to cover complex details
- d) Easy post protection fixings to steelwork eg service hangers

LIMITATIONS (check with manufacturer)

- a) May be suitable for dry internal environments only
- b) May be more expensive than sprayed insulation
- c) May require blast cleaned surface and compatible primer

PROTECTION THICKNESS

Thickness recommendations given in 'Fire Protection of Structural Steel in Building' have normally been derived from fire tests on orthodox H or I rolled sections. For other sections the recommended thickness for a given section factor and fire rating should be modified as follows.

CASTELLATED SECTIONS

The thickness of fire protection material on a castellated section should be 20% greater than that required for the section from which it was cut

HOLLOW SECTIONS

For intumescent materials applied to hollow sections the manufacturers should have carried out separate tests and appraisal

FOR MORE DETAILED INFORMATION SEE:-
 "Fire Protection of Structural Steel in Building"
 published jointly by:
 ASFCM - (0252 336318) and
 The Steel Construction Institute - Tel: 0344 23345

Sheet Code
 iSF/M03
 January 1991

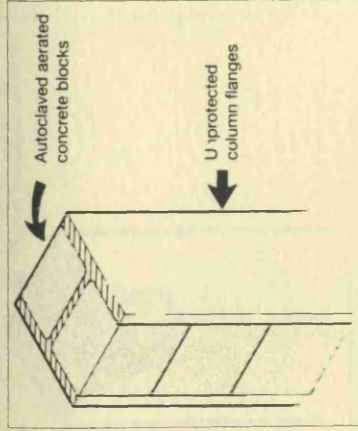
STEELWORK IN FIRE INFORMATION SHEET

This series of information sheets is intended to illustrate methods of achieving fire resistance in steel structures. It should not be used for design without consulting detailed design guidance referenced below.

MO4

BLOCK - FILLED COLUMNS

30 MINUTES



METHOD

Unprotected universal sections with section factors up to 69m² (see overleaf) can attain 30 minutes fire resistance by fitting autoclaved aerated concrete blocks between the flanges tied to the web at approximately 1m intervals.

PRINCIPLE

Partial exposure of steel members affects fire resistance in two ways:-

Firstly the reduction of exposed surface area reduces the rate of heating by radiation and thus increases the time to reach failure temperature.

Secondly, if fire exposure creates both hot and cold regions in the cross section, plastic yielding occurs in the hot region and load is transferred to the stronger cooler region. Thus a non-uniformly heated section has a higher fire resistance than one heated evenly.

ADVANTAGES

- Reduced cost - compared with total encasement with insulation
- More slender finished columns occupy less floor space
- Good durability - high resistance to impact and abrasion damage

LIMITATIONS

With unprotected steel the method is limited to 30 minute fire rating. When higher ratings are required exposed steel must be treated with the full insulation or intumescent coating thickness recommended for the higher rating.

This method should not be used when the blockwork also forms a separating wall. In this case the column will be heated on one side only and thermal bowing may cause the wall to crack or collapse. In such cases the flange(s) should be protected. Alternatively, if the limit of wall deformation is known, the bowing can be calculated to ensure no integrity failure.

FOR MORE DETAILED INFORMATION SEE:-
BRE Digest 317, Building Research Advisory Service,
Fire Research Station, Borehamwood,
Herts WD6 2BL
Telephone 081 953 6177

Sheet Code
ISF/M04
January 1991

METHODS OF ACHIEVING 30 MINUTES FIRE RESISTANCE

COLUMN SECTIONS - AXIALLY LOADED ⁽¹⁾ FREE STANDING

SERIAL SIZE mm	MASS/METRE kg	PROTECTION METHOD RECOMMENDED
305 x 406	393 and over	No fire protection required
356 x 406	340 and under	Block filling with autoclaved aerated concrete blocks
305 x 305	All weights	
254 x 254	All weights	
203 x 203	52 and over	
203 x 203	46 ⁽²⁾	
152 x 203	All weights	Apply fire protection material as per manufacturers' recommendations

BEAM SECTIONS ACTING AS PORTAL FRAME STANCHIONS ⁽¹⁾

914 x 419	All weights	No fire protection required
914 x 305		
*610 x 305		
*914 x 305	253 and under	Block filling with autoclaved aerated concrete blocks
838 x 292		
762 x 267		
686 x 254		
*610 x 305		
610 x 229		
533 x 210		
457 x 191		
457 x 152		
406 x 178		
356 x 171	54	
305 x 165		
305 x 127		
254 x 146	48	
	43	
Other beam sizes		
Apply fire protection material as per manufacturers' recommendations		

Notes:

- This table applies to sections designed to BS 5950 Part 1:1990 provided the load factor (γ_f) does not exceed 1.5
- To achieve 30 min fire resistance, a 203 x 203 x 46 kg/m column with blocked in webs should be loaded only up to 80% of the maximum allowable per BS 449: Part 2: 1969 or BS 5950: Part 1: 1990
- The table revises BRE Digest 317 (1986) in accordance with BS 5950: Part 8: 1990

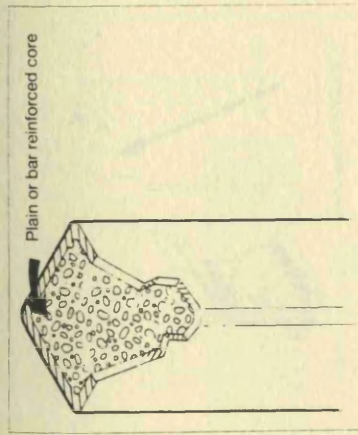
STEELWORK IN FIRE INFORMATION SHEET

This series of information sheets is intended to illustrate methods of achieving fire resistance in steel structures. It should not be used for design without consulting detailed design guidance referenced below.

M05

CONCRETE FILLED HOLLOW COLUMNS

UP TO 2 HRS



METHOD

Unprotected square or rectangular hollow sections can attain up to 120 minutes fire resistance by filling with plain, fibre reinforced or bar reinforced concrete.

PRINCIPLE

Heat flows through the steel wall into the concrete core which being a poor conductor heats up slowly.

As the temperature increases the steel yield strength reduces and the load is progressively transferred into the concrete core.

The steel acts as a restraint to the concrete preventing spalling and hence the rate of degradation of the concrete.

ADVANTAGES

- Steel acts as a permanent shuffling
- More slender finished columns occupying less floor space
- Good durability - high resistance to impact and abrasion damage

LIMITATIONS

- A minimum column size of 140mm x 140mm or 100mm x 200mm is required for plain or fibre reinforced sections
- A minimum column size of 200mm x 200mm or 150mm x 250mm is required for bar reinforced sections.
- CHS columns are not included due to insufficient data at present.

FOR MORE DETAILED INFORMATION SEE:-

BS 5950 Part 8

Concrete filled column design manual TD 296 from

British Steel General Steels Welded Tubes (0536 402121)

Sheet Code

ISF/M05

January 1991

CONCRETE FILLED RECTANGULAR HOLLOW SECTIONS

The fire resistance of externally unprotected concrete filled hollow sections is dependent on three main variables:

- The concrete strength selected
- The ratio of axial load and moment
- The addition of fibre or bar reinforcement

CONCRETE STRENGTH

The core capacity and hence its fire resistance is directly related to the concrete strength selected.

AXIAL LOAD AND MOMENT

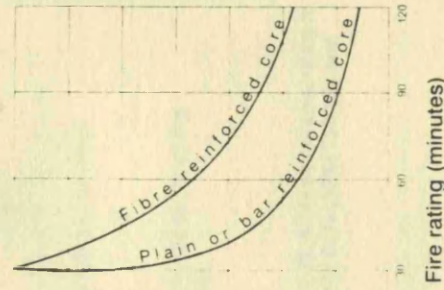
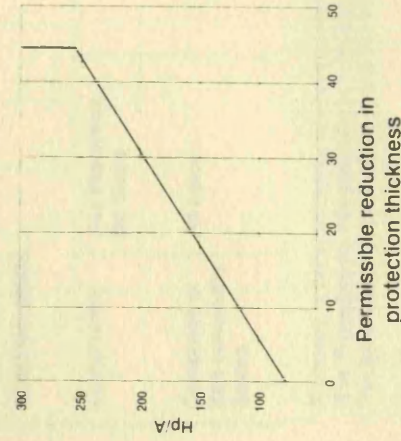
Plain concrete does not perform well in tension and when subject to axial load and moment it is necessary to produce a resultant compressive stress in the core.

REINFORCEMENT

Fibre reinforcement will enhance the core axial capacity yet retain the advantage of filling into a section without obstructions. Bar reinforcement will enhance the moment capacity.

COMBINED PROTECTION

As an alternative the concrete filled section can be designed for full factored loads and provided with external fire protection. The thickness of the external fire protection is assessed as for an unfilled section, and, due to the effect of the core, the thickness can be reduced.



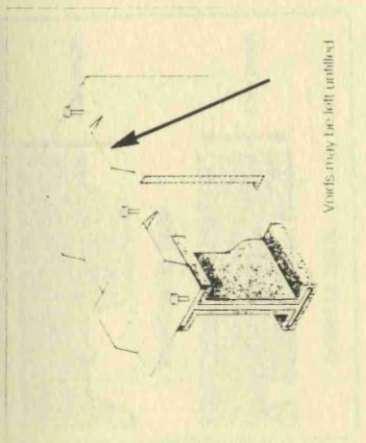
STEELWORK IN FIRE INFORMATION SHEET

COMPOSITE BEAMS - UNFILLED VOIDS

This series of information sheets is intended to illustrate methods of achieving fire resistance in steel structures. It should not be used for design without consulting detailed design guidance referenced below.

COMPOSITE SLABS WITH PROFILED METAL DECK WITH UNFILLED VOIDS

UP TO 2 HRS



METHOD

In a composite construction using profiled metal deck floors it is unnecessary to fill the deck voids above the top flange for any fire resistance period using dovetail deck, or up to 90 minutes using trapezoidal deck.

PRINCIPLE

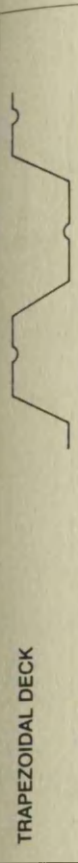
In a composite beam/slab member the neutral axis in bending lies in, or close to, the beam top flange. Thus the top flange makes little significant contribution to the structural behaviour of the total composite system and its temperature can be allowed to increase with little detriment to performance in fire.

ADVANTAGES

- a) Saving in time on site
- b) Saving in cost for filling voids
- c) It is unnecessary to build up the full thickness of protection on toes of upper flange
- d) Void filling is unnecessary when using dovetail deck

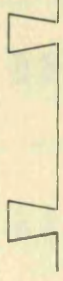
LIMITATIONS

- Voids must be filled where:-
- a) Trapezoidal deck is used for fire ratings over 90 minutes
- b) Trapezoidal deck is used in non-composite construction
- c) Any type of deck crosses a fire separating wall



Construction	Fire Protection On Beam	Fire Resistance (minutes)	
		Up to 60	Over 90
Composite Beams	BOARD or SPRAY	No increase in thickness*	Increase thickness by 10% (or use thickness* appropriate to beam Hp/A + 15% whichever is less)
	INTUMESCENT	Increase thickness* by 20% (or use thickness* appropriate to beam Hp/A + 30 % whichever is less)	Increase thickness* by 30% (or use thickness* appropriate to beam Hp/A + 50 % whichever is less)
Non-Composite Beams	All types	Fill Voids	

Construction	Fire Protection On Beam	Fire Resistance (minutes)



* Thickness is the board spray or intumescent thickness given for 30, 60 or 90 minutes rating in "Fire Protection for Structural Steel in Buildings", published by ASFCM (0252 336318) and The Steel Construction Institute (0344 23345)

FOR MORE DETAILED INFORMATION SEE:-

Technical Report 087
 "Fire resistance of composite beams"
 The Steel Construction Institute
 (0344 23345)

Sheet Code
 ISF/M06
 January 1991

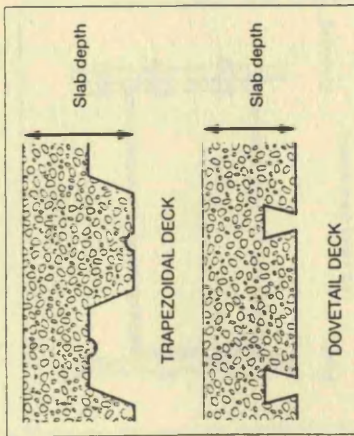
STEELWORK IN FIRE INFORMATION SHEET

M07

This series of information sheets is intended to illustrate methods of achieving fire resistance in steel structures. It should not be used for design without consulting detailed design guidance referenced below.

COMPOSITE SLABS WITH PROFILED METAL DECK

UP TO 2 HRS



METHOD

Fire resistance of composite slabs up to 90 mins can be achieved using normal A142 mesh reinforcement. This can be increased to 120 mins if heavier mesh is used and the slab depth increased (see overleaf).

Other cases outside the limits overleaf can be evaluated by the "Fire Engineering Method" (See below)

PRINCIPLE

Mesh reinforcement, which is not designed to act structurally under normal conditions, makes a significant contribution to structural continuity in fire.

ADVANTAGES

- Standard mesh, without additional reinforcing bars, may be used.
- No fire protection is required on the deck soffit.

LIMITATIONS

- Applies only to slabs designed to BS5950 Part 4
- Mesh overlaps should exceed 50 times bar diameters
- Mesh bar ductility should exceed 12% elongation in tension (to BS 4449)
- Mesh should lie between 20 & 45mm from slab upper surface
- Imposed load should not exceed 6.7 kN/m² (including finishes)

FOR MORE DETAILED INFORMATION SEE:-

SCI Publication 059

"Fire resistance of composite floors with steel decking"

The Steel Construction Institute - (0344 23345) and

CIRIA Special publication 42 CIRIA (071 222 8891)

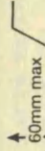
Sheet Code

ISF/M07

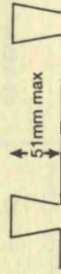
January 1991

FIRE RESISTANT COMPOSITE SLABS

Maximum Span (m)	Fire Rating (h)	Minimum Dimensions			Mesh Size						
		Sheet thickness	Slab depth (mm)								
			NWC ^(a)	LWC ^(a)							
2.7	1	0.8	130	120	A142						
						3.0	1	0.9	130	120	A142
2	0.9	155	140	A193							
					3.6	1	1.0	130	120	A193	
1 1/2	1.2	140	130	A193							
											2



Maximum Span (m)	Fire Rating (h)	Minimum Dimensions			Mesh Size					
		Sheet thickness	Slab depth (mm)							
			NWC ^(a)	LWC ^(a)						
2.5	1	0.8	100	100	A142					
						1 1/2	0.8	110	105	A142
1 1/2	0.9	130	120	A142						
					2	0.9	140	130	A193	
3.6	1	1.0	125	120						A193
					1 1/2	1.2	135	125	A193	



1) Imposed load not exceeding 5kN/m² (+ 1.7kN/m² ceiling and services)

2) NWC = Normal weight concrete

3) LWC = Light weight concrete

NOTE: Minimum slab depths given in BS 5950 part 8 are to satisfy the insulation criterion only. Figures given in the table above incorporate a strength criterion also and thus may exceed the minimum depth given in the code.

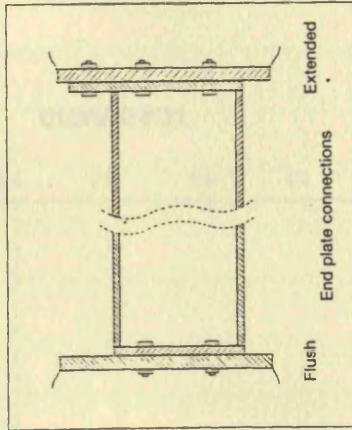
STEELWORK IN FIRE INFORMATION SHEET

MOB

This series of information sheets is intended to illustrate methods of achieving fire resistance in steel structures. It should not be used for design without consulting detailed design guidance referenced below.

BEAM - COLUMN CONNECTIONS

30 MINUTES



METHOD

Most beams can achieve 30 minutes fire resistance without additional protection by mobilising the moment capacity of the connections to reduce the effective load ratio of the beam at the fire limit state (see overleaf).

PRINCIPLE

It is known that so-called "simple" connections can resist moments but this is usually ignored in design. At the fire limit state large rotations are permitted and moments may be transferred to adjacent members. Reduction of moment in the beam increases the limiting temperature and thus the fire resistance of the beam.

ADVANTAGES

- Elimination of fire protection for 30 minutes rating of most beams.
- Reduction of fire protection thickness for higher ratings.

LIMITATIONS

- Applies only to end plate connections designed to be "simple" in normal design
- Does not apply to continuous frames (eg portal frames)
- Bolt sizes are M16, 20 or 24 in grades 4.6 or 8.8
- Applies only to internal beams with span variation less than 25%
- Special considerations are required for edge columns or for beam-beam connections which do not align through the web

FOR MORE DETAILED INFORMATION SEE:-

SCI Technical Report 086
 "Enhancement of fire resistance by beam column connections" published by
 The Steel Construction Institute (0344 233445)

Sheet Code

ISF/M08
 January 1991

INCREASE IN LIMITING TEMPERATURE

Connections provide an increase in limiting temperature over that of a simply supported beam. The limiting temperature of the simply supported beam is a function of the load ratio. The increase in limiting temperatures due to the connection has been determined conservatively as:

For flush end plates $T^{\circ}C = 135 Mc/Mp$

For extended end plates $T^{\circ}C = 160 Mc/Mp$

Valid over a range of $0.15 < Mc/Mp < 0.7$

Where $Mc =$ "cold" moment capacity of the connection (obtained by calculation)
 $Mp =$ "cold" moment capacity of the beam

MAXIMUM SECTION FACTORS FOR 30 MINUTES FIRE RESISTANCE OF INTERNAL NON - COMPOSITE BEAMS.

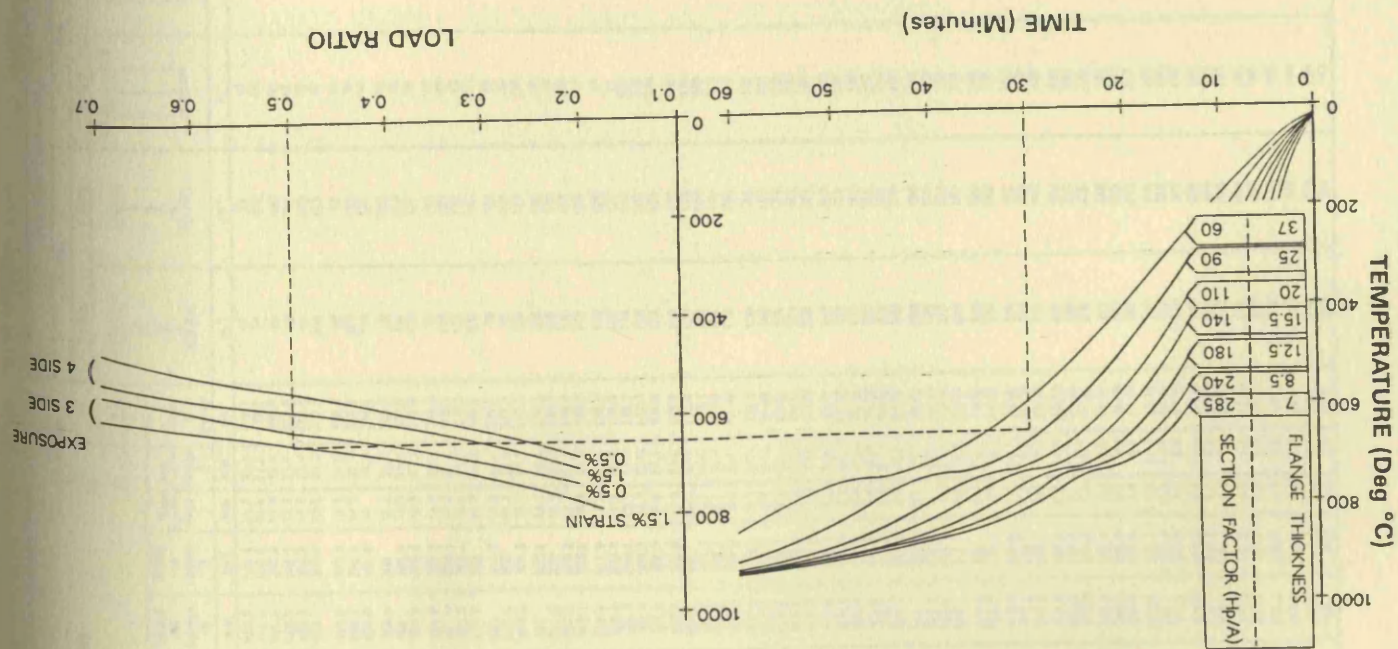
CONNECTION TYPE	APPLIED LOAD RATIO OF SIMPLE BEAM	EFFECTIVE LOAD RATIO	LIMITING TEMPERATURE OF BEAM ($^{\circ}C$)	MAXIMUM SECTION FACTOR (m^{-1}) OF BEAM
Extended end plates Moment capacity > 0.6 Mp	0.40	0.20	780	230
	0.45	0.23	770	210
	0.50	0.25	755	180
	0.55	0.28	735	120
Flush end plates Moment capacity > 0.3 Mp	0.35	0.24	765	200
	0.40	0.27	745	150
	0.45	0.30	725	110
	0.50	0.34	710	105
	0.55	0.37	695	95

Notes:

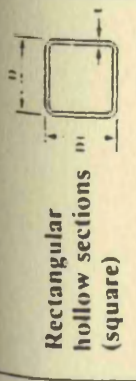
- Beam supporting concrete slabs
- Internal beam connected to internal column by connections of the above type
- Load ratio takes into account reduced load factors at limit state
- Capacity of bolt group in shear is taken as 50% of their design capacity when determining their normal loadcarrying capacity

LIMITING TEMPERATURE - BEAMS

DESIGN TEMPERATURE



Case No.	Members in compression						
	0.7	0.6	0.5	0.4	0.3	0.2	
(1)	510	540	580	615	655	710	Uniform heating on all faces; braced members in simple construction: Slenderness ratio ≤ 70 Slenderness ratio ≤ 180
(2)	460	510	545	590	635	635	
(3)							Members in bending Supporting concrete or composite deck floors: Unprotected members, or protected members complying with clause 2.3 (a) or (b) Other protected members
(4)	590	620	650	680	725	780	
(5)	460	510	545	590	635	690	Not supporting concrete floors: Unprotected members, or protected members complying with Clause 2.3 (a) or (b) Other protected members
(6)	520	555	585	620	660	745	
(7)	460	510	545	590	635	690	Members in tension All cases



Designation Size D x D mm	Designation		Area of section cm ²	Mass per metre kg	Section factor H _p /A	
	Thickness t mm	Thickness t mm			3 sides	4 sides
					m ⁻¹	m ⁻¹
20 x 20	2.0	1.2	1.42	1.12	425	565
20 x 20	2.5	1.35	1.72	1.35	350	465
25 x 25	2.0	1.43	1.82	1.43	410	550
25 x 25	2.5	1.74	2.22	1.74	340	450
30 x 30	3.0	2.04	2.60	2.04	290	385
30 x 30	3.2	2.15	2.74	2.15	275	365
30 x 30	3.5	2.14	2.72	2.14	330	440
30 x 30	4.0	2.51	3.20	2.51	280	375
40 x 40	3.2	2.65	3.38	2.65	265	355
40 x 40	3.5	2.92	3.72	2.92	325	430
40 x 40	4.0	3.45	4.40	3.45	275	365
40 x 40	4.5	3.66	4.64	3.66	260	345
50 x 50	4.0	4.46	5.68	4.46	210	280
50 x 50	5.0	5.40	6.88	5.40	175	235
50 x 50	5.5	3.71	4.72	3.71	320	425
50 x 50	6.0	4.39	5.60	4.39	270	355
50 x 50	6.5	5.04	6.55	5.04	255	335
60 x 60	5.0	5.72	7.38	5.72	205	275
60 x 60	5.5	6.97	8.88	6.97	170	225
60 x 60	6.3	8.49	10.8	8.49	140	185
60 x 60	7.0	5.34	6.80	5.34	265	355
60 x 60	7.5	5.67	7.22	5.67	250	330
60 x 60	8.0	6.97	8.88	6.97	205	270
70 x 70	5.0	8.54	10.9	8.54	165	220
70 x 70	6.3	10.5	13.3	10.5	135	180
70 x 70	8.0	12.8	16.3	12.8	110	145
70 x 70	9.0	6.28	8.00	6.28	260	350
70 x 70	10.0	7.46	9.50	7.46	220	295
80 x 80	5.0	10.1	12.9	10.1	165	215
80 x 80	6.3	12.5	15.9	12.5	130	175
80 x 80	8.0	15.3	19.5	15.3	110	145
80 x 80	9.0	7.22	9.20	7.22	260	350
80 x 80	10.0	8.39	10.9	8.39	220	295
90 x 90	5.0	11.7	14.9	11.7	160	215
90 x 90	6.3	14.4	18.4	14.4	130	175
90 x 90	8.0	17.8	22.7	17.8	105	140
90 x 90	9.0	7.72	12.4	7.72	220	290
90 x 90	10.0	8.91	14.6	8.91	160	215
100 x 100	5.0	13.3	20.9	13.3	130	170
100 x 100	6.3	16.4	25.9	16.4	105	140
100 x 100	8.0	20.4	25.9	20.4	105	140
100 x 100	9.0	12.0	15.3	12.0	195	260
100 x 100	10.0	14.8	18.9	14.8	160	210
100 x 100	11.0	17.0	23.4	17.0	130	170
100 x 100	12.5	22.9	29.1	22.9	105	135
100 x 100	16.0	27.9	35.5	27.9	85	115

H _p /A up to	Dry thickness (mm) to provide fire resistance of					
	½ hour	1 hour	1½ hours	2 hours	3 hours	4 hours
30	10	10	10	10	15	25
50	10	10	10	14	21	29
70	10	10	12	17	27	36
90	10	10	14	20	31	42
110	10	10	16	22	34	47
130	10	10	17	24	37	51
150	10	11	18	25	40	54
170	10	12	19	27	42	57
190	10	12	20	28	44	59
210	10	13	21	29	45	
230	10	13	21	30	47	
250	10	14	22	31	48	
270	10	14	23	31	49	
290	10	14	23	32	50	
310	10	14	23	33	51	

Linear interpolation is permissible between values of H_p/A

APPENDIX B

**STRUCTURAL OPTIMIZATION OF CORRUGATED CORE AND WEB CORE
SANDWICH PANELS SUBJECTED TO UNIAXIAL COMPRESSION (selected
parts from [58])**

SUMMARY

This report presents the development of rational methods of structural optimization for flat, corrugated core and web-core sandwich panels subjected to uniaxial compressive loads.

These methods provide a means by which such panels can be designed with absolute minimum weight, yet retaining structural integrity (i.e., structurally optimum) for a given load index, panel width, panel length, and face and core materials. Of equal importance is that these methods provide a means for rational material selection through the comparison of weights of optimum construction for several material systems as a function of load index. The methods account for both isotropic or orthotropic face and core materials and various boundary conditions. Three types of core are considered: triangulated core (single truss core) construction, web-core construction, and "hat-shaped" core construction.

Chapter 1 presents the methods of optimization for the triangulated core (truss-core) construction. Chapter 2 presents methods of optimization for web-core construction. Chapter 3 presents methods of optimization for the "hat-shaped" core construction. Chapter 4 presents examples for several material systems using these constructions, as well as providing comparisons between these core constructions and honeycomb core construction. Chapter 5 presents some conclusions drawn from this investigation.

NAEC-ASL-1109

The methods developed herein are applicable to panels at elevated or lowered temperatures, under steady state and nearly uniform temperatures. Only the stress-strain curve, or preferably the tangent modulus-stress curve, for each temperature under consideration is necessary.

NAEC-ASL-1109

NOTATION

- a Panel dimension in the x direction, in.
- \bar{A}_c Area of the core per unit width of corrugation cross-section parallel to the yz plane, in. (see Equations 1.1, 2.1, and 3.1)
- b Panel dimension in the y direction, in.
- d_f Dimension in the y direction given in Figures 4 and 5
- D_{q1} Transverse shear stiffness, per unit width, of a beam cut from the panel in the i direction ($i=x,y$), lbs./in. (see Equations 1.8, 1.9, 2.4, 3.4, and 3.5)
- D_i $\frac{1}{2} E_i t_f h^2$, lbs.-in. ($i=x,y$)
- D_j Flexural stiffnesses associated with an orthotropic plate, lbs.-in. ($j=1,2,3$)
- E Modulus of elasticity, lbs./in.²
- E_c Modulus of elasticity of corrugated core sheet material, lbs./in.²
- E_f Modulus of elasticity of face sheet material, lbs./in.²
- E_0 Definition given by Equation 1.66
- E_T Tangent modulus, lbs./in.²
- E^0 $(E_c/E_f)\rho$
-
- E Reduced modulus of elasticity, lbs./in.²
- G_c Shear modulus of corrugated core sheet material, lbs./in.²

NAPC-ASL-1109

- h_c Core depth, in.
- K Extensional stiffness of the facing sheets, lbs./in.
- I_c Moment of inertia of the core, per unit width of the corrugation cross-section parallel to the yz plane, taken about the centroidal axis of the corrugation cross-section, in.³ (see Equations 1.2, 2.2, and 3.2)
- I_f Moment of inertia per unit width of the faces considered as membranes, with respect to the sandwich plate middle surface, in.³ (see Equation 1.8, 2.6, and 3.6)
- K Buckling coefficient
- n Number of half waves in the x direction
- N_c Definition given by Equation 1.79
- N_x Compressive in-plane load in the x direction per unit panel width, lbs./in.
- P $d_f + h_c \tan \theta$
- r_i Transverse shear flexibility ratio (see Equation 2.8) ($i=x, y$)
- S Definition given by Equations 1.6 and 3.5
-
- t_c Thickness of core web, in.
- t_f Thickness of facing material, in.
- V Definition given by Equation 1.10 ($= r_y$)
- W Total weight per unit planform area of panel construction, lbs./in.²

NAEC-ASL-1109

- V_i Weight per unit planform area of core (i-c) or facing (i-f) materials
- V_{ad} Weight of adhesive or other joining material between facing and core per unit planform area, lbs./in.²
- x Panel in-plane coordinate (see Figure 2)
- y Panel in-plane coordinate (see Figure 2)
- z Panel coordinate normal to mid-plane of panel (see Figures 1 and 4)
- β a/b
- δ_i In-plane axial compressive deformation, in. (see Equation 1.15) i=c,f
- ϵ In-plane strain
- η Plasticity reduction factor
- θ Angle web material makes with a line normal to plane of faces
- ν Poisson's ratio
- ρ_i Density, lbs./in.³ (i=c,f)
- σ Stress, psi
- Ω $[(1-\nu_c^2)/(1-\nu_f^2)]^{1/2}$
- Ω_0 Definition given by Equation 1.80

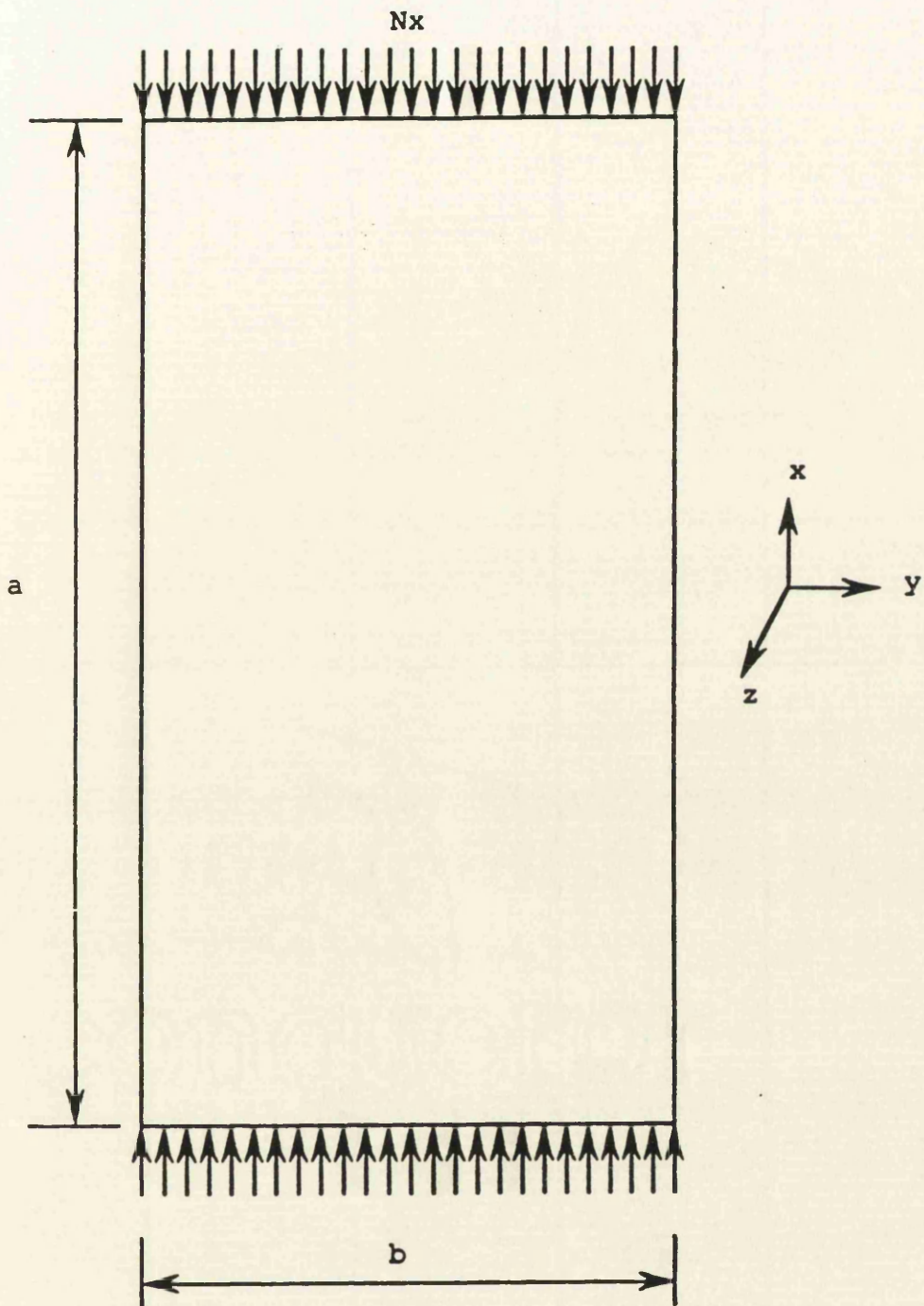


Figure 2

NAEC-ASL-1309

to the corrugation, the x direction, is found to be

$$D_{q_x} = \frac{G_c t_c h_c^2 \cos \theta}{(h_c + d_f \cos \theta)(d_f + h_c \tan \theta)} \quad (\text{lb./in.}) \quad (3.4)$$

The transverse shear stiffness in planes perpendicular to the direction of the corrugations is given by

$$D_{q_y} = \frac{S h_c E_c}{(1 - \nu_c^2)} \left(\frac{t_c}{h_c}\right)^3 \quad (\text{lbs./in.}) \quad (3.5)$$

The values of S to use in this expression are given in Reference 1 by Figure 3, as functions of h_c/t_c , t_c/t_1 , θ , and y/h_c . In this work, $p = d_f + h_c \tan \theta$, θ of Reference 3 is $(90^\circ - \theta)$ in this report, and t_1 of Reference 3 is t_f in this report.

The moment of inertia per unit width, \bar{I}_f , of the faces considered as membranes with respect to the sandwich plate middle surface is found to be

$$\bar{I}_f = \frac{t_f h_c^2}{2} \quad (3.6)$$

Since $t_f \ll h_c$ the core depth (h_c) can be taken as the distance between the centerlines of the faces.

NAEC-ASL-1109-1072

where $m =$ the number of half sine waves in the x direction

$$\beta = a/b$$

$$\eta = E_c \bar{I}_c / E_f \bar{I}_f$$

$$r_x = \frac{2 E_f \bar{I}_f}{b^2 D_{q_x}}$$

$$r_y = \frac{2 E_f \bar{I}_f}{b^2 D_{q_y}}$$

The general characteristics of this equation are discussed in more detail in Chapter 1, Section C-1.

2. Face Plate Instability

Referring to Figure 5, the facings can buckle in the regions between points B and E. Since the support conditions at B and E, the unloaded edges, are unknown precisely, it is conservative to assume that they are simply supported. For such a case the lower bound of the buckling coefficient for this condition, where the length to width ratio is greater than unity, is equal to 4. The well known buckling equation to describe this instability, written in terms of this construction, is found to be

$$\sigma_F = \frac{\pi^2 E_F t_F^2}{3(1-\nu_F^2)(d_F + 2h_F \tan \theta)^2} \quad (3.9)$$

Likewise, it is possible for the face plate between A and B to buckle. In this region, since the core material and the face material are intimately joined or bonded in some way,

the plate element has a thickness of $(t_c + t_f)$. If the construction involves the same material for both facing and core, the expression for the critical stress is found to be, assuming simply supported edges,

$$\sigma_c = \frac{\pi^2}{3(1-\nu^2)} \frac{E (t_c + t_f)^2}{d_f^2} \quad (3.10)$$

The expression will be more complicated if the face and core materials differ because there will be a shift in the neutral axis from the centroid.

3. Web Plate Instability

Similarly the local plate elements of the core case become unstable due to the core being directly subjected to a portion of the axial loading, N_x . The conservative assumption is also made here that the web elements from B to C and D to E in Figure 5 are simply supported along the unloaded edges, since the actual boundary conditions are somewhere between the simply supported and clamped boundary condition. Hence $K = 4$ for these elements which have a length in the x direction greater than the dimensions of B to C and D to E in Figure 5.

In terms of the symbols of Figure 5, the plate buckling equation is easily determined to be

$$\sigma_c = \frac{\pi^2 E_c}{3(1-\nu_c^2)} \frac{t_c^2}{h_c^2} \cos^2 \theta \quad (3.11)$$

Equation (3.11) is of course identical to Equation (1.12).

NAEC-ASL-1:79

4. Load-Stress Relationship

Following the developments of Chapter 1, Section C-4, it is easily shown that for uniform strain on the loaded edges

$$\sigma_c = \sigma_f \frac{E_c}{E_f} \quad (3.12)$$

Likewise, it is seen that

$$N_x = \sigma_c \bar{A}_c + 2\sigma_f t_f \quad (3.13)$$

Substituting (3.1) and (3.12) into (3.13), the load-stress relationship for this construction is given by

$$N_x = \sigma_f \left[\frac{E_c}{E_f} \frac{t_c (h_c + d_f \cos \theta)}{\cos \theta (d_f + h_c \tan \theta)} + 2t_f \right] \quad (3.14)$$

Again relations (3.12) and (3.13) are only applicable when both the face material and core material are stressed below their proportional limit. However, when the core and face materials are the same then $\sigma_c = \sigma_f$ and Equation (3.14) applies over the entire stress range.

5. Weight Relation

The weight equation is seen to be

$$W = \rho_c \bar{A}_c + 2\rho_f t_f + W_{ad}$$

which for this particular geometry becomes

$$W - W_{ad} = \frac{\rho_c t_c (h_c + d_f \cos \theta)}{\cos \theta (d_f + h_c \tan \theta)} + 2\rho_f t_f \quad (3.15)$$

NAEC-ASL-1199

D. Structural Optimisation of Panels with Faces and Core of the Same Isotropic Material

The governing equations pertaining to this construction given in the previous subsection can be simplified if the facing and core are made of the same isotropic materials; namely,

$E_o = E_f = E$, $\nu_o = \nu_f = \nu$, and $\sigma_o = \sigma_f = \sigma$. The results are:

$$N_x = \frac{\pi^2 \bar{E} t_f h_c^2 k}{2b^2} \quad (3.16)$$

$$\sigma = \frac{\pi^2 \bar{E} t_f^2}{3(1-\nu^2)(d_f + 2h_c \tan \theta)^2} \quad (3.17)$$

$$\sigma = \frac{\pi^2 \bar{E} (t_c + t_f)^2}{3(1-\nu^2) d_f^2} \quad (3.18)$$

$$\sigma = \frac{\pi^2 \bar{E}}{3(1-\nu^2)} \frac{t_c}{h_c^2} \cos^2 \theta \quad (3.19)$$

$$N_x = \sigma \left[\frac{t_c (h_c + d_f \cos \theta)}{\cos \theta (d_f + h_c \tan \theta)} + 2b_f \right] \quad (3.20)$$

$$W_{\text{Wed}} = \rho \left[\frac{t_c (h_c + d_f \cos \theta)}{\cos \theta (d_f + h_c \tan \theta)} + 2b_f \right] \quad (3.21)$$

In the above, the \bar{E} is a reduced modulus of elasticity if the stresses are above the proportional limit.

Immediately from (3.20) and (3.21), it is seen that

$$\frac{N_x}{b} = \left(\frac{W_{\text{Wed}}}{b} \right) \frac{\sigma}{\rho} \quad \text{and} \quad \frac{W_{\text{Wed}}}{b} = \left(\frac{N_x}{b} \right) \frac{\rho}{\sigma} \quad (3.22)$$

NAEC-ASL-1109

The philosophy of optimization expressed in Chapter 1, Section D is utilized here.

Looking at the set of Equations (3.16) through (3.22) the known or specified quantities are the applied load per inch (N_x) and the panel width (b) which can be grouped together as the load index (N_x/b), and the material properties E , ν and ρ . The buckling coefficient K is a slowly varying parameter of the dependent variables which is considered here as a constant, but will be discussed in the next section.

The dependent variables are t_c , t_p , θ , σ , d , and $W = V_{ad}$. Thus there are six equations and seven unknowns.

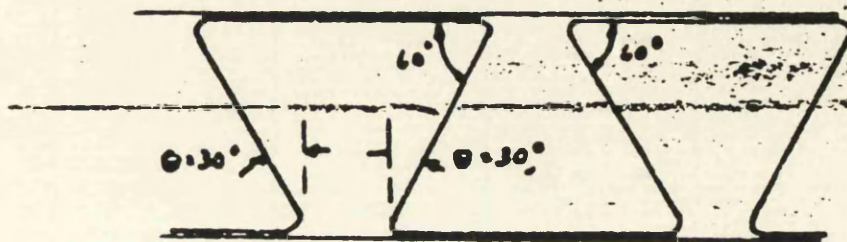
Turning first to Equations (3.17), (3.18), and (3.19) it is found that the minimum weight structure for the construction shown by Figure 5 occurs when

$$\theta = -30^\circ$$

$$\text{and } t_c = \frac{2t_p h_c}{(\beta d_p - 2h_c)} = \frac{2(1-\nu^2)^{1/2} h_c \sigma}{\pi E h_c} \quad (3.23)$$

$$\text{and } t_p = \frac{(\beta d_p - 2h_c)(1-\nu^2)^{1/2} \sigma h_c}{\pi E h_c}$$

Thus the minimum weight panel with this type of construction has the geometry shown in the centerline sketch below.



NAFC-ASL-1109

This leaves much to be desired from a practical viewpoint, because of the larger angles through which the core material must employ small radius bends in conjunction with the comparatively large regions AB over which loading is required. However, to have the angle $\theta > 30^\circ$, implies that the critical stress for the plate element from A to B will be greater than either the critical stress for the plate element from B to E, or the core plate element from B to C.

Although a geometry in which $\theta > 30^\circ$ is not a true minimum weight construction for hat-shaped corrugated core construction, it is of interest to investigate the "optimum" geometry under the constraint that $\theta \geq 0^\circ$ (to avoid a small radius bend in the core material of greater than 90°), which implies the elimination of Equation (3.18) in the following development. Thus, such construction can be compared to the triangulated core (truss core) and the web core construction, optimized in Chapters 1 and 2, respectively. Now, there are five equations and seven unknowns. It would therefore be desirable through manipulating the governing equations to obtain the weight equation in terms of two dependent variables. However, due to the complexity of the equations, it is not possible to uncouple the dependent variables in such a manner to accomplish this. However, appealing to the fact that the dimension d_p is often determined by manufacturing limitations and restrictions, or could even be specified by some other consideration, we can consider it as a constant, and investigate the optimum construction for a number of specific values of d_p . The weight equation

MAEC-ASL-1109

can now be obtained in terms of the variables h_c and θ (although other variables could possibly have been employed).

$$W_{\text{total}} = \frac{3\rho(d_f + 2h_c \tan\theta)^2 \pi^2 E h_c^4 k^2 (1-\nu^2)}{4b^4 \theta} \quad (3.24)$$

In the range of variable θ , $0^\circ \leq \theta \leq 90^\circ$, it is obvious that the weight will be least when $\theta = 0^\circ$.

With $\theta = 0$, the set of governing equations becomes the following:

$$N_x = \frac{\pi^2 E t_p h_c^2 k}{2b^2} \quad (3.25)$$

$$\sigma = \frac{\pi^2 E t_p^2}{3(1-\nu^2) d_f^2} \quad (3.26)$$

$$\sigma = \frac{\pi^2 E t_c^2}{3(1-\nu^2) h_c^2} \quad (3.27)$$

$$N_x = \sigma \left[\frac{t_c (h_c + d_f)}{d_f} + 2t_p \right] = (W_{\text{total}}) \frac{\sigma}{\rho} \quad (3.28)$$

$$W_{\text{total}} = \rho \left[\frac{t_c (h_c + d_f)}{d_f} + 2t_p \right] = N_x \frac{\rho}{\sigma} \quad (3.29)$$

With the set (3.25) through (3.29), it is still not possible to separate the variables in such manner as to obtain explicit solutions, as was done in the case of the triangulated core construction, the tub-core construction, or the honeycomb core construction in Reference 6. A numerical, iterative scheme must therefore be employed.

NAEC-ASL-1109

A great variety of iterative techniques could be employed. However, experience with numerical examples, discussed in Chapter 4 of this report, indicates the following as the most direct.

From (3.26) it is easily seen that

$$\frac{t_F}{b} = \frac{3^{1/2} (1-\nu^2)^{1/2} \left(\frac{d_F}{b}\right) \sigma^{1/2}}{\pi E^{1/2}} \quad (3.30)$$

From (3.25) and (3.30),

$$\frac{h_s}{b} = \frac{2^{1/2} (N_x/b)^{1/2}}{\pi^{1/2} E^{1/2} K^{1/2} 3^{1/2} (1-\nu^2)^{1/2} \left(\frac{d_F}{b}\right)^{1/2} \sigma^{1/2}} \quad (3.31)$$

From (3.27) and (3.31), it is seen that

$$\frac{t_s}{b} = \frac{(3)^{1/4} (1-\nu^2)^{1/2} (2)^{1/2} \left(\frac{h_s}{b}\right)^{3/2} \sigma^{1/2}}{\pi^{3/2} E^{1/2} K^{1/2} \left(\frac{d_F}{b}\right)^{1/2}} \quad (3.32)$$

Substituting (3.30), (3.31), and (3.32) into (3.28), the following relation is obtained.

$$\frac{N_x}{b} = \sigma \left\{ \frac{2(3)^{1/2} (1-\nu^2)^{1/2} \left(\frac{d_F}{b}\right) \sigma^{1/2}}{\pi E^{1/2}} + \frac{(3)^{1/4} (2)^{1/2} (1-\nu^2)^{1/2} (N_x/b)^{1/2} \sigma^{1/2}}{\pi^{1/2} E^{1/2} K^{1/2} \left(\frac{d_F}{b}\right)^{1/2}} + \frac{2(N_x/b)}{\pi^{1/2} E^{1/2} K^{1/2} \left(\frac{d_F}{b}\right)^{1/2}} \right\} \quad (3.33)$$

This is the "universal relation" relating the applied load (N_x/b) to the stress σ , for a given or specified value of (d_F/b) .

NAEC-ASL-1109

In this optimization procedure, use is made of the fact that in solving (3.33) for a given load (N_x/b), for various specified values of (d_r/b) , that value of (d_r/b) which results in the highest value of stress σ is the value of (d_r/b) which will result in minimum weight, according to Equation (3.22), since $\frac{W - W_{ad}}{b}$ is inversely proportional to σ .

The iterative procedure is now explained in detail for a panel with specified load index (N_x/b), to obtain a minimum weight construction.

1. Known quantity is $\theta = 0$.
2. Select a material of construction.
3. Estimate a value of the buckling coefficient K .
4. Select a value of (d_r/b) .
5. Estimate a stress value.
6. Determine \bar{N} for the assumed stress in Step 5.

Below the proportional limit \bar{N} will be used, above the proportional limit $\bar{N} = \sqrt{EK_c}$ may be used (see footnote, Chapter 1, Section 2)

7. Substitute these into Equation (3.33) to see if an equality is obtained. If the right hand side is less than N_x/b specified, the assumed stress is too low, and conversely. Repeat steps 5, 6, and 7 until an equality is obtained. This is the solution for the selected value of (d_r/b) .

8. Select another value of (d_r/b) and repeat steps 4 through 7 until a value of (d_r/b) is found which

NAEC-ASL-1109

has the highest value of σ as a solution.

9. For the value of (d_r/b) which has the highest value of σ as its solution, solve for (t_r/b) , (t_c/b) , and (h_c/b) using Equations (2.27), (2.28), and (2.29).

10. With these values, using relations derived previously, solve for

$$a. \eta = \frac{F_c}{F_r} = \frac{1}{6} \frac{(t_c/b)}{(t_r/b)} \frac{[\frac{h_c}{b} + 3 \frac{(d_r/b)}{b}]}{(d_r/b)}$$

$$b. r_3 = \frac{\pi^2 E I_f}{b^4 D_{xy}} = \frac{\pi^2}{2} \left(\frac{t_r}{b} \right) \left(\frac{h_c}{b} \right) \frac{h_c^3}{5} \frac{(h_c/b)^3}{(b^2/b)^3}$$

where S is found in Figure 3, Reference 1

Note: θ of Reference 3 is $(90^\circ - \theta)$ in this

report and $y = d_r$.

$$a. r_2 = \frac{\pi^2 (1+\nu) (t_r/b) [(h_c/b) + (d_r/b)] (d_r/b)}{(t_r/b)}$$

11. Solve Equation (3.8) for K . Because of the characteristics of K , one may assume a value of $m = 1$ and $\beta = 1.6$ for a good approximation. However if an exact value of K is required one can let $m = 1$, and vary β until a minimum is obtained.

12. Compare the calculated value of K from step 11 with the value assumed in step 3. If they do not match, repeat steps 4 through 12 until the assumed value equals the calculated value.

13. For the final solution of step 12, values of t_r/b , t_c/b , and h_c/b will have been calculated in step 9 and

APPENDIX AREFERENCES

1. Libove, Charles, and Hubka, Ralph E., "Elastic Constants For Corrugated-Core Sandwich Plates", NACA TN 2289, February 1951.
2. Anderson, Melvin S., "Optimum Proportions of Truss-Core and Web-Core Sandwich Plates Loaded in Compression", NACA TN D-96, September 1959.
3. Seide, Paul, "The Stability Under Longitudinal Compression of Flat Symmetric Corrugated-Core Sandwich Plates With Simply Supported Loaded Edges and Simply Supported or Clamped Unloaded Edges", NACA TN 2679, April 1952.
4. Anon., "Sandwich Construction For Aircraft, Part II", AEC-R3, Second Edition, 1955, issued by the Department of the Air Force Air Research and Development Command; Department of the Navy, Bureau of Aeronautics; Department of Commerce, Civil Aeronautics Administration.
5. Anderson, Melvin S., "Local Instability of the Elements of A Truss-Core Sandwich Plate", NACA TR R-30, 1959.
6. Vinson, J. R., and Shore, S., "Methods of Structural Optimization For Flat Sandwich Panels", U. S. Naval Air Engineering Center Report No. NAEC - ASL - 1083, 15 April 1965.

APPENDIX C
STRAIN GAUGE INSTALLATION INSTRUCTIONS

The following instructions have to be followed in order to install a strain gauge.



Strain Gage Installations with M-Bond 200 Adhesive

INTRODUCTION

Micro-Measurements Certified M-Bond 200 is an excellent general-purpose laboratory adhesive because of its fast room-temperature cure and ease of application. When properly handled, M-Bond 200 can be used for high-elongation tests in excess of 60 000 microstrain, for fatigue studies, for one-cycle proof tests to over +200°F (+95°C) or to below -300°F (-185°C). The normal operating temperature range is -25° to +150°F (-30° to +65°C). M-Bond 200 is compatible with all Micro-Measurements strain gages and most common structural materials. When bonding to plastics, it should be noted that for best performance, the adhesive flowout should be kept to a minimum. For best reliability, it should be applied to surfaces between the temperatures of +70° and +85°F (+20° to +30°C), and in a relative humidity environment of 30% to 65%. M-Bond 200 catalyst has been specially formulated to control the reactivity rate of this adhesive. The catalyst should be used sparingly for best results. Excessive catalyst can contribute many problems: e.g., poor bond strength, age-embrittlement of the adhesive, poor glue-line thickness control, extended solvent evaporation time requirements, etc.

Since M-Bond 200 bonds are weakened by exposure to high humidity, adequate protective coatings are essential. This adhesive will gradually become harder and more brittle with time, particularly if exposed to elevated temperatures. For these reasons, M-Bond 200 is not generally recommended for installations exceeding one or two years.

For proper results, the procedures and techniques presented in this bulletin should be used with qualified Micro-Measurements installation accessory products (refer to Micro-Measurements Catalog A-110). M-LINE accessories used in this procedure are:

- CSM-1 Degreaser or GC-6 Isopropyl Alcohol
- Silicon Carbide Paper
- M-Prep Conditioner A ✓
- M-Prep Neutralizer 5A ✓
- GSP-1 Gauze Sponges
- CSP-1 Cotton Applicators
- PCT-2A Cellophane Tape

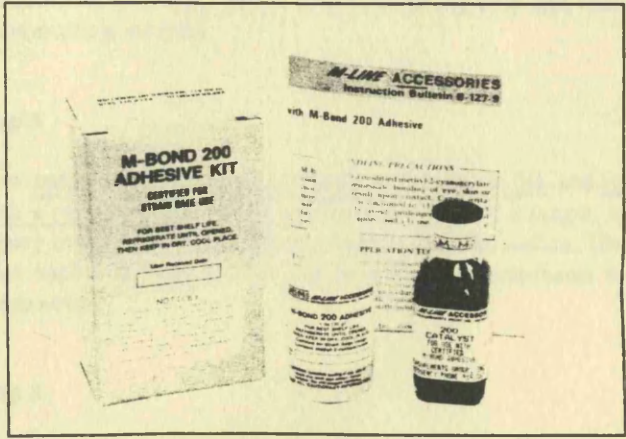
Various installation techniques are described on professionally prepared videotapes available from the Measurements Group. Request Bulletin 318 for details.

SHELF AND STORAGE LIFE

Unopened M-Bond 200 adhesive has a shelf life of nine months when stored under normal laboratory conditions. Life can be extended if upon receipt the *unopened* material is refrigerated [+40°F (+5°C)]. Due to possible condensation problems which will degrade adhesive performance, care should be taken to insure that the M-Bond 200 has returned to room-temperature equilibrium before opening. Refrigeration after opening is not recommended.

HANDLING PRECAUTIONS

M-Bond 200 is a modified alkyl cyanoacrylate compound. *Immediate bonding of eye, skin or mouth may result upon contact. Causes irritation.* The user is cautioned to: (1) *avoid contact with skin;* (2) *avoid prolonged or repeated breathing of vapors;* and (3) *use with adequate ventilation.* For additional health and safety information, consult the material safety data sheet which is available upon request.



MEASUREMENTS GROUP UK LTD

STROUDLEY ROAD, BASINGSTOKE, HANTS. RG24 0FW
Tel 0256 462131 Fax 0256 471441 Telex 858521



GAGE APPLICATION TECHNIQUES

The installation procedure presented on this and the following pages is somewhat abbreviated and is intended only as a guide in achieving proper gage installation with M-Bond 200. *Micro-Measurements Instruction Bulletin B-129* presents recommended procedures for surface preparation, and lists specific considerations which are helpful when working with most common structural materials.

Step 1

Thoroughly degrease the gaging area with a solvent, such as CSM-1 Degreaser or GC-6 Isopropyl Alcohol (Fig. 1). The former is preferred, but there are some materials (e.g., titanium and many plastics) which react with chlorinated solvents. In these cases GC-6 Isopropyl Alcohol should be considered. All degreasing should be done with uncontaminated solvents – thus the use of "one-way" containers, such as aerosol cans, is highly advisable.

Step 2

Preliminary dry abrading with 220- or 320-grit silicon-carbide paper (Fig. 2a) is generally required if there is any surface scale or oxide. Final abrading is done by using 320- or 400-grit silicon-carbide paper on surfaces thoroughly wetted with M-Prep Conditioner A; this is followed by wiping dry with a gauze sponge. Repeat this wet abrading process, then dry by slowly wiping through with a gauze sponge, as in Fig. 2b.

With a 4H pencil (on aluminum) or a ballpoint pen (on steel), burnish (do not scribe) whatever alignment marks are needed on the specimen. Repeatedly apply M-Prep Conditioner A and scrub with cotton-tipped applicators until a clean tip is no longer discolored. Remove all residue and Conditioner by again slowly wiping through with a gauze sponge. Never allow any solution to dry on the surface because this invariably leaves a contaminating film and reduces chances of a good bond.

Step 3

Now apply a liberal amount of M-Prep Neutralizer 5A and scrub with a cotton-tipped applicator. See Fig. 3. With a single, slow wiping motion of a gauze sponge, carefully dry this surface. Do not wipe back and forth because this may allow contaminants to be redeposited.

Step 4

Using tweezers to remove the gage from the mylar envelope, place the gage (bonding side down) on a chemically clean glass plate or gage box surface. If a solder terminal is to be incorporated, position it on the plate adjacent to the gage as shown. A space of approximately 1/16 in (1.6 mm) should be left between the gage backing and terminal. Place a 4- to 6-in (100- to 150-mm) piece of Micro-Measurements No. PCT-2A cellophane tape over the gage and terminal. Take care to center the gage on the tape. Carefully lift the tape at a shallow angle (about 45 degrees to specimen surface), bringing the gage up with the tape as illustrated in Fig. 4.



Fig. 1

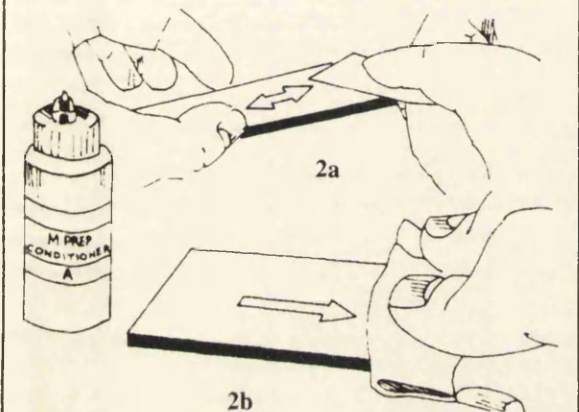


Fig. 2



Fig. 3

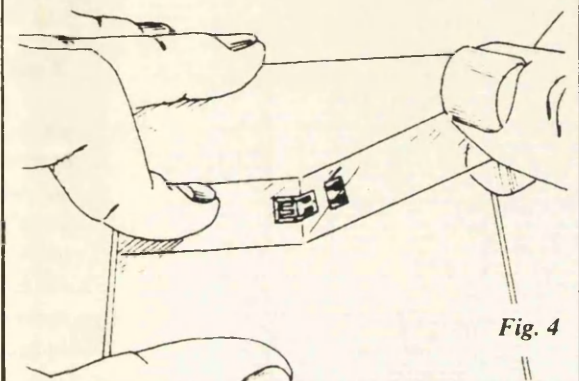


Fig. 4

Step 5

Position the gage/tape assembly so that the triangle alignment marks on the gage are over the layout lines on the specimen (Fig. 5). If the assembly appears to be misaligned, lift one end of the tape at a shallow angle until the assembly is free of the specimen. Realign properly, and firmly anchor down at least one end of the tape to the specimen. Realignment can be done without fear of contamination by the tape mastic if Micro-Measurements No. PCT-2A cellophane tape is used because this tape will retain its mastic when removed.

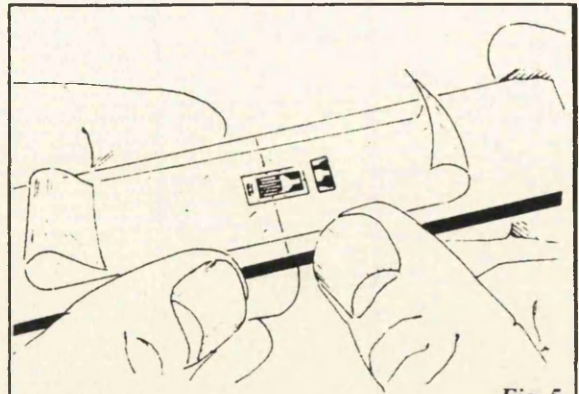
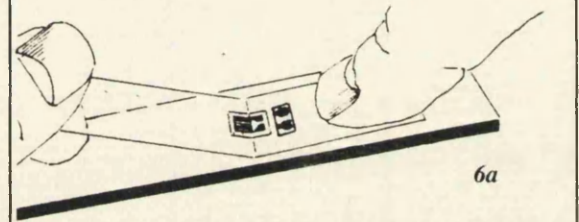


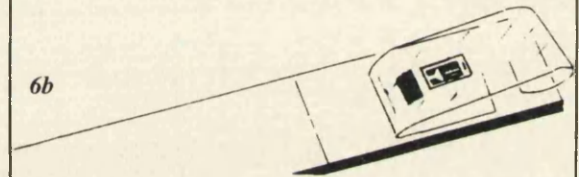
Fig. 5

Step 6

Lift the gage end of the tape assembly at a shallow angle to the specimen surface (about 45 degrees) until the gage and terminal are free of the specimen surface (Fig. 6a). Continue lifting the tape until it is free from the specimen approximately 1/2 in (10 mm) beyond the terminal. Tuck the loose end of the tape under and press to the specimen surface (Fig. 6b) so that the gage and terminal lie flat, with the bonding surface exposed.



6a



6b

Fig. 6

Note: Micro-Measurements gages have been treated for optimum bonding conditions and require no pre-cleaning before use unless contaminated during handling. If contaminated, the back of any gage can be cleaned with a cotton applicator slightly moistened with M-Prep Neutralizer 5A.

Step 7

M-Bond 200 catalyst can now be applied to the bonding surface of the gage and terminal. M-Bond 200 adhesive will harden without the catalyst, but less quickly and reliably. Very little catalyst is needed and should be applied in a thin, uniform coat. Lift the brush-cap out of the catalyst bottle and wipe the brush approximately 10 strokes against the lip of the bottle to wring out most of the catalyst. Set the brush down on the gage and swab the gage backing (Fig. 7). Do not stroke the brush in a painting style, but slide the brush over the entire gage surface and then the terminal. Move the brush to the adjacent tape area prior to lifting from the surface. Allow the catalyst to dry at least one minute under normal ambient conditions of +75°F (+24°C) and 30% to 65% relative humidity before proceeding.

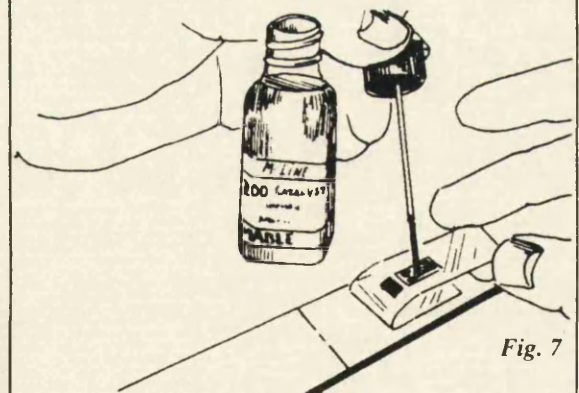


Fig. 7

Note: The next three steps must be completed in the sequence shown, within 3 to 5 seconds. Read Steps 8, 9, and 10 before proceeding.

Step 8

Lift the tucked-under tape end of the assembly, and, holding in the same position, apply one or two drops of M-Bond 200 adhesive at the fold formed by the junction of the tape and specimen surface (Fig. 8). This adhesive application should be approximately 1/2 in (13 mm) outside the actual gage installation area. This will insure that local polymerization, taking place when the adhesive comes in contact with the specimen surface, will not cause unevenness in the gage glue line.

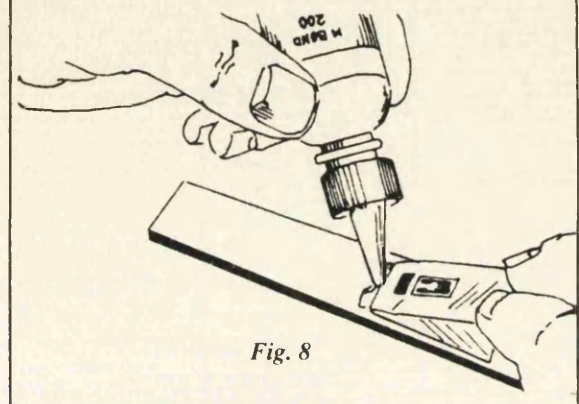


Fig. 8

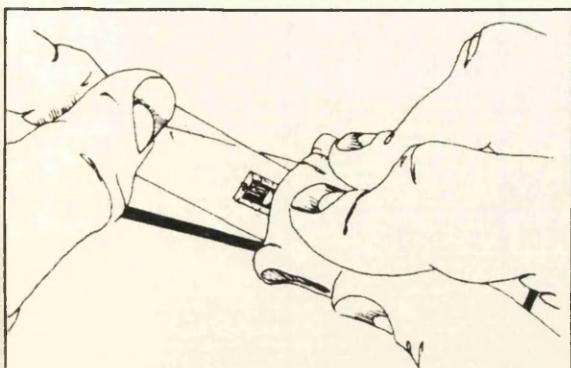


Fig. 9

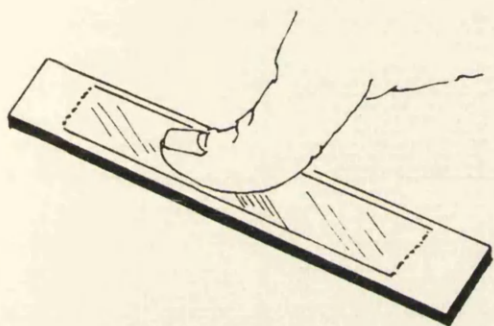


Fig. 10

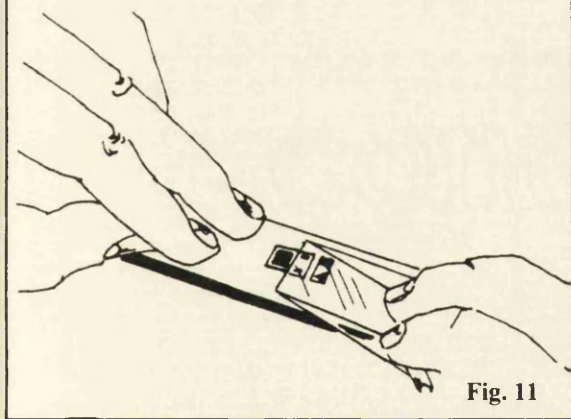


Fig. 11

Step 9

Immediately rotate the tape to approximately a 30-degree angle so that the gage is bridged over the installation area. While holding the tape slightly taut, slowly and firmly make a single wiping stroke over the gage/tape assembly with a piece of gauze (Fig. 9) bringing the gauze back down over the alignment marks on the specimen. Use a firm pressure with your fingers when wiping over the gage. A very thin, uniform layer of adhesive is desired for optimum bond performance.

Step 10

Immediately upon completion of wipe-out of the adhesive, firm thumb pressure must be applied to the gage and terminal area (Fig. 10). This pressure should be held for at least one minute. In low humidity conditions (below 30%) or if the ambient temperature is below +70°F (+20°C), this pressure application time may have to be extended to several minutes. Where large gages are involved, or where curved surfaces such as fillets are encountered, it may be advantageous to use preformed pressure padding during the operation. Pressure-application time should again be extended due to the lack of "thumb heat" which helps to speed adhesive polymerization. Wait two minutes before removing tape.

Step 11

The gage and terminal strip are now solidly bonded in place. To remove the tape, pull it back directly over itself, peeling it slowly and steadily off the surface (Fig. 11). This technique will prevent possible lifting of the foil on open-faced gages or other damage to the installation. It is not necessary to remove the tape immediately after gage installation. The tape will offer mechanical protection for the grid surface and may be left in place until it is removed for gage wiring.

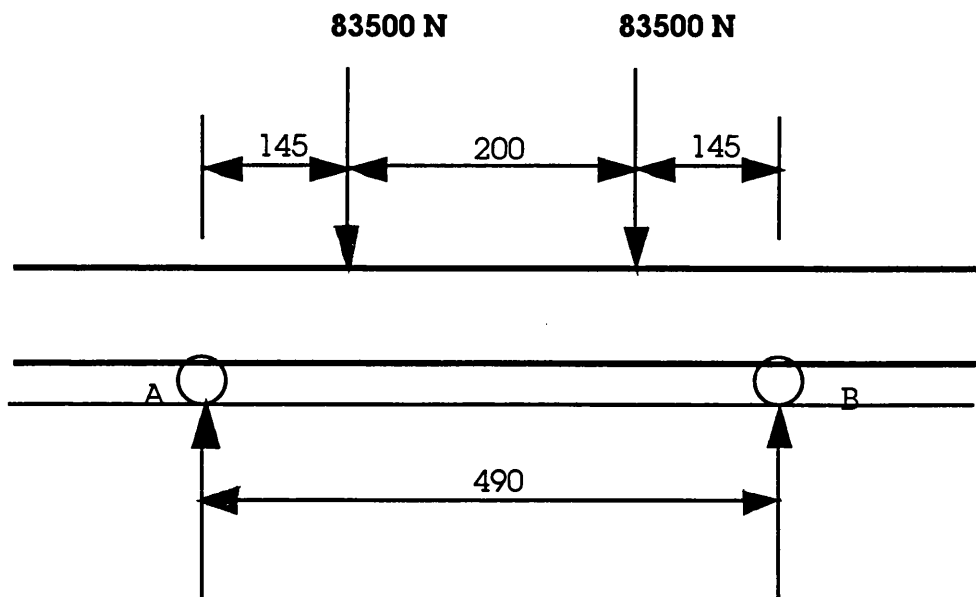
FINAL INSTALLATION PROCEDURE

1. Select appropriate solder, referring to *Micro-Measurements Catalog A-110*, and attach leadwires. Prior to any soldering operations, open-faced gage grids should be masked with PDT-1 drafting tape to prevent possible damage.
2. Remove the solder flux with *M-LINE Rosin Solvent, RSK-1*.
3. Select and apply protective coating according to the protective coating selection chart found in *Micro-Measurements Catalog A-110*.

APPENDIX D

CALCULATIONS FOR THE DETERMINATION OF THE BENDING STRESS AND
COMPRESSION STRESS

In the following case we have:



The maximum bending moment M_{\max} is given by:

$$M_{\max} = 83,500 \times 145 = 12,107,500 \text{ Nmm} = 12,107.5 \text{ KNmm}$$

$$\text{we assume that } s_d = s_y \times 1.5 = 230 \times 1.5 = 345 \text{ N/mm}^2$$

Then:

$$I/y_{\text{required}} = M/s_d = 12,107,500/345 = 35,094.2 \text{ mm}^3$$

Which means that the required maximum section modulus is approximately 35 cm^3 and all models should have a section modulus value below 35 cm^3 .

THEORETICAL VALUES					
MODEL NUMBER	0-4b	1-4b	2-4b	3-4b	4-4b
Ec (N/mm ²)	220000	220000	210000	220000	210000
Ef (N/mm ²)	230000	220000	230000	230000	230000
Theta (rad)	0.35	0.44	0.44	0.35	0.44
Ac per unit width (mm)	3.088	1.775	1.899	3.449	2.880
Ic per unit width (mm ³)	1673.67	697.03	1467.38	4812.05	2519.45
If per unit width (mm ³)	3394.80	1583.99	5113.07	9792.04	5874.92
Gc (N/mm ²)	84615.38	84615.38	80769.23	84615.38	80769.23
Gf (N/mm ²)	88461.54	84615.38	88461.54	88461.54	88461.54
DQx (N/mm)	140986.82	70598.55	84716.64	190021.25	131647.89
Yield Load (N)	60000	15000	36000	59000	36000
Lever (mm)	145.00	145.00	145.00	145.00	145.00
Max Mb (Nmm)	8.70E+06	2.18E+06	5.22E+06	8.56E+06	5.22E+06
Deflection (mm)	1.19	0.64	0.42	0.29	0.64
Stress (N/mm ²)	110.38	84.58	76.18	40.81	81.08

THEORETICAL VALUES			
MODEL NUMBER	1-c	2-c	4-c
FLANGE BREADTH (mm)	20.0	20.0	20.0
CORE DEPTH (mm)	55.28	81.57	87.00
ANGLE (degrees)	25.00	25.00	25.00
ANGLE (rad)	0.436	0.436	0.436
PLATE THICKNESS (mm)	1.00	1.50	1.50
WEB THICKNESS (mm)	1.00	1.00	1.50
CORE AREA PER UNIT WIDTH (mm)	1.769	1.895	2.873
CORE MOMENT OF INERTIA PUW (mm ³)	673.084	1433.097	2436.730
E_c (N/mm ²)	220000	210000	210000
E_f (N/mm ²)	220000	230000	230000
EXTENSIONAL STIFFNESS (N/mm)	8.29E+05	1.09E+06	1.29E+06
G_c (N/mm ²)	84615.38	80769.23	80769.23
DQ_x (N/mm)	69739.16	84178.53	130524.46
S from graphs	10.0	22.0	16.5
DQ_y (N/mm)	791.125	763.027	1697.841
FACES MOMENT OF INERTIA PUW (mm ³)	1527.939	4990.249	5676.750
PLATE ASPECT RATIO (a/b)	3.167	2.604	5.009
MODEL LENGTH (mm)	566	593	595.5
MODEL WIDTH (mm)	178.71	227.73	118.89
MODEL WEIGHT (Kg)	2.68	5.495	2.725
PARAMETER HTA	0.441	0.262	0.392
PARAMETER r_x	1.490	2.595	6.984
PARAMETER r_y	131.313	286.268	536.936
m	0.4	0.288	0.67
n	0	0	0
SIMPLY SUPPORTED k	0.025	0.017	0.027
CLAMPED k	0.038	0.026	0.041
SS COMPRESSIVE LOAD (KN)	45.441	122.142	115.249
C COMPRESSIVE LOAD (KN)	70.434	189.320	178.636
sf (BE) (N/mm ²)	155.339	202.694	182.904
Stress (N/mm ²)	104.564	169.820	255.849
EXPERIMENTAL COMPRESSIVE LOAD (KN)	72.1	191.25	179.5

THEORETICAL VALUES		
MODEL NUMBER	0-3b	3-3b
Ec (N/mm ²)	220000	220000
Ef (N/mm ²)	230000	230000
Theta (rad)	0.35	0.35
Ac per unit width (mm)	3.088	3.449
Ic per unit width (mm ³)	1673.67	4812.05
If per unit width (mm ³)	3394.80	9792.04
Gc (N/mm ²)	84615.38	84615.38
Gf (N/mm ²)	88461.54	88461.54
DQx (N/mm)	140986.82	190021.25
Yield Load (N)	32000	29000
Lever (mm)	245.00	245.00
Max Mb (Nmm)	7.84E+06	7.11E+06
Deflection (mm)	0.41	0.09
Stress (N/mm ²)	99.47	33.90

APPENDIX E
THE ORION PROCEDURE

1. **ON**
2. **CHAN**
3. Enter channel numbers
1
4. **Enter**
5. Select item to be defined
Sensor
6. Select measurement type
Volts
7. Select DC or AC measurement
DC
8. Select item to be defined
Alarm
9. Select alarm
Change
10. Enter change size
Enter
11. **CHAN**
12. Enter channel numbers
3-20, 21-40, 41-60
13. **Enter**
14. Select item to be defined
Sensor
15. Select measurement type
Strain
16. Select bridge configuration
1/4 bridge
17. Select thermal drift compensation
On
18. Select dummy
Rem 120
19. Select energization current

8 mA

20. Enter gauge factor

2.07

21. **Enter**

22. **CHAN**

23. Enter channel numbers

2

24. **Enter**

25. Select item to be defined

Sensor

26. Select measurement type

Volts

27. Select DC or AC measurement

DC

28. **TASK**

29. Enter task number

8

30. **Enter**

31. Enter task title

[SHIFT] LOAD

32. **Enter**

33. Select task function

Scan

34. Select task trigger source

Timer

35. Enter delay to start

Enter

36. Enter number of scans

Enter

37. Select continuous or fixed interval scan

Cont

38. Enter channels to be scanned

1

39. **Enter**

40. Select measurement rate

- 10/s**
41. Select end-of-scan processing
On
42. Select data to be logged
All
43. Select when to output task header
LogData
44. Select output device
Print
45. Select format required
Compact
46. Enter tasks triggered on alarm
8
47. **Enter**
48. Enter tasks aborted on alarm
Enter
49. Ready for command
50. **TASK**
51. Enter task number
7
52. **Enter**
53. Enter task title
[SHIFT] STRAIN
54. **Enter**
55. Select task function
Scan
56. Select task trigger source
Timer
57. Enter delay to start
Enter
58. Enter number of scans
Enter
59. Select continuous or fixed interval scan
Cont
60. Enter channels to be scanned

3-20, 21-40, 41-60

61. **Enter**
62. Select measurement rate
10/s
63. Select end-of-scan processing
On
64. Select data to be logged
All
65. Select when to output task header
LogData
66. Select output device
Print
67. Select format required
Compact
68. Enter tasks triggered on alarm
7
69. **Enter**
70. Enter tasks aborted on alarm
Enter
71. Ready for command
72. **TASK**
73. Enter task number
6
74. **Enter**
75. Enter task title
[SHIFT] DEFLECTION
76. **Enter**
77. Select task function
Scan
78. Select task trigger source
Timer
79. Enter delay to start
Enter
80. Enter number of scans
Enter

81. Select continuous or fixed interval scan

Cont

82. Enter channels to be scanned

2

83. **Enter**

84. Select measurement rate

10/s

85. Select end-of-scan processing

On

86. Select data to be logged

All

87. Select when to output task header

LogData

88. Select output device

Print

89. Select format required

Compact

90. Enter tasks triggered on alarm

6

91. **Enter**

92. Enter tasks aborted on alarm

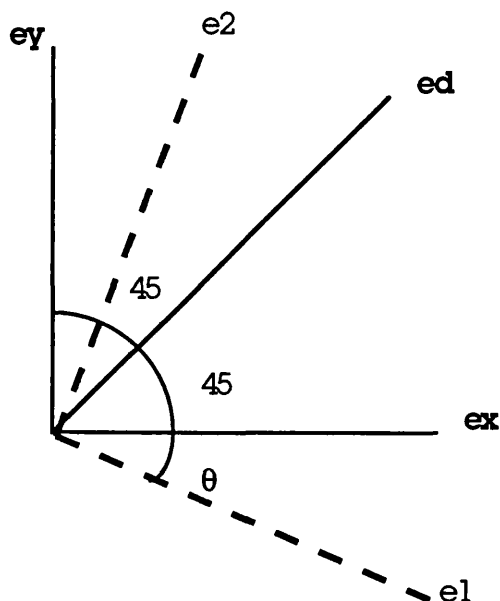
Enter

93. Ready for command

94. **RUN**

APPENDIX F

FORMULAE FOR CALCULATING THE PRINCIPAL STRESSES AND PRINCIPAL
AXES USING A 45-ANGLE ROSETTE



The principal strains e_1 and e_2 are given by the following expressions:

$$e_1 = \frac{1}{2}(e_x + e_y) + \frac{\sqrt{2}}{2} \sqrt{(e_x - e_d)^2 + (e_d - e_y)^2}$$

$$e_2 = \frac{1}{2}(e_x + e_y) - \frac{\sqrt{2}}{2} \sqrt{(e_x - e_d)^2 + (e_d - e_y)^2}$$

The orientation of the principal axes can be easily found by calculating:

$$\tan 2\theta = \frac{2e_d - e_x - e_y}{e_x - e_y}$$

Consequently, the principal stresses σ_1 and σ_2 are given by the following expressions:

$$\sigma_1 = \frac{E}{1-\nu^2}(e_1 + \nu e_2)$$

$$\sigma_2 = \frac{E}{1-\nu^2}(e_2 + \nu e_1)$$

Finally, the stresses s_x and s_y are:

$$\sigma_x = \frac{\sigma_1 + \sigma_2}{2} + \frac{\sigma_1 - \sigma_2}{2} \cos 2\theta$$

$$\sigma_y = \frac{\sigma_1 + \sigma_2}{2} - \frac{\sigma_1 - \sigma_2}{2} \cos 2\theta$$